



UNIL | Université de Lausanne

Unicentre

CH-1015 Lausanne

<http://serval.unil.ch>

---

Year : 2019

## Early Modifications of the Adipose Tissue linking Obesity and Metaflammation

Caputo Tiziana

Caputo Tiziana, 2019, Early Modifications of the Adipose Tissue linking Obesity and  
Metaflammation

Originally published at : Thesis, University of Lausanne

Posted at the University of Lausanne Open Archive <http://serval.unil.ch>

Document URN : urn:nbn:ch:serval-BIB\_609FD80231BE6

### **Droits d'auteur**

L'Université de Lausanne attire expressément l'attention des utilisateurs sur le fait que tous les documents publiés dans l'Archive SERVAL sont protégés par le droit d'auteur, conformément à la loi fédérale sur le droit d'auteur et les droits voisins (LDA). A ce titre, il est indispensable d'obtenir le consentement préalable de l'auteur et/ou de l'éditeur avant toute utilisation d'une oeuvre ou d'une partie d'une oeuvre ne relevant pas d'une utilisation à des fins personnelles au sens de la LDA (art. 19, al. 1 lettre a). A défaut, tout contrevenant s'expose aux sanctions prévues par cette loi. Nous déclinons toute responsabilité en la matière.

### **Copyright**

The University of Lausanne expressly draws the attention of users to the fact that all documents published in the SERVAL Archive are protected by copyright in accordance with federal law on copyright and similar rights (LDA). Accordingly it is indispensable to obtain prior consent from the author and/or publisher before any use of a work or part of a work for purposes other than personal use within the meaning of LDA (art. 19, para. 1 letter a). Failure to do so will expose offenders to the sanctions laid down by this law. We accept no liability in this respect.



**UNIL** | Université de Lausanne

Faculté de biologie  
et de médecine

Centre Intégréatif de Génomique

# **Early Modifications of the Adipose Tissue linking Obesity and Metaflammation**

**Thèse de doctorat ès sciences de la vie (PhD)-programme  
Integrated Experimental and Computational Biology**

présentée à la

Faculté de biologie et de médecine  
de l'Université de Lausanne

par

**Tiziana CAPUTO**

Maîtrise universitaire en Biotechnologie Pharmaceutique  
diplômée de l'Université de Milan

**Jury**

Prof. Luc Tappy, Président  
Prof. Béatrice Desvergne, Directrice de thèse  
Dr Federica Gilardi, Co-directrice  
Prof. Johan Auwerx, expert  
Prof. Maurizio Crestani, expert  
Prof. Lluis Fajas Coll, expert

Lausanne 2019





UNIL | Université de Lausanne

Faculté de biologie  
et de médecine

Centre Intégréatif de Génomique

# **Early Modifications of the Adipose Tissue linking Obesity and Metaflammation**

Thèse de doctorat ès sciences de la vie (PhD)-programme  
Integrated Experimental and Computational Biology

présentée à la

Faculté de biologie et de médecine  
de l'Université de Lausanne

par

**Tiziana CAPUTO**

Maîtrise universitaire en Biotechnologie Pharmaceutique  
diplômée de l'Université de Milan

## **Jury**

Prof. Luc Tappy, Président  
Prof. Béatrice Desvergne, Directrice de thèse  
Dr Federica Gilardi, Co-directrice  
Prof. Johan Auwerx, expert  
Prof. Maurizio Crestani, expert  
Prof. Lluís Fajás Coll, expert

Lausanne 2019

# Imprimatur

Vu le rapport présenté par le jury d'examen, composé de

<b>Président·e</b>	Monsieur Prof. Luc <b>Tappy</b>
<b>Directeur·trice de thèse</b>	Madame Prof. Béatrice <b>Desvergne</b>
<b>Co-directeur·trice</b>	Madame Dre Federica <b>Gilardi</b>
<b>Expert·e·s</b>	Monsieur Prof. Lluis <b>Fajas Coll</b>
	Monsieur Prof. Johan <b>Auwerx</b>
	Monsieur Prof. Maurizio <b>Crestani</b>

le Conseil de Faculté autorise l'impression de la thèse de

## **Madame Tiziana Caputo**


Master in pharmaceutical biotechnology Università degli Studi di Milano, Italie

intitulée

## **Early modifications of the adipose tissue linking obesity and metaflammation**

Lausanne, le 27 février 2019

pour le Doyen  
de la Faculté de biologie et de médecine



Prof. Luc Tappy

# Acknowledgements

This thesis is the fruit of a journey started 5 years ago in the Béatrice Desvergne laboratory. I would like to thank Béatrice for hosting me in her lab in the Centre for Integrative Genomics and for giving me the opportunity to complete my PhD and become an “almost” independent researcher. Thanks Béatrice for trusting me all along the journey and for all your personal inputs to develop my scientific and not scientific personality.

This project would not have started without the work, the help and the support of Federica Gilardi. Thanks Fede simply for being there every time I have a problem, a doubt or just a depressing moment.

Thanks to Nicolas Guex for his great support and his contagious enthusiasm. Thanks to our collaborators Aurelien Thomas and Nasim Bararpuor for sharing their work, ideas and results.

Thanks to Marco Pagni and Thuong Van Du Tran for their work and the priceless bioinformatics support.

A big thanks to Catherin Moret for the help with the histological work and to all the people in the genomic technology facility of the CIG for all the sequencing performed.

I'm extremely grateful to have shared my life in the lab with amazing colleagues. My special thanks goes to Barbara for the great musical moments we had together, to Greta for the uncountable psychological sessions, to Michael, to Coralie and to Khan for their precious help. Many thanks to Carine for this last year together, for all the coffees and for her Swiss made

organizational skills and finally, thanks to Mariano for the testosterone dosage he was bringing in the lab.

I would like to thank all the people in the CIG and particularly the ones on the 5<sup>th</sup> floor with whom I spent some funny moments and shared ideas. Particularly, thanks to Anita, Laia and Judit for all the gossip sessions, all the hilarious moments we had together but especially for the technical support. Part of the last result section would not be there without your help girls 😊.

Thanks to my family for the support and thanks to my mother for her unconditional love.

Finally, a special thanks to Jessica for the love, the care, the encouragements and for being my safe haven in all these years.

# Table of Contents

Summary.....	6
Résumé .....	7
Abbreviations.....	8
Introduction .....	12
<b>I From chronic overnutrition to metaflammation and insulin resistance: adipose tissue and liver contribution .....</b>	<b>14</b>
<b>I.1 Profound remodeling of the visceral white adipose tissue in over-nutrition and obesity .....</b>	<b>15</b>
I.1.1 Visceral WAT and subcutaneous WAT.....	15
I.1.2 Cellular and tissular responses of the vWAT in obesity.....	17
I.1.3 Adipose tissue pro-inflammatory responses induced in obesity: secretion of pro-inflammatory cytokines and modulation of adipokine secretion.....	19
I.1.4 Recruitment of inflammatory and immune cells in the WAT .....	21
I.1.5 Local metabolic consequences of vWAT remodeling .....	28
<b>I.2 Diet-induced modifications occurring in the liver .....</b>	<b>30</b>
I.2.1 NAFLD as a result of the imbalance between uptake and export of lipid in the liver .....	30
I.2.2 From NAFLD to NASH: the role of inflammation in the liver in obesity and overnutrition ...	32
I.2.3 The Adipose Tissue-Liver crosstalk in metaflammation .....	34
<b>I.3 Linking metabolism and inflammation: insulin sensitivity as the central piece .....</b>	<b>39</b>
I.3.1 Insulin signaling in the liver and pathways to insulin resistance in the context of obesity...39	
I.3.2 Molecular pathways that link inflammation and insulin resistance .....	42
I.3.3 Lipid mediators of insulin resistance .....	45
<b>I.4 Metaflammation and specific aspects of PPARs.....</b>	<b>48</b>
<b>I.5 CONCLUSIONS AND PERSPECTIVES.....</b>	<b>52</b>
<b>II The adipose tissue properties and its diverse depots .....</b>	<b>54</b>
<b>II.1 Heterogeneity of the adipose tissue (AT) .....</b>	<b>54</b>
<b>II.2 Molecular pathways driving adipogenesis.....</b>	<b>56</b>
<b>Aim of the project .....</b>	<b>62</b>
<b>Materials and Methods .....</b>	<b>65</b>
<b>I In vivo methods .....</b>	<b>66</b>
I.1 Animals and diet .....	66
<b>II Ex vivo methods.....</b>	<b>67</b>
II.1 Quantitative PCR and Gene expression analyses .....	67
II.2 RNA sequencing (RNA-seq) .....	67
II.2.1 Sequencing data analysis:.....	68



II.3	ChIP on adipose tissue .....	68
II.4	ChIP-seq.....	69
II.4.1	ChIP-seq computational analysis.....	70
II.5	Metabolomics .....	72
II.6	Histology and immunohistochemistry .....	73
II.6.1	Cell Size quantification .....	73
II.7	Western blotting.....	73
III	Statistical analysis.....	74
III.1	Differential expression analysis.....	74
III.2	Ruv correction of RNA-seq dataset.....	75
III.3	Pathway analysis .....	75
III.4	Cluster analysis on ChIP-seq dataset .....	76
Results	.....	77
I	Establishing the final experimental design via a pilot experiment .....	78
I.1	Chromatin immunoprecipitation protocol optimization .....	78
I.1.1	Epigenetic markers selection and optimization of ChIP protocol for each epigenetic mark.....	78
I.2	<i>In vivo</i> pilot experiment .....	81
I.2.1	High fat diet efficiency.....	81
I.2.2	Assessment of the best intermediate time point to study the inflammatory response .....	84
I.2.3	Determination of the needed number of mice at each time point .....	88
II	Full scale <i>in vivo</i> experimental design .....	89
II.1	Design of the full scale experiment .....	89
II.2	Phenotypic evaluation of the response to HFD .....	91
II.3	Full scale <i>in vivo</i> experiment: Quality control and pooling strategy .....	93
II.3.1	Inflammatory response at 8 weeks of HFD treatment and sample selection .....	93
II.3.2	Inflammatory response at 20 weeks of HFD treatment and pooling strategy .....	98
II.4	Full scale <i>in vivo</i> experiment: analysis performed .....	100
II.4.1	ChIP seq: quality controls and general observations.....	100
II.4.2	RNA-seq: quality control and general observations .....	103
II.4.3	Metabolomics: general approach and methodology .....	107
III	Distinct epigenetics and expression profiles of the scWAT and vWAT, in normal conditions .....	108
IV	Different responses at early time point (1week) highlight a distinctive plasticity of the vWAT and scWAT .....	112
IV.1	Epigenetic analyses between early and late time points pinpoint the Wnt pathway.....	112
IV.2	Transcriptomic analysis emphasizes deregulation of histone genes in the vWAT.....	119
IV.3	Modification of the mitochondrial activity in the scWAT.....	125
IV.3.1	Adipocytes in culture maintain the characteristic of their origin, visceral or subcutaneous, but not the specific response to lipid overload .....	130

**V Analysis at the 8-week time-point confirmed the prevalence of inflammation in the vWAT 136**

**VI Omics integration .....138**

    VI.1.1 Data set preparation for integration ..... 139

**Discussion .....146**

**I Overview .....147**

**II Power and limits of the tools used .....148**

**III Intrinsic differences of the two white adipose tissue depots, .....150**

**IV Inhibition of AP differentiation in the vWAT may cause hypertrophic adipocytes and cell death .....151**

**V Early changes occurring in over nutrition in scWAT .....153**

**Appendix.....156**

**References .....186**

# Summary

Obesity is associated with many metabolic disturbances, among which insulin resistance, dyslipidaemia and type 2 diabetes. The low-grade systemic inflammatory response or metaflammation is a well-established consequence of the diet-induced obesity and is thought to play an important role in the development of these co-morbidities.

The aim of this thesis was to reveal the early events that occur in the white adipose tissue (WAT) upon high fat diet (HFD) and which explain its pathological modifications associated to the development of the metaflammation process. For that purpose, we placed mice under HFD or control diet for 1 week, 8 weeks, and 20 weeks. At each time point, a number of parameters were analysed using a combination of systems approaches, *i.e.* transcriptomics, epigenomics and metabolomics approaches, comparing the modifications occurring in two independent WAT depots, the visceral WAT (vWAT), prone to inflammation, and the subcutaneous WAT (scWAT), which does not develop inflammation.

The analyses carried out first show that the two tissues present, under baseline conditions, a number of intrinsic differences in epigenetic organization, gene transcription and metabolites. . The evaluation of genome wide histone acetylation driven by HFD pinpoints a number of significant changes in chromatin organization at many genomic loci in the vWAT. More particularly, we show that in vWAT, but not in scWAT, genomic regions associated with development and cell differentiation genes undergo loss of histone acetylation, suggesting a specific inhibition of adipocyte differentiation in the vWAT. These events are already visible after only one week of HFD. Other experimental data show that the activation of the anti-adipogenic pathway Wnt- $\beta$ catenin, via an increase of Wnt10b, could contribute to dampen adipocyte differentiation in vWAT.

In contrast, under HFD, scWAT undergoes plastic expansion over time. Histological observations show that, in the control situation, scWAT differs from vWAT for the presence of many small beige adipocytes with high mitochondrial activity. In the initial phase of HFD treatment, the decrease in mitochondrial activity suggested by the transcriptomic analyses, is corroborated by the decrease in protein levels of the components of the electron transport chain and the decrease in mitochondrial DNA. The concomitant disappearance of small beige adipocytes suggests a phenotypic change in the latter, which leads to the generation of white fat cells and increases the fat storage capacity.

In conclusion, our results show that one crucial difference in the response of vWAT and scWAT to HFD is represented by the antiadipogenic signals that are rapidly activated specifically in vWAT, but not in scWAT. Such response, by interfering with the normal differentiation of adipocyte progenitors, leads to hypertrophic expansion of the existing mature adipocytes, which ultimately causes cell death and the inflammatory response. Releasing the inhibition of adipocyte differentiation in the vWAT would therefore be a possible mean for reducing the inflammatory response and the subsequent obesity-related insulin resistance.

# Résumé

L'obésité, est associée à de nombreux troubles métaboliques, parmi lesquels l'insulinorésistance, la dyslipidémie et le diabète de type 2. La réponse inflammatoire systémique de bas grade, ou métaflammation, est une conséquence bien établie de l'obésité et joue probablement un rôle important dans le développement de ces comorbidités.

Le but de cette thèse était de mettre en évidence les événements précoces qui se produisent dans le tissu adipeux blanc (white adipose tissue, WAT) lors d'un régime riche en graisses (high fat diet, HFD), et qui contribueraient au développement du processus de métaflammation. Pour ce faire, nous avons placé des souris sous HFD ou sous régime de contrôle pendant 1 semaine, 8 semaines et 20 semaines. Dans chaque condition, un certain nombre de paramètres ont été analysés en combinant plusieurs approches dites de système, soit la transcriptomique, l'épigénomique et la métabolomique. Ces analyses ont été effectuées dans deux types de tissu adipeux, le tissu adipeux viscéral (vWAT), sujet à l'inflammation, et le tissu adipeux sous-cutané (scWAT), qui ne développe aucune inflammation.

Les analyses effectuées montrent en premier lieu que les deux tissus présentent, en conditions de base, un certain nombre de différences intrinsèques au niveau de l'organisation épigénétique, de la transcription des gènes et des métabolites. En comparant à l'échelle du génome les modifications des marques d'acétylation des histones induites par le régime riche en graisse, on constate, dans le vWAT, des changements importants de l'organisation de la chromatine au niveau de nombreux loci génomiques. Plus particulièrement, nous montrons que, dans le vWAT et non dans le scWAT, les régions génomiques associées aux gènes liés au développement et à la différenciation cellulaire subissent une perte d'acétylation des histones, ce qui suggère un inhibition de la différenciation adipocytaire dans le vWAT. Ces changements sont déjà visibles après seulement une semaine et renforcés après huit semaines de HFD. D'autres données expérimentales montrent que l'activation de la voie antiadipogène Wnt- $\beta$ catenin, via une augmentation de Wnt10b, pourrait contribuer à inhiber la différenciation des adipocytes dans le vWAT.

A l'opposé, le scWAT subit, sous HFD, une expansion plastique au fil du temps. Les observations histologiques montrent que, dans la situation contrôle, le scWAT diffère du vWAT par la présence de nombreux petits adipocytes beiges, à forte activité mitochondriale. Dans la phase initiale du traitement HFD, la diminution de l'activité mitochondriale est corroborée par la diminution des niveaux de protéines des composants de la chaîne des transporteurs d'électrons et la diminution de l'ADN mitochondrial. Associé à la disparition des petits adipocytes beiges, cela suggère un changement phénotypique de ces derniers qui aboutit à la génération d'adipocytes blancs et à l'augmentation de la capacité de stockage de graisse.

En conclusion, ces résultats montrent que des signaux anti-adipogéniques sont rapidement activés dans le vWAT par le traitement HFD. Cette réponse, qui interfère avec la différenciation normale des progéniteurs adipocytaires, mène à une expansion hypertrophique des adipocytes adultes existants, et, par conséquence, induit la mort cellulaire la réponse inflammatoire. La levée de l'inhibition de la différenciation des adipocytes dans le tissu adipeux viscéral serait donc un moyen possible de réduire la réponse inflammatoire et la résistance à l'insuline liée à l'obésité qui en résulte.

# Abbreviations

AA	Aminoacids
ACADM	Medium-chain Acyl-CoA Dehydrogenase
ACOX1	Acyl-CoA Oxidase 1
ADAM8	Metallopeptidase Domain-8
ADRP	Adipose Differentiation-Related Protein
ALT	Alanine Aminotransferase
AMPK	Adenosine Monophosphate-Activated Protein Kinase
AP-1	Activator Protein-1
aPKC	Atypical Protein Kinase C
ATF6	Activating Transcription Factor 6
ATM	Adipose Tissue Resident Macrophages
BAT	Brown Adipose Tissue
C/EBPs	CCAAT/Enhancer Binding Proteins
CCL2	CC- motif Chemokine Ligand 2
CCL3	CC- motif Chemokine Ligand 3
CCL4	CC- motif Chemokine Ligand 4
CCR2	CCL2 Receptor 2
CPT	Carnitine Palmitoyl Transferase Carrier
CRP	C-Reactive Protein
CXCL10	C-X-C motif Chemokine 10
DAG	Diacyl-Glycerol
DNL	<i>De Novo</i> Lipogenesis
ER	Endoplasmic Reticulum
ERK	Extracellular signal-Regulated Kinase
FABP4	Fatty-Acids Binding-Protein 4
FATP1	LPL Fatty Acids Transporter
FFA	Free Fatty Acids
FGF21	Fibroblast Growth Factor 21

Foxo	Forkhead box
GCK	Glucokinase
GLUT4	Glucose Transporter 4
GSK-3	Glycogen Synthase Kinase 3
HGP	Hepatic Glucose Production
HIF1 $\alpha$	Hypoxia Inducible Factors
ICAM-1	Intracellular Adhesion Molecule
IFN $\gamma$	Interferon $\gamma$
IgG	Immunoglobulin G
IKK $\beta$	Inhibitor of Nuclear Factor I $\kappa$ B
IL-1RA	IL-10 and IL-1 Receptor Antagonist
IL15	Interleukin 15
IL6	Interleukin 6
iNOS	Nitric Oxide Synthase
IR	Insulin Receptor
IRE1	Inositol-Requiring Enzyme 1
IRFs	Interferon Regulatory Factors
IRS1/IRS2	Insulin Receptor Substrate 1 and 2
JNK	Jun N-terminal Kinases
LPL	Lipoprotein Lipase
MAC-1	Macrophage Antigen 1
MAPK	Mitogen-Activated Protein Kinases
MAPK	Mitogen Activated Protein Kinases
MCP1	Macrophage Chemoattractant Protein 1
MIP-1 $\alpha$	Macrophage Inflammatory Protein 1 $\alpha$
mTORC	Rapamycin complex
NAFLD	Non Alcoholic Fatty Liver Disease
NASH	Non Alcoholic Steatohepatitis
NCoR1	Nuclear Receptor Co-Repressor
NCR1	NK Cell-activating Receptor

NEFA	Non-Esterified Fatty Acids
NFκB	Nuclear Factor κB
NK	Natural Killer
NLR	Leucine rich Repeat
NLRP3	NLR-and Pyrin domain containing 3
PAI-1	Plasminogen-Activator Inhibitor type 1
PERK	PKR-like ER Kinase
PI3K	Phosphatidylinositol 3-Kinase
PKR	RNA-activated Protein Kinase
PPARα	Peroxisome Proliferator-Activated Receptors α
ROS	Radical Oxygen Species
S6K	S6 Kinase
scWAT	Subcutaneous White Adipose Tissue
SLC25A20	Carnitine Acycarnitine Translocase
SOCS3	Suppressor of Cytokine Signaling 3
SPTLC	Serine Palmitoyl-Transferase
SREBP1c	Sterol Regulatory Element-Binding Protein 1c
T2D	Type 2 Diabetes
TGs	Triglycerides
T <sub>H</sub> 1	CD4 <sup>+</sup> T helper 1 cells
TIMP1	Tissue Inhibitor of Metallo-Proteinase 1
TLR4	Toll-Like Receptor 4
TNF-α	Tumor Necrosis Factor alpha
TZD	Thiazolidinediones
UCP1	Uncoupling Protein 1
UPR	Unfolded Protein Response
VCAM-1	Vascular Cell Adhesion Molecule
VEGF	Vascular Endothelial Growth Factor
VLDL	Very low Density Lipoprotein
vWAT	Visceral White Adipose Tissue

WAT	White Adipose Tissue
$\alpha$ -SMA	$\alpha$ -Smooth Muscle Actin
$\beta$ -ox	$\beta$ -oxydation



# **Introduction**

# **From chronic overnutrition to metaflammation and insulin resistance: adipose tissue and liver contribution**

*Tiziana Caputo, Federica Gilardi\*, and Béatrice Desvergne\**

*Center for Integrative Genomics, Genopode, Lausanne Faculty of Biology and Medicine CH-1015 Lausanne,  
Switzerland*

\*Corresponding authors

This part of the introduction has been published in July 2017

<https://doi.org/10.1002/1873-3468.12742>

## **I From chronic overnutrition to metaflammation and insulin resistance: adipose tissue and liver contribution**

Obesity is a complex chronic disorder with a multifactorial etiology, involving genetics, hormones, diet and life style. It is characterized by a massive increase in adipose tissue due to the imbalance between daily energy intake and energy expenditure. In the last 30 years, obesity has become a worldwide epidemic affecting both adult and children and turning into an extremely important public health problem<sup>1</sup>. Indeed, it is associated to many different (co)morbidities, such as cardiovascular diseases, type 2 diabetes (T2D), hypertension, certain cancers and sleep-disordered breathing, such as sleep apnea, contributing to an increase risk of mortality as well as reduced life expectancy. Although carrying a large amount of fat is not necessarily harmful, two interlinked systemic disorders contribute to the high morbidity, i.e. insulin resistance and inflammation, the latter being thought to play an important role in the pathogenesis of the former<sup>2</sup>. The link between these two processes is illustrated by the increased levels of several inflammatory cytokines in serum of T2D patients compared to healthy subjects. Up to 30% of obese patients are considered as “metabolically healthy obese individuals” because of their normal fasting glucose, normotension, high insulin sensitivity and inflammatory status<sup>3,4</sup>. This concept was substantiated in many clinical studies, although a study showing that insulin-sensitive and insulin-resistant has recently challenged it obese have similar insulin-dependent transcriptional response in subcutaneous adipose tissue<sup>5</sup>.

## **I.1 Profound remodeling of the visceral white adipose tissue in over-nutrition and obesity**

In humans, adipose tissue is distributed over the entire body with many compartments that differ in terms of metabolic activity, sympathetic innervation, and contribution to local and systemic signaling. Whereas the brown adipose tissue (BAT) is orientated towards use of lipids, coupled to a thermogenic process, the white adipose tissue (WAT) is the main location for lipid storage, expanding in response to high fat or over-nutrition. The WAT is prone to develop inflammation upon obesity and thus is the focus of the present review.

### **I.1.1 Visceral WAT and subcutaneous WAT**

When considering the impact on the development of metabolic disorders, two main types of WAT have been identified: the subcutaneous WAT (scWAT) which is located under the dermal compartment of the skin, and the visceral WAT (vWAT) further divided into the mesenteric WAT wrapped around the intestine, the retroperitoneal WAT surrounding the kidney, and the omental WAT positioned in the lower part of the abdominal cavity covering the stomach. This anatomic classification of the vWAT is not strictly reproduced in mice where omental fat is absent, and the tissue presenting the properties of visceral fat in mouse is the gonadal fat.

Visceral and subcutaneous adipose tissues have different behaviors, particularly highlighted in obesity and related metabolic disorders. These differences are of three types. Firstly, adipokine nature and secretion profile of vWAT and scWAT differ. For example, the expression and secretion of Interleukin 6 (IL6) and Plasminogen-Activator Inhibitor type 1 (PAI-1) are higher in

the visceral WAT, whereas leptin and adiponectin are higher in subcutaneous WAT<sup>6,7</sup>. Secondly, the adipokines produced by the scWAT are secreted into the systemic circulation, whereas those produced by vWAT are secreted into the portal system, thus having a more direct impact on hepatic metabolism. Thirdly, the rate of lipolysis and fatty acids mobilization<sup>8</sup> is also different, the visceral adipose tissue appearing to be more sensitive to lipolytic effects of catecholamines and less sensitive to the antilipolytic effects of insulin, that mobilizes fatty acids into the portal vein. Whereas these differences are possibly due to the vWAT vs. scWAT specific environment, which includes the innervation and vasculature proper to each depot, recent reports suggested that physiological heterogeneity within the adipose tissues could also stem from different developmental programs, leading to cell-autonomous differences<sup>9,10,11</sup>.

These differences explain at least in part the major distinct response of each WAT depot upon obesity in human and in experimental models, including genetically induced obese mice, *ob/ob* and *db/db*, lacking the coding gene for leptin or for leptin receptor, respectively, as well as diet induced obese mice.

In the rest of this chapter, we will thus discuss how the remodeling of the visceral WAT in over-nutrition and obesity is a sequential process that starts with the development of mature hypertrophic adipocytes that have to face oxidative and endoplasmic reticulum (ER) stress. Their altered secretome initiates the inflammation process, with the recruitment of a large number of macrophages as well as the modification of the profile of pre-existing adipose tissue resident macrophages. Finally, activated macrophages lead to the recruitment and activation of T lymphocytes, which altogether sustain the progression of obesity-induced inflammation. Recent knowledge concerning this process is discussed below. However, it must be reminded that the

triggering stimuli as well as the exact temporal sequence of inflammatory cell infiltration and their cross-talk with stressed adipocytes is not completely clear, due to its intrinsic complexity and the difficulties in taking into account the various experimental contexts (e.g. animal model, type of diet, selected time points).

### **I.1.2 Cellular and tissular responses of the vWAT in obesity**

WAT has the unique capacity to undergo dramatic remodeling in response to nutritional factors by increasing the size of individual cells (hypertrophy) and by recruiting new adipocytes from the resident pool of progenitors (hyperplasia). These processes, which aim to positively improve the lipid storage capacity of the body, are however accompanied, particularly in vWAT, by a reduction of tissue vascularization, leading to areas with lower oxygen availability and hypoxia<sup>12,13</sup>. This results in the vWAT by the alteration of some cellular and tissular responses and by an undesirable infiltration and activation of immune and inflammatory cells, observed both in experimental models and in humans.

The first response of the adipose tissue to the high levels of circulating lipids is a hypertrophic growth of the pre-existing mature adipocytes as a result of the triglyceride accumulation in the unilocular lipid droplet. The hyperplasia process also starts quite rapidly since in mice adipogenesis and adipocyte precursor proliferation are already activated 3 days after the beginning of a high fat diet feeding in vWAT depots, with the subsequent creation of a pool of precursors that will turn into mature adipocytes over a prolonged exposition to the diet (seven weeks)<sup>14</sup>. Notably, the hypertrophic process – rather than the hyperplasia – seems to be the most damaging for the cells and thus for the tissue.

At the cellular level, one of the consequences of the hypertrophic response is the decrease of insulin-dependent glucose uptake because of a dysregulation of cortical actin remodeling and the consequent impairment of insulin-dependent glucose transporter 4 (GLUT4) translocation to the plasma membrane<sup>15</sup>. Another alteration in hypertrophic adipocytes is the accumulation of radical oxygen species (ROS)<sup>16</sup> and dysfunction of the endoplasmic reticulum, a membranous network controlling synthesis, maturation, and trafficking of secreted and membrane proteins. The accumulation of unfolded proteins in the ER lumen induces an adaptive response known as unfolded protein response (UPR) that is mediated by three major transducers: the PKR-like ER Kinase (PERK), the Inositol-Requiring Enzyme 1 (IRE1) and the Activating Transcription Factor 6 (ATF6). Along this line, chronic obesity is associated with endoplasmic reticulum stress in adipose tissue<sup>17</sup> and free fatty acids (FFA; also called non-esterified fatty acids) induce ROS generation as well as endoplasmic reticulum stress by activation of UPR signaling pathways in adipocytes.<sup>18</sup>

At the tissular levels, adipocyte hypertrophy is associated with a relative deficiency of vasculature that creates a local imbalance between oxygen supply and consumption, which, in turn, leads to an increase in the level of angiogenic factors and the expression of inflammation and ER stress associated genes<sup>19</sup>. In mice exposed to high fat diet, sign of hypoxia can be detected after 3 days of diet together with increased protein level of its main mediator, the Hypoxia Inducible Factors (HIF1 $\alpha$ ), Vascular Endothelial Growth Factor (Vegf) expression levels and accumulation of lactate. The link between hypoxia and the appearance of inflammation in vWAT, was demonstrated in both mouse models of both HIF1 $\alpha$  genetic deletion and transgenic overexpression establishing its critical role in the inflammatory response and in the onset of insulin<sup>20,13</sup>.

Altogether, these alterations are responsible, at least in part, for the subsequent inflammatory response and decreased insulin sensitivity, as discussed below.

### **I.1.3 Adipose tissue pro-inflammatory responses induced in obesity: secretion of pro-inflammatory cytokines and modulation of adipokine secretion**

The first evidence showing the implication of adipose tissue in the obesity-related inflammatory response came twenty years ago, when Hotamisligil et al.<sup>21</sup> demonstrated that the production of Tumor Necrosis Factor alpha (TNF- $\alpha$ ) was induced in the visceral fat pad of obese rodents and that the neutralization of this cytokine improved their insulin sensitivity. Excessive nutrient consumption triggers an inflammatory process, also called “metaflammation”<sup>2,22</sup>, that is initiated and sustained by metabolic cells, which are at the interface between metabolic inputs and the inflammatory outputs. Metaflammation is characterized by being low-grade compared to the acute inflammatory response, and chronic, as cytokine expression and immune cell infiltration appear gradually and remain unresolved over time. WAT is likely the primary site where metaflammation originates, although, to a certain degree, other metabolic tissues, such as liver (as discussed later), pancreas and gut cells associated with the gut microbiota are also involved, with important consequences for metabolic homeostasis.

Upon nutrient overload, the inflammatory process is likely initiated by the cellular and tissular damages, described above. These alterations lead to two main processes. First, they increase the number of dead adipocytes showing necrotic-like abnormalities<sup>23,24</sup>. In turn, these necrotic events trigger the recruitment of inflammatory cells that secrete pro-inflammatory soluble mediators. In parallel, the adipocytes themselves undergo a global and profound change in their secretome profile, with an increased release of mediators of the clotting process, such as PAI-1, but also an



increased expression and secretion of pro-inflammatory cytokines<sup>25,26</sup> and alterations in the level of several adipokines<sup>27</sup>.

As mentioned above, TNF- $\alpha$  was the first identified major pro-inflammatory cytokine released from the obese adipose tissue, in mice and in humans<sup>28,29</sup>. It is mainly expressed by monocytes and macrophages that infiltrate the obese adipose tissue, as well as by obese adipocytes<sup>21</sup> and has a central role in many different inflammatory diseases.

CC- motif Chemokine Ligand 2 (CCL2) also known as Macrophage Chemoattractant Protein 1 (MCP1), is one key chemokine expressed by the adipocytes whose levels positively correlate with the increased adiposity and whose presence is sufficient to induce the recruitment and infiltration of macrophages in the adipose tissue initiating the inflammatory response and obesity-related insulin resistance<sup>30</sup>. Whereas the work of Kirk *et al.* reported no differences in adipose tissue inflammation or macrophages accumulation in CCL2 deficient mice<sup>31</sup>, other studies showed that lack of CCL2 or of its receptor CCR2 in the adipose tissue reduces macrophage accumulation and ameliorates the metabolic profile as well as the insulin sensitivity and hepatic steatosis of obese mice<sup>30,32</sup>.

IL6 and IL18 are cytokines produced by the adipose tissue and positively correlated with the adiposity level<sup>33,34</sup>, even in a regimen of weight loss<sup>35,36</sup>. However, the metabolic consequence of the increase of these two cytokines remains controversial, as discussed later.

The adipokines also play a role in modulating inflammatory responses. Adiponectin has anti-inflammatory properties, via inhibition of TNF- $\alpha$  synthesis in endothelial and hepatic cells and induction of the production of anti-inflammatory cytokines such as IL-10 and IL-1 Receptor Antagonist (IL-1RA) in macrophages and dendritic cells<sup>37</sup>. Adiponectin reduction observed in obesity limits these anti-inflammatory effects. In contrast, leptin increases circulating levels of

pro-inflammatory mediators released by various cell types, including macrophages. Leptin is an adipokine involved in the regulation of food intake through the central nervous system. Mice lacking leptin (*ob/ob* mice) are hyperphagic and develop obesity and insulin resistance, which can be reverted by the administration of leptin<sup>38</sup>. Leptin circulating levels are positively associated with the adipose tissue mass, suggesting a possible leptin resistance in obese patients as they do not show the expected anorexic response<sup>38</sup>. The pro-inflammatory activity of leptin is mainly mediated by its ability to increase the production of TNF- $\alpha$  and IL6 by monocytes, and of CC-chemokine ligands by macrophages<sup>39-41</sup>. In addition, it increases the production of IL2 and Interferon  $\gamma$  (IFN $\gamma$ ) and suppresses the production of the anti-inflammatory cytokine IL4 in T cells<sup>42</sup>. In the obese adipose tissue, pro-inflammatory signals such as TNF- $\alpha$ ,<sup>43</sup> stimulate the production of leptin, which in turn maintains and exacerbates the inflammatory response.

Resistin is another major secreted adipokine whose levels increase with obesity and correlate with both inflammation and insulin resistance in animal models<sup>44</sup>. The pro-inflammatory action of resistin in human mononuclear cells is mediated by the increase of the expression levels of TNF- $\alpha$  and IL6 in monocytes<sup>44</sup> and of adhesion molecules (VCAM1, ICAM1 and pentraxin 3) in vascular cells that enhance leukocyte adhesion<sup>45</sup>.

Altogether, the obesity- or overnutrition-driven changes in the secretion profiles of these cytokines and adipokines in the vWAT are part of the process that leads to the recruitment of inflammatory/immune cell in this tissue.

#### **I.1.4 Recruitment of inflammatory and immune cells in the WAT**

Macrophages are at the front line of the inflammatory process, prevailing in terms of number and tissue remodeling activity<sup>46</sup>. In lean mice, around 10-15% of the vWAT cells are positive for

F4/80<sup>+</sup>, which identifies macrophages. These so-called adipose tissue resident macrophages (ATM) have an alternatively activated M2 phenotype (Arg1<sup>+</sup>, CD206<sup>+</sup>, CD301<sup>+</sup>) and localize in the interstitial spaces between adipocytes, uniformly distributed through the adipose tissue. M2 macrophages are crucial for the adipose tissue homeostasis, particularly for their production of IL10, a regulatory anti-inflammatory cytokine. However upon obesity, the secretion by the hypertrophic adipocytes of pro-inflammatory cytokines such as CCL2, CCL5 and others<sup>47</sup> as well as that caused by the presence of increased number of necrotic adipocytes<sup>48,49</sup> leads to the recruitment of circulating monocytes towards the stressed tissue, monocytes which then are activated in macrophages (figure. 1). In total, in obese mice, macrophages can reach 45-60% of the vWAT cell population<sup>50</sup>. They localize primarily in “crown-like structure” surrounding dying adipocytes<sup>51,52</sup> and have a classical pro-inflammatory M1 phenotype (CD11c<sup>+</sup>, nitric oxidase synthase 2<sup>+</sup>, TNF- $\alpha$ <sup>+</sup>). They produce pro-inflammatory cytokines, such as TNF- $\alpha$ , iNOS and IL6, which further promote obesity-associated inflammation in mice<sup>52</sup>, but also in obese patients where the accumulation of macrophages has been shown to correlate with higher circulating level of TNF- $\alpha$ <sup>53,54</sup>

Another concurrent effect, which contributes to the worsening of obesity-related inflammation, is mediated by paracrine action of leptin on immune cells. Leptin has been reported as a strong mediator of monocytes proliferation, macrophages phagocytosis, cytokine expression and chemotaxis<sup>55</sup> by stimulating the production of IL2, IL12 and IFN $\gamma$ <sup>56</sup>. Moreover, mast cells in the adipose tissue of obese mice contribute to leptin production, which in turn affects macrophage polarization towards the M1 pro-inflammatory status. Consistently, mast cells from leptin-deficient mice are able to polarize macrophages towards the less inflammatory M2 phenotype<sup>57</sup>.

Finally, other stimuli in the context of obesity can influence macrophage recruitment and activation, such as fatty acids, fetuin-A, Krüppel-like factor 4<sup>58</sup> or cold exposure<sup>59</sup>. Unsaturated fatty acids have been identified as promoters of macrophage activation in obesity through a mechanism mediated by the binding to the pattern recognition receptor Toll-like receptor 4 (TLR4)<sup>60</sup>. Recent observations suggested that FFAs are not direct ligands of TLR4 but bind *via* fetuin-A, a glycoprotein produced by the liver that may act as a transporter of FFAs in the circulation and as endogenous ligand for TLR4, presenting in this way FFAs to the receptor<sup>61</sup>. All these effects favor not only recruitment of macrophages to the inflated adipose tissue, but also their polarization to M1 type. However, some studies have demonstrated a mixed M2/M1 phenotype in adipose tissue of obese mice and humans<sup>62-64</sup>, while others depicted a complex scenario where the most abundant “metabolically-activated” (MMe) macrophages have a different phenotype compared to classically activated M1 macrophages, suggesting that their activation is occurring via mechanisms that are different from those occurring during infection<sup>65</sup>.

Currently, an active research field is studying ways to counteract the inflammatory response in white adipose tissue by pushing the rise in number and activity of brite (brown in white) cells, in order to boost the whole-body energy expenditure but also to improve adipose tissue inflammation and thus insulin resistance<sup>66</sup>. Indeed, prolonged cold exposure increases adiponectin secretion that in turn is responsible for the activation and recruitment of anti-inflammatory M2-type macrophages<sup>67</sup>.

After the first wave of newly recruited M1 macrophages, that have the role to clear necrotic adipocytes and remodel the extracellular matrix<sup>24</sup>, and with the persistence of excessive nutrient intake, the activation of the adaptive immune system response is occurring in the adipose tissue.

Indeed, activated M1 cells act as antigen presenting cells, via MHC class I and II molecules, thereby initiating the response of the adaptive immune system and amplifying the adipose tissue obesity-driven inflammation (Figure 1).

Among the immune cells of the adaptive response, CD4<sup>+</sup> T cells are thought to play an important role in the progression of the obesity-related inflammatory response. T helper lymphocytes expressing CD4 can be subdivided into a T<sub>H</sub>1 and T<sub>H</sub>2 sub-lineage, based on their secretion profile. T<sub>H</sub>1-cells tends to secrete pro-inflammatory cytokines responsible for the elimination of pathogens and the perpetuation of the inflammatory response. On the other hand, T<sub>H</sub>2-cells produce anti-inflammatory cytokines including IL4, 5, 10 and 13, which promote antibody synthesis but inhibit several functions of phagocytic cells. Compared to the scWAT of obese mice as well as to vWAT of lean mice, the vWAT of diet-induced obese mice exhibits a higher number of pro-inflammatory CD4<sup>+</sup> T<sub>H</sub>1 cells secreting IFN $\gamma$  (Figure 1). This contributes to the creation of a feed forward loop in the obese vWAT, where the increased production of IFN $\gamma$  by T<sub>H</sub>1 cells favors the classical (proinflammatory) activation of macrophages<sup>68</sup>. The importance of another subset of CD4<sup>+</sup> T cells, the regulatory CD4<sup>+</sup>Foxp3<sup>+</sup> T<sub>reg</sub> cells, in the vWAT is highlighted by its relative defection upon inflammatory response of the adipose tissue in obesity. This particular population of WAT T<sub>reg</sub> seems to be extremely important for metabolic processes and for the regulation of inflammatory response in vWAT. They are present in high number in lean mice (40-80% of CD4<sup>+</sup> T cells in vWAT), while they are dramatically reduced down to 30% of the initial population during obesity<sup>69</sup>. However, how this particular new cell compartment contributes to the worsening of the inflammatory response is not yet clarified.

Another immune cell type contributing to the creation of a modified milieu in the AT, are the CD8<sup>+</sup> T, whose depletion improves insulin sensitivity in diet-induced obese mice. These cells

localize in close proximity to M1 cells in the crown-like structures, suggesting a possible crosstalk between CD8<sup>+</sup> and M1 cells. This hypothesis is also supported by the fact that M1 cells that are co-cultured with CD8<sup>+</sup> cells increase their production of TNF- $\alpha$ <sup>70</sup> (Figure 1).

B cells, another class of cells belonging to the adaptive immune system, are also playing a role in the pathogenesis of obesity-related insulin resistance. In mouse model of diet-induced obesity, B cells accumulate in vWAT at early stage (i.e. by 4 weeks), and contribute to the worsening of insulin sensitivity. This mechanism is in part mediated by their effect on CD8<sup>+</sup> and T<sub>H</sub>1 cells, which are induced to produce proinflammatory cytokines, and in part by their own release of Immunoglobulin G (IgGs). In line with this observation, B cell depletion using CD20 monoclonal antibody reduced the levels of pro-inflammatory mediators such as IFN $\gamma$  and TNF- $\alpha$  and ameliorated glucose metabolism<sup>71</sup>.

This already complex scenario has been recently enriched by two reports that highlighted the essential role of Natural Killer (NK) cells in this process. This specialized subset of lymphocytic cells has normally two functions. First, they can destroy tumor and infected cells using the cytolytic activities of enzymes such as perforin and granzyme. Second, they are able to modulate the activity of many immune cells by secreting many different pro and anti-inflammatory cytokines, including TNF- $\alpha$ , IFN $\gamma$  and IL10<sup>72</sup> (Figure 1). Two different groups demonstrated that NK cell number dramatically increase in the vWAT of HFD-exposed mice and that these cells have a major role in the recruitment and the M2-M1 macrophage polarization<sup>73,74</sup>. Wensveen et al. showed how NK cells start to accumulate in the vWAT within few days of high fat diet, with the maximum number detected at 2 weeks, and this correlates with the up-regulated expression of NK Cell-activating Receptor (NCR1) ligand in adipocytes. In turn, NCR1 is thought to activate vWAT-resident NK cells thereby inducing the production of IFN $\gamma$ , a strong modulator of M1

polarization (Figure 1). Similar results come from the work of Lee et al., where the authors show how the modified milieu, created by a prolonged high fat diet (12 weeks), induce in the vWAT the production of pro-inflammatory cytokines, such as CCL3, CCL4, CXCL10 and IL15, which serve as chemo-attractants for NK cells. NK cells are then responsible for the production of CCL2 and TNF- $\alpha$ , which will promote monocyte recruitment and activation respectively. Together these works agree on the crucial role of NK cells in the early and late phases of obesity, showing how selective depletion of this particular immune cell population is able to improve metabolic phenotype and insulin resistance of HFD treated mice.

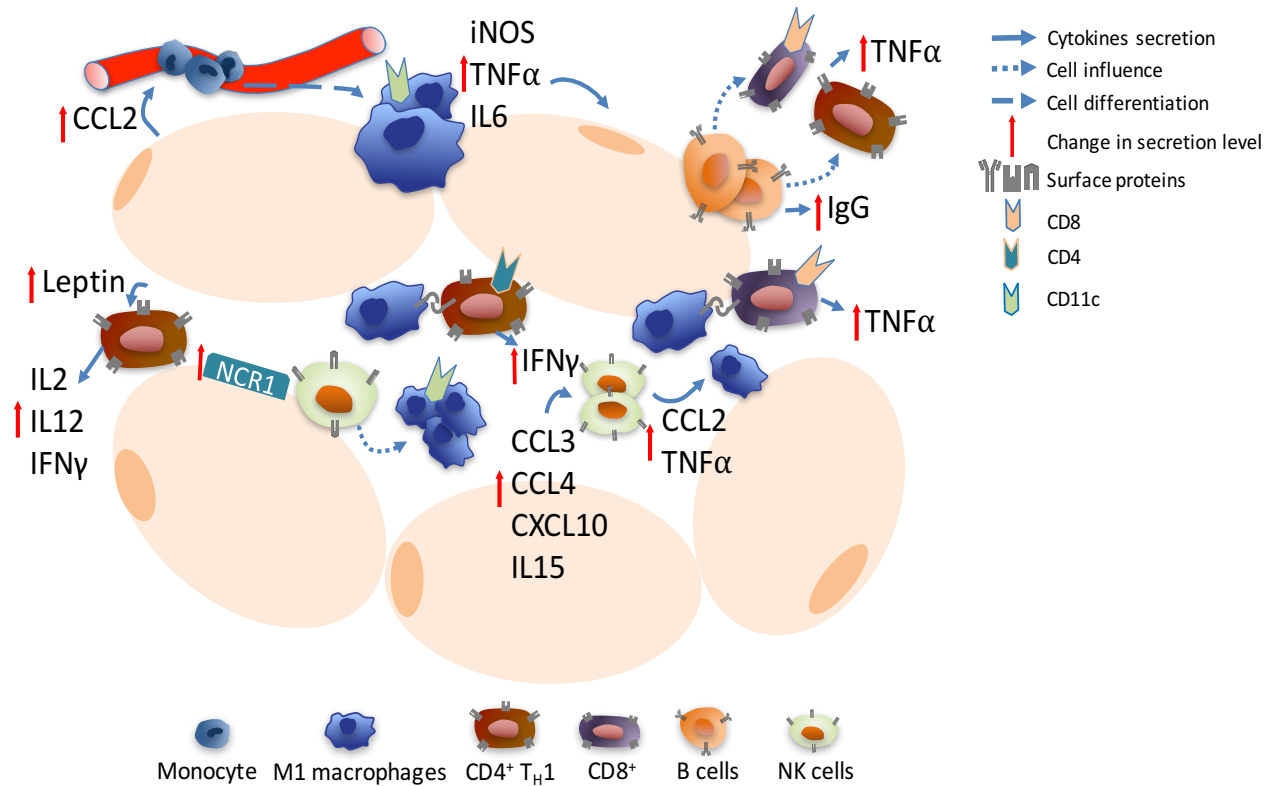


**Figure 1: Recruitment of inflammatory and immune cells in WAT.**

Upon over nutrition adipocytes secrete pro-inflammatory cytokines: CC- motif chemokine ligand 2, 3 and 4 (CCL2, CCL3, CCL4), C-X-C motif chemokine 10 (CXCL10), interleukin 15 (IL15), which induce recruitment and activation of inflammatory and immune cells. Monocytes are recruited from the circulation and are activated to become M1 macrophages producing Tumor Necrosis Factor alpha (TNFα), Interleukin 6 (IL6) and inducible Nitric Oxide Synthase (iNOS). M1 macrophages activate cells of the adaptive immune response: CD4<sup>+</sup> T helper 1 cells (T<sub>H</sub>1), CD8<sup>+</sup>, producing interferon γ (IFNγ) and TNFα; B cells, releasing immunoglobulins G (IgGs). Obese adipocytes favor the recruitment of natural killer cells (NK) through upregulation of NK cell-activating receptor (NCR1) ligand. The increased adipocyte secretion of leptin contributes to the activation of CD4<sup>+</sup> cells that worsen the inflammation via secretion of interleukin 2, 12 (IL2, IL12) and IFNγ.



### **I.1.5 Local metabolic consequences of vWAT remodeling**

Cellular and tissular damages together with the inflammation of the vWAT along obesity development have local metabolic consequences which are interconnected: a decreased insulin sensitivity and a limitation of the capacity of the vWAT to store lipids.

While chapter 4 is dedicated to insulin signaling and its perturbation upon obesity, we can here mention two specific actions in adipocytes with that respect. First, we have seen that the remodeling of the cortical actin in adipocytes impacts the insulin-dependent translocation of the glucose transporteur Glut4 to the membrane. Second, in mice, the enhanced secretion of the adipokine Resistin interferes with the normal insulin signaling by increasing the expression of the Suppressor Of Cytokine Signaling 3 (SOCS3), a known inhibitor of insulin action in adipocytes<sup>75</sup>. Other more systemic mechanisms are likely to operate and are reviewed in the chapter 4.

One paradoxical consequence of the adipose tissue remodeling and its decreased insulin sensitivity during over-nutrition is a limitation of the vWAT to further accumulate lipids. This occurs through several mechanisms. The first one is the fact that adipocytes are less sensitive to the anti-lipolytic effects of insulin. This results in a sustained lipolysis even in fed state, which augments the efflux of FFAs in the systemic circulation (Figure 2). The second fact is that pro-inflammatory cytokines produced by inflamed WAT, such as IL6 and TNF- $\alpha$ , reduce the activity of Lipoprotein Lipase (LPL)<sup>76</sup> (Figure 2), the enzyme that hydrolyzes TGs contained in Very low Density Lipoproteins (VLDLs) and chylomicrons at the surface of capillary endothelium<sup>77</sup>. This reduction thus impairs the uptake of FA into the adipose tissue for storage. Consistent with this important role in the regulation of lipid flux, LPL upregulation in the adipose tissue protects

against the ectopic accumulations of lipids by increasing the portion of FAs stored in the adipocytes with beneficial effects on obesity-induced insulin resistance<sup>78</sup>. Interestingly, scWAT maintains its ability to correctly store lipids upon HFD feeding, as demonstrated in Interferon Regulatory Factors 5 (IRF5) deficient mice<sup>79</sup>. Thus, a strategy directed at limiting vWAT expansion to the expenses of the scWAT might be beneficial for the whole body homeostasis. However, some clinical studies are reporting the observation that vWAT and scWAT have no difference in terms of adipose tissue macrophage (ATM) accumulation in severe obese patients<sup>80</sup>. This controversy may be linked to the fact that in the extreme conditions of obesity even the scWAT loses the capacity to properly store lipids, leading to the accumulation of activated ATM.

Thus, inflammation and insulin resistance are major processes that, in the early phase, take place in the vWAT upon overnutrition and obesity development. The consequences are not only local but results in a systemic low-grade inflammation and increased levels of circulating FFA that will particularly affect the liver

## **I.2 Diet-induced modifications occurring in the liver**

The liver has a central metabolic role. More specifically in the context of this review, the liver regulates metabolic homeostasis across the alternance of fed and fasting states on daily basis. In context of chronic overnutrition, the liver must cope on the one hand with the direct alteration of these homeostatic metabolic responses. On the other hand, the liver must also cope with metabolites and inflammatory signals coming from the adipose tissue as described above.

### **I.2.1 NAFLD as a result of the imbalance between uptake and export of lipid in the liver**

As clarified by the World Gastroenterology Association, NAFLD is a condition defined by excessive fat accumulation in the form of triglycerides (steatosis) in the liver. A subgroup of NAFLD patients displays liver cell injury and inflammation in addition to excessive fat (steatohepatitis), a condition designated as Non Alcoholic Steatohepatitis (NASH).

In obesity, hepatosteatosis represents the first step of NAFLD. Hepatosteatosis correlates quite well with abdominal adiposity and its incidence is showing the same positive trend as obesity. In a simplified manner, hepatosteatosis results from increased fatty acid uptake, decreased fatty acid use, and decreased export in form of VLDL. Adipose tissue-derived FFAs are the major source of hepatic fatty acids and they represent 59% of liver fat in NAFLD patients<sup>81</sup>. The increased fatty acid uptake is sustained by the increased expression of CD36 in the liver and skeletal muscle of obese patients with NAFLD compared to obese subjects with normal intra hepatic TG content<sup>82</sup>. At the same time, the down-regulation of CD36 and the enhanced lipolysis that take place in the adipose tissue, further exacerbate the flux of FFAs towards the liver and the skeletal muscle in NAFLD patients (Figure 2). The role of FFA uptake in hepatosteatosis was further corroborated

in animal model of NAFLD lacking transporters such as CD36 and FATPs, where reduction of liver fatty acid influx prevented steatosis<sup>83,84</sup>.

The remaining part of hepatic TG stores derives from dietary fatty acids and *de novo* Lipogenesis (DNL). The increase in DNL precedes the development of steatosis and is due in part to the insulin resistance of the muscle, which provokes an increased flux of ingested carbohydrates towards the liver<sup>85</sup>. Compared to healthy subjects, in patients with NAFLD the newly synthesized lipids account for a much higher percentage of the total intra-hepatic fatty acids (15-23% vs 5%)<sup>86</sup>. Highly lipogenic hepatocytes undergo a phenotypic change characterized by enhanced expression of adipogenic genes such as Sterol Regulatory Element-Binding Proteins (SREBPs), Adipose Differentiation-Related Protein (ADRP) and PPAR $\gamma$ <sup>87,88</sup>.

At the same time, oxidation of fatty acids in the liver is reduced, contributing to their consequent accumulation in the liver. More particularly, the expression of the nuclear receptor PPAR $\alpha$ <sup>89</sup> is blunted, resulting in a reduction of fatty acid transport to the mitochondria, via reduction of Carnitine Palmitoyl Transferase 1 (CPT1) expression, and decreased fatty acid  $\beta$ -oxidation. Reciprocally, liver specific deletion of PPAR $\alpha$  also caused the development of hepatic steatosis in ageing in mice fed a standard diet<sup>90</sup>. Finally, the TG outflow rate through VLDL contributes to the maintenance of hepatosteatois. Although subjects with NAFLD have greater VLDL secretion than those with normal intrahepatic TG content, this secretion does not increase linearly with the increasing TG amount but rather reaches a plateau. Therefore, the increase in VLDL secretion rate, in NAFLD patients, is not able to compensate for the increased rate of TG accumulation<sup>91</sup>.

Hepatosteatois *per se* is not necessarily deleterious, and may remain clinically silent, i.e. the metabolic functions of the liver are unaffected by the “simple” accumulation of lipids. However, in a number of cases, which in human reach one-third<sup>92</sup> of the NAFLD patients, complications

can ultimately lead to NASH, where inflammation and fibrosis are severely altering liver functions

### **I.2.2 From NAFLD to NASH: the role of inflammation in the liver in obesity and overnutrition**

A prolonged over-nutrition condition triggers in some case the progression of NAFLD from the simple hepatosteatosis to the development of inflammation, fibrosis and NASH<sup>93</sup>. A “multi-hit” hypothesis is presently widely accepted to explain this evolution. As described above, liver lipid accumulation and insulin resistance (see also chapter I.4) appears early in NAFLD and worsens steatosis as a result of increased DNL. These alterations expose the liver to “multi-hits”, which include mitochondrial dysfunction, oxidative damage, altered hepatocyte apoptosis, increased levels of fibrogenic and pro-inflammatory mediators and activation of stellate and Kupffer cells<sup>89</sup>. We will focus below on the inflammatory process, which is a main contributor to the worsening of the liver status.

The inflammatory response of the liver parallels the increase in hepatic lipid accumulation and the development of obesity. Hepatic inflammatory mediators include C-Reactive Protein (CRP), PAI-1, fibrinogen and IL-6, which mark the presence of a “subacute inflammation” in the liver<sup>94</sup>. However, as for the adipose tissue, the immune cells are the major contributors of liver inflammation.

Two different populations of macrophages mainly drive the inflammatory response in liver: the resident macrophages, known as Kupffer cells, and the recruited macrophages, which migrate

into the liver during obesity<sup>95</sup>. Kupffer cells derive from embryonic progenitors of the yolk sac and are found in the liver sinusoids in close proximity with sinusoidal endothelial cells<sup>96</sup>, where they protect against pathogenic compounds. However, their activation, induced by toxic lipid droplets present in the liver, seems to represent the “first hit” of NAFLD/NASH pathogenesis<sup>97</sup>. Activated Kupffer cells further enhance hepatic inflammation via the secretion of monocyte chemoattractant CCL2<sup>98</sup>, which triggers the recruitment and activation of monocytes from the bloodstream. These monocytes are able to infiltrate the liver as a result of liver injury and to differentiate into pro-inflammatory M1 macrophages<sup>99</sup>. The primary role of Kupffer cells is supported by the fact that their depletion, using clodronate injections, results in improved liver steatosis and insulin resistance<sup>100</sup>.

However, liver inflammation is also sustained by other immune cells that entertain complex cross-regulation and activation with Kupffer cells and macrophages<sup>101</sup>. Dendritic cells are antigen presenting cells that participate to the innate immune defense in the liver and provide support to macrophages. NK cells are the major lymphocyte population in the liver, representing 30-50% of total lymphocytes<sup>102</sup>. NKs as well as T cells are not contributing to the steady-state condition of the liver but are extremely important during the inflammatory response. Activated Kupffer cells are responsible for the stimulation of these cells through a signaling pathway initiated by TLRs. TLR2 or 3 induce Kupffer cells secretion of IL18 and IL1 $\beta$ , thus activating NK cells<sup>103</sup>, while TLR4 is responsible for the upregulation of adhesion molecules such as ICAM1 and VCAM on Kupffer cells and hepatic stellate cells, which are then mediating T cell trapping and activation<sup>104</sup>. In addition, neutrophils are polymorphonuclear leukocytes important in sustaining the liver inflammation process. Hepatic infiltration of neutrophils is an acute response to liver injury, hepatic stress or systemic inflammatory signals<sup>105</sup> that aggravates the

inflammatory reaction by the secretion of cytotoxic reactive oxygen and nitrogen species or of pro-inflammatory cytokines such as IL1 $\beta$  and TNF<sup>106</sup>. Neutrophil dysfunction is also associated with the development of liver fibrosis and cirrhosis in NASH. Indeed, the neutrophil-to-lymphocyte ratio is higher in patients with NASH and advanced fibrosis, and has been proposed as a non-invasive marker to predict advanced liver disease<sup>107</sup>.

Chronic liver inflammation is also associated with tissue damage and remodeling as well as fibrosis<sup>108</sup>. Hepatic macrophages are able to induce differentiation of hepatic stellate cells, the primary cells involved in liver fibrosis, into myo-fibroblasts and to promote their survival with the secretion of TNF and IL1<sup>109</sup>. The establishment of a modified microenvironment, where inflammation and fibrosis coexist enhancing liver injury, is thought to be at the base of the progression of liver steatosis to NASH.

### **I.2.3 The Adipose Tissue-Liver crosstalk in metaflammation**

As described above, there are two main processes that start in the adipose tissue and have an impact on the liver environment: the development of systemic low-grade inflammation in obesity, and the increase afflux of FFAs to the liver due to increased lipolysis, together with the inhibition of LPL activity. The importance of WAT lipolysis was also recently highlighted by the efficiency of the pharmacological inhibition of the adipose triglyceride lipase in decreasing insulin resistance and hepatosteatosis in mice<sup>110</sup>.

In addition to this metabolic regulation, adipose tissue-derived adipokines and pro-inflammatory cytokines can directly act on liver metabolism and the development of NAFLD<sup>111</sup>. Adiponectin, for example, has a protective role in the progression of hepatic steatosis to fibrosis and NASH. In

the model of diet-induced obesity in rats, adiponectin overexpression stimulates hepatic  $\beta$ -oxidation and protects the liver from steatosis and inflammation, thus improving insulin sensitivity<sup>112</sup>. Indeed, adiponectin inhibits hepatic DNL and gluconeogenesis by reducing the expression of the lipogenic transcription factor SREBP1-c and the rate limiting enzyme Phosphoenolpyruvate Carboxy-Kinase (PEPCK), respectively<sup>113</sup>. In addition, adiponectin improves glucose utilization by activating an Adenosine Monophosphate-Activated Protein Kinase (AMPK-dependent pathway)<sup>114</sup>. In agreement with mouse studies, adiponectin levels are reduced in patients with NAFLD<sup>115</sup> and negatively correlate with liver alanine aminotransferase and  $\gamma$ -glutamyltranspeptidase<sup>116</sup>, which are indicators of liver lesions.

Leptin, on the other hand, negatively influences the onset and the progression of NAFLD, being positively correlated with serum level of Alanine Aminotransferase (ALT) in humans<sup>117</sup>. Moreover, it acts as pro-fibrogenic mediator by stimulating the production of  $\alpha$ -Smooth Muscle Actin ( $\alpha$ -SMA), collagen 1 and the Tissue inhibitor of Metallo-Proteinase 1 (TIMP1) in human stellate cells<sup>118</sup>. However, it has been shown that leptin produced by the adipose tissue has an insulin sensitizer effect in the liver and skeletal muscle with regularization of pancreatic  $\beta$ -cell activity<sup>119</sup>. TNF- $\alpha$  and IL-6 also correlated with the progression of NAFLD to NASH and with the onset of insulin resistance by increasing the production of SOCS3 in the liver<sup>120</sup>.



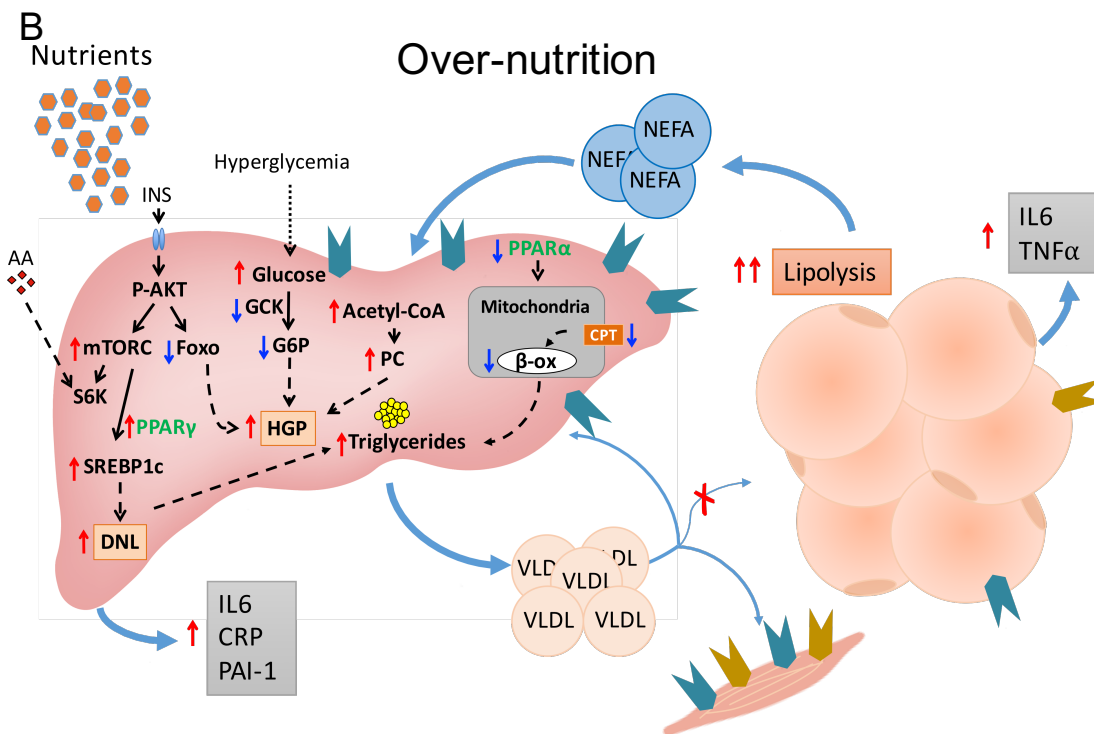
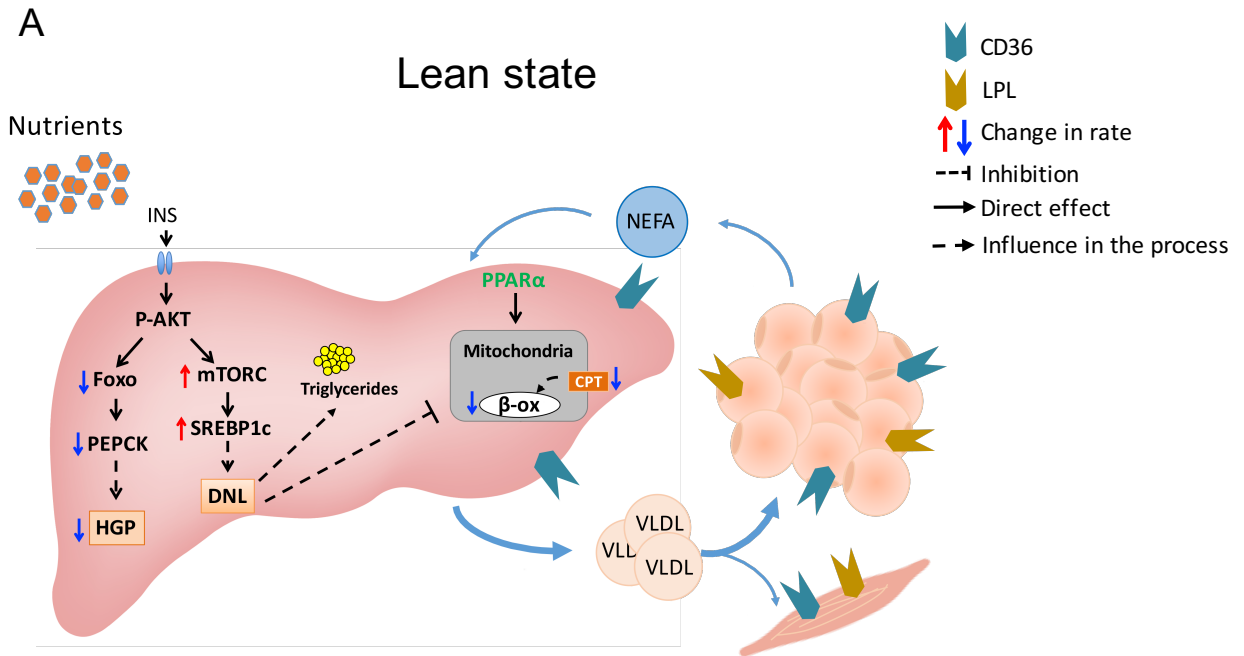


**Figure 2:** Liver-adipose tissue crosstalk in lean and over-nutrition state.

**(A).** Lean state. Insulin signaling in the liver induces phosphorylation of the protein kinase AKT. AKT-dependent downregulation of forkhead box (Foxo) transcription factor reduces the transcription of gluconeogenic genes, such as PhosphoEnolPyruvate CarboxyKinase (PEPCK), and hepatic glucose production (HGP). AKT-dependent upregulation of the mammalian target of rapamycin complex (mTORC) upregulates Sterol Regulatory Element-Binding Protein 1c (SREBP1c) thus inducing de novo lipogenesis (DNL) and triglyceride (TG) synthesis. DNL inhibits both the transport of fatty acids in the mitochondria via carnitine palmitoyl transferase carrier (CPT) and the  $\beta$ -oxydation ( $\beta$ -ox), which is controlled by peroxisome proliferator-activated receptors  $\alpha$  (PPAR $\alpha$ ). Hepatic TGs are secreted in the circulation in form of very low density lipoproteins (VLDLs) to reach muscle and adipose tissue where they are uptaken, through the action of CD36 and lipoprotein lipase (LPL). In adipose tissue, insulin inhibits the release of non-esterified fatty acids (NEFAs).

**(B).** Over-nutrition. In obesity, hepatic DNL and HGP are both active. PPAR $\gamma$  is upregulated in hepatosteatosis, further inducing DNL and hepatic TG content. Aminoacids (AA) derived from the diet influence mTORC/S6 kinase (S6K) pathway that through an inter-tissue connection affects LPL activity in the adipose tissue and thus increases circulating TGs. Hepatic VLDL secretion increases, but their uptake by adipose tissue is reduced because of the low expression of CD36 and LPL. Conversely, CD36 and LPL are more expressed in muscles and liver that therefore internalize more VLDLs. HGP upregulation is due to different processes: 1) lower utilization of glucose due to reduced glucokinase (GCK) activity, 2) Increased adipose tissue lipolysis due to insulin resistance and consequent increase in the releasing of NEFAs in the circulation. Hepatic acetyl-CoA content and pyruvate carboxylase (PC) activity increase, with consequent higher transformation of pyruvate into glucose. In obesity, both liver and adipose tissue undergo an inflammatory response with production of pro-inflammatory cytokines: Interleukin 6 (IL6), Tumor Necrosis Factor alpha (TNF- $\alpha$ ), C-reactive protein (CRP), plasminogen activator inhibitor 1 (PAI-1).

Finally, the adipose tissue-derived FFAs may directly act as signaling molecules in the liver via interacting with the transcription factor PPAR $\alpha$ , triggering the expression of its target genes and more particularly Fibroblast Growth Factor 21 (FGF21)<sup>121,122</sup>. In turn, FGF21 is part of the reciprocal cross-talk from the liver to the adipose tissue. It is produced mainly by the liver in the fasted state, and has a direct effect on adipose tissue, stimulating both lipolysis and the expression of adiponectin<sup>123</sup>. This signaling to adipose tissue is required for FGF21 activity on increasing insulin sensitivity. However, it also has adipose tissue independent activity, more particularly on increasing energy expenditure<sup>124</sup>. It is considered as a good candidate for the treatment of T2D and metabolic syndrome primarily for its ability to reduce plasma TGs in rodents and humans<sup>125,126</sup>. FGF21 would act via reducing VLDL secretion in the liver and re-directing TG-rich lipoproteins towards WAT, via increased activity of CD36 and LPL in this tissue<sup>127</sup>. Other hepatokines might be discovered, since a systematic analyses of the secretome of steatotic hepatocytes identified 32 hepatokines differentially secreted by steatotic versus non-steatotic hepatocytes. Among them, Fetuin B is increased in patients with hepatosteatosis, and its silencing in mice improved glucose tolerance<sup>128</sup>.

### **I.3 Linking metabolism and inflammation: insulin sensitivity as the central piece**

With the onset of T2D, obese patients display an array of metabolic alterations including hyperinsulinemia, hyperglycemia and hypertriglyceridemia. High levels of insulin are not able to lower the glycemia: thus the name of insulin resistance. This insulin signaling has been at best studied in the liver, but resistance appears in all metabolic tissues, particularly the adipose tissue, which will be discussed herein in light of their links to metaflammation.

#### **I.3.1 Insulin signaling in the liver and pathways to insulin resistance in the context of obesity.**

Insulin signaling has been extensively studied. Briefly, in terms of processes, the peak of insulin in the postprandial period drives both a reduction of hepatic glucose production (HGP), and an increase in the rate of lipid production via DNL. In insulin resistant liver, the insulin-dependent activation in DNL is maintained, but there is a failure in decreasing glucose production, a process known as “selective hepatic insulin resistance”<sup>129</sup> (Figure 2).

In this context, the observation by Lu et al. that mice lacking Akt1, Akt2 and forkhead box transcription factor 1 (Foxo1) do not show any defect in insulin-mediated suppression of gluconeogenesis<sup>130</sup>, raised the question whether other mediators could have a role in the postprandial reduction of HGP mediated by insulin<sup>131</sup>. The idea that an inter-tissue connection could participate in regulating this metabolic process comes from the observation that the insulin-dependent suppression of HGP is occurring even in mice with liver specific ablation of insulin

receptor<sup>132</sup>. Subsequently, Perry and colleagues<sup>133</sup> demonstrated that HGP is highly sensitive to hepatic acetyl-CoA, whose concentration depends on the levels of circulating FFAs. When insulin fails to suppress lipolysis in adipose tissue, the high FFA flux to the liver determines a rise in the levels of hepatic acetyl-CoA, which, in turn, maintain high the pyruvate carboxylase activity and the conversion of pyruvate into glucose (Figure 2). The critical role of FFAs in the regulation of HGP in obesity-related insulin resistance was also pointed by Titchenell et al<sup>134</sup>. These authors suggested that, in fact, insulin action in the liver directly controls only hepatic lipogenesis, while HGP is regulated by insulin in an indirect way through the modulation of the levels of circulating FFAs. Both these reports thus highlighted the key role of FFAs as mediators of the tight connection between liver and adipose tissue in the regulation of HGP in insulin resistant mice. It must be noted however that recent studies highlighted some contexts in which hepatic lipid production is necessary and even beneficial. More particularly, the accumulation of mono-unsaturated fatty acids such as oleate rather than poly- and unsaturated fatty acids, seems rather protective against insulin resistance and glucose intolerance<sup>121,135</sup>.

Finally, an additional level of complexity comes from the role of amino acids, which in obesity can activate the Mammalian Target Of Rapamycin Complex 1/ S6 Kinase (mTORC1/S6K) signaling pathway<sup>136</sup>. This signal then activates an inter-tissue neuronal pathway acting on the adipose tissue that results in a reduction of LPL activity and consequent elevation in serum TGs<sup>137</sup>.

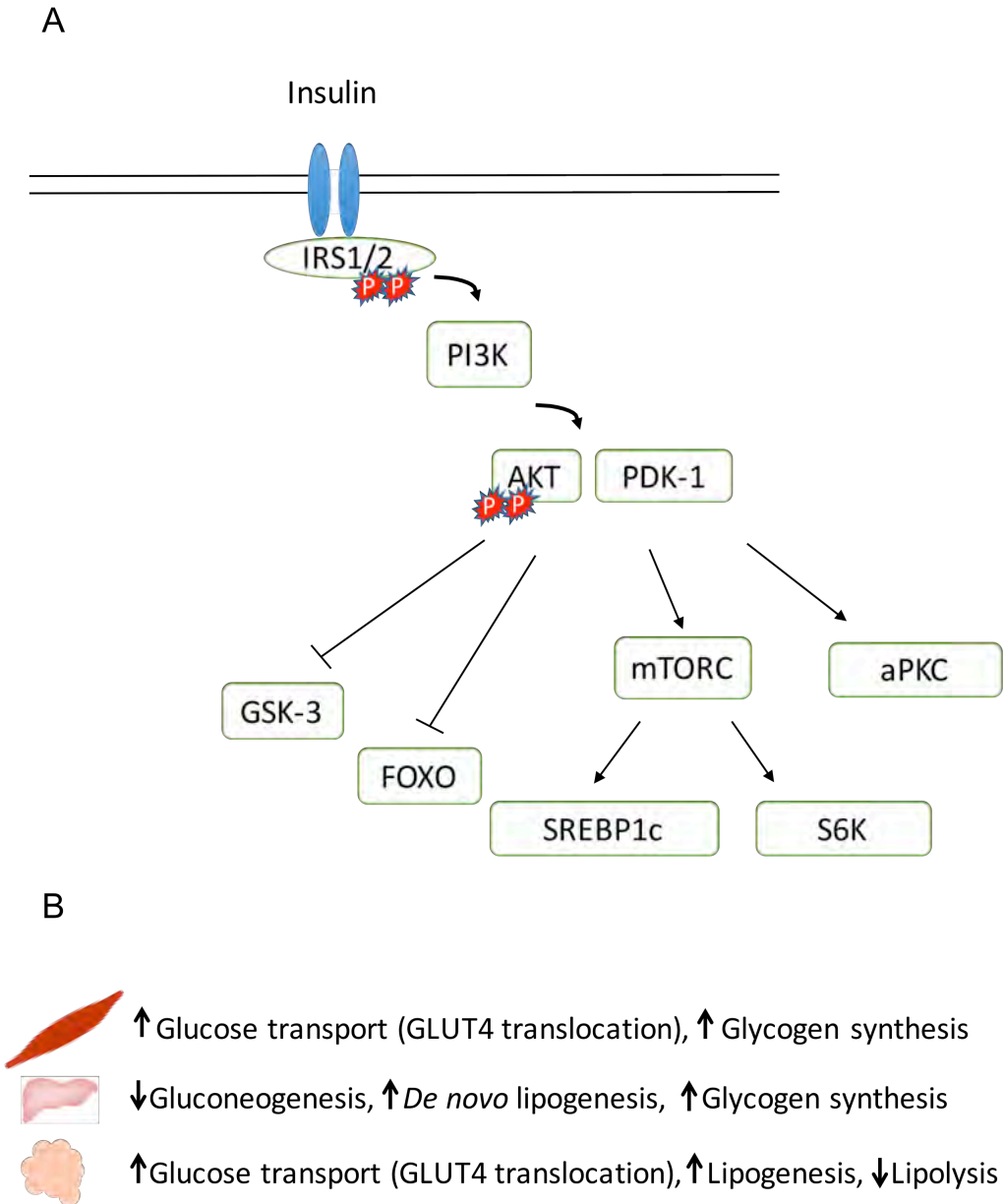


**Figure 3: Insulin signalling pathway.**

*A. The interaction of insulin with the membrane Insulin Receptor (IR) and Insulin Receptor Substrate 1 and 2 (IRS1/IRS2) are represented. The activation of the Phosphatidylinositol 3-Kinase (PI3K) mediates the action of insulin on intermediary metabolism, via activation of AKT. PI3K-dependent activation of Sterol Regulatory Element-Binding Protein 1c (SREBP1c) and S6 Kinase (S6K) is mediated by the mammalian target of rapamycin complex 1 (mTORC1). In contrast, AKT activation inhibits the activity of Glycogen Synthase Kinase 3 (GSK-3) and the Forkhead box (FOXO) transcription factors, mainly resulting in the inhibition of the activity and transcription of downstream target. Other consequences of PI3K/AKT activation are the activation of the atypical Protein Kinase C (aPKC), which is responsible for the glucose transport in muscles and adipose tissue.*

### **I.3.2 Molecular pathways that link inflammation and insulin resistance**

The link between inflammation and the onset of insulin resistance in obese patients remained obscure until the hypoglycemic effects of salicylates were re-investigated, leading to the identification of the Inhibitor of Nuclear Factor  $\kappa$ B (I $\kappa$ B) kinase  $\beta$  (IKK $\beta$ )/ NF $\kappa$ B axis as their molecular target<sup>138</sup>. Concomitantly, increased adiposity and dysregulation of lipid metabolism were shown to correlate with the activation of a diverse range of stress-responsive pathways including the Jun N-terminal Kinases (JNK), IKK $\beta$ , and inflammasome, which are important mediators of the inflammatory response.

JNKs are members of the Mitogen-Activated Protein Kinases (MAPK) family, which are induced in response to cellular stress signals<sup>139</sup> and are able to phosphorylate and activate the protein cJun, a member of the Activator Protein-1 (AP-1) transcription factor family. Their role in the induction of insulin resistance has been largely studied in the past and several mechanisms are proposed to explain how JNKs can induce insulin resistance in response to excess of adiposity. First, JNKs are responsible for the phosphorylation of Irs1 in serine-307, inhibiting the interaction of Irs1 with the insulin receptor<sup>140</sup>, whose signaling is normally occurring through the counter-regulatory serine/threonine phosphorylation. Second, JNK1 and 2 are proposed as key mediators in macrophages to allow their recruitment and activation in the obese vWAT. Mice lacking JNK1/2 specifically in myeloid cells are largely protected from the inflammation associated to diet-induced obesity, with less severe insulin resistance, decreased accumulation of macrophages and a relative lower expression of M1-specific cytokines<sup>141</sup>. Finally, JNKs have a role in the reduction of FA oxidation and in the onset of steatosis and insulin resistance in the

liver, mainly acting as a negative regulator of PPAR $\alpha$  activity and FGF21 expression in hepatocytes, via the activation of the Nuclear Receptor Co-Repressor (NCoR1) complex<sup>142</sup>.

IKK $\beta$  is another inflammatory kinase playing a critical role in the onset of insulin resistance. Its activity is highly selective toward its physiological substrates, the I $\kappa$ B protein inhibitors of NF $\kappa$ B. Phosphorylation by IKK $\beta$  directs I $\kappa$ B $\alpha$  to proteasomal degradation, thus allowing the release of NF $\kappa$ B, a master transcriptional regulator of inflammation. Once delivered from its complex with I $\kappa$ B $\alpha$ , NF $\kappa$ B translocates into the nucleus, where it affects the expression of numerous target genes involved in insulin resistance<sup>143,144</sup>. It has been shown that NF $\kappa$ B is activated in the liver of mice fed a high fat diet, whereas a reduction of its activity or an increased expression of IKK $\beta$  significantly improve glucose and lipid metabolism<sup>143,145</sup>.

As described above, IRS1, the first transducer of insulin signaling, can be phosphorylated by JNKs. Besides this regulation, IRS1 is also the target of other kinases such as RNA-activated Protein Kinase (PKR), Extracellular signal-Regulated Kinase (ERK), Protein Kinase C $\theta$  (PKC $\theta$ ), mTOR and SOCS, whose activity is influenced by the inflammatory status. Thus, insulin signaling is sensitive to the antagonizing effects of multiple mediators belonging to different cellular pathways related to the inflammatory response. Further highlighting this interference, inflammatory kinases also counteract insulin sensitivity by directly activating transcription factors such as the AP-1, NF $\kappa$ B and Interferon Regulatory Factors (IRFs) and thus modulating the expression of genes important in inflammation but also in glucose, cholesterol metabolism and fatty acid synthesis<sup>146</sup>, as detailed below.

Many of the pro-inflammatory cytokines and adipokines that are produced in obese vWAT, including TNF- $\alpha$ , IL6, IL1b and resistin, were shown to modulate the activation of the stress-



response kinase JNK and IKK $\beta$ . Therefore, a feed-forward loop arises in obesity, where increased adiposity induces the production of pro-inflammatory cytokines, which, in turn, activate cellular signaling pathways leading to the onset of insulin resistance.

TNF- $\alpha$  was the first adipose tissue-secreted cytokine directly linking inflammation and insulin resistance<sup>21</sup>. It exerts its action on the adipose tissue by enhancing adipocyte lipolysis and increasing Irs1 serine phosphorylation through a mechanism dependent on the activation of JNK1/2 in visceral adipose tissue<sup>147</sup>. TNF- $\alpha$  levels are increased in the adipose tissue and in the plasma of obese individuals<sup>28</sup>, where it correlates with markers of insulin resistance<sup>29</sup>. Moreover, mouse models of genetic loss-of-function for TNF- $\alpha$ , TNF Receptors 1/2, JNKs, are all protected when challenged with high fat diet<sup>148,149</sup>. However, the use of TNF- $\alpha$  as target to treat insulin resistance in diabetic patients did not turn to be successful. Clinical trials using short and long-term administration of TNF- $\alpha$  antagonists were able to reduce systemic inflammatory markers but showed poor effects on insulin resistance<sup>150-152</sup>.

IL6 is a pro-inflammatory cytokine produced mainly by the adipose tissue that is thought to play a role in the onset of insulin resistance. This action would be mediated by IL6-induced reduction in GLUT4 and Irs1 expression levels through the activation of the JACK-STAT signaling pathway and the increased expression of SOCS3<sup>153</sup>. However, the direct link between IL6 and obesity-induced insulin resistance is controversial. On the one hand, it is thought to suppress insulin ability to modulate gluconeogenesis in liver and this was demonstrated both in mice<sup>154</sup> and *in vitro*, using HepG2 human cell line<sup>155</sup>. On the other hand, IL6 deficiency worsens hepatic insulin resistance and inflammation in a mouse model of diet induced obesity<sup>156</sup>. These contradictory results on IL6 role in insulin resistance can be in part explained by its multiple

action in different organs (i.e. skeletal muscle or liver) and in part by its different sources (i.e. muscle and adipose tissue).

The action of IL18 is also debated in the literature with negative effects on insulin sensitivity reported in a rat model of metabolic syndrome<sup>157</sup>, whereas, IL18 deficient mice show hyperphagia, obesity and insulin resistance<sup>158</sup>.

Finally, the adipokine resistin was initially reported as major player in insulin resistance, thus its name. Mice lacking resistin are protected from diet-induced hyperglycaemia, due to AMPK increased activity and reduced expression of gluconeogenic genes<sup>159</sup>. However, in humans, the role of resistin is less clear and quite debated, with reports showing a positive association between resistin levels and the development of obesity, insulin resistance and T2D<sup>160</sup> and others refuting any kind of association with the development of metabolic syndrome<sup>161,162</sup>. One of the possible explanations of the difference between mice and human is the different pattern of resistin expression, which, in mice, is totally restricted to adipocytes, whereas in humans is exclusively observed in macrophages and monocytes<sup>163,164</sup>.

### **I.3.3 Lipid mediators of insulin resistance**

The altered lipid flux that prevails in obesity has been associated to insulin-resistant states, being both the cause and the result of insulin resistance. Circulating fatty acids can impair insulin signaling mainly in two ways.

On the one hand fatty acids can interfere with the downstream pathways of insulin binding<sup>165</sup>, via the interaction of long saturated fatty acids, such as palmitate, with the receptors TLR2, TLR4 and Nucleotide-binding oligomerization domain, Leucine rich Repeat (NLR)-and Pyrin domain containing 3 (NLRP3)<sup>166,167</sup>. Upon ligand binding, TLRs triggers a signaling cascade that leads to

the activation of IKK $\beta$  and mitogen activated protein kinases (MAPKs) such as p38, JNK and ERK1/2. In parallel, NLRP3 can be activated by host-derived molecules, including excess ATP, glucose, ceramides, reactive oxygen species, that are abundant in obese individuals. NLRP3 activation initiates the assembly of the inflammasome, a large multiprotein complex which governs the maturation of the proinflammatory cytokines IL-1 $\beta$  and IL-18<sup>168-170</sup>. The key role of this complex in the obesity-induced adipose tissue inflammatory response has been demonstrated by the blunted response to ceramide of macrophages derived from the adipose tissue of Nlrp3 knockout mice, which display a reduction of macrophage M1 polarization of in the fat tissue<sup>170</sup>.

All these multiple pathways activated by overnutrition converge onto the stimulation of the major inflammatory kinases JNK and IKK $\beta$ , which, as described above, interfere with insulin signal transduction.

On the other hand, the accumulation of intracellular lipid products, such as diacylglycerols (DAG) and ceramides can directly be the cause of insulin resistance. This last mechanism raises the concept of lipotoxicity, as referred to the ability of excessive lipids to contribute to the pathophysiology of metabolic syndrome and T2D<sup>171</sup>. Once entered in the cell, fatty acids are rapidly esterified with coenzyme A to form acyl-CoAs. These intermediates are then transferred to a glycerol backbone to form mono-, di- and triacylglycerols. In the liver, the link between DAG accumulation and insulin resistance is attributed to the activation of Protein Kinase C $\epsilon$  (PKC $\epsilon$ )<sup>172</sup>, which binds and inhibits insulin receptor kinase activity. By knocking down the hepatic PKC $\epsilon$  expression using specific antisense oligonucleotides, Samuel *et al.* were able to protect rats from lipid induced hepatic insulin resistance, independently of the increased hepatic lipid levels<sup>173</sup>.

Ceramides represent another class of fatty acid derivatives whose intracellular levels are strongly associated with insulin resistance<sup>174,175</sup>. Their biosynthesis occurs through the condensation of saturated fatty acids (preferentially palmitate) with amino acids (preferentially serine) to form 3-ketosphingamine, the scaffold for all sphingolipids. The sphingoid backbone subsequently acquires additional fatty acids leading to the production of a series of sphingolipids that include ceramides and other more complex products<sup>176</sup>. Inhibition of ceramide production through the administration of myriocin, a potent inhibitor of Serine Palmitoyl-Transferase (SPTLC), prevents the development of insulin resistance and diabetes in obese mice<sup>177,178</sup>. This insulin sensitizing effect is mediated by a reduction of the circulating levels of leptin and a concomitant increase of adiponectin and FGF21. A decreased of ceramide production was also observed in mice carrying an intestinal-specific Farnesoid X Receptor (*Fxr*) gene deletion and resulted in a down-regulation of hepatic SREBP1c and decreased *de novo* lipogenesis<sup>179</sup>. Further supporting the beneficial effect of the hampering of ceramide production, myriocin administration, as well as *Sptlc2* ablation specifically in adipose tissue, induces macrophage M2 polarization, most prominently in the scWAT, with concomitant increase of serum anti-inflammatory cytokine IL10 and reduction of pro-inflammatory cytokines IL6, MCP1, and TNF- $\alpha$ <sup>180</sup>. Conversely, elevated intracellular ceramide levels have been shown to stimulate the ability of phosphatase 2A to dephosphorylate AKT, thus interfering with insulin signaling<sup>175</sup>. Notably, both saturated fatty acids and TNF- $\alpha$  induce SPTLC expression, and the subsequent production of ceramide, via activation of TLR4<sup>174,181</sup> and their action is mediated by IKK $\beta$ . In the case of the TNF $\alpha$ -mediated cascade, this is an emblematic example of how an inflammatory stimulus can promote the production of lipid intermediates, which, in turn, impairs insulin action.

Lastly, a compelling body of evidence has accumulated in recent years showing how intracellular fluctuations of several metabolites, as a function of the metabolic status, may influence the activity of chromatin regulators. The resulting epigenetic changes at the level of DNA and histone modifications have a major influence on the control of gene transcription during embryonic development as well as in the differentiated tissues of the adult organism.

Example of metabolites influencing chromatin-modifying enzymes include acetyl-CoA, which is the universal donor for acetylation reactions,<sup>182</sup> and S-adenosylmethionine, which acts as a methyl donor substrate stimulating DNA methyltransferase reactions<sup>183</sup>. The crosstalk between metabolites and epigenetic regulation is described in detail elsewhere<sup>184</sup>.

#### **I.4 Metaflammation and specific aspects of PPARs**

Peroxisome proliferator-activated receptors (PPARs) are nuclear receptors that function as ligand-activated transcriptional regulators, with both activation and repression mechanisms, depending on the condition/target. Three PPAR isoforms exist, PPAR $\alpha$ , PPAR $\beta/\delta$  and PPAR $\gamma$ , which are characterized by distinct functions and expression patterns. Their peculiar role in the regulation of glucose and lipid metabolism and inflammation puts PPARs at the crossroad of many molecular pathways involved in metaflammation development. This paragraph will mainly consider PPAR activity in the adipose tissue and the liver, the tissue focus of this review, and their potential use as therapeutic target for the treatment of obesity<sup>185,186</sup>

PPAR $\alpha$  has a crucial role in regulating hepatic fatty acid catabolism and clearance, as demonstrated by its target genes such as CPT1, Carnitine Acycarnitine Translocase (SLC25A20), Medium-chain Acyl-CoA Dehydrogenase (ACADM), Acyl-CoA Oxidase 1 (ACOX1), that

globally induce fatty acid oxidation<sup>187</sup>. In addition, PPAR $\alpha$  enhances the expression of the FGF21, a secreted factor that further stimulates hepatic fatty acid utilization, but that also improves systemic insulin sensitivity through its extra-hepatic enhancement of glucose transporter 1 expression<sup>125,188</sup>. PPAR $\alpha$  displays also anti-inflammatory activity, by interfering with NF $\kappa$ B activation<sup>189</sup>. Altogether, these features make PPAR $\alpha$  an interesting therapeutic target for obesity, particularly in presence of hepatosteatosis. Selective PPAR $\alpha$ -agonists, such as fibrates were efficiently used for decades in hyperlipidemic patients to lower plasma triglycerides<sup>190</sup>. However, and despite encouraging results obtained in mouse models of NAFLD, these molecules did not prove advantageous in the treatment of NAFLD/NASH in humans, likely due to their lower potency in humans, compared to mice<sup>191</sup> (reviewed in<sup>191</sup>). Furthermore, a number of side effects (i.e. increased risk of acute kidney injury, rhabdomyolysis and gallstone formation) were associated to their long-lasting use<sup>192</sup>.

Another key positive modulator of FA oxidation, particularly in skeletal muscle, is PPAR $\beta/\delta$ . However, in the liver, FA oxidation is mainly under the control of PPAR $\alpha$ , while PPAR $\beta/\delta$  selective activation suppresses hepatic gluconeogenesis, enhances carbohydrate catabolism<sup>193</sup>, and has anti-inflammatory effects in the liver by dampening Kupffer cell activation<sup>194</sup>. In the adipose tissue, PPAR $\beta/\delta$  inhibits FFA release. While the selective PPAR $\beta/\delta$  ligand GW501516 was discontinued from clinical trials for favoring tumor development in several organs, KD3010<sup>195</sup> is currently in phase III clinical trial for the treatment of obesity, NASH and T2D. A detailed description of other PPAR $\beta/\delta$  agonist can be found elsewhere<sup>196</sup>.

In the adipose tissue, PPAR $\gamma$  is the master regulator of adipogenesis<sup>197</sup> and its activation with Thiazolidinediones (TZDs) leads to *de novo* differentiation of adipocytes. TZDs are potent insulin sensitizer agents, but their clinical use in the last years has been strongly limited due the

associated risk of increased body weight, bone fractures, congestive heart failure and bladder cancer<sup>198,199</sup>. In humans, PPAR $\gamma$  activation triggers apoptosis of large fat cells in vWAT and scWAT and induces differentiation of pre-adipocytes only in scWAT<sup>200</sup>, thus favoring scWAT adiposity<sup>201</sup>. The formation of new adipocytes with the activation of genes such as Fatty-Acids Binding-Protein 4 (FABP4), CD36, LPL Fatty Acids Transporter (FATP1) and SREBP1<sup>202</sup>, improves the uptake and storage of plasmatic FFAs in AT, with the subsequent reduction of circulating TGs and of lipotoxic accumulation in non-storage specialized tissues, such as liver and muscles<sup>203</sup>. TZDs also enhance FFA mobilization upon fasting and ameliorate the postprandial suppression of FFA release triggered by insulin<sup>204</sup>. Interestingly, chronic treatment of human adipocytes with TZDs initiates a “browning program” characterized by induction of Uncoupling Protein 1 (Ucp1)<sup>205,206</sup> and of several components of the mitochondrial transport chain<sup>207</sup>, thus initiating a tissue remodeling program that is considered as a promising way to combat obesity through consumption of lipids to produce heat.

Besides their effects on adipogenesis, PPAR $\gamma$  agonists also promote the expression of components of the insulin signaling pathway, including the IRS2 and CAP<sup>208,209</sup>, that contributes to enhance adipocyte insulin sensitivity. In addition, PPAR $\gamma$  activation restores the expression and secretion levels of different adipokines such as adiponectin, resistin<sup>210</sup>, IL6, TNF- $\alpha$ <sup>211</sup>, PAI-1, MCP1 and angiotensinogen<sup>212</sup> that are altered in obesity. Thus, TZDs display also beneficial effects on the development of adipose tissue inflammation upon chronic over nutrition. Importantly, such anti-inflammatory properties of PPAR $\gamma$  agonists are the result of their action not only in adipocytes, but also in all the PPAR $\gamma$ -expressing immune cells residing in adipose tissue. In macrophages, PPAR $\gamma$  acts as negative regulator of classical pro-inflammatory M1 polarization<sup>213</sup> and promotes the shift towards the alternative M2 macrophage activation in

response to IL4<sup>214</sup>, thus reducing the expression of inflammatory markers such as Metallopeptidase Domain-8 (ADAM8), Macrophage Inflammatory Protein 1 $\alpha$  (MIP-1 $\alpha$ ), Macrophage Antigen 1 (MAC-1), F4/80 and CD68<sup>215</sup>. In M2 macrophages PPAR $\gamma$  is required to induce  $\beta$ -oxidation and mitochondrial biogenesis<sup>216</sup> as well as expression of Arginase 1(Arg1), a specific M2 marker. In obesity, PPAR $\gamma$  has been proposed to play a crucial anti-inflammatory role in the so-called metabolically activated macrophages in the adipose tissue<sup>65</sup>. Consistently, mice lacking PPAR $\gamma$  in myeloid cells when challenged with a high fat diet are more prone to develop obesity and insulin resistance, mainly due to mitochondrial dysfunction and altered glucose disposal in adipose tissue<sup>216,217</sup>.

More recently, PPAR $\gamma$  has been shown to play a role also in regulating the accumulation of T<sub>reg</sub> cells in vWAT. T<sub>reg</sub> specific PPAR $\gamma$  ablation reduces the population of vWAT T<sub>reg</sub> cells on normal chow diet, while injection of PPAR $\gamma$  agonist into HFD treated mice specifically induces an expansion of T<sub>reg</sub> population in adipose tissue<sup>218</sup>, with beneficial consequences on the tissue inflammatory pattern.

One special note must be made about hepatic PPAR $\gamma$  activity in obesity. PPAR $\gamma$ , whose hepatic expression is very low in lean subjects, is strongly up-regulated in steatotic liver. As a consequence, TZD treatment in obese/NAFLD patients favors the transcription of the lipogenic transcription factors SREBP1c in the liver, thus increasing the hepatic production of TGs and the maintenance of steatosis<sup>219</sup>. This explains why, in spite of their ability to reduce lipotoxicity by favoring lipid storage in adipose tissue, TZDs are not able to counteract the development of NAFLD in mice exposed to high fat diet.

In conclusion, although the long-lasting use of PPAR agonists highlighted the occurrence of considerable side effects that raise the necessity to improve their long-term safety profile, the



modulation of PPAR activity is still an attractive possibility to ameliorate obesity-related inflammation, insulin resistance and NAFLD. The development of safer PPAR agonists still requires a deeper understanding of PPAR signaling and their changes in obesity. As an example, in the obese state PPAR $\gamma$  was recently shown to undergo phosphorylation at serine 273, a post-transcriptional modification that alters the transcriptional effects of PPAR $\gamma$  and its sensitivity to ligands<sup>220,221</sup>. The new synthetic compound SR1664, which was shown to block this phosphorylation of serine 273, has been recently proposed as an antidiabetic drug<sup>222</sup>. Another appealing approach that has been explored in the pharmacological use of PPAR agonists is the combination of the therapeutic benefits of the activation at least two PPAR isoforms with the development of dual PPAR agonists. Although so far most of these molecules displayed safety issues, saroglitazar, a dual PPAR $\alpha/\gamma$  activator, has currently been approved in India for the treatment of diabetic patients with NAFLD<sup>223</sup>. Finally, a more systematic consideration of species-related differences, when comparing the activity of PPAR agonists in mice and humans, would be also beneficial for the successful development of new therapeutic ligands<sup>224</sup>. The systematic and complementary use of system biology approaches, evaluating PPAR activity in a given tissue/cell, but integrating such information in the context of the whole organism, will perhaps allow accounting for PPAR agonist pleiotropic effects without considering only a single receptor-dependent pathway.

## **I.5 CONCLUSIONS AND PERSPECTIVES**

Obesity, especially visceral adipose tissue overload, is associated with many metabolic disturbances, and more particularly insulin resistance, dyslipidemia and NAFLD. In the last years enormous efforts have been made to uncover new mechanisms contributing to the onset of insulin

resistance. Particular progresses were made in understanding how nutritional overload, as well as particular classes of metabolites and lipids can induce a plethora of pathological modifications in different metabolic organs that can alter their physiological activity.

The low-grade inflammatory response or metaflammation is a well-established consequence of the diet-induced obesity and the characterization of the mechanism of recruitment and activation of different immune cells population is a very active research field. However, the attempt to study the modulation of the immune response playing with the balance between pro- and anti-inflammatory cells has been pursued mainly in mouse model whose immune system is, for some aspects, different from humans, leaving an open question on the feasibility of a treatment based on a delicate equilibrium that should favor metabolic outcome without causing other perturbations.

The hope to develop efficient cure to improve insulin resistance in obesity using unique target, such as PPARs (but also for example AKT or JNK pathways) faded away over the last years, with the evidence that the model in which one factor is the primary responsible for the onset of insulin resistance is clearly too simplistic, as is the idea that targeting one single factor will correct the myriad of defects. Considering the fact that obesity is a disease where multiple organs, endocrine pathways and inflammatory responses are involved, the future challenge will be to develop a holistic approach where knowledge of different systems are processed together in order to see how they are interconnected in humans. This is the ambitious goal of system medicine, and only once it will be achieved, the entry door for personalized medicine.

## **II The adipose tissue properties and its diverse depots**

In this chapter, we give additional information on the adipose tissue.

### **II.1 Heterogeneity of the adipose tissue (AT)**

The adipose tissue is a highly plastic tissue composed of preadipocytes, mature adipocytes and stromal-vascular cells, coexisting with nerve terminals, blood vessels and lymph nodes, and immersed in a complex collagen matrix. In our body, many different adipose tissue depots exist, the main difference being between white and brown adipose tissue.

The white adipocytes store lipids in one large lipid droplet surrounded by a thin layer of cytoplasm. However, not all the white depots share the same characteristic. For instance, subcutaneous WAT (scWAT) and, the visceral WAT (vWAT) have distinct properties in terms of cell composition and response to the obesity-induced inflammation. With respect to the origin, these two WAT develop separately. ScWAT appears at mouse embryonic day 16.5-17.5<sup>225,226</sup>, while vWAT develops later, becoming visible at postnatal day 7<sup>227</sup>. At the cellular level the adipocytes originate from the adipocyte progenitors which are contained in the so-called Stromal Vascular Fraction (SVF). These cells have a mesodermal origin and develop from the mesenchyme<sup>228</sup>. Some studies showed the apposition of vascular structures to the developing fat pad advancing the hypothesis of a possible connection between adipogenesis and angiogenesis<sup>229,230</sup>. However, scWAT is not made uniquely of white adipocytes but it also hosts clusters of “beige” or “brite” (brown in white) adipocytes. In spite of their phenotype, these cells

do not have the same origin of the brown cells, which derive from a common precursor Pax7<sup>+</sup>/Myf5<sup>+</sup>, which is generating both brown adipocytes and muscle cells<sup>231</sup>.

The brown adipocytes accumulate lipids in several small lipid droplets and are characterized by a high number of densely packed mitochondria. The BAT is the main site of non-shivering thermogenesis and this is due to a unique biochemical property of the mitochondria in this tissue that contains the uncoupling protein 1 (UCP1). This brown specific protein has the function of dissipating the proton gradient produced by the respiratory chain, therefore reducing the efficiency of ATP synthesis and resulting in the formation of heat. This special thermogenic function has an important impact on energy expenditure in rodents. Accordingly, BAT ablation or dysfunction induces the acquisition of obese phenotype<sup>232,233</sup> and conversely, its activation via cold exposure attenuates weight gain in genetic and dietary mouse models<sup>234,235</sup>. Adult humans have also active BAT in the para-clavicular and spinal region<sup>236,237,238</sup>. The indication that BAT activation promotes a negative energy balance, by increasing energy expenditure and reducing body weight, has led to an increasing interest in understanding BAT biology in order to explore a possible therapeutic application for the treatment of obesity. Interestingly, some multi-locular UCP1<sup>+</sup> cells are also present in the WAT, especially in the subcutaneous adipose tissue<sup>239,240</sup>. It has been also shown that, white fat cells can differentiate to beige or brite (“brown in white”) fat cells in response to different stimuli such as cold exposure or  $\beta$ 3-adrenergic stimulation<sup>241,242</sup>. To date, two theories exist to explain the origin of beige/brite adipocytes: 1) *de novo* differentiation from resident progenitors and 2) the transdifferentiation. The first theory hypothesizes the existence of a specific population of adipocyte progenitors, which, upon specific stimulation, become beige preadipocytes<sup>243</sup>. This is occurring with the activation of a transcriptional program that increases the expression level of characteristic genes like *Ucp1*, *Prdm16* and *Zfp516* as well

as *Pgc1 $\alpha$*  which is important for mitochondrial biogenesis<sup>244,245</sup>. Indeed, beige cells appear to have multilocular lipid droplets and increased mitochondrial mass compared to white adipocytes. The second theory proposes that mature white adipocytes are the source for beige cells. This theory is supported by the observation that cold-induced beige adipocytes are converted to white adipocytes after five weeks of exposure to warm<sup>246</sup>. Moreover, an intermediate adipocyte phenotype, between the typical white and brown morphology, was observed during cold exposure, suggesting the participation of the adipocytes to the process of interconversion<sup>247</sup>.

HFD-feeding represents also a stimulus to activate BAT and increase BAT mass. Such phenomenon is known as diet-induced thermogenesis (DIT)<sup>248</sup>. Of note, this process does not induce the recruitment of beige cells in scWAT, suggesting that the increased thermogenic capacity induced by cold vs. by HFD is not regulated via the same way. However, a clear picture of how HFD-feeding regulates thermogenesis is missing. Further studies are needed to identify a therapeutic strategy, which would treat obesity by increasing energy expenditure via activation and expansion of BAT mass.

## **II.2 Molecular pathways driving adipogenesis**

Adipocytes derive from mesenchymal stem cells through a differentiation process that has been usually described as the two phases of adipogenesis. The first, which is referred to as determination phase, is characterized by the commitment of pluripotent stem cells to adipocyte lineage and the creation of a pre-adipocyte pool that has lost the capacity to differentiate into other cell types. In the second phase, the terminal differentiation, these pre-adipocytes acquire the characteristic of mature adipocytes as insulin sensitivity and adipokine secretion<sup>249</sup> and the

machinery necessary for lipid storage and synthesis. This two-step differentiation process requires a temporally highly-regulated transcriptional network that has been studied over the past three decades. In mammalian cells the Peroxisome Proliferator-Activator Receptor  $\gamma$  (PPAR $\gamma$ ) and CCAAT/Enhancer Binding Protein  $\alpha$  (C/EBP $\alpha$ ) are the main regulators of adipogenesis and they share a number of target genes<sup>250,251</sup>. PPAR $\gamma$  is commonly referred to as the “master regulator” of adipogenesis, because it is both necessary and sufficient for adipocyte differentiation<sup>252</sup>. Notably, nothing, transcription factor (TF) or cellular process, is capable of promoting or rescuing adipogenesis in the absence of PPAR $\gamma$ . Moreover, this extremely important TF not only induces differentiation but also maintains the differentiation state. Indeed, blunting PPAR $\gamma$  expression in mature NIH 3T3 cells induces de-differentiation, with loss of lipid accumulation and reduced expression of adipocyte markers<sup>253</sup>.

The C/EBP family members (C/EBP $\alpha$ ,  $\beta$  and  $\delta$ ) are also among the TFs implicated in adipocyte differentiation. Their expression is temporally regulated, with an early induction of C/EBP $\beta$  and C/EBP $\delta$  that leads to C/EBP $\alpha$  expression. The importance of these TFs was demonstrated *in vivo* with different mouse models in which deletion of C/EBP genes results in severe abnormalities in fat<sup>254</sup>. However, despite the strong effect on fat development, these TFs cannot overcome the lack of PPAR $\gamma$ .

Another important group of pro-adipogenic regulators includes SREBP1c, Endothelial PAS domain protein 1 (EPAS1), Signal Transducer and Activator of Transcription 5 (STAT5) and KROX20, as well as the large family of C2H2 zinc-finger proteins KLFs, which regulate different processes, as apoptosis, proliferation and differentiation. The ADD1/SREBP1c is a well-known adipogenesis regulator, whose levels are found increased during *in vitro* differentiation of 3T3 cells. Moreover, the regulation of cholesterol levels mediated by SREBP1c has a regulatory

function on PPAR $\gamma$  expression levels<sup>255,256,255</sup>. EPAS1, also known as hypoxia-inducible factor 2 $\alpha$ , is an important TF involved in vascular remodeling as well as in the ROS management. Its role in adipogenesis has been demonstrated in cultured cells where its expression level is increased 6 days after induction of adipogenic differentiation. It plays a role, more particularly, in the regulation of glucose uptake and thus, in lipid synthesis<sup>256</sup>. STAT5 is a mediator of the prolactin/GH-signaling and may play a regulatory role on PPAR $\gamma$  expression and TG accumulation at later stages of NIH 3T3 cells differentiation<sup>257,258</sup>. KROX20, also known as Early Growth Response 2 (Egr2), is a TF belonging to the zinc finger family and is highly expressed in the adipose tissue. During adipogenesis it exerts a positive effect on the early step of differentiation, by increasing *C/ebp $\beta$*  transcription. However, C/EBP $\beta$ -independent mechanisms are also hypothesized, since KROX20 and C/EBP $\beta$  have a synergistic effect on the differentiation of NIH 3T3 cells and only the expression of both results in the differentiation to a fully mature adipocyte<sup>259</sup>.

Finally, KLFs have different pattern of expression in adipocytes and can either promote or impair adipogenesis<sup>260,261</sup>. KLF4 is an important regulator of the “determination phase”, it is transiently expressed in the first 24h of differentiation and, together with KROX20, induces *C/ebp $\beta$*  gene expression<sup>262</sup>. Other KLFs that act as positive regulator of differentiation include KLF15<sup>260</sup>, KLF5<sup>263</sup> and KLF6, which inhibit the expression of Delta like-1 /pre-adipocyte factor-1 (DLK1/PREF1) in 3T3-L1 cells<sup>264</sup>. However, some of the KLF proteins act as negative regulator of adipocyte differentiation, such as KLF3<sup>261</sup> and KLF2, which repress *Ppar $\gamma$ 2* promoter activity when overexpressed *in vitro*<sup>265</sup>.

Recent studies demonstrated that extracellular signaling can influence the pre-adipocyte adipogenic capacity. For example, the highly conserved secreted proteins of the WNT family

regulate cell fate and development through paracrine and autocrine mechanisms. WNT binding to surface receptor activates an intracellular signaling cascade that regulates gene expression via canonical ( $\beta$ -catenin mediated) or non-canonical pathways<sup>266</sup>. The hallmark of the canonical Wnt pathway is the accumulation and translocation of  $\beta$ -catenin into the nucleus (Figure 4). In the absence of WNT, the cytoplasmic  $\beta$ -catenin is targeted by the  $\beta$ -catenin destruction complex which is composed of AXIN, Protein Phosphatase 2A (PP2A), Adenomatosis Polyposis Coli (APC), Glycogen Synthase Kinase 3 $\beta$  (GSK3 $\beta$ ) and Casein Kinase 1 $\alpha$  (CK1 $\alpha$ )<sup>267</sup>. This complex phosphorylates the  $\beta$ -catenin and targets it for ubiquitination and subsequent proteosomal degradation<sup>268</sup>. Binding of WNT to its receptor complex, composed of Frizzled (FZ) and LRP5/6, triggers a series of events that end up with the dissociation of the destruction complex and cytosolic accumulation of the  $\beta$ -catenin. One of the events provoked by WNT binding is the translocation to the membrane of AXIN, which binds to the cytoplasmic tail of LRP5/6<sup>269,270</sup>. The binding of AXIN is considered to be the turning point in the activation of the canonical Wnt pathway, by inducing the activation of the phosphoprotein Dishevelled (DSH), which induces in turn the inhibition of the kinase GSK3 $\beta$ . This series of events prevents  $\beta$ -catenin degradation and consequently promotes its translocation to the nucleus, where it acts as a transcriptional co-activator<sup>271</sup>. Many binding partners of  $\beta$ -catenin have been discovered, among these the best characterized is the complex LEF/TCF<sup>272</sup>.

The first link between Wnt signaling and adipogenesis came with the observation that activation of the canonical Wnt pathway in NIH 3T3 cells impairs differentiation to mature adipocytes<sup>273</sup>. In contrast, Wnt pathway disruption leads to spontaneous adipogenesis in pre-adipocytes, indicating that WNT protein may function as a “brake” during adipocytes differentiation. A possible reciprocal repression between  $\beta$ -catenin and C/EBP $\beta$  or PPAR $\gamma$  is also suggested by the fact that



the activation of these factors lead to increased proteosomal degradation of  $\beta$ -catenin<sup>274</sup>. This mechanism requires GSK3 $\beta$  activity as well as physical association between PPAR $\gamma$  and  $\beta$ -catenin<sup>275</sup>.

One of the Wnt-family members that have been extensively studied in adipogenesis is WNT10b, because of its anti-adipogenic effect and its role in shifting the development of progenitors from adipogenesis towards osteoblastogenesis<sup>276</sup>. When overexpressed in adipocytes *in vivo*, *Wnt10b* impairs WAT and BAT formation<sup>277</sup>. Its expression is restricted to pre-adipocytes and stromal cells and not to mature adipocytes.

In addition to the canonical, Wnt non-canonical pathway has also been linked to adipogenesis. However, WNT proteins activating this signaling have a pro-adipogenic function, which is thought to be mediated by the antagonizing effects on the canonical pathway. The most studied Wnt family members with proved pro- adipogenic function are WNT4 and WNT5a that have been shown to impair  $\beta$ -catenin nuclear translocation and thus, stimulate NIH 3T3 cell differentiation to mature adipocytes<sup>278-280</sup>.

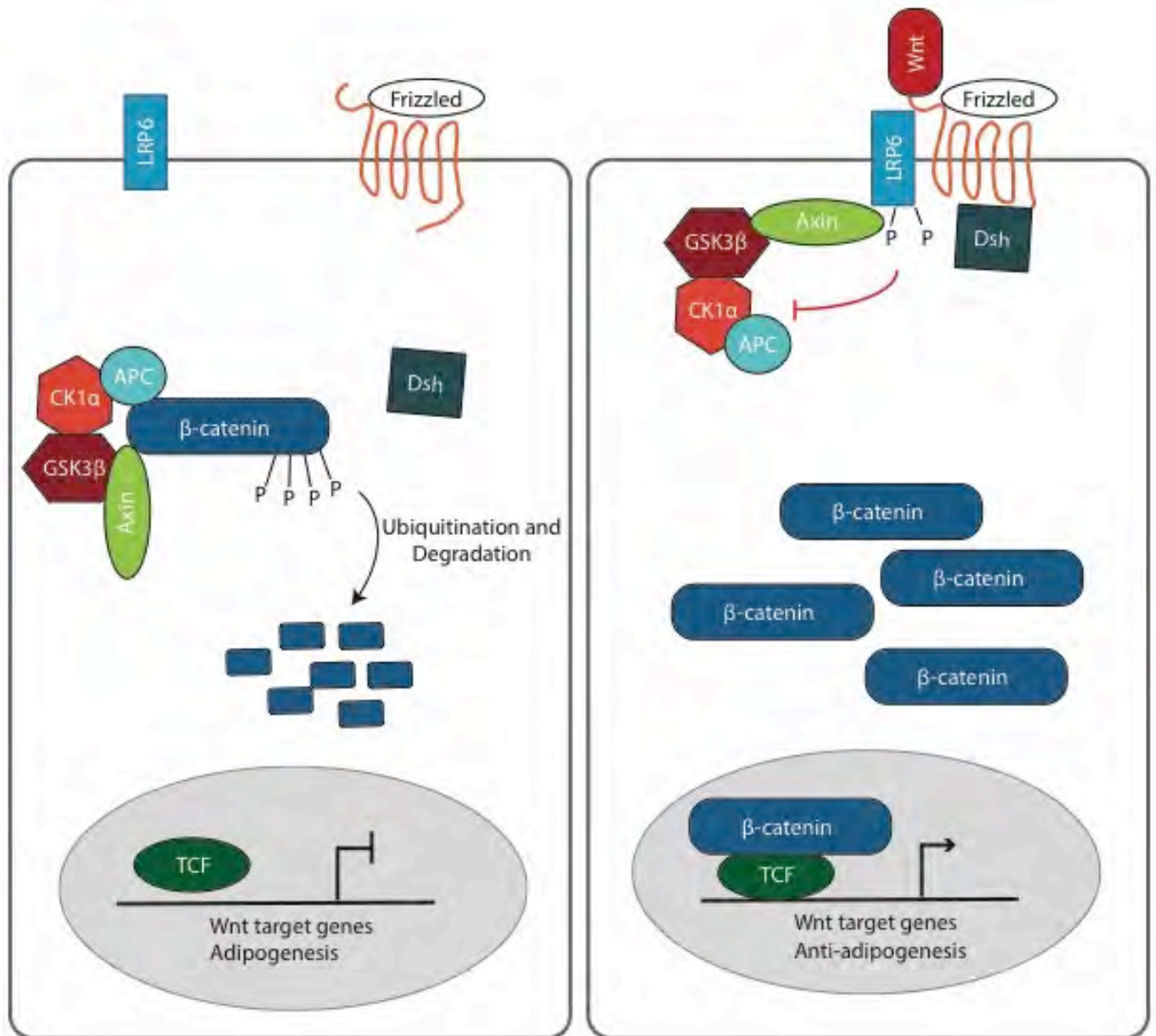


**Figure 4: Canonical Wnt/β-catenin pathway**

Binding of Wnt protein to its receptors LRP6 and Frizzled induces the recruitment of Dishevelled (Dsh) to the membrane and the consequent phosphorylation of LRP6. This leads to the dissociation of the “destruction complex” formed by Axin, Adenomatosis Polyposis Coli (APC), Glycogen Synthase Kinase 3β (GSK3β) and Casein Kinase 1α (CK1α), as well as the accumulation of β-catenin in the cytoplasm. When β-catenin is not phosphorylated, and thus not targeted for degradation, it enters the nucleus and acts as co-activator, binding to TCF/LEF binding sites.

# **Aim of the project**

Human obesity recently became a global epidemic, causing mortality especially because of the many associated co-morbidities. The cause of obesity is linked to the increased energy intake. Indeed, the elevated availability of high-calorie food, coupled with the adoption of a sedentary life style, results in a positive energy balance, where the energy introduced is much higher of the energy consumed. The consequence is an expansion of the adipose tissue and a subsequent weight gain. Although carrying a large percentage of fat is not necessarily detrimental, human obesity is accompanied by systemic chronic inflammation, which is thought to play an important role in the pathogenesis of obesity-related insulin resistance<sup>281</sup>. Despite the number of reports describing the mechanisms by which inflammation induces insulin resistance, very little is known about the molecular processes that lead to the onset of inflammation in obesity. Environmental inputs, such as nutrition, can modulate cell metabolism and the intracellular concentration of a number of metabolites, which can be sensed and, in turn, give rise to inflammation and stress responses in different metabolic tissues<sup>282</sup>. In addition, these metabolites can alter the activity of transcription factors and chromatin modifier enzymes, thus potentially causing specific changes in the chromatin structure<sup>283,284</sup>. Along this line, epigenetic regulation is a key component of the activation of the inflammatory response in immune cells<sup>285</sup>. These observations raise the important question of whether and how alterations of metabolite balance induced in obesity are conveyed to chromatin and what is the contribution of the subsequent epigenetic alterations in triggering the inflammatory response in metabolic tissues.

In order to decipher the pivotal changes promoted in adipose tissue by high caloric nutrient intake and involved in triggering inflammation we propose to (i) follow the evolution of WAT dysfunctions in a mouse model of diet-induced obesity and (ii) explore the response in both the

visceral adipose tissue (vWAT) and subcutaneous adipose tissue (scWAT), each of them having a different response with respect to inflammation.

The present PhD work aims at systematically dissecting the transcriptomic, epigenomic and metabolomic responses in the fat tissue of a mouse model of diet-induced obesity. The final goal is to identify the alterations that play a causal role in the onset of inflammation. For that purpose, the following specific tasks aim at 1) identifying the epigenetic signature promoted by excessive nutrient intake (High Fat Diet); 2) integrating metabolomic, epigenomic, and gene expression changes triggered by excessive food intake and 3) identifying the specific early events in the scWAT and vWAT that drive the development of the obesity-associated chronic inflammation in the vWAT and not in the scWAT. For this purpose we treated control mice with HFD for 1, 8 and 20 weeks. These time points correspond to different stages of the HFD induced inflammatory progression, with the acute response at 1 week, the appearance of macrophage infiltration in vWAT between 6 and 8 weeks and the chronic inflammation at 20 weeks.

# **Materials and Methods**

## **I In vivo methods**

### **I.1 Animals and diet**

Mice were housed 5 per-cage in temperature-controlled room (24 °C) with a 12-hours light/dark cycle. Animals had free access to food and water.

Six-weeks old C57/BL6 male mice are fed with either a HFD (n=170) containing 60% of calories coming from fat or a matched control diet (n=180) with 10% of calories from fat for 1, 8 and 20 weeks.

The calculation of the food intake was calculated manually weighing food.

Glycaemia was measured every week after 5 hour fasting, starting at 9 am until 12 am.

Mice were staggered for the beginning of the HFD in order to have groups of mice matched for the period of HFD feeding. This was decided according to the dissection protocol and the precise number of mice (20; 10 CTR & 10 HFD) that could be dissected in a time period of 2 hours. This time frame was needed to ensure the sampling to be made in the same circadian window for all the mice avoiding any interference of the circadian clock in the epigenetic and metabolomic analyses

## II Ex vivo methods

### II.1 Quantitative PCR and Gene expression analyses

WAT was dissected, frozen in liquid nitrogen and stored at -80°C. Total RNA was extracted and purified using RNesy Mini columns (Qiagen) according to the manufacturer's instruction, quantified and retrotranscribed using the iScript cDNA Synthesis kit (BIO RAD). The analyses were performed using SYBR Green Real-Time PCR on an Agilent Mx3005P or an Applied Biosystems 7900HD Real Time PCR system. Triplicates were checked for reproducibility, and then averaged. No reverse transcriptase controls were included to check for genomic contamination and no template control (H<sub>2</sub>O) were included to exclude formation of primer dimers. Fold difference in gene expression was calculated as  $2^{-\Delta\Delta C_t}$  using cyclophilin B as endogenous control gene. Mice fed with control diet were used as the “comparer”.

### II.2 RNA sequencing (RNA-seq)

RNA-seq was performed on visceral WAT (vWAT) and subcutaneous WAT (scWAT) from 6 groups of mice. The groups were as follows: 1) 1 week fed with control diet, 2) 1 week fed with HFD diet, 3) 8 weeks fed with control diet, 4) 8 weeks fed with HFD diet, 5) 20 weeks fed with control diet, 6) 20 weeks fed with HFD diet. For each group 6 biological replicates were used and each replicate was generated from a pool of mice: 10 mice for pool at 1 week, 6 mice for pool at 8 weeks and 5 mice for pool at 20 weeks.

RNA was extracted and purified using RNesy Mini columns (Qiagen) and RNA quality was assessed using Agilent Bioanalyzer. Libraries were prepared using the NuGen RNA-seq kit



(NuGen) and sequenced 8 for lane (total 8 lanes) on an Illumina HiSeq2000 to obtain approximately between 20 and 30 million single-end reads.

### II.2.1 Sequencing data analysis:

Purity-filtered reads were adapters and quality trimmed with Cutadapt and filtered for low complexity with reaper<sup>286</sup>. Reads were aligned against *Mus musculus* version GRCm38 genome using STAR<sup>286</sup>. The number of read counts per gene locus was summarized with htseq-count<sup>287</sup> using *M. musculus* Ensembl version GRCm38.86 gene annotation. Quality of the RNA-seq data alignment was assessed using RSeQC<sup>288</sup>.

Reads were also aligned to the *M. musculus* Ensembl version GRCm38.86 transcriptome using STAR<sup>286</sup> and the estimation of the isoforms abundance was computed using RSEM<sup>289</sup>.

Statistical analysis was performed for genes in R (R version 3.2.3). Genes with low counts were filtered out according to the rule of 1 count per million (cpm) in at least 1 sample. Library sizes were scaled using TMM normalization (EdgeR package version 3.14.0)<sup>290</sup> and log-transformed with limma voom function (Limma package version 3.26.9)<sup>291</sup>.

### II.3 ChIP on adipose tissue

Adipose tissues were dissected, frozen in liquid nitrogen and stored at -80°C.

The tissues were first reduced to powder and then cross-linked. Two different cross-linking condition were used, (a) 0,5% formaldehyde for 8 min at RT, (b) 20 mM EGS for 20min at RT followed by 8 min with 0,5% formaldehyde, this condition was adapted for ChIP of p300. The cross-linking is then stopped using 125mM of glycine. The shearing condition used was 12 cycles 30''ON/60'' OFF, using a Bioruptor Pico (Diagenode).

The antibody tested were:

H2Ac, marker of accessible chromatin (Millipore, 06-866)

H3K9Ac, marker of active promoters (Abcam, ab4441)

H3K4me1, marker of enhancer (Abcam, ab8895)

H3K27Ac, marker of active enhancer (Abcam, ab4729)

p300, marker of active enhancer (SC-584)

H3K4me3, marker of active promoters (Abcam, ab8580)

pSer5Poll II, marker of active transcriptional elongation (Abcam, ab5131)

RNAPoll II, marker of transcriptional elongation (SC-67318)

## **II.4 ChIP-seq**

Adipose tissues were dissected, frozen in liquid nitrogen and stored at -80°C.

Each tissues preparation was performed on 8 grams of tissue that was first reduced to powder and then cross-linked with 0,5% formaldehyde for 8 min at RT on a shaking platform. The cross-linking is then stopped using 125mM of glycine. The shearing condition used was 12 cycles 30''ON/60'' OFF, using a Bioruptor Pico (Diagenode).

The antibody used were:

H3K27Ac, marker of active enhancer (Abcam, ab4729)

H3K4me1, marker of enhancer (Abcam, ab8895)

RNAPoll II, marker of transcriptional elongation (Santa Cruz, 67318)

The DNA was stored at -20°C until the verification of ChIP enrichment by qPCR and ChIP-seq library preparation.

Library preparation was performed using Diagenode kit (C05010013) according to the manufacturer's instruction, with the ligation of barcoded adapter to allow a multiplexed sequencing of 8 libraries per lane.

ChIP-seq was performed on visceral WAT (vWAT) and subcutaneous WAT (scWAT) from 6 groups of mice. The groups were as follows: 1) 1 week fed with control diet, 2) 1 week fed with HFD diet, 3) 8 weeks fed with control diet, 4) 8 weeks fed with HFD diet, 5) 20 weeks fed with control diet, 6) 20 weeks fed with HFD diet. For each group 2 biological replicates were used and each replicate was generated from a pool of mice: 32 mice for pool at 1 week, 20 mice for pool at 8 weeks and 17 mice for pool at 20 weeks. All the mice used for pool preparation were selected based on their inflammatory response as described in the result section (II.3).

#### **II.4.1 ChIP-seq computational analysis**

100 bases Single-ended tags were mapped to mouse genome Ensemble GRCm38 (mm10) by Illumina pipeline Casava 1.82 using Elandv2e.

##### **Filter:**

We filtered all the tags that did not pass the filter, tags that contain Ns or more than 5 mismatches, and tags that were mapped outside chromosome sizes of mm10.

##### **Files generated:**

-For analysis: BED files were generated from all the tags remained after filter. The total tags for each sample from then on are referred to these numbers.

-For USCS genome viewer: bedGraph and bigWig files were generated from the BED files and scaled by the total tag number for each sample.

**IP quality control:**

CHANCE was used measure IP strength using BED files

Significant bins identification:

We used ChiP-Cor ([https://ccg.vital-it.ch/chipseq/chip\\_cor.php](https://ccg.vital-it.ch/chipseq/chip_cor.php)) to analyze the correlation between 5' and 3' tags position and determined the average ChIP fragment length for each sample.

The mm10 genome was divided into 500 bases long consecutive, non-overlapping bins to calculate the ChIP signal. For each bin, each sample has its own value of tag density which is the AUC (area under the curve) created by the tags piled-up from BED file, strand-shifted by half of the fragment length produced by ChIP-Cor. The bin values were scaled by the total tags for each sample and 30 pseudo-counts were added to stabilize the variance of low scores. The same quantifications were done for all the INPUT samples. All the values were then log<sub>2</sub> converted.

The log<sub>2</sub> scaled bin values of each ChIP sample and of the corresponding time-tissue-treatment INPUT sample were used to compute ratio-mean distribution. This distribution was sectioned into 200 step-wise proportions along the mean axis. Smoothing function lowess with smoother-span 0.2 was applied for only the negative-ratio bin population of each step-wise proportion. From the predicted distribution of smooth function, the mirrored bins were selected on the positive-ratio population. Distribution function was applied for this positive-ratio population with the mean and standard deviation derived from smooth function. The p-values were adjusted for false discovery rate (Benjamini–Hochberg). All bins with adjusted p-value less than 0.05 were considered significant.

This “origami” comparison was done for each replicates of ChIP sample over each replicate of INPUT sample.

We also repeated the same whole genome analysis using bins shifted of half bin size (250 bases) in order to collect all the regions where the signal would be split over two consecutive 500 nt bins.

The significant bins in both replicates and both bin sets (non-shift and 250-shifted) were pooled into consistency analysis. A bin was considered consistently significant if it was found in both replicates, either in the same or shifted position. The final bin set was determined for each sample.

#### **Merging regions:**

All the collected bins for all time points, tissues, diet treatments and IP treatments were pooled and merged with maximum distant of 250–two bins separated by 250 bases would be merged–into significant regions. We have 72314 significant regions in total. The tag density within each region were collected and scaled by total tags of each sample and by each region width.

## **II.5 Metabolomics**

Metabolites were extracted from 20mg of each adipose depot by using a conventional methanol-based solvent mixture. This non-discriminant extraction aims to precipitate high-molecular weight species while avoiding the possible loss of metabolites and their information<sup>292</sup>. Each extract was then aliquoted for further analyses.

The aliquots were analyzed on Reverse Phase Liquid Chromatography (RPLC) Mass Spectrometry (MS) in both positive and negative polarities for un-targeted measuring of features.

## **II.6 Histology and immunohistochemistry**

scWAT and vWAT were dissected, fixed in a IHC zinc fixative (BD Pharmingen, Cat n° 550523), embedded and sectioned. Sections were stained with hematoxylin and eosin. Immunofluorescences were performed using the following antibody: rat anti-mouse F4/80 (ABCAM, cat n° ab6640), mouse anti Arginase 1 (BD biosciences, cat n° 610709).

### **II.6.1 Cell Size quantification**

Six pictures were taken randomly at the magnification of 10X for all the Haematoxylin and Eosin sections. Adipocyte size was calculated on each picture using the Adiposoft software as a plug-in of Fiji. This automated program retrieves the number and the area of each counted cell. All the information per section was pulled together and a distribution of the cell size was obtained using the function histograms in R. The number of cells was counted in a range of size going from zero to the maximal cell size for each group. A summary box plot was produced showing the variability in the cell number in slots of 50  $\mu\text{M}^2$  each.

## **II.7 Western blotting**

Proteins were extracted from powdered tissue using mPER lysing buffer (78501) with added protease inhibitor (Roche) and phosphatase inhibitor (Roche) cocktails. The lysates were left 1h at 4°C on a rotating wheel and then sonicated 5 cycles 30''ON/30'' OFF, using a Bioruptor Pico (Diagenode). Debris and fat were cleaned from lysates by centrifugation. Protein concentration was determined by Pierce BSA protein assay Kit (23227). After dilution with mPER and Laemmli, 15-10  $\mu\text{g}$  of protein was separated by electrophoresis using NuPAGE™ SDS-

polyacrylamide gels (Invitrogen) and transferred on nitrocellulose membrane using wet transfer. Membranes were blocked 1 hour in 5% milk protein, dissolved in tris-buffered saline with 0.05% tween (TBS-T) at room temperature and then incubated over-night at 4°C with primary antibodies. Bound primary antibodies were detected using peroxidase-coupled secondary antibodies and enhanced chemiluminescence (SuperSignal West Pico, 34080). Blots were exposed digitally using the Fusion FX system (Vilber) and bands were quantified using ImageJ software. Protein levels were normalized using housekeeping protein (Gapdh or Vinculin) and data are expressed as arbitrary units.

### **III Statistical analysis**

#### **III.1 Differential expression analysis**

Statistical quality controls were performed through sample PCA (all samples and samples per week).

Differential expression was computed with limma<sup>293</sup> by fitting samples into three linear models per time point and performing the following groups of comparisons:

Comparisons at week 1

Visceral HFD vs visceral control (W1V.H-W1V.C)

Comparisons at week 8

Visceral HFD vs visceral control (W8V.H-W8V.C)

Comparisons at week 20

Visceral HFD vs visceral control (W20V.H-W20V.C)

Moderated t-test was used for each contrast.

The result files contain one row per gene. Columns contain the log<sub>2</sub> average expression across all samples in the model (AveExpr), the log fold change (logFC), the t or F statistic (t or F), the p-value of the test (P.Value), the adjusted p-value computed by the Benjamini-Hochberg method, controlling for false discovery rate (FDR or adj.P.Val. Next columns are the associated gene annotation including gene name and description and so on.

### **III.2 Ruv correction of RNA-seq dataset**

Unwanted variation due to epididymus contamination was removed using RUVr (RUVseq package version 1.6.2)<sup>294</sup>.

### **III.3 Pathway analysis**

Pathway analysis were performed with R using tools called Signalling Pathway Impact Analysis (SPIA)<sup>295</sup> or ClusterProfiler<sup>296</sup>.

SPIA analysis was performed on the full RNA-seq dataset (16709 protein coding genes) without any a priori selection for fold change. The program was provided with pValue and fold change coming from the comparison HFD versus Control (see Differential expression analysis). The differentially expressed genes were defined with pValue cut-off lower than 0.05.

ClusterProfiler with Gene Ontology (GO) annotation was applied, when specified, on list of genes coming from other analysis with pValue cut-off lower than 0.05 and adjusted p-value computed by the Benjamini-Hochberg method.



### **III.4 Cluster analysis on ChIP-seq dataset**

Clustering analysis were performed in R using hierarchical clustering and complete method on the fold change of selected genomic regions. Cut-off for tree selection was applied looking at the best grouping and set at 15, in order to retrieve 15 different clusters.

# **Results**

## **I Establishing the final experimental design via a pilot experiment**

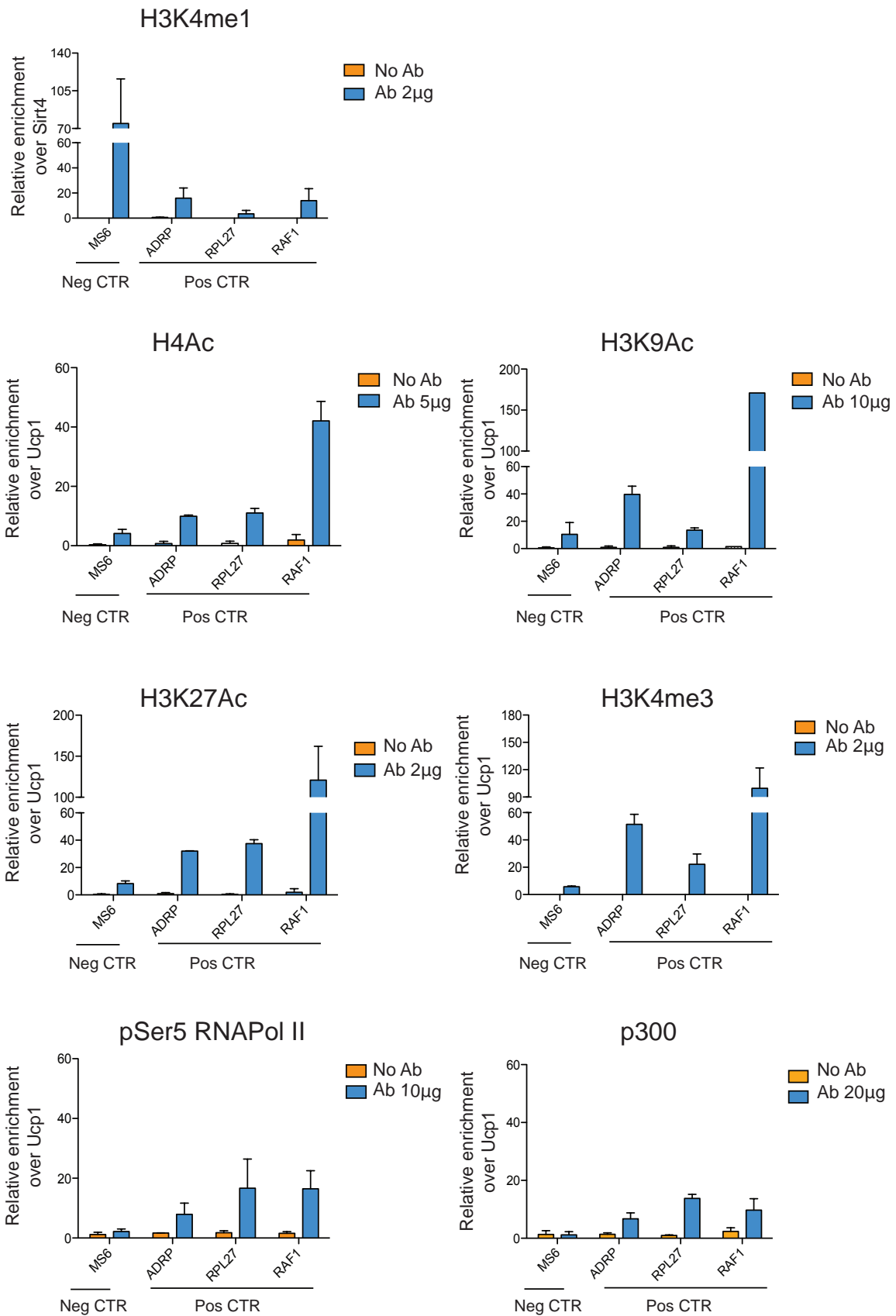
### **I.1 Chromatin immunoprecipitation protocol optimization**

#### **I.1.1 Epigenetic markers selection and optimization of ChIP protocol for each epigenetic mark**

The identification of the epigenetic modifications possibly involved in the onset of obesity-related inflammation in the white adipose tissue is achieved by the application of high-throughput sequencing technologies coupled with ChIP. In order to have a broad view of the HFD impact on the epigenetic landscape, we focused our attention on the histone acetylation status that influences chromatin packaging and the accessibility of transcription factors to local chromatin regions, and on the distal regulatory elements, which are critical for context-specific gene regulation and are associated with characteristic chromatin marks.

We tested the following histone marks:

- Histone 4 acetylation (H4Ac) that reflects chromatin accessibility<sup>297</sup>;
- Histone 3 lysine 9 acetylation (H3K9Ac), marker of active promoters<sup>297</sup>;
- Histone 3 lysine 4 mono-methylation (H3K4me1), which is constitutively associated to enhancers<sup>297</sup>;
- Histone 3 lysine 27 acetylation (H3K27Ac), to monitor active enhancers<sup>297</sup>;
- The cofactor p300, marker of active enhancers sensitive to environmental stimuli<sup>298</sup>;
- Histone 3 lysine 27 tri-methylation (H3K27me3), associated to silenced chromatin;
- Phospho-Serine 5 (pSer5)v and total RNA polymerase II (Pol II) to define the relationship between histone modification changes and actively transcribed genes.



---

**Figure 1:** ChIP protocol validation of different histone modification markers, the cofactor p300 and phosphorylated active RNAPol II (pSer5 RNAPol II) in WAT. In all the graphs, we report the best condition for the immunoprecipitated sample in term of antibody amount, and the no antibody (No Ab) condition, as negative control. Each marker has been tested for three positive controls (*ADRP*, *RPL27* and *RAF1*) and two negative controls (*UCP1* and *MS6*), except *H3K4me1* for which *Sirt4* and *MS6* were used as negative controls. The percentage of input has been normalized to *Ucp1* or *Sirt4* (*H3K4me1*) signal

---

ChIP protocols were optimized for each of these histone modification marks. For each antibody, different concentrations (2, 5, 10 and 20 µg) were tested in order to identify the concentration giving the optimal ratio between enrichment levels and background signals. To evaluate ChIP efficiency, we defined a panel of control sequences mapping at the transcription-starting site (TSS) of genes actively transcribed or not in mature adipocytes. As positive controls, we considered genes such as the Adipose Differentiation-Related Protein (*Adrp*), Ribosomal Protein L27 (*Rpl27*), *Raf-1* and *Pparg*. As negative controls, we chose the *Ucp1* gene, generally not expressed in vWAT, and a gene transcribed by the RNAPol III (*Ms6*).

The second step of this protocol optimization process was to adjust the crosslinking conditions and chromatin shearing process in order to improve the efficiency of ChIP, especially for the cofactor p300. This important transcriptional co-activator is not directly bound to the DNA and is thus, more difficult to immunoprecipitate using the standard ChIP protocol. Nevertheless, by using a stronger crosslinker and a gentler sonication system, we were able to improve the immunoprecipitation efficiency of p300 and of all the histone modification marks. As shown in Figure 1, we obtained a nice enrichment of the positive sequences and a good specificity of the signal compared to the no antibody condition for all the considered markers.

A specific hint must be given concerning the intriguing enrichment pattern obtained for the marker of enhancer, *H3K4me1*, which seemed to be enriched also at the TSS of our negative control *Ucp1* (data not shown). This is in line with many ChIPseq analyses where this mark

displays a dynamic distribution spread in promoter, intronic and intergenic regions<sup>297</sup>. For this reason, as negative control H3K4me1 we added a sequence designed on the TSS of Sirtuin 4 (*Sirt4*) that, according to Raghav et al.<sup>299</sup>, in mature adipocytes is bound by the nuclear corepressor receptor corepressor 2 (NCoR2) and its TSS did not show any H3K4me1 tag enrichment

## **I.2 *In vivo* pilot experiment**

### **I.2.1 High fat diet efficiency**

Different diet-inducing obesity (DIO) formulas have been described in the literature to mimic the high caloric nutrient intake and reproduce the obese pathogenic process. In particular, two HFD formulas are the most commonly used, one containing 45% and 35% of calories coming from fat and carbohydrate, respectively<sup>300</sup>, and the other one with a higher percentage of fat (60%)<sup>301</sup>. Although extreme in term of fat content, thus not perfectly reflecting the human food intake, we fed the mice with a 60% HFD (cat. D12492), to push the onset of obesity-induced inflammation in our experimental group. A specific control diet for this specific HFD, which matched for the amount of sucrose (7%, cat. D12450J), was used instead of the regular chow diet, which contains 35% of sucrose (purple line in Figure 2). In order to avoid any bias due to acute effects in changing the chow dietary regimen, we started the experimentation right after the weaning (4 weeks old mice), feeding both control and HFD groups for two weeks with the appropriate control diet (Figure 2).

To test that this matched control diet would not affect food intake and growth, we first went through a pilot experiment, feeding mice with the D12450J control diet or the chow diet normally

used in our animal facility (Figure 2A). As shown in Figure 2B, we did not observe any change, neither in body weight nor in the food consumption, suggesting that this control diet is well tolerated and does not induce weight loss. Following this first assessment, we tested the HFD efficiency in a group of 20 mice, 10 of them being switched to HFD after the 2 weeks of conditioning with control diet, while the other 10 continuing on the control diet. After six weeks of this regimen, the measurement of the body weight confirmed that HFD was efficient in inducing body weight gain, giving significant differences already at 2 weeks of treatment (Figure 2C).

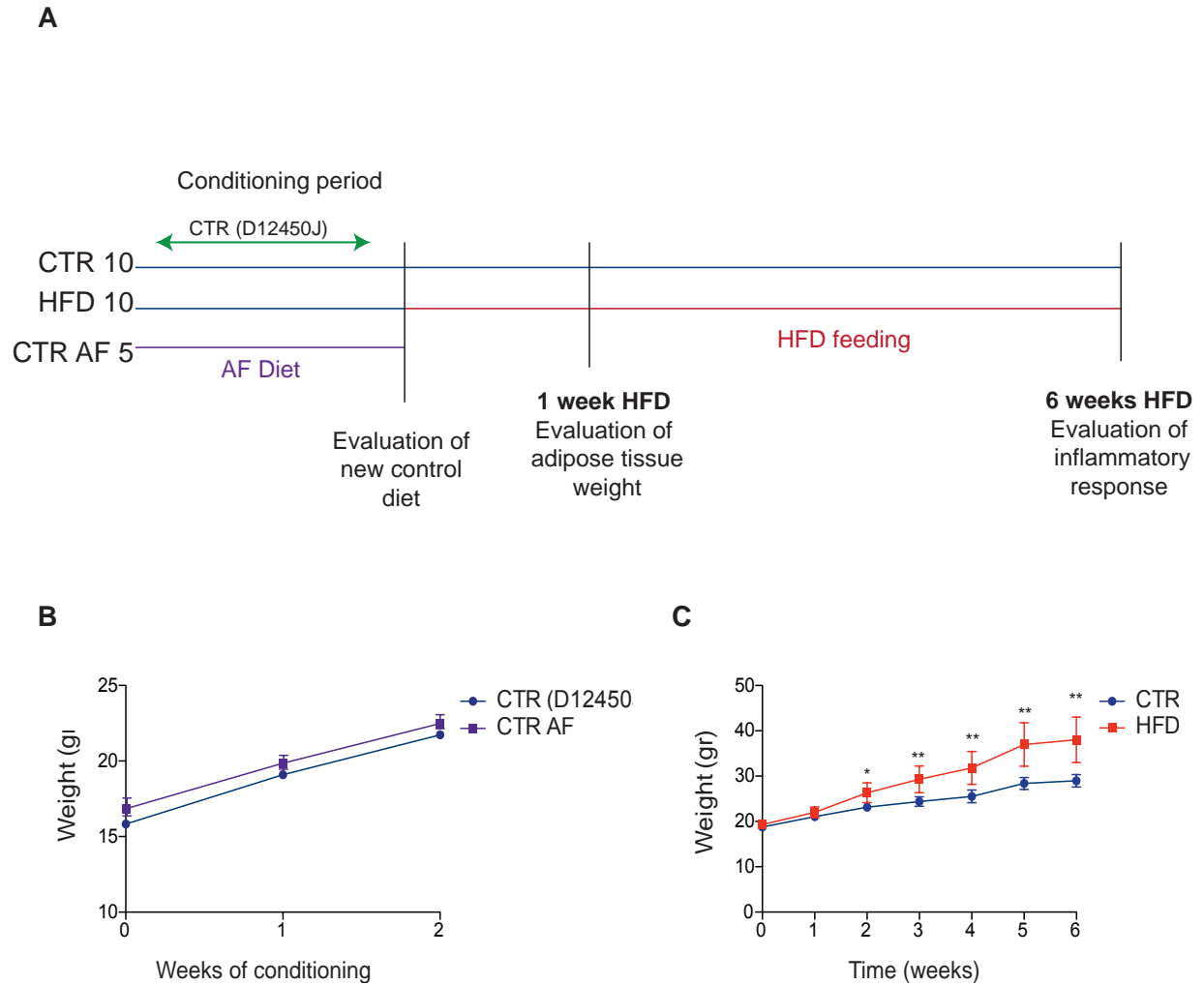


**Figure 2:** (A) Study design for the pilot experiment. Twenty 4-weeks old mice are fed with the new control diet D12450J (low sucrose but isocaloric with the usual chow diet) for two weeks, while, as control, 5 age-matched mice are fed with the control diet regularly used in the animal facility (AF diet, purple line). After the conditioning period, half of the mice (10) in control diet (blue line) is shifted to a 60% HFD for 1 or 6 weeks (orange line) (B) Weight gain of 20 and 5 mice fed for two weeks respectively with a 7% (D12450J) or a 35% (CTR Animal Facility) sucrose control diet. (C) Weight gain along 6 weeks of HFD treatment \* $pVal < 0.05$ , \*\* $pVal < 0.01$ .



### **I.2.2 Assessment of the best intermediate time point to study the inflammatory response**

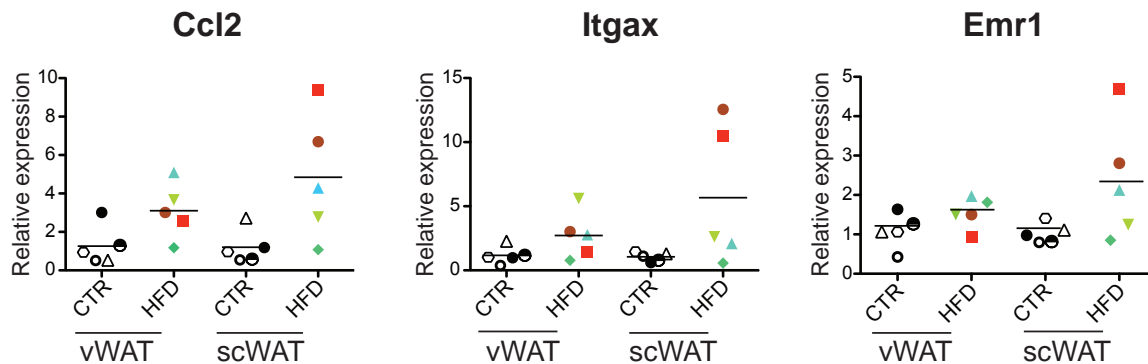
The time points initially chosen to follow the evolution of the diet-induced obesity (1, 6 and 20 weeks) were based on evidence reported in the literature, showing the time course of the inflammatory response along the HFD treatment. However, the exact timing of appearance of activated macrophages in the vWAT is controversial, with different reports showing the first increase of markers of activated macrophages starting from 3 until 8 weeks of HFD treatment <sup>301,302</sup>.

Therefore, it was necessary to carefully evaluate the inflammatory response along the treatment period in order to identify the time point in which a macrophage infiltration is significantly occurring. We thus checked the inflammation status after 6 weeks of HFD feeding, in the small group of mice from the pilot experiment (5 control and 5 HFD). The analyses of the inflammatory response were based on the expression level of a panel of inflammatory genes, including markers of M1 macrophages and cytokines (Figure 3) and on histological analyses on both vWAT and scWAT, using Arg-1 and F4/80 as markers of M2 or M1 macrophages, respectively (Figure 4).

In the gene expression analysis (Figure 3) the three markers of activated macrophages, *Ccl2* (MCP1), *Itgax* (CD11c) and *Emr1* (F4/80), exhibited a coordinated increase in 2 out of 5 mice, indicating that, at this time point, not all the mice have established inflammatory response in the vWAT. This heterogeneous response was further found in the expression profile of a panel of inflammatory cytokines, such as *Tnf* (TNF $\alpha$ ), *Il1b*, *Il6* and *Cxcl12* (SDF1), which are secreted by both adipocytes and macrophages in an established inflammatory situation. Indeed, the levels of *Tnf* and *Cxcl12* showed only a trend to increase without reaching a statistical significance. Altogether, these observations suggested that, after 6 weeks of HFD, vWAT starts to recruit

immune cells, but the response is not yet homogeneous in all mice. Importantly, and as expected, no signs of inflammation were observed in the scWAT, neither at the level of macrophage infiltration nor at the level of cytokines secretion.

A



B

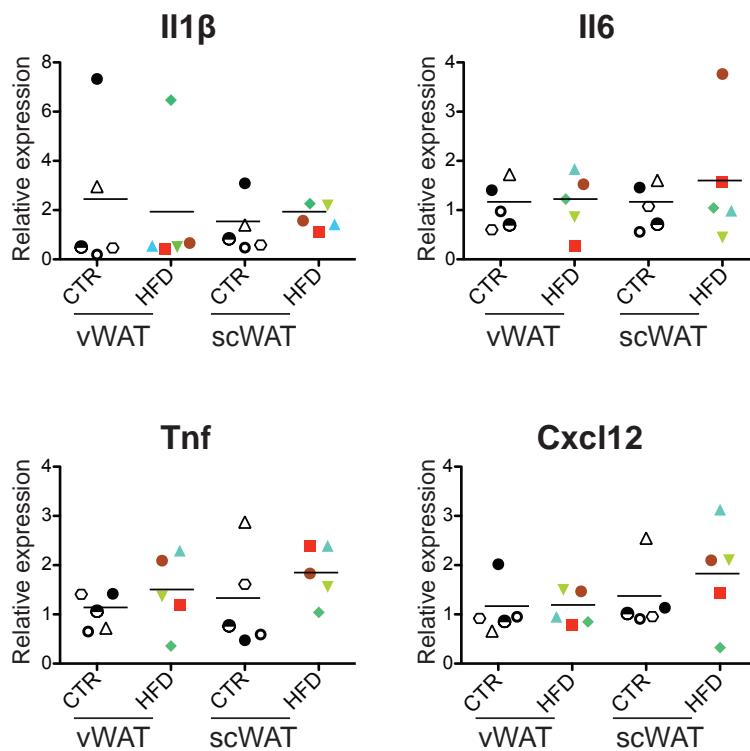


**Figure 3:** Gene expression analysis of markers of activated macrophages, *Ccl2* (*MCP1*), *Itgax* (*Cd11c*) and *Emr1* (*F4/80*) (A) and cytokines, *Il1b*, *Il6*, *Tnf* (*TNF $\alpha$* ) and *Cxcl12* (*SDF1*) (B) in both visceral and subcutaneous adipose tissues of mice fed with D12450J control or HFD diet

Histological analyses confirmed the gene expression results. As represented in Figure 4A for the vWAT, we could identify resident M2 macrophages (Arg1<sup>+</sup>) in both control and HFD mice, whereas only 2 out of 5 mice showed F4/80<sup>+</sup> activated macrophages. These results were strengthened by the Hematoxylin & Eosin staining, which showed some macrophages surrounding adipocytes.

As expected, the same histological analyses performed in scWAT revealed no sign of F4/80<sup>+</sup> cells in both control and HFD mice (Figure 4B). The different inflammatory response observed in these two white adipose tissue depots, which is consistent with many reports in the literature, strengthens the hypothesis that the comparison of the epigenetic and metabolomics profiles in vWAT and scWAT may highlight the crucial alterations that play a role in the onset of the inflammatory response.

Taken together these results proved the efficiency of the diet in inducing body weight gain and inflammatory activation. However, at 6 weeks of HFD treatment, only 2 mice showed a marked vWAT inflammation, with high expression of markers of activated macrophages at the gene and protein level. According to this, we decided to feed mice for 2 additional weeks in the final protocol, in order to increase the number of mice exhibiting an initiated inflammatory response.

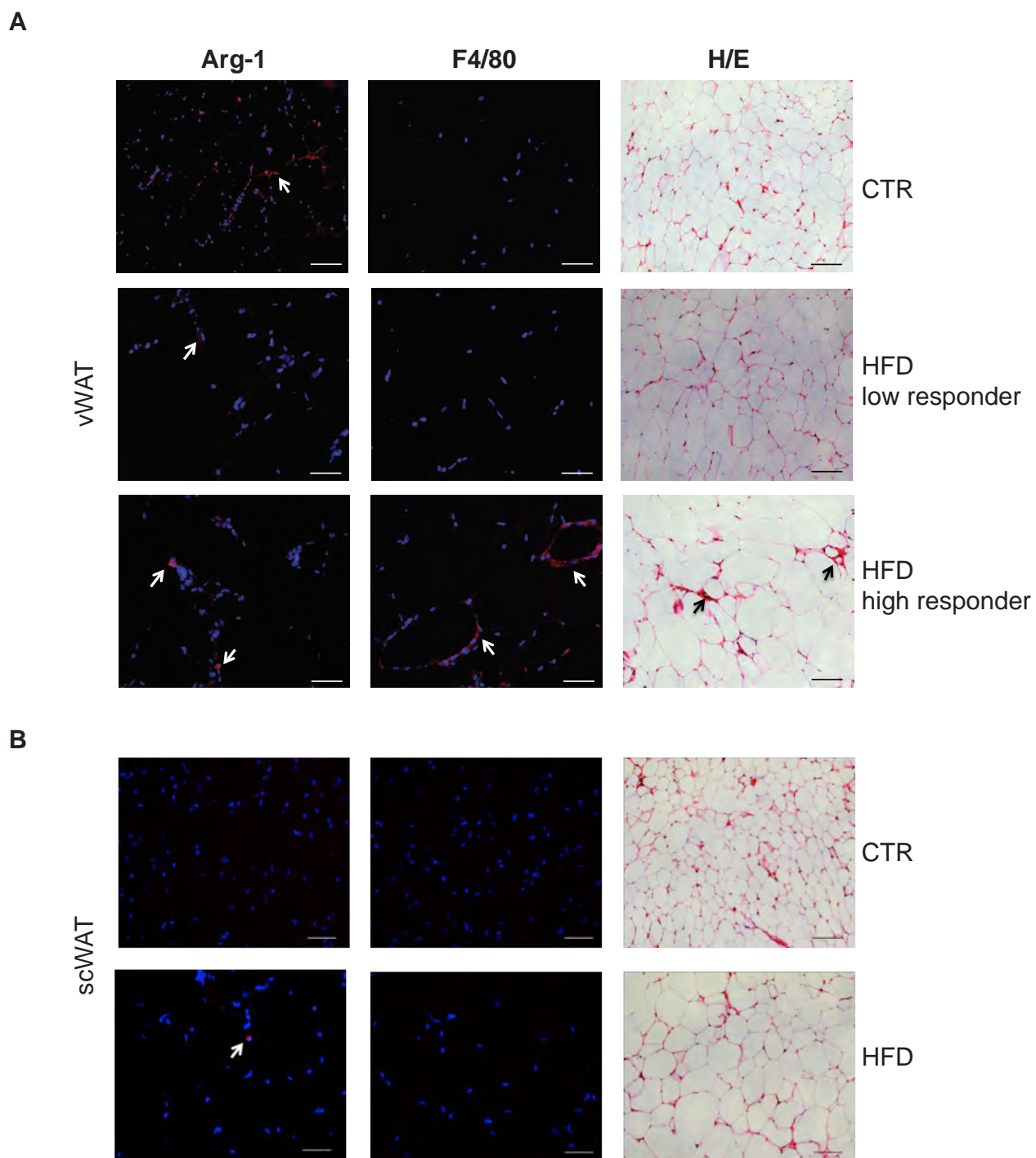


**Figure 4:** Protein expression analysis of markers of M2 ( $Arg-1^+$ ) or M1 macrophages ( $F4/80^+$ ). (A) Immunofluorescence (IF) and H/E staining in visceral white adipose tissue (vWAT). The following conditions are reported: control (CTR), HFD-adipose tissue with no sign of inflammatory response (low responder) and HFD-adipose tissue with sign of inflammatory response (high responder). (B) IF and H/E staining in the subcutaneous adipose tissue (scWAT). Arrows indicate IF positive cells. Bars indicate  $100\mu\text{m}$ .

### I.2.3 Determination of the needed number of mice at each time point

The preliminary experiments allowed us to evaluate the sample size, i.e. the number of mice, needed for giving sufficient materials for all the analyses to be performed. The calculation took into consideration the small amount of WAT present in 7 weeks old mice and the estimated number of adipocytes present in chronic inflamed adipose tissue. Indeed, after several weeks of HFD, the expansion of the WAT is more likely due to an increase in the adipocytes size, rather than to an increase in the number of these cells. Based on the weight of WAT recovered in average in the different conditions (Table 1), and based on the amount of tissue needed for ChIP (8 grams/chromatin preparation) but also for metabolomic, transcriptomics, inflammatory and histological analyses, and the need of performing replicates in order to have statistically significant results, we decided to treat 140, 110 and 100 mice respectively for 1, 8 and 20 weeks.

Mice age	Adipose tissue amount (gr)
7 weeks	0.21 ± 0.08
20 weeks (CTRdiet)	0.7 ± 0.3
20 weeks (12 weeks HFD)	1.3 ± 0.5

*Table 1: averaged WAT mass at different ages.*

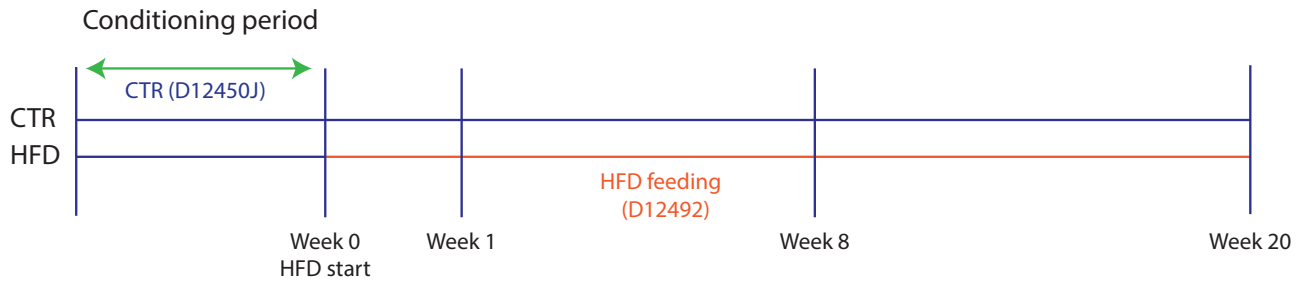
## **II Full scale in vivo experimental design**

### **II.1 Design of the full scale experiment**

As defined through the pilot experiment, 350 four-weeks old C57/BL6 male mice are fed for two weeks with control (D12450J) diet. After this conditioning period, mice were shifted either to a HFD (n=170) containing 60% of calories coming from fat or a matched control diet (n=180) with 10% of calories from fat for 1, 8 and 20 weeks (Figure 5). These time points correspond to different stages of the HFD induced inflammatory progression, with the acute response at 1 week, the appearance of macrophage infiltration in vWAT evaluated at 6-8 weeks and the chronic inflammation at 20 weeks.

At each of the three time points, the blood and two different white adipose tissue depots are collected, namely visceral adipose tissue (vWAT), represented by the epididymal fat pad and subcutaneous adipose tissue (scWAT), represented by the inguinal fat pad. Anatomically well separated, these two energy storage compartments are biologically different in terms of secretion of adipokines and receptor expression patterns that influence their response to afferent signals. More particularly, vWAT has been demonstrated to undergo a more massive activation in terms of inflammatory response upon HFD compared to scWAT, as demonstrated by a higher rate of macrophage infiltration.

A



B

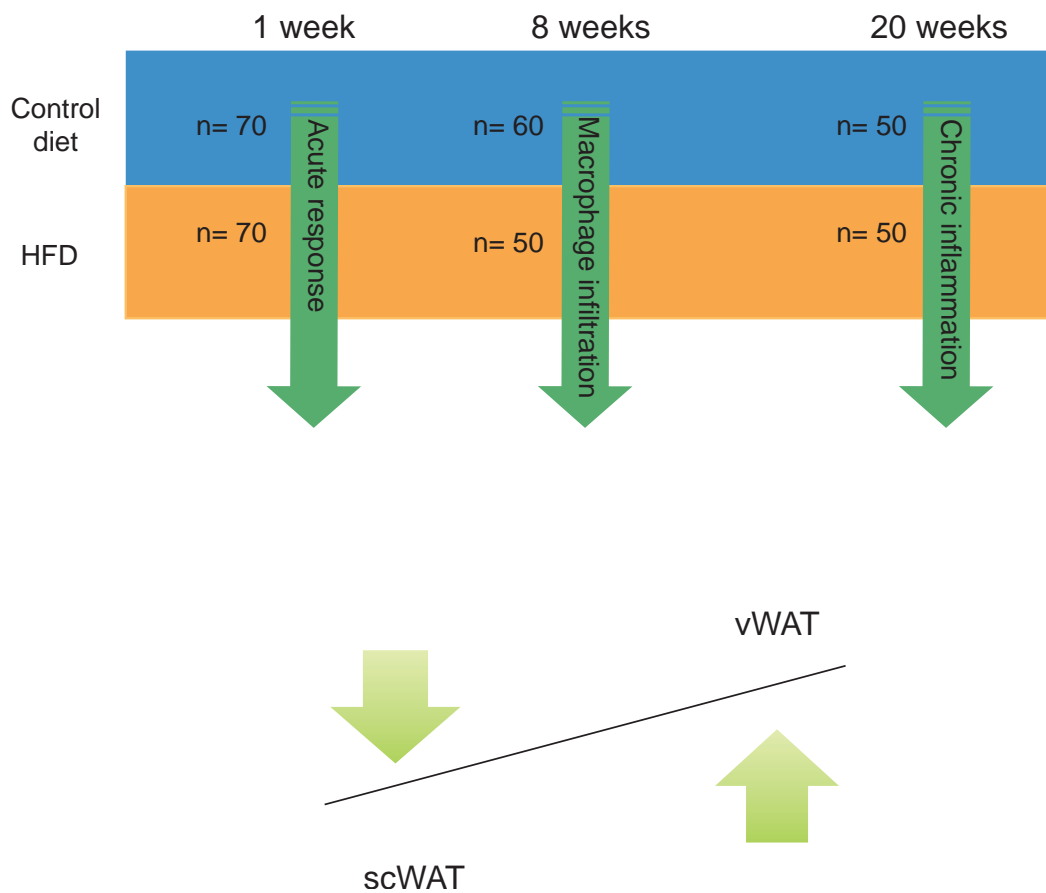


**Figure 5:** Study design for full experiment. 350 4-weeks old mice are fed with the new control diet D12450J (low sucrose but isocaloric with the usual chow diet) for two weeks. After the conditioning period 70 mice were shifted to a 60% HFD for 1 week, 50 mice for 8 weeks and 50 mice for 20 weeks.

## II.2 Phenotypic evaluation of the response to HFD

The evolution of the diet-induced obesity was followed by regular measurements of weight and glycaemia in both control and HFD groups. As shown in Figure 6A, we observed a statistically significant difference in the gain of weight between controls and HFD already after 1 week of treatment. Of note, the HFD group did not develop a strong diabetic phenotype along the feeding period evaluated by glycaemia measurements (Figure 6B).

To confirm that the increase in body weight was directly correlated to the expansion of WAT, we evaluated at the time of sacrifice the individual amount of epididymal (vWAT) and inguinal fat (scWAT) at each time point (Figure 7) As expected, we observed a significant increase in WAT weight at 1 and 8 weeks for both scWAT and vWAT.

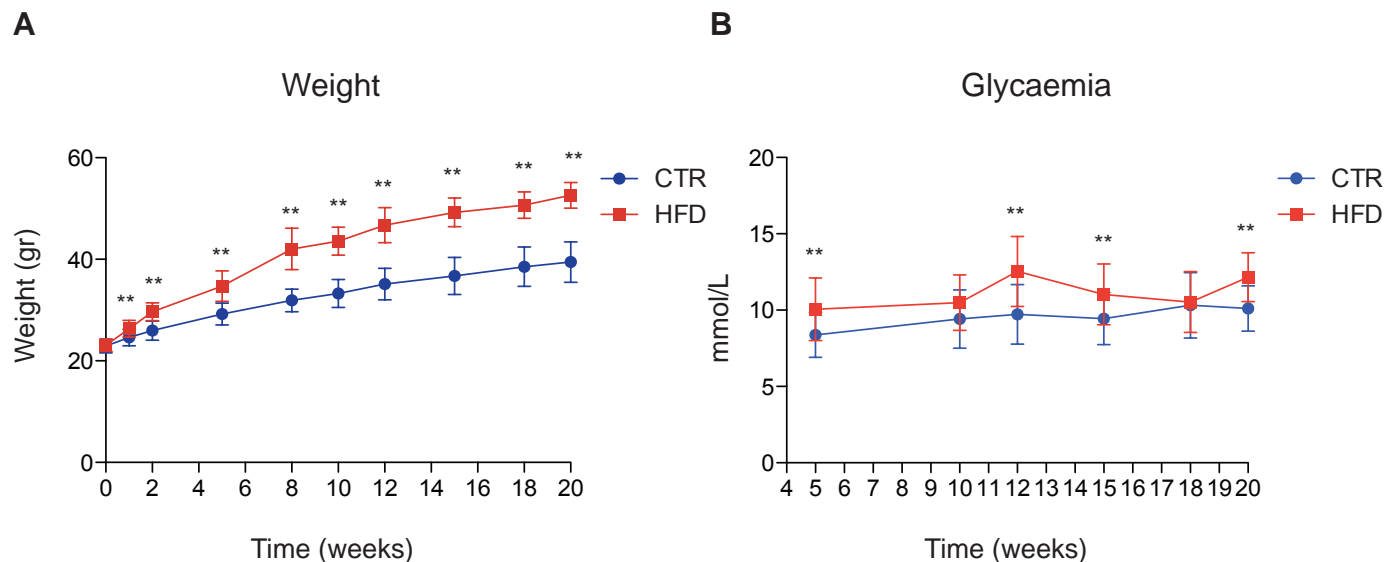


**Figure 6:** (A) Weight gain and (B) fasting glycaemia (5h) evolution along the 20 weeks of HFD treatment. \* $pVal < 0.05$ , \*\* $pVal < 0.01$ .



Interestingly, at 20 weeks the amount of scWAT is largely increased (4 gr on average), whereas there was no difference in the weight of vWAT between the control and the HFD group. On one hand, this is in part explained by the physiological weight gain normally occurring during aging in the control group. However, there was also a paradoxical decrease in the amount of vWAT, from 2.5gr to 1.6gr on average in the HFD group (Figure 7). In contrast, the scWAT compartment is displaying a plastic behavior with progressive expansion upon high caloric nutrition, possibly linked to anatomical availability of space.

Altogether, our data definitively prove the efficiency of the HFD in inducing the obese phenotype in our experimental group.

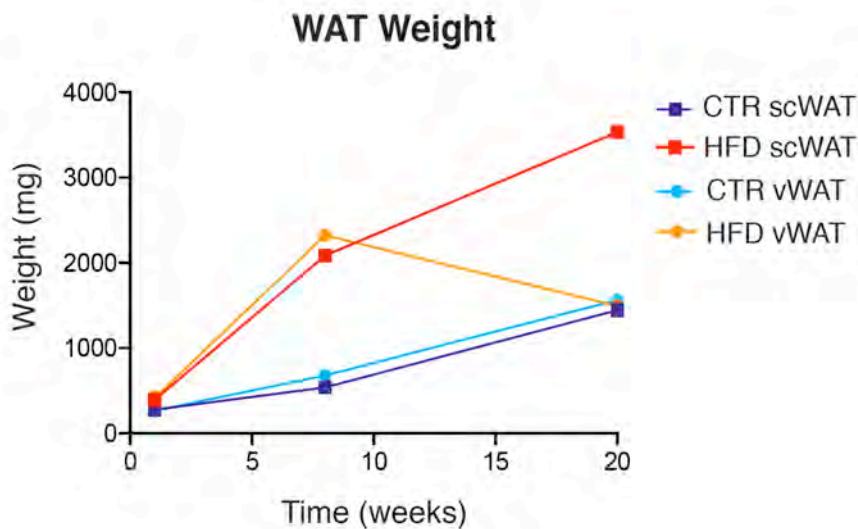


**Figure 7:** Ex vivo measurements of vWAT and scWAT weight after 1, 8 and 20 weeks of HFD treatment.

### **II.3 Full scale in vivo experiment: Quality control and pooling strategy**

Based on the amount of adipose tissue needed for ChIP-seq, as explained in the section I.2.3, it was necessary to establish a strategy for pooling the mice at each time point. Since the aim of the project was to identify changes responsible for the development of obesity-induced inflammation, we used the vWAT inflammation as the key criteria for pooling. After 1 week of HFD, inflammation has not yet started, and the mice were arbitrarily pooled at this time point. In contrast, a detailed evaluation of the systemic and local inflammation was performed in all the mice fed with HFD for 8 and 20 weeks in order to define pools of mice with a homogeneous inflammatory status and avoid, later, a bias due to a different response to the diet. In particular, we measured the circulating levels of proinflammatory cytokines like TNF $\alpha$ , IL1 $\beta$  and IL6, as well as insulin, leptin and resistin that are known to be altered upon obesity and are linked to inflammation. At the tissue level, we assessed the infiltration of macrophages as well as other immune cells. Immunostaining of a panel of markers were performed in the vWAT and scWAT, namely F4/80 (M1 macrophages), Nitric Oxide Synthase 2 (M1 macrophages), Arginase 1 (M2 macrophages), CD8 (Cytotoxic T cells) and CD4 (Helper T cells). The expression levels of inflammatory genes were also measured. It included the gene expression of *Tnf*, *Ccl-2* interleukin-1 receptor antagonist (*Il-1Ra*), and *Itgax*, which are known markers of immune cell recruitment and activation.

#### **II.3.1 Inflammatory response at 8 weeks of HFD treatment and sample selection**

Insulin, resistin and leptin levels as well as the vWAT gene expression of *Tnf*, *Ccl-2* and *Itgax* were evaluated in 61 vWAT collected at the 8 weeks time point. All these measurements, in

addition to the individual mouse weight, were used as variables to perform a Principal Component Analysis (PCA). As shown in Figure 8, a group of HFD treated mice clustered close to the control group. These mice were considered as “low responder” mice, in terms of inflammatory response, whereas the others were assigned to the “high responder” group (Figure 8).

To better establish this categorization in low or high responder, we added a second level of information, by coupling histological analyses to the PCA. As represented by the staining in Figure 9, resident M2 macrophages (Arg1<sup>+</sup>) appear to be present in both controls and HFD mice, whereas the pro-inflammatory F4/80<sup>+</sup> M1 activated macrophages were present only in the “high responder” mice that were falling in the positive axis of the principal component 1 (Figure 8). The Hematoxylin & Eosin was also revealing a stronger macrophage infiltration in the high responders compared to the low responders and to the controls, as shown by the presence of “crown-like structures” in the adipocytes surrounding areas. Taken together, the PCA and the histological analysis, gave us strong evidence that the mice in the positive dimension of the principal component 1 had clear inflammatory response and could be classified as high responders (~75% of HFD treated mice). Because the aim of the project is to identify the events that contribute to the onset of inflammation, the “low responder” mice were excluded.

These data suggested that the chosen experimental approach is appropriate to our aim. A sufficient number of HFD mice were presenting a quite homogeneous inflammatory phenotype for the considered parameters and could be pooled to perform the epigenetic analyses. Using the group of high responders mice, we then performed the ChIP-seq analysis on 2 biological replicates each of them containing 20 mice. Each of these 2 pools of mice was then split into 3 to

generate 6 biological replicates (6 mice per group) for the RNA-seq experiment (Figure 10A & B).

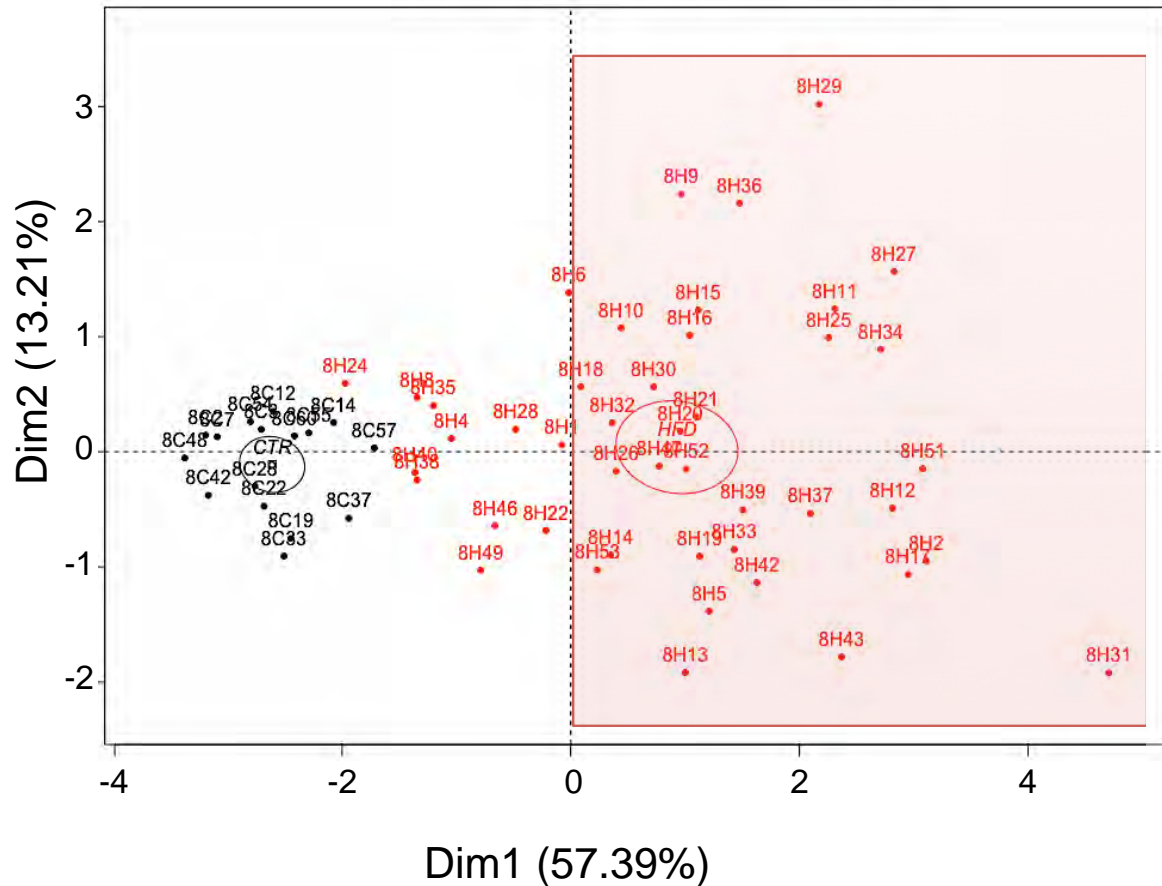


**Figure 8:** Principal Component Analysis (PCA) performed on 61 mice treated for 8 weeks either with CTR (16) or HFD diet (45). 7 variables were used: gene expression levels of *Ccl2* (*MCP1*), *Itgax* (*CD11c*) and *Cxcl12* (*SDF1*), plasmatic levels of insulin, resistin and *Leptin*, and individual mouse weight. In the plot, the control group is represented in black while the HFD mice in red. A red panel was added to indicate the mice selected as “High Responders”. Each point represents a mouse. The nomenclature of the mice is as follow:

The first number is the week of treatment

The following letter is referring to the type of diet, C in black or H in red

The last number is the discriminant of the individual mouse

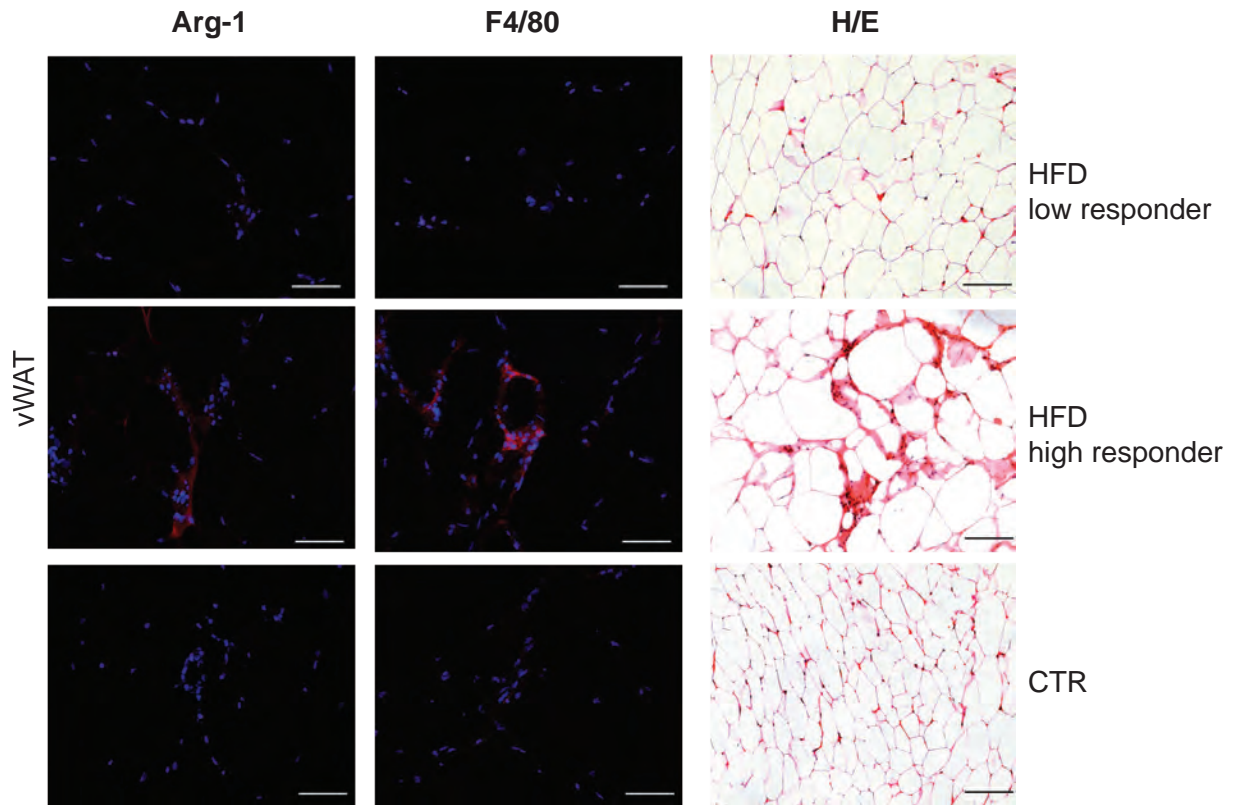
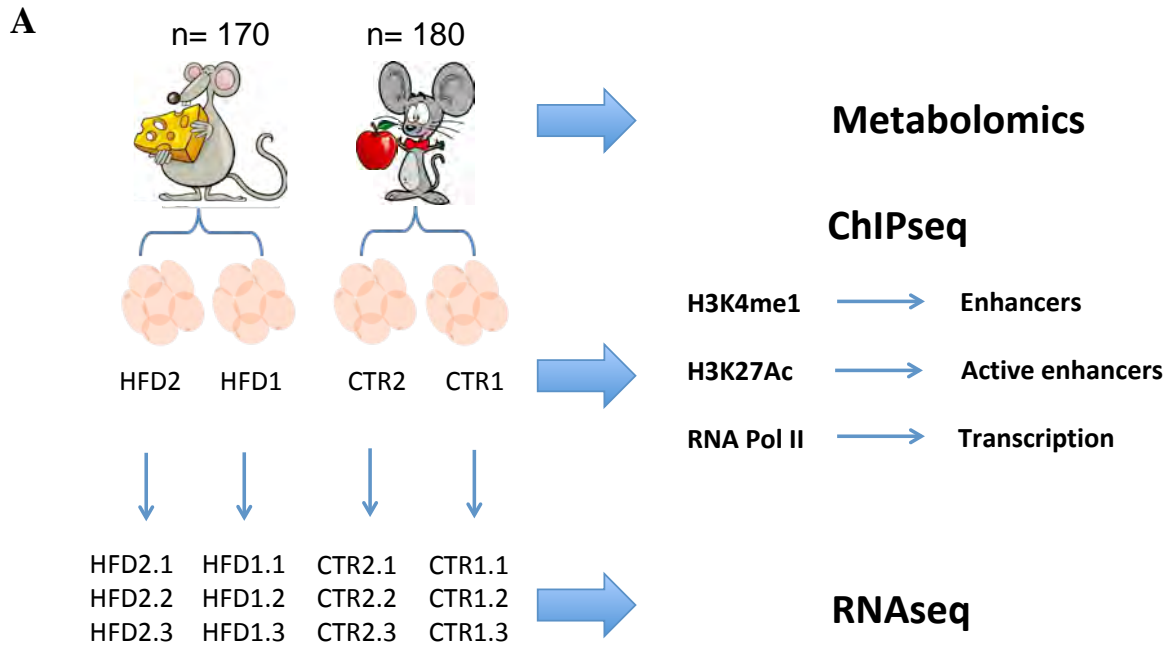


**Figure 9:** Examples of Immunofluorescence and H/E staining performed in the visceral adipose tissue (vWAT) of mice after 8 weeks of HFD. Control group (CTR), low responder HFD (low expression of inflammatory markers) and high responder (high expression of inflammatory markers) HFD. Bars indicate 100 μm.



**B**

		Weeks		
		1	8	20
ChIP-seq	Replicates	2	2	2
	mice/pool	32	20	17
RNA-seq	Replicates	6	6	6
	mice/pool	10	6	5

**Figure 10:** Experimental procedure and pooling strategy. (A) Single mouse extraction was performed for Metabolomics. 2 biological replicates were used to perform ChIP-seq on H3K4me1, H3K27Ac and RNAPol II. 6 biological replicates were used for RNA-seq. (B) number of mice used for each pool at the different time points.

Interestingly, the presence of these two subpopulations of HFD-fed mice differing in terms of obesity-driven inflammation raises the question of which mechanisms are underlying their distinct behavior. By pooling separately low responders and high responders HFD samples, this difference could be exploited to highlight epigenetic modifications occurring exclusively in the high responders that could play a critical role in the inflammatory onset. However, due to time constraints, this has not yet been exploited.

### **II.3.2 Inflammatory response at 20 weeks of HFD treatment and pooling strategy**

A similar characterization of individual inflammatory response was performed on mice fed for 20 weeks with HFD. Principal Component Analysis was performed on 58 samples (20 CTR and 38 HFD) using the same variables used at 8 weeks (expression levels of *Ccl2*, *Itgax*, *Cxcl12* as well as plasmatic levels of insulin, leptin and resistin). As for the 8-weeks time point we decided to consider as high responder the mice in the positive dimension of the component 1 and exclude only one mouse falling in the negative region (Figure 11). Similarly to the 8-weeks time-point, 2 pools of mice (17 mice each) per condition were prepared for ChIP-seq. For the RNA-seq instead, we used 6 pools of 5 mice (see Figure 10 for the replicates scheme).

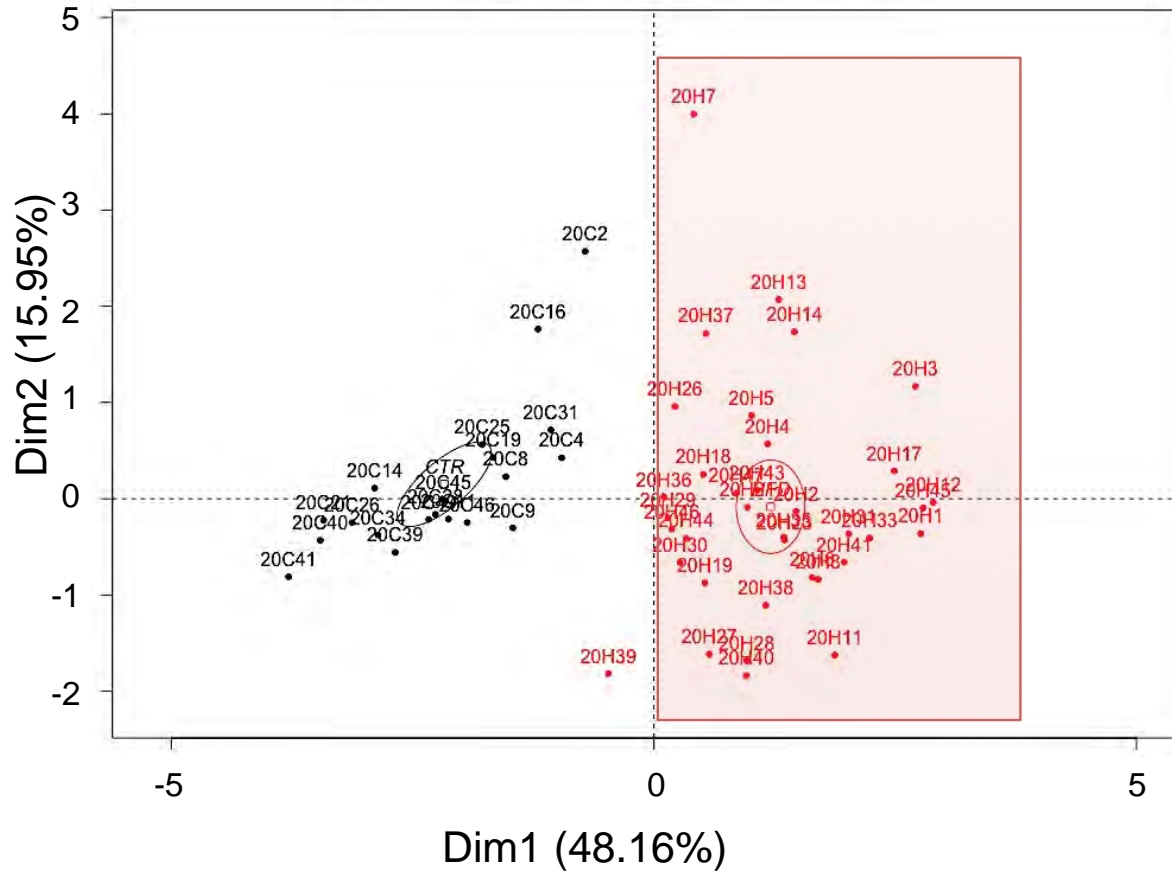


**Figure 11:** Principal Component Analysis (PCA) performed on 58 mice treated for 20 weeks either with CTR (20) or HFD diet (38). 7 variables were used: gene expression levels of *Ccl2* (*Mcp1*), *Itgax* (*CD11c*) and *Cxcl12* (*SDF1*), plasmatic levels of insulin, resistin and leptin and individual mouse weight. In the plot the control group is represented in black while the HFD mice in red. A red panel was added to indicate the mice selected as “high responders”.



## **II.4 Full scale in vivo experiment: analysis performed**

### **II.4.1 ChIP seq: quality controls and general observations**

To characterize the diet-induced changes in the global enhancer and promoter organization, we profiled the genome-wide landscape of H3K27Ac and H3K4me1 histone modifications, as well as the phosphorylated isoform of RNAPol II (5PSerRNAPol II), by performing ChIP-seq analysis in both vWAT and scWAT at all the time points. To check the efficiency of each single immunoprecipitations (IPs), we performed bioinformatics analysis using a tool known as CHANCE (ChIP-seq ANalytics and Confidence Estimation). The IP strength is calculated by comparing the IP cumulative percentage enrichment over the relative background signal given by the input, namely the chromatin precipitation performed without the use of any antibody. This tool is not perfect for our dataset, as it is using a previous version of the mouse annotation (mm9). However, this is negligible since both the inputs and the IPs are mapped to the same genome annotation. These analyses confirmed that the IPs were technically successful for H3K27Ac and H3K4me1, but not for 5SerPol II where the antibody worked only for some sample of the first time point (Figure 12). We thus repeated the ChIP using an antibody recognizing the total form of the RNAPol II. New CHANCE analysis confirmed that these IPs were perfectly working.

We then divided the genome into 500 bases long consecutive and non-overlapping bins to calculate the signal for both IP and input and used a function called “origami” to calculate the IP enrichment over the input for all the bins in the genome. A final step was used to merge the bins into regions (72314) that were the same for all the time points and the 2 tissues. The signal in these regions was scaled according to the total tags in each sample and to the region width, generating the data thus used for subsequent analyses,

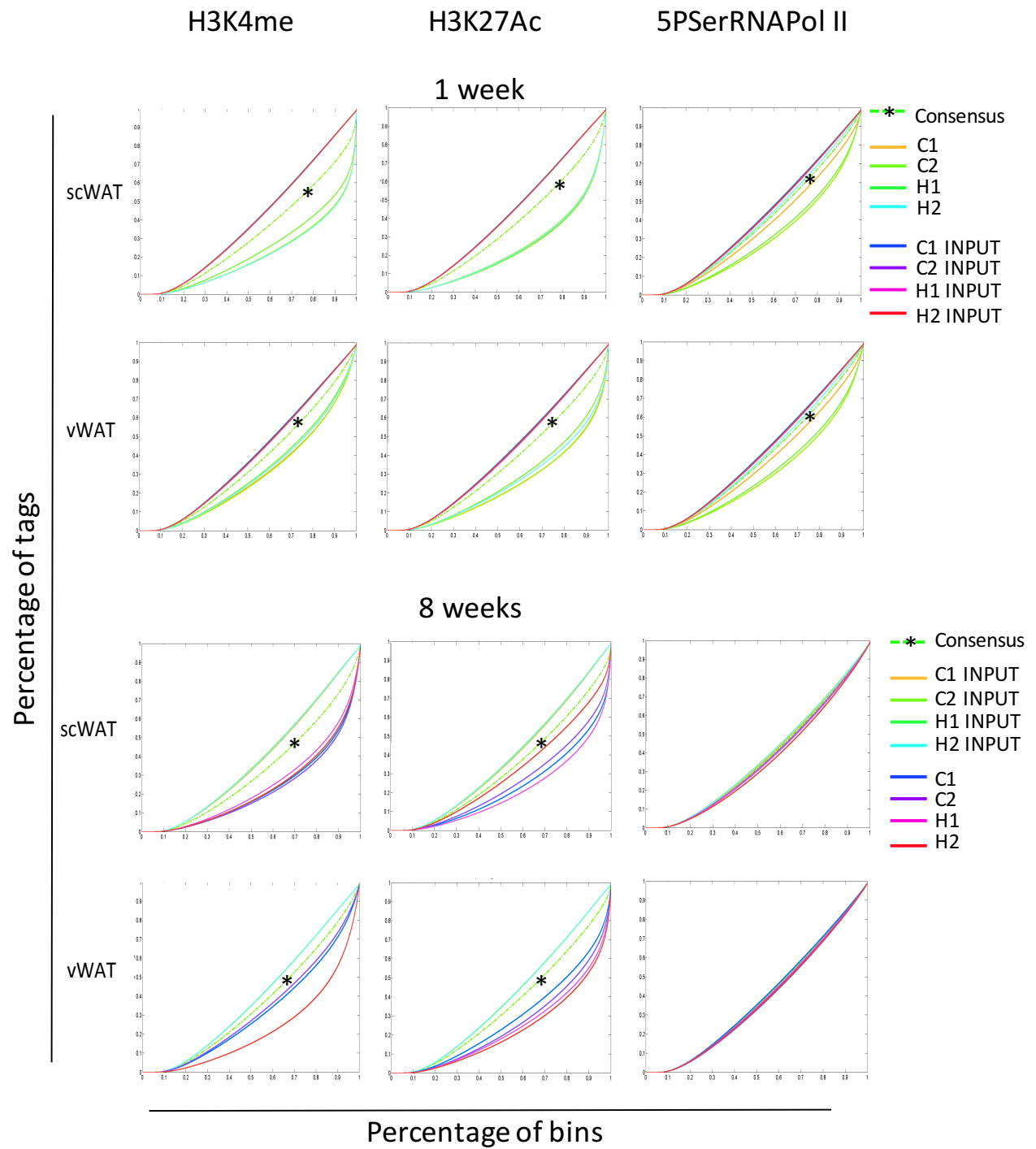


**Figure 12:** CHANCE output for the multi-IP normalization module. For each plot, the x-axis corresponds to percentages of bins (from 0 to 1), which represent 500bp pieces of the genome, giving the idea of the percentage of genome. The y-axis corresponds to percentages of the total number of reads. In each plot 4 curves are present, relative to two control (C1, C2) and two HFD (H1, H2) replicates together with their respective INPUT lines. The point at which the distance between the IP and input percentages is maximized shows the percentage of genome for which the IP is enriched compared to the input. The green dotted line (\*) represents the “consensus”, an in silico built profile based on signal processing techniques designed to identify regions of mutual enrichment. The greater the separation between IP and Input, the better the IP enrichment will be. Each column represent a ChIP and each row a different conditions (type of tissue, length of the diet). In all the ChIP performed using 5PSerRNAPol II antibody the difference in enrichment between the inputs and the IPs are not statistically significant.

#### II.4.2 RNA-seq: quality control and general observations

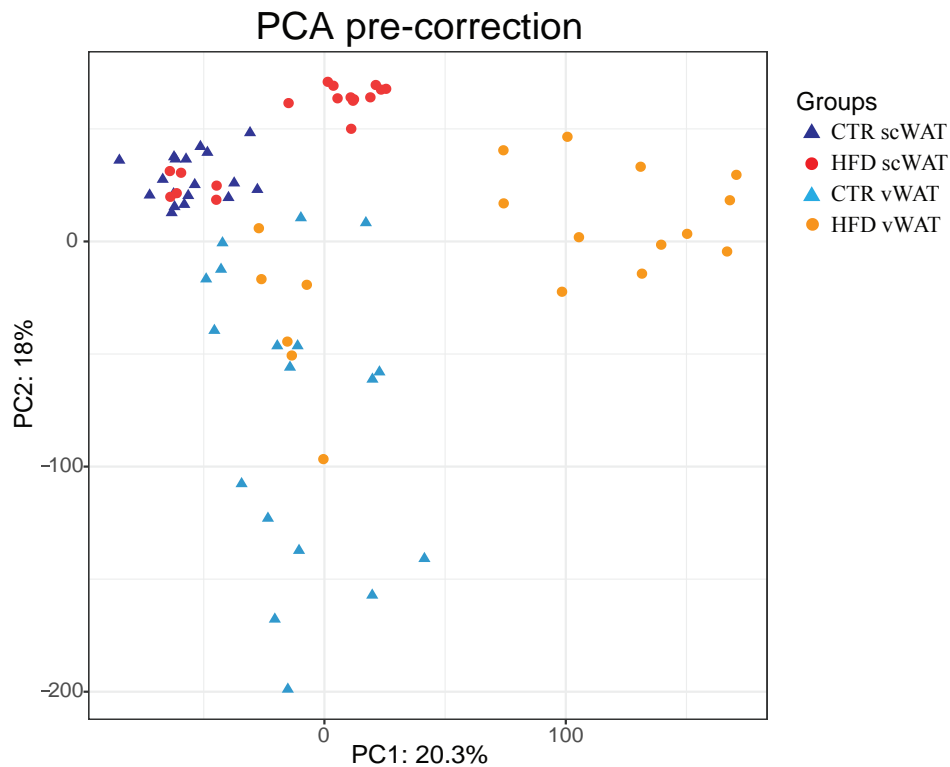
A first quality control (QC) check was applied on the RNA-seq, establishing that all the QC metrics were within the optimal values. We thus proceeded to the RNA-seq analysis, taking into account only the protein coding genes (16709) as shown in table 2. In a second QC test, we performed PCA to assess the quality of the replicates using all the genes as variables and all the experimental conditions. This analysis revealed a non-coherent clustering of the 6 biological replicates coming from the samples prepared from visceral adipose tissue of mice under control diet in all the time points (Figure 13A). The fact that only the control vWAT was affected made us think of a possible contamination by other tissues surrounding the visceral fat, more specifically the epididymis. We thus looked for candidate genes exclusively expressed in the epididymis and not in the fat, such as reproductive homeobox 5 (*Rhox5*), perm adhesion molecule 1 (*Spam1*) and the F-actin-capping protein subunit alpha 3 (*Capza3*), and checked their expression in the RNA-seq dataset. As shown in Figure 14 the epididymal contamination is clear in 2 out of the 6 replicates in all the time points. In these two replicates, the expression of these genes is amazingly high compared to the other samples, reflecting a contamination of the vWAT by the adjacent epididymal tissue. The strategy used to address this problem and remove the influence of these genes on the global variability of the dataset was to add a normalization step by removing the unwanted variation, with the help of an R tool called RUVseq<sup>294</sup>. This method can be applied to large heterogeneous studies where a batch effect is expected but there is no predefined factor of interest to correct, i.e. specific set of genes. This normalization enables the data set correction by removing the unwanted variation, but maintaining the variation of interest, gene expression changes in control vs HFD treated mice for example. This gave us a new data set where the

unwanted variation introduced by the tissue contamination has been normalized. As shown by the PCA in Figure 13B, the clustering of the control vWAT replicates improved.

Category	Total	Sum > 0	In analysis
3prime_overlapping_ncRNA	2	1	0
antisense	2343	2229	636
bidirectional_promoter_lncRNA	47	47	28
IG_LV_gene	4	2	0
IG_or_TR_gene	490	427	162
IG_or_TR_pseudogene	203	105	1
IG_pseudogene	2	0	0
lincRNA	3960	3271	848
macro_lncRNA	1	1	0
miRNA	2202	1136	49
misc_RNA	563	315	27
Mt_rRNA	2	2	2
Mt_tRNA	22	11	5
polymorphic_pseudogene	54	38	12
processed_pseudogene	6970	5134	338
processed_transcript	755	712	394
protein_coding	22018	20705	16709
pseudogene	101	82	16
ribozyme	22	12	2
rRNA	354	122	2
scaRNA	51	29	7
scRNA	1	0	0
sense_intronic	263	257	168
sense_overlapping	25	23	6
snoRNA	1508	577	75
snRNA	1383	705	38
sRNA	2	1	0
TEC	2593	2459	1138
transcribed_processed_pseudogene	184	155	61
transcribed_unitary_pseudogene	6	6	5
transcribed_unprocessed_pseudogene	179	144	67
unitary_pseudogene	24	22	8
unprocessed_pseudogene	2375	1135	72
TOTALS	48709	39865	20876

**Table 2:** The first column gives the name of different gene categories. The second column shows the total number of all the genes falling in the specific category. The third column shows the number of genes per category after selecting only the genes that have at least 1 read count in at least 1 sample. The last column represents the number of genes that have at least 1 count per million (cpm) in at least 1 sample. These genes are the ones we take into account in our analysis.

A



B

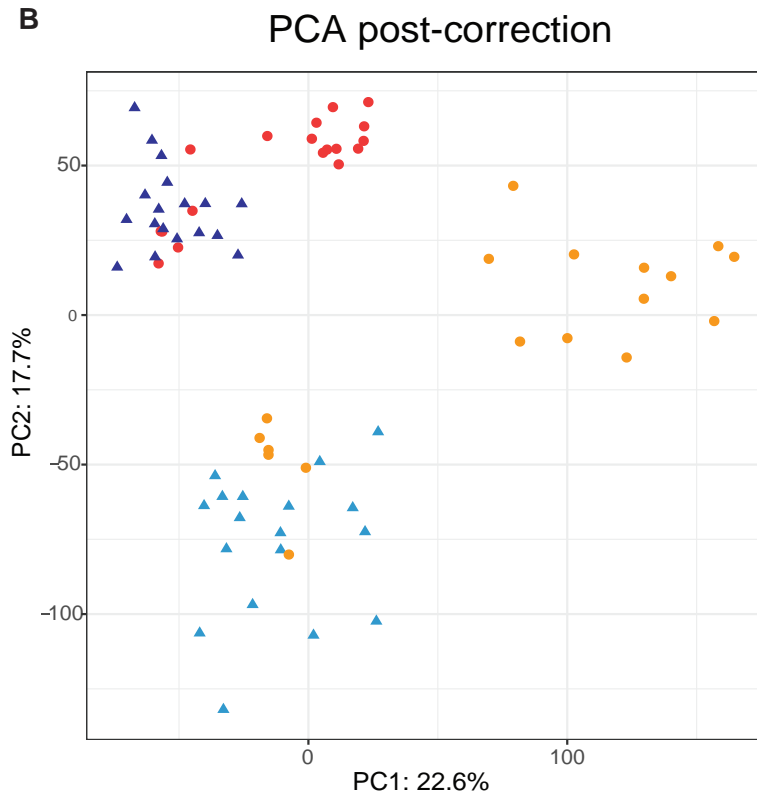


**Figure 13:** Principal component analysis (PCA) performed before (A) and after (B) Ruv correction. In each panel all the time points, tissues as well as all the replicates are showed. (A & B): A shape code is defining the treatment: triangles are representing the control and dots the HFD treated mice. Different colours are assigned to distinguish the diet and the tissue. Blue represents the subcutaneous controls, red represents subcutaneous HFD, light blue represents visceral controls and orange the visceral HFD. After the Ruv correction (B) the intra-group variability is reduced improving the separation between groups. Ruv correction is used here to remove the unwanted variation introduced by epididymis contamination in the vWAT.

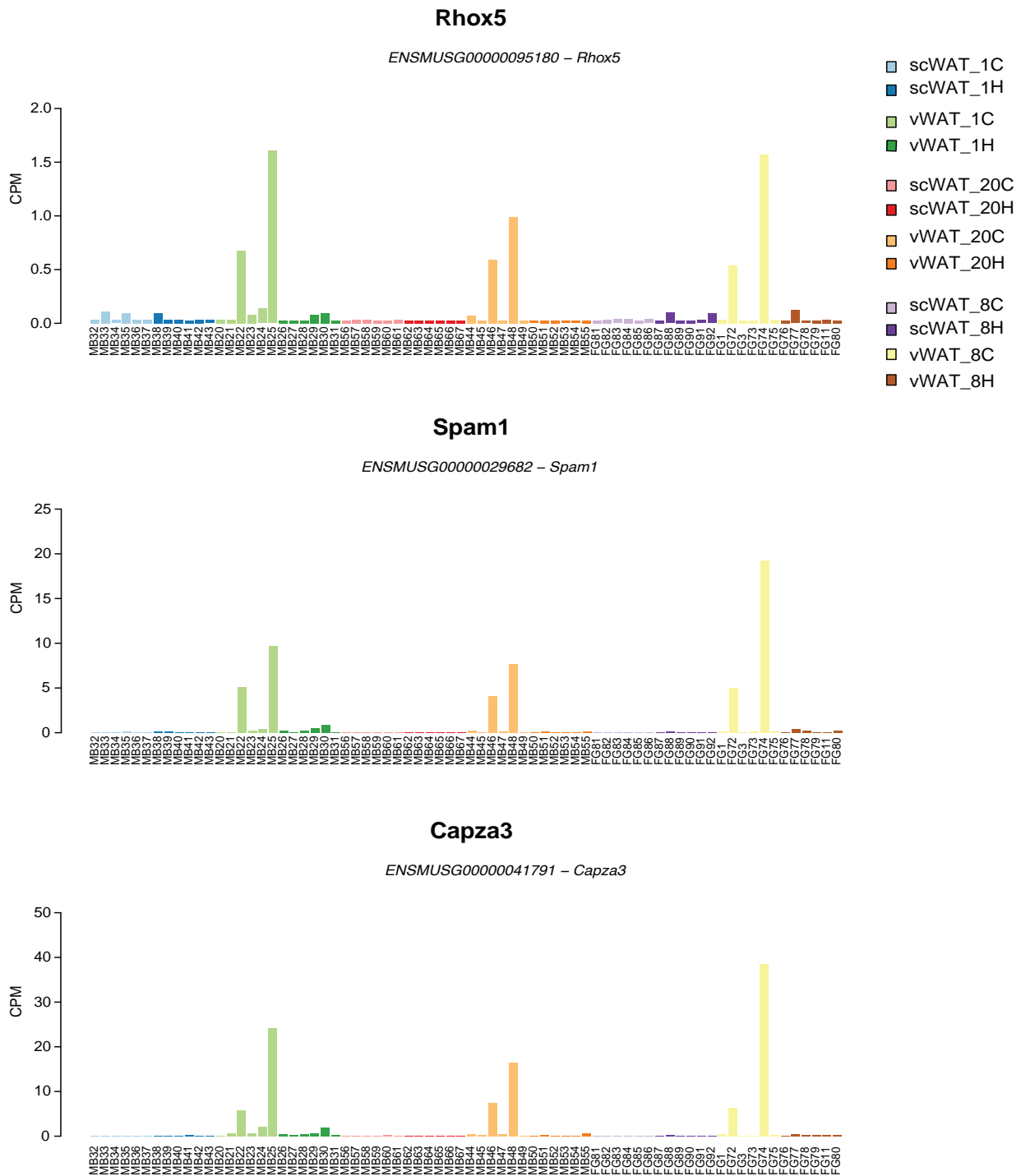


**Figure 14:** Example of epididymis specific genes. Each panel represents the expression of an epididymis specific gene (indicated above the panel). The y-axis represents the count per million (CPM) and on x-axis each histogram represent a sample. A color code is assigned to each group of biological replicates. The expression of these epididymis specific genes is consistently high in different samples of the visceral controls in all the time points (i.e MB25 and MB22, MB46 and 48).

### **II.4.3 Metabolomics: general approach and methodology**

Part of the project was dedicated to the characterization of metabolite changes occurring in the white adipose tissue in the context of obesity. These analyses were performed by the group of Professor Aurélien Thomas, in the frame of the collaborative project Inlawat, in which the present PhD works is embedded.

For this part, we performed the metabolite measurement on single mouse extracts. The samples were analyzed through Reverse Phase liquid chromatography (RPLC) mass spectrometry (MS) in both positive and negative polarities. These analyses were performed on the 1-week and 8-weeks time points, on both scWAT and vWAT.



### **III Distinct epigenetics and expression profiles of the scWAT and vWAT, in normal conditions**

We first explored the basal differences between the two tissues, vWAT and scWAT, independent of the diet effect. For that question, we focus on the global epigenetic landscape of H3K27Ac as well as the transcriptomics, using an unbiased approach.

Principal component analysis was performed using as variables all the 72314 genomic regions profiled by ChIP-seq (see paragraph II.4.1, page 101) in all 24 samples, corresponding to the replicates of the different tissues at different time points. The same analysis was performed using the 16709 protein coding genes and the 72 corresponding samples of the RNA-seq (see paragraph II.4.2, page 104). The PCA plots and the samples clusters revealed a strong difference between the tissues, at both epigenetic and transcriptomic level, that was independent of the diet, since the vWAT of both controls and HFD treated mice are clustering far from the scWAT (Figure 15A). Moreover, the PCA performed on the RNA-seq dataset revealed, in each tissue, a strong diet effect that is more pronounced in the vWAT compared to the scWAT.

Using the RNA-seq data, we identified two sets of genes that, independently of the age of mice, are significantly more expressed in vWAT (791 genes) and in scWAT (298 genes). Pathway analysis of these genes first identified several pathways related to development (Figure 16). This is consistent with the possible different origin of adipocyte precursors, with a mesodermal origin for the vWAT, and a skeletal muscle derived origin for the scWAT. The results also highlight in scWAT a more pronounced expression of genes important for fatty acids metabolism and oxidation, and suggest a higher mitochondrial activity, as revealed by the enrichment in terms

linked to mitochondrial respiration. In the vWAT, the differentially expressed genes belong to pathways related to cell shape, growth, and motility.

We then looked at the epigenetic architecture of the promoter and gene body of few genes coding for transcription factors that are known to be tissue specific, specifically *Wt1* and *Tcf21* for the vWAT, and *Tbx15* and *Lhx8* for the scWAT. As shown in Figure 16B, we observe important H3K4me1 tag enrichment on the promoter of both *Wt1* and *Tbx15* genes. Such pattern is in line with the knowledge that this histone modification is a broad marker specifying enhancer identity but not activation. H3K27Ac instead conveys the information concerning gene activation. For this marker, there is indeed a tissue specific enrichment in tags on these two promoters as shown in the Figure 16B. This further demonstrates that these enhancers are active exclusively in one of the tissues.

These observations revealed the clear intrinsic differences of the two adipose tissue tissues, not only in global gene expression, but also in the epigenomic organization.

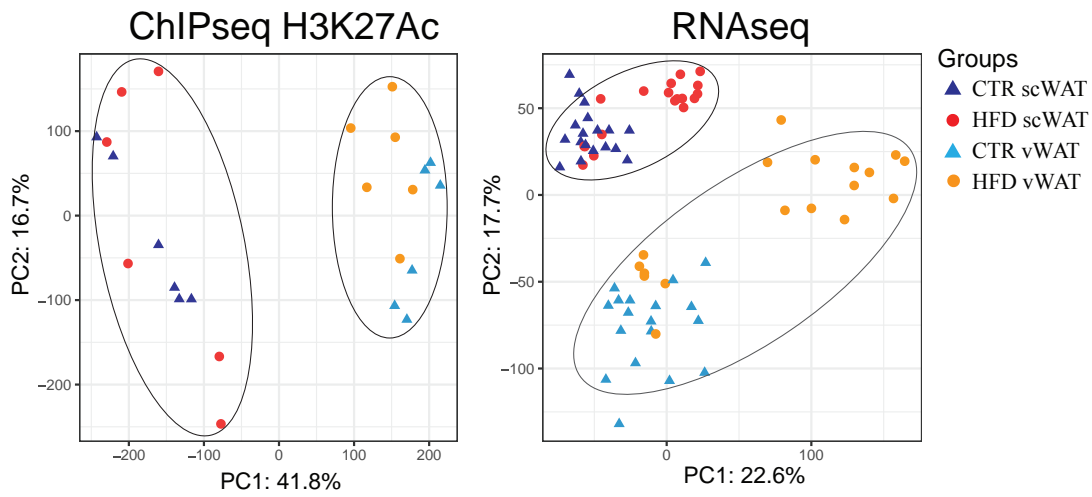
---

**Figure 15:** (A) Principal Component Analysis (PCA) performed using the full ChIP-seq dataset relative to the H3K27Ac on the left, and the full RNA-seq dataset on the right. In each panel the dots represent a sample. A shape code is defining the treatment: triangles are representing the control and dots the HFD treated mice. The number of dots and triangles are representative of the number of replicates: 2 per time point for the ChIP-seq and 6 per time point for the RNA-seq.

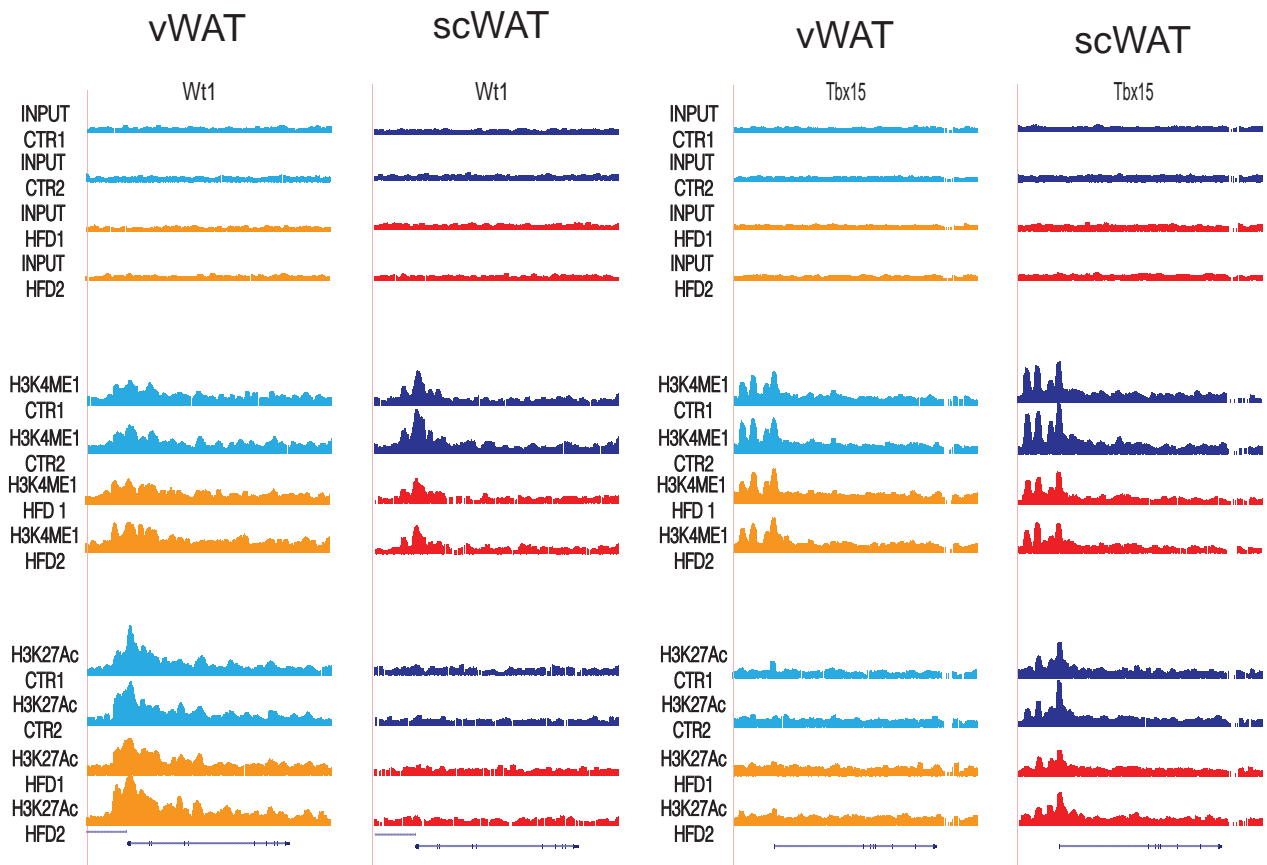
(B) Genome browser view of tag enrichment. In each panel the first four lines represent the inputs, the four lines in the middle represents the H3K4me1 IPs and the last four the H3K27Ac IPs. The two-left panels show tag enrichment on the promoter and gene body of a visceral adipose tissue specific gene, *Wt1*. The two-right panels show tag enrichment on the promoter and gene body of a subcutaneous adipose tissue specific gene, *Tbx15*.

Different colours are assigned to distinguish the diet and the tissue (A & B): blue represents the subcutaneous controls, red represents subcutaneous HFD, light blue represents visceral controls and orange the visceral HFD.

A



B



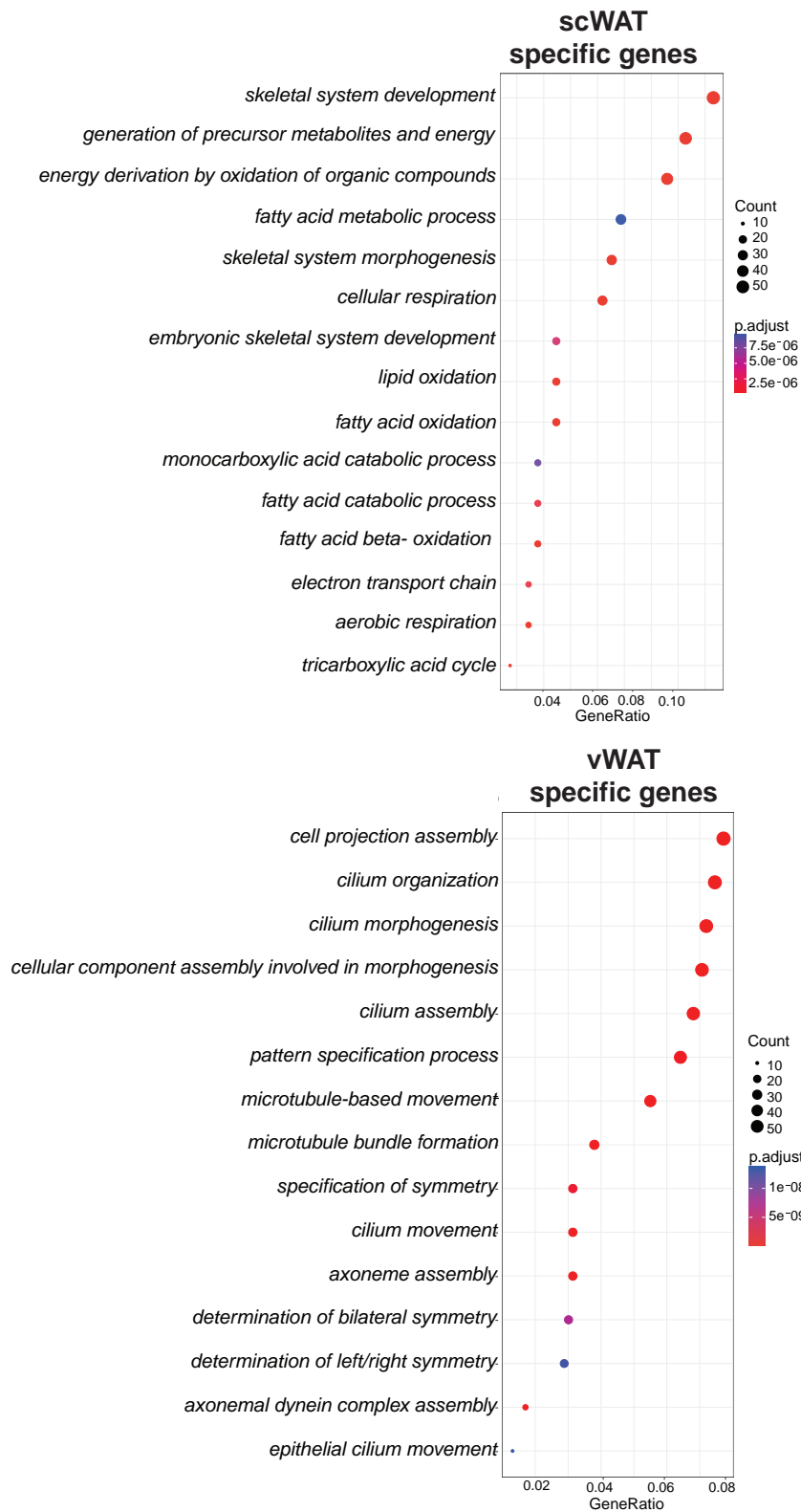


**Figure 16:** Gene ontology pathway enrichment analysis of subcutaneous adipose tissue (scWAT) specific genes and visceral adipose tissue (vWAT) specific genes.

## **IV Different responses at early time point (1week) highlight a distinctive plasticity of the vWAT and scWAT**

The general aim of our study was to highlight biological changes induced by the over nutrition that could explain the different outcome observed in the visceral and subcutaneous adipose tissues. We thus started the analyses by looking at the early changes (1 week of diet) that would allow to understand the mechanisms of the different responses in the scWAT vs. the vWAT observed at the later time point.

### **IV.1 Epigenetic analyses between early and late time points pinpoint the Wnt pathway**

Our first interest was the identification of genomic regions acquiring epigenetic modifications after 1 week of diet.

We first used H3K27Ac, a marker of active enhancer, and performed statistical analyses to compare control- and HFD-treated mice in the two tissues at the different time points (Figure 17). This analysis allowed the identification of the regions with a statistically significant difference ( $p\text{Val} < 0.05$ ) together with their fold change, corresponding to the red and green dots in the volcano plots shown in Figure 17. We then retrieved all the regions that were significantly changed either in the vWAT or in scWAT at 8 weeks (5984 regions) and analyzed their behavior also at one week. For that purpose, we performed a cluster analysis, using their Log fold change at 8 and 1 weeks. As seen in the heatmap (Figure 18A), most of the tested regions show quite a similar pattern between the scWAT and the vWAT. However, two interesting clusters showed a distinctive pattern in the two tissues both at 1 and 8 weeks (Figure 18A).

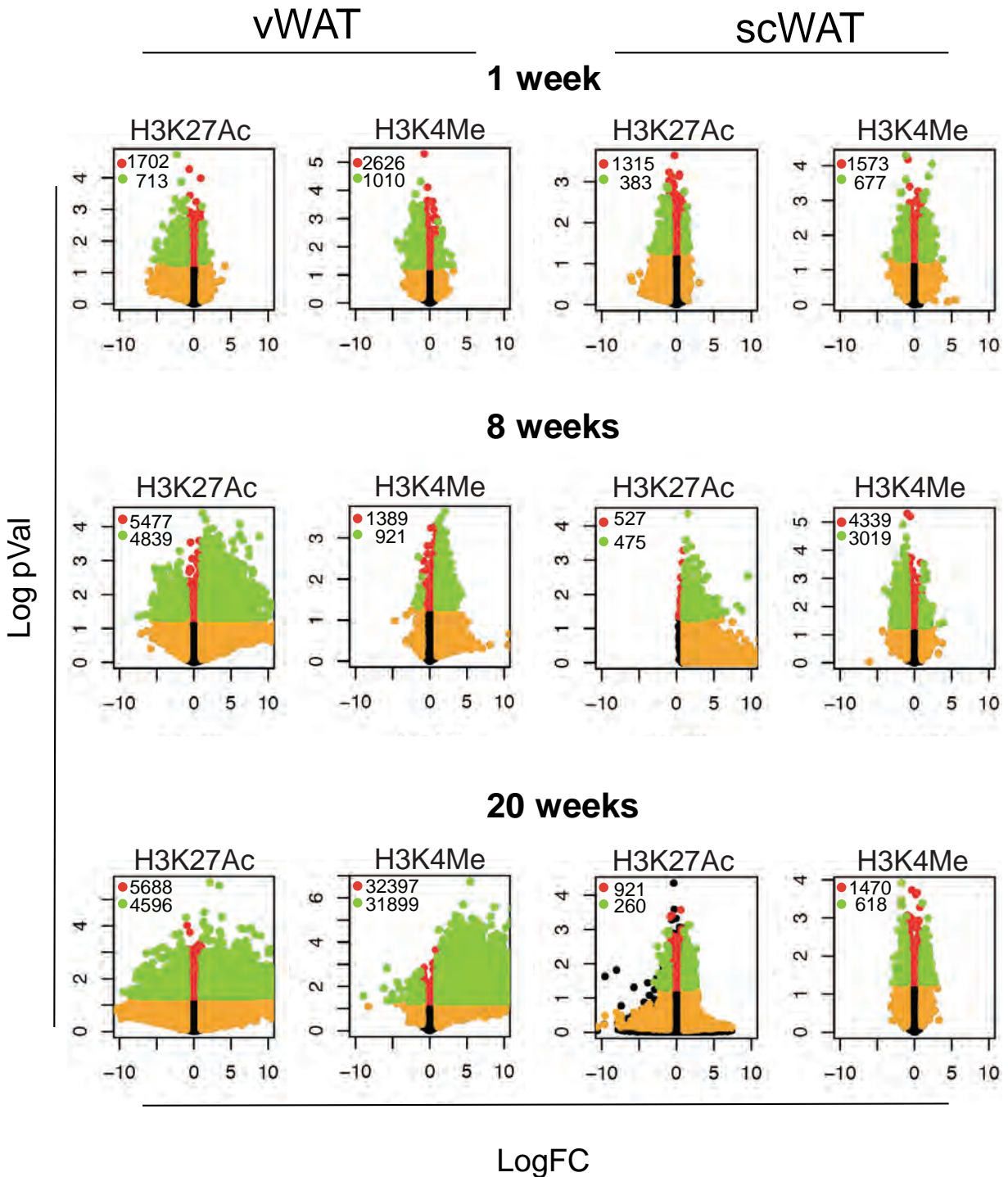


**Figure 17:** ChIP-seq volcano plots. In each panel the x-axis and the y-axis represent respectively the Log fold change (LogFC) and the Log P value of the comparison between control and HFD treated mice. Each dot represents a genomic region that can be coloured in 1) red if its P value is lower than 0.05, 2) green if its P value is lower than 0.05 and the LogFC absolute value is higher of 1, 3) orange if its LogFC absolute value is higher of 1, 4) black if it is falling into any of the 3 categories.

The regions of the first cluster (359 regions) were characterized by having an increased H3K27Ac occurring with the diet in scWAT in contrast to reduced acetylation levels in vWAT. This behavior was already present at 1 week but was more marked after 8 weeks of diet. The second cluster (711 regions) presented the same acetylation profile but with less marked differences between 1 and 8 weeks in the vWAT.

To refine this analysis, we analyzed back the tag density obtained in ChIP-seq for the H3K4Ac, H3K4me1 and RNAPolIII over the 359 regions of cluster 1 (Figure 18B). Interestingly, the acetylation and methylation levels between vWAT and scWAT are extremely different in normal conditions, with an averaged tag density much lower in the scWAT. This suggests that the enhancers that are differentiating the response to HFD in the two depots are in normal condition more accessible for transcription in vWAT than in scWAT. The analysis also shows that the level of RNAPol II on the regions belonging to cluster 1 are in line with those of H3K27Ac, with an average tag density significantly reduced in vWAT at 8 weeks. On the other hand, H3K4me1 levels are significantly reduced at 1 week but not changing at 8 weeks, suggesting that this regulation is happening only in the early phase of overfeeding. Finally, it must be noted that the changes in H3K27Ac tag density in the scWAT, are not statistically significant (Figure 18B). Thus the distinct pattern between vWAT and scWAT mainly stems from the decreased H3K27Ac and RNAPolIII marks in the regions of the cluster 1, and with a lesser intensity in the regions of the cluster 2.

To dig insight the biological functions of these regions, we annotated them to the closest gene from the center of each region. This step gave us a list of 323 genes from the first cluster and 674 genes from the second one. Gene Ontology annotations (Figure 18C & D) obtained with the genes of the first cluster gave a strong enrichment of pathways linked to fatty acid metabolism,

for the presence of genes like *Ppara*, *Hacd2*, *Psapl1*, *Scd4*, *Elovl6*, *Gpat2*, *Acsf2*, *Pla2g5*, *Alox12*, *Pck1*, *Degs1*, *Acsbg1*, which are associated to sphingolipid and long fatty acid metabolism. This cluster also contains developmental genes (*Nrp2*, *Irx4*, *Mfng*, *Tshz2*, *Shroom3*, *Nat8f2*, *Ackr3*, *Celsr1*, *Ambra1*, *Fzd4*, *Sufu*, *Farp1*, *Slit3*, *Wnt4*, *Hoxa3*, *Slc26a8*, *Smoc1*, *Asb1*, *Etl4*, *Fgf1*, *Sik1*, *Ihh*, *Pitx2*, *Bmp8a*, *Zfp423*) and some genes that are part of the Wnt pathway (*Wnt4*, *Rspo1*, *Fzd4*, *Mmp7*, *Camk2b*, *Axin2*). ). Pretty similar to the first, the second cluster is enriched in terms involved in cell commitment and regulation of cell growth. Taken together, the decreased H3K27Ac marks in these regions in the vWAT would therefore suggest that upon HFD treatment the visceral fat undergoes a reduction in fatty acid metabolism and a perturbation in cell growth and cell differentiation, when compared to the scWAT.

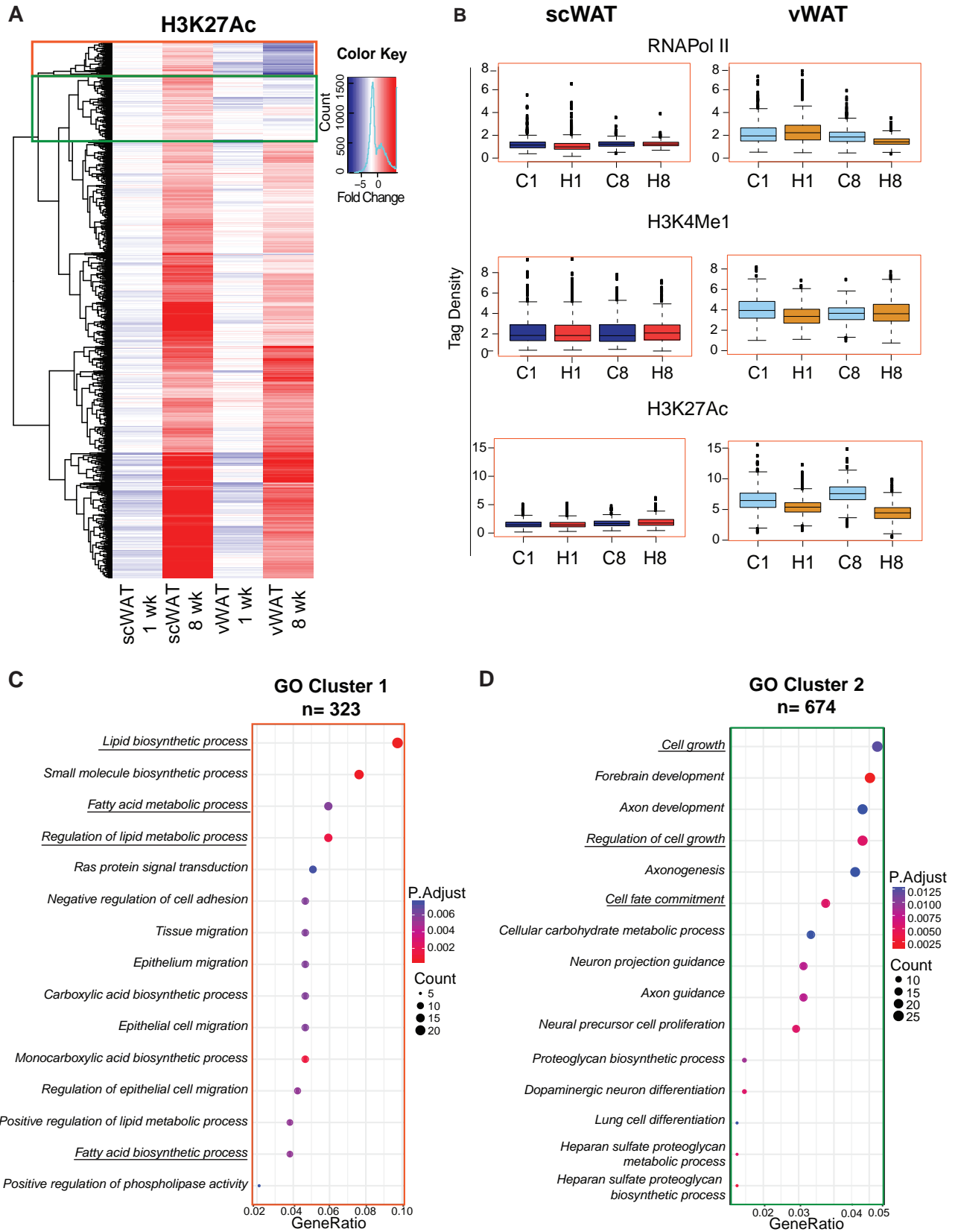
---

**Figure 18:** (A) ChIP-seq cluster analysis. Hierarchical cluster analysis and heatmap showing the Log fold (LogFC) change of genomic regions (5984), obtained with the comparison between control and HFD treated mice. In the panel, blue and red represent, respectively, LogFC lower and higher than 0. The orange and the green rectangle highlight the clusters of interest.

(B) Box plot of average tag density on the 359 regions in the cluster 1 (orange) for RNAPolIII, H3K4me1 and H3K27Ac.

(C& D) Pathway Enrichment analysis performed on genes annotated respectively in the orange or green clusters. In each panel the x-axis shows the gene ratio. The dots are coloured based on the significance of each pathway and the size represents the number of genes that are annotated in the pathways

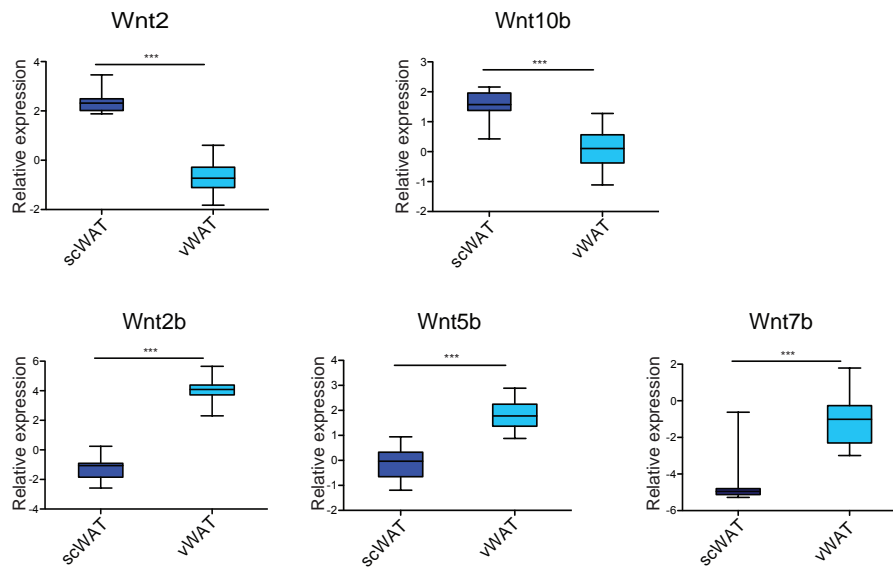




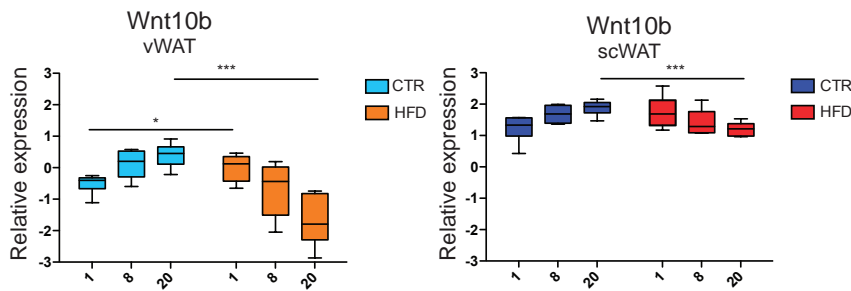
Among the different hits highlighted by ChIP-seq analysis, we were particularly interested in the Wnt pathway, which was represented both in cluster 1 (*Wnt4*, *Rspo1*, *Fzd4*, *Mmp7*, *Camk2b*, *Axin2*) and in cluster 2 (*Usp34*, *Nle1*, *Prickle1*, *Gsk3b*, *Tcf7l2*, *Src*, *Nfkb1*, *Dlx5*, *Mitf*, *Zfp703*, *Tnks*, *Cttnb1*, *Smad3*). Wnt is known to contribute to the regulation of adipocyte differentiation. We, thus, checked the expression of different Wnt genes, which have distinct properties with respect to adipogenesis. Interestingly, many Wnt genes are already differentially expressed in the vWAT and scWAT in control mice, with decreased *Wnt2* and *Wnt10b* and increased *Wnt2b*, *Wnt5b* and *Wnt7b*, in vWAT compared to scWAT (Figure 19A). This suggesting that Wnt pathway and its action might be intrinsically different in the two tissues. Considering the role of Wnt in controlling adipogenesis and knowing that defects in adipogenesis can have an impact on the generation of hypertrophic adipocytes, we hypothesized a possible involvement of Wnt as a crucial player in the different response of vWAT and scWAT to HFD diet. Consistent with this idea, *Wnt10b*, which is a well-known negative regulator of adipogenesis<sup>303,304</sup>, has an increased expression after 1 week of diet exclusively in the vWAT (Figure 19B). To further test the possible implication of the canonical Wnt pathway, we looked at the  $\beta$ -catenin phosphorylation status in the tissue. As shown in Figure 19C, the  $\beta$ -catenin phosphorylation was reduced in the vWAT exclusively, after 1 week of HFD. Lower level of phosphorylated  $\beta$ -catenin indicates that the protein is less targeted for proteasomal degradation and thus, free to access the nucleus and activates the transcription of anti-adipogenic genes.

Collectively these results show that *Wnt10b* and the activation of the canonical Wnt/ $\beta$ -catenin pathway may be important in differentiating the vWAT and scWAT early response to HFD. Moreover, this pathway could contribute to the regulation of the epigenetic landscape of the genomic regions that are linked to cell differentiation.

A



B



C

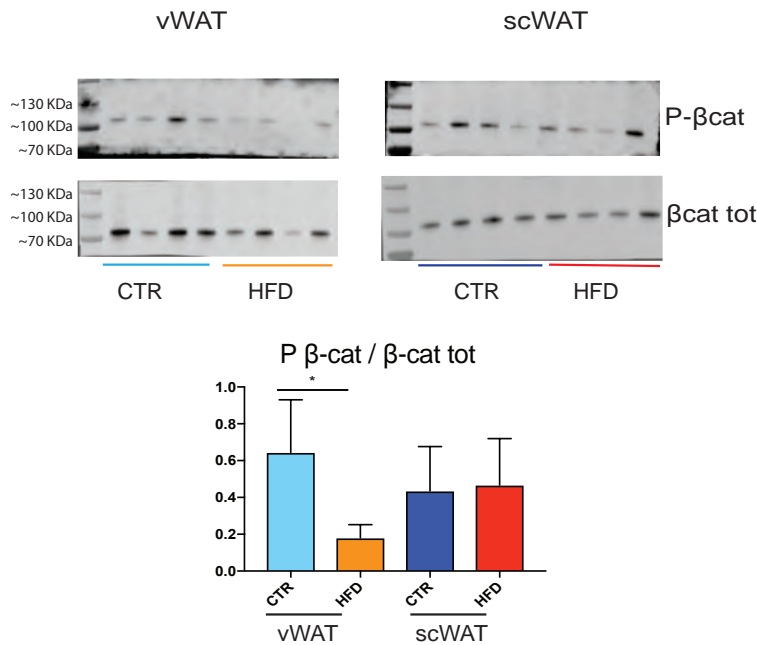


**Figure 19:** (A) Gene expression level of visceral or subcutaneous specific genes. The y-axis shows the normalized log count per million values. In each box plot is showed the average of the controls in the dataset (6 per time point). (B) Wnt10b expression level in visceral and subcutaneous adipose tissue. (C) Western blot performed with antibodies against the phosphorylated and the total β-catenin. In the picture four controls and four mice treated for 1 week with HFD are showed. Vinculin is used as loading control. On the bottom is showed the relative quantification as ratio between phosphorylated and total β-catenin.

---

## IV.2 Transcriptomic analysis emphasizes deregulation of histone genes in the vWAT

We then focused our attention on the transcriptomic changes occurring in the two tissues, in the acute response to the diet. To explore the early response to the diet in the two tissues at the transcriptional level, we compare control and HFD treated mice in the two tissues, separately and at the different time points (Figure 20). We used this analysis to retrieve the pValue and the Fold Change for further pathway analyses that we performed using an R tool called Signalling Pathway Impact Analysis (SPIA). This tool uses pVvalue of the entire dataset to highlight significant pathways. The result obtained, using the SPIA tool highlighted some common pathways deregulated in both vWAT and scWAT. Two main pathways emerged: ECM-receptor interaction and focal adhesion, likely reflecting the changes in a huge number of gene coding for membrane proteins (Figure 21; see also Figure 24). These changes in membrane proteins are possibly due to the hypertrophic response to the diet happening in the two adipose tissues.

In contrast, some pathways happened to be significant exclusively in one of the tissues. Specifically, Systemic Lupus Erythematosus (SLE) and Alcoholism were deregulated in vWAT. Since these pathways were meaningless for the biology of the adipose tissue, we identified, within these pathways, the genes that were changing with the diet (Table 3). A careful inspection of these genes revealed that both SLE and Alcoholism pathways in the vWAT were statistically significant because of changes in genes common to both pathways. Indeed, 27 histone genes, coding for all the variants of nucleosomal histones (H2A, H2B, H3, H4) were more expressed in HFD condition compared to control. The increase in histone gene transcription is usually associated to cell proliferation. We thus looked at the cell size distribution in sections colored

with hematoxylin and eosin of both vWAT and scWAT, in order to highlight changes in the number of cells in different range of size. As shown in Figure 22, we observed a striking difference in the two tissues in the frequency of the cell population ranging between 0 - and 50  $\mu\text{m}^2$ . Indeed, the count of small cells is dropping significantly in scWAT in response to HFD, while no change is occurring in vWAT. Finally, cells of intermediate size ranging from 50 to 300 $\mu\text{m}^2$ , are decreasing in vWAT in HFD condition, emphasizing the shift in cell size distribution towards a population of bigger cells. In line with the hypertrophic effect of the over-nutrition, a significant increase in the very big cells ( $> 1300\mu\text{m}^2$ ) was measured in both vWAT and scWAT.

Collectively, our results showed that the number of small cells is well maintained in the vWAT but not in the scWAT after 1 week of HFD, while hypertrophy, with increased frequency of big cells is present in the two tissues.

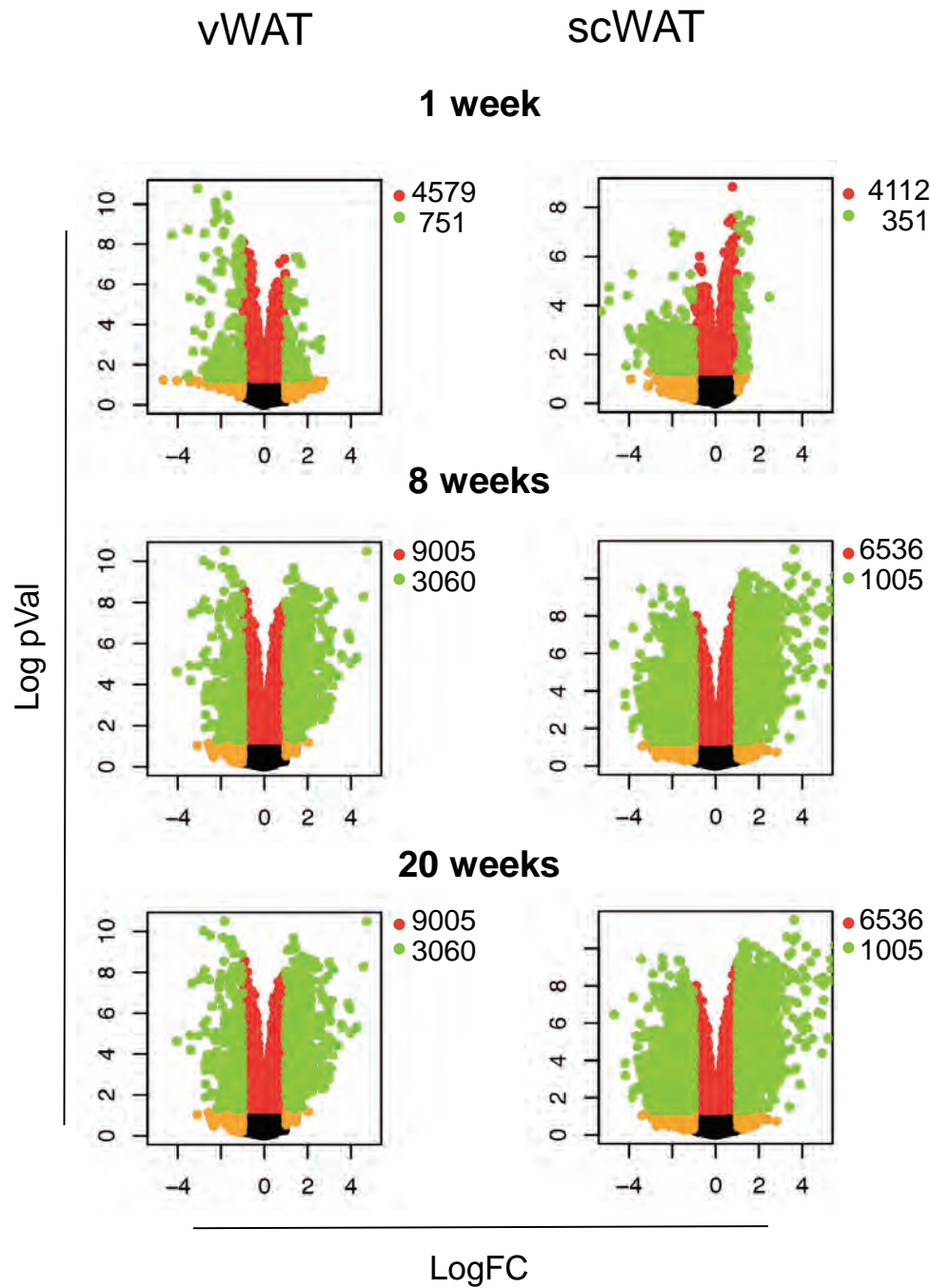


**Figure 20:** RNA-seq volcano plots. In each panel the x-axis and the y-axis represent respectively the Log fold change and the Log Pvalue of the comparison between control and HFD treated mice. Each dot represents a gene that is coloured in 1) red if its PValue is lower that 0.05, 2) green if its PValue is lower that 0.05 and the LogFC absolute value is higher of 1, 3) orange if its LogFC absolute value is higher of 1, 4) black if it is not falling in the other 3 categories

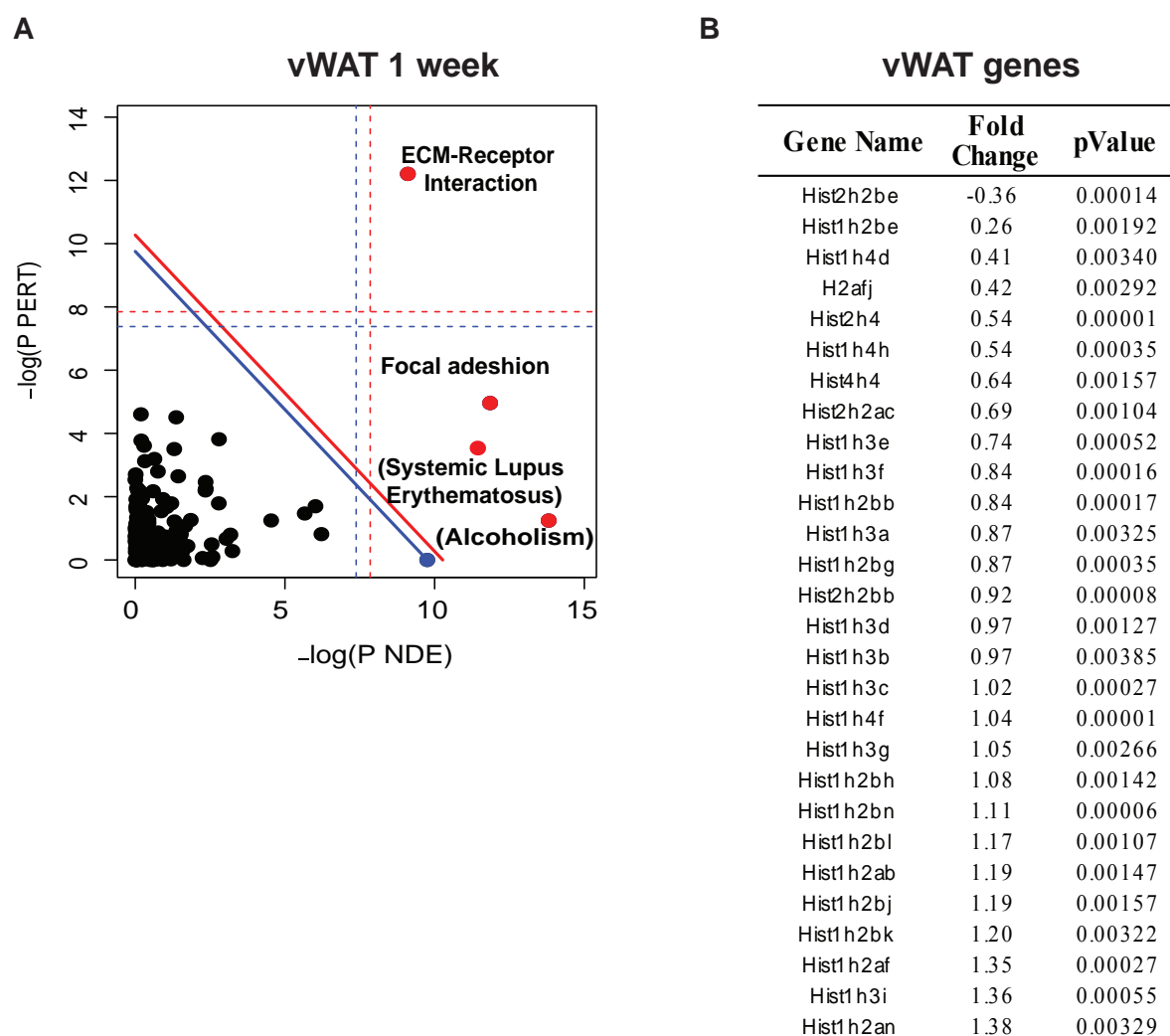


**Figure 21:** (A) Signalling Pathway Impact Analysis (SPIA) performed at 1 week. Two-dimensional plots illustrating the relationship between the two types of evidence considered by SPIA. The X-axis shows the over-representation evidence (PNDE), while the Y-axis shows the perturbation evidence (PERT). Each pathway is represented by a point. Pathways above the oblique red line are significant at 5% after Bonferroni correction, while those above the oblique blue line are significant at 5% after FDR correction. The vertical and horizontal thresholds represent the same corrections for the two types of evidence considered individually. (B) List of genes deregulated in the visceral adipose tissue, which are in common between Systemic Lupus Erythematosus and Alcoholism.

Systemic Lupus Erythematosus			Alcoholism		
Gene Name	Fold Change	p.Value	Gene Name	Fold Change	p.Value
Hist2h2be	-0.36	0.00014	Creb3l4	-1.39	0.00291
Hist1h2be	0.26	0.00192	Hist2h2be	-0.36	0.00014
Snrpb	0.31	0.00359	Hdac2	-0.24	0.00089
C4b	0.35	0.00525	Atf2	-0.18	0.00334
C1qb	0.38	0.00065	Gnas	0.17	0.00039
Hist1h4d	0.41	0.00340	Atf4	0.18	0.00373
C1qa	0.42	0.00057	Creb3	0.18	0.00038
H2afj	0.42	0.00292	Hist1h2be	0.26	0.00192
C1qc	0.44	0.00012	Calm3	0.27	0.00359
Hist2h4	0.54	0.00001	Hras	0.30	0.00251
Hist1h4h	0.54	0.00035	Ntrk2	0.31	0.00002
Hist4h4	0.64	0.00157	Hdac5	0.31	0.00268
Hist2h2ac	0.69	0.00104	Adora2a	0.36	0.00191
Hist1h3e	0.74	0.00052	Gnai2	0.37	0.00001
Hist1h3f	0.84	0.00016	Gnb2	0.38	0.00070
Hist1h2bb	0.84	0.00017	Creb3l1	0.39	0.00224
Hist1h3a	0.87	0.00325	Hist1h4d	0.41	0.00340
Hist1h2bg	0.87	0.00035	H2afj	0.42	0.00292
Hist2h2bb	0.92	0.00008	Hist2h4	0.54	0.00001
Hist1h3d	0.97	0.00127	Hist1h4h	0.54	0.00035
Hist1h3b	0.97	0.00385	Hist4h4	0.64	0.00157
Hist1h3c	1.02	0.00027	Hist2h2ac	0.69	0.00104
Hist1h4f	1.04	0.00001	Hist1h3e	0.74	0.00052
Hist1h3g	1.05	0.00266	Hist1h3f	0.84	0.00016
Hist1h2bh	1.08	0.00142	Hist1h2bb	0.84	0.00017
Hist1h2bn	1.11	0.00006	Hist1h3a	0.87	0.00325
Hist1h2bl	1.17	0.00107	Hist1h2bg	0.87	0.00035
Hist1h2ab	1.19	0.00147	Hist2h2bb	0.92	0.00008
Hist1h2bj	1.19	0.00157	Hist1h3d	0.97	0.00127
Hist1h2bk	1.20	0.00322	Hist1h3b	0.97	0.00385
Hist1h2af	1.35	0.00027	Hist1h3c	1.02	0.00027
Hist1h3i	1.36	0.00055	Hist1h4f	1.04	0.00001
Hist1h2an	1.38	0.00329	Hist1h3g	1.05	0.00266
			Adcy5	1.06	0.00000
			Hist1h2bh	1.08	0.00142
			Hist1h2bn	1.11	0.00006
			Hist1h2bl	1.17	0.00107
			Hist1h2ab	1.19	0.00147
			Hist1h2bj	1.19	0.00157
			Hist1h2bk	1.20	0.00322
			Hist1h2af	1.35	0.00027
			Hist1h3i	1.36	0.00055
			Hist1h2an	1.38	0.00329

**Table 3:** Deregulated genes in visceral adipose tissue upon 1 week of HFD. List of genes present in Systemic Lupus Erythematosus and alcoholism pathways with their Fold Change and p.Value .



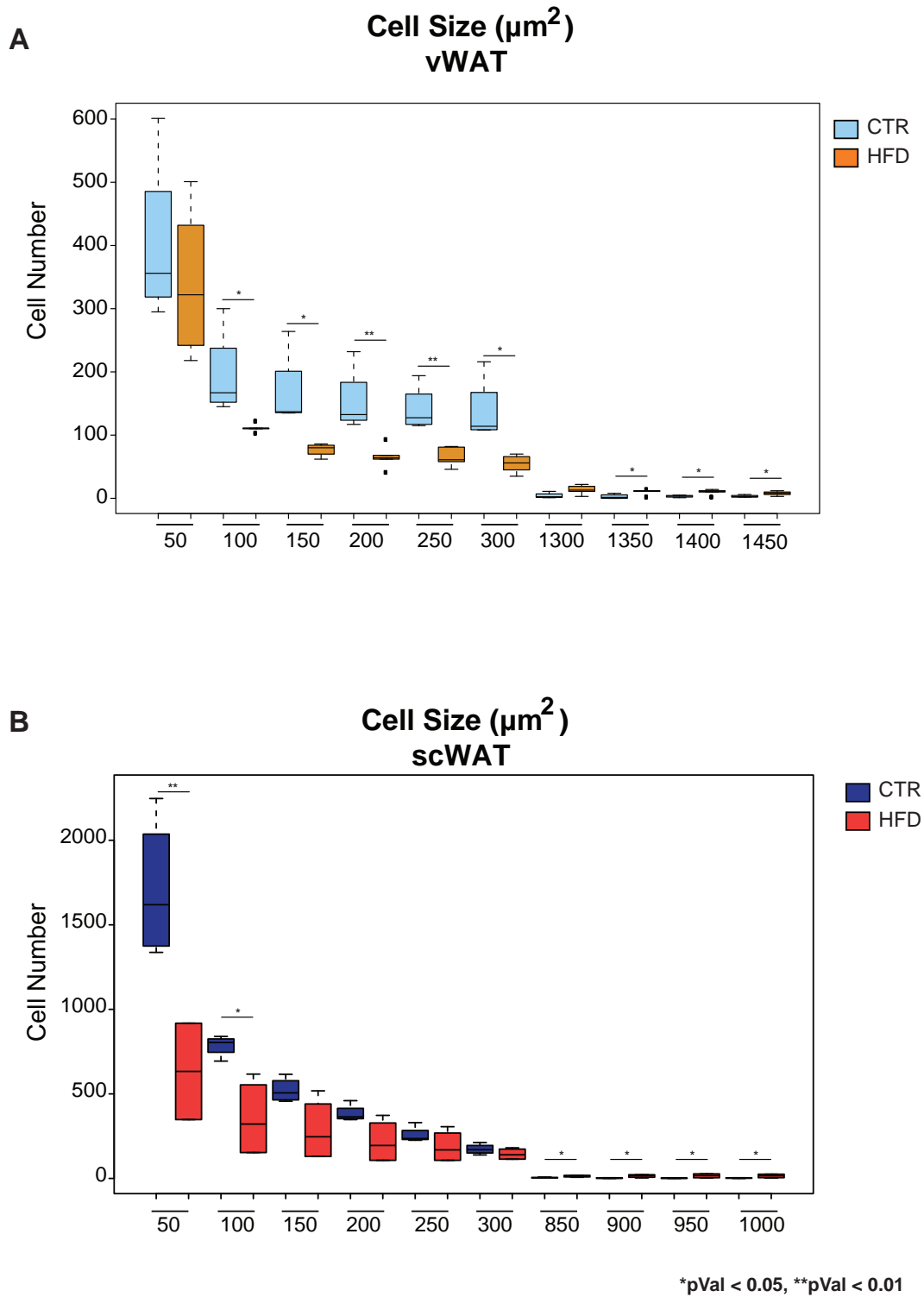


**Figure 22:** Boxplots of cell size distribution calculated on sections of visceral (A) and subcutaneous adipose tissue (B) in controls and 1 week HFD treated mice. The y-axis shows the cell number and the x-axis the cell size, divided in ranges of  $50 \mu\text{m}^2$ . A strong difference in cell size is observed in the first two size ranges ( $0-50$  and  $50-100 \mu\text{m}^2$ ) between controls and HFD treated mice. Cells bigger than  $800 \mu\text{m}^2$  are more frequent in HFD mice in both tissues.

### **IV.3 Modification of the mitochondrial activity in the scWAT**

The pathway enrichment analysis performed on the scWAT results gave the same kind of apparently not coherent pathways as we had seen in the vWAT. In the scWAT, the highlighted pathways were linked to central nervous degenerative disease, such as Huntington, Parkinson and Alzheimer disease (Figure 23A). Once again we looked at the individual genes in the pathways (Table 4). Similarly to the vWAT, we discovered that a group of genes, mainly belonging to the Electron Transport Chain (ETC), were shared between the three pathways. These mitochondrial genes were all down regulated in the scWAT upon 1 week of diet (Figure 23B).

To validate this observation, we looked at the protein levels of some of the ETC proteins by Western blot, as well as at the mitochondrial abundance estimated using the quantification of mitochondrial DNA in the two tissues in both control and HFD situation. As shown in Figure 24A, we could validate the reduction of the complexes I, III, IV in HFD condition in the scWAT. This reduction in mitochondrial protein is correlated to an overall reduction in the mitochondrial mass as showed by the reduction of mitochondrial DNA. Together, these observations support the hypothesis that the observed down-regulation of the mitochondrial respiration can be due to a global reduction of the mitochondrial number (Figure 24B).

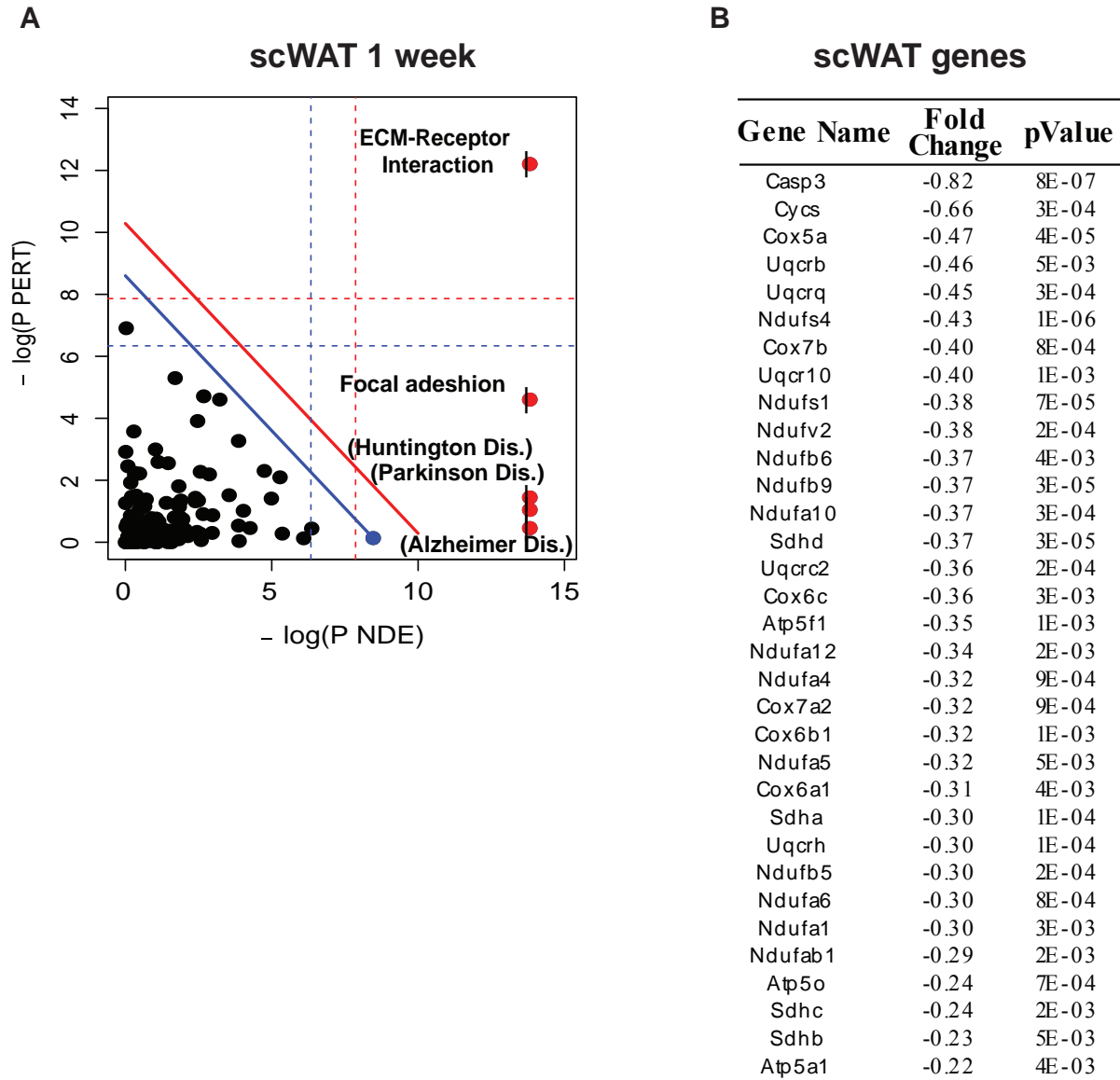


**Figure 23:** (A) Signalling Pathway Impact Analysis (SPIA) performed at 1 week. Two-dimensional plots illustrating the relationship between the two types of evidence considered by SPIA. The X-axis shows the over-representation evidence (PNDE), while the Y-axis shows the perturbation evidence (PTERT). Each pathway is represented by a point. Pathways above the oblique red line are significant at 5% after Bonferroni correction, while those above the oblique blue line are significant at 5% after FDR correction. The vertical and horizontal thresholds represent the same corrections for the two types of evidence considered individually. (B) List of genes deregulated in the subcutaneous adipose tissue, which are in common between Parkinson disease, Huntington disease and Alzheimer disease.

Parkinson Disease			Alzheimer Disease			Huntington Disease		
Gene Name	Fold Change	p.Value	Gene Name	Fold Change	p.Value	Gene Name	Fold Change	p.Value
Casp3	-0.82	8E-07	Casp3	-0.82	8E-07	Casp3	-0.82	8E-07
Ndufs4	-0.43	1E-06	Cycs	-0.66	3E-04	Cycs	-0.66	3E-04
Ubb	0.44	1E-05	Cox5a	-0.47	4E-05	Cox5a	-0.47	4E-05
Ndufb9	-0.37	3E-05	Uqcrb	-0.46	5E-03	Uqcrb	-0.46	5E-03
Sdhd	-0.37	3E-05	Uqcrq	-0.45	3E-04	Uqcrq	-0.45	3E-04
Cox5a	-0.47	4E-05	Ndufs4	-0.43	1E-06	Ndufs4	-0.43	1E-06
Ndufs1	-0.38	7E-05	Cox7b	-0.40	8E-04	Cox7b	-0.40	8E-04
Sdha	-0.30	1E-04	Uqcr10	-0.40	1E-03	Uqcr10	-0.40	1E-03
Uqcrh	-0.30	1E-04	Ndufs1	-0.38	7E-05	Ndufs1	-0.38	7E-05
Ndufv2	-0.38	2E-04	Ndufv2	-0.38	2E-04	Ndufv2	-0.38	2E-04
Ndufb5	-0.30	2E-04	Ndufb6	-0.37	4E-03	Ndufb6	-0.37	4E-03
Uqcrc2	-0.36	2E-04	Ndufb9	-0.37	3E-05	Ndufb9	-0.37	3E-05
Pink1	0.36	2E-04	Ndufa10	-0.37	3E-04	Ndufa10	-0.37	3E-04
Ndufa10	-0.37	3E-04	Sdhd	-0.37	3E-05	Sdhd	-0.37	3E-05
Uqcrq	-0.45	3E-04	Uqcrc2	-0.36	2E-04	Uqcrc2	-0.36	2E-04
Cycs	-0.66	3E-04	Cox6c	-0.36	3E-03	Cox6c	-0.36	3E-03
Atp5o	-0.24	7E-04	Atp5f1	-0.35	1E-03	Atp5f1	-0.35	1E-03
Cox7b	-0.40	8E-04	Ide	-0.34	3E-03	Ppif	-0.34	3E-03
Ndufa6	-0.30	8E-04	Ndufa12	-0.34	2E-03	Ndufa12	-0.34	2E-03
Ndufa4	-0.32	9E-04	Ndufa4	-0.32	9E-04	Ndufa4	-0.32	9E-04
Cox7a2	-0.32	9E-04	Cox7a2	-0.32	9E-04	Cox7a2	-0.32	9E-04
Atp5f1	-0.35	1E-03	Cox6b1	-0.32	1E-03	Cox6b1	-0.32	1E-03
Uqcr10	-0.40	1E-03	Ndufa5	-0.32	5E-03	Ndufa5	-0.32	5E-03
Cox6b1	-0.32	1E-03	Cox6a1	-0.31	4E-03	Cox6a1	-0.31	4E-03
Sdhc	-0.24	2E-03	Sdha	-0.30	1E-04	Sdha	-0.30	1E-04
Ndufab1	-0.29	2E-03	Uqcrh	-0.30	1E-04	Uqcrh	-0.30	1E-04
Ndufa12	-0.34	2E-03	Ndufb5	-0.30	2E-04	Ndufb5	-0.30	2E-04
Lrrk2	-0.27	2E-03	Ndufa6	-0.30	8E-04	Ndufa6	-0.30	8E-04
Cox6c	-0.36	3E-03	Ndufa1	-0.30	3E-03	Ndufa1	-0.30	3E-03
Ndufa1	-0.30	3E-03	Ndufab1	-0.29	2E-03	Ndufab1	-0.29	2E-03
Ppif	-0.34	3E-03	Atp5o	-0.24	7E-04	Atp5o	-0.24	7E-04
Cox6a1	-0.31	4E-03	Sdhc	-0.24	2E-03	Sdhc	-0.24	2E-03
Vdac2	-0.20	4E-03	Sdhb	-0.23	5E-03	Sdhb	-0.23	5E-03
Ndufb6	-0.37	4E-03	Atp5a1	-0.22	4E-03	Atp5a1	-0.22	4E-03
Atp5a1	-0.22	4E-03	Capn2	0.23	6E-04	Pparg	-0.21	2E-03
Uqcrb	-0.46	5E-03	Calm3	0.29	2E-03	Tfam	-0.21	6E-03
Ndufa5	-0.32	5E-03	Psen2	0.36	1E-05	Vdac2	-0.20	4E-03
Sdhb	-0.23	5E-03	Apbb1	0.37	9E-04	Creb3	0.16	1E-03
			App	0.41	9E-07	Hip1	0.27	2E-03
			Lrp1	0.48	5E-05	Cltb	0.34	2E-05
			Apoe	0.48	2E-05	Creb3l1	0.44	8E-04
						Dnah3	0.79	5E-03

**Table 4:** Deregulated genes in subcutaneous adipose tissue upon 1 week of HFD. List of genes present in Parkinson, Alzheimer and Huntington disease pathways, with their Fold Change and p.Value .

The scWAT was previously shown to harbor both white and beige adipocytes<sup>231,242</sup>, and therefore to have a higher mitochondrial mass compared to the visceral fat. To investigate if tissue composition was altered in scWAT upon HFD, we performed histological analysis to quantify the number of beige adipocytes (UCP1<sup>+</sup>) in control and HFD treated mice. As shown in Figure 24C, the scWAT appear to have many cluster of small UCP1<sup>+</sup> cells with multi-locular lipid droplets, characteristic of beige adipocytes, which are strongly reduced upon HFD. The reduction in UCP1<sup>+</sup> cells also correlated with a drop in the number of cells ranging up to 100  $\mu\text{m}^2$  (Figure 22B), suggesting that the small cells, which are lost upon HFD, are possibly contributing to the hypertrophic expansion of white UCP1<sup>-</sup> adipocytes.

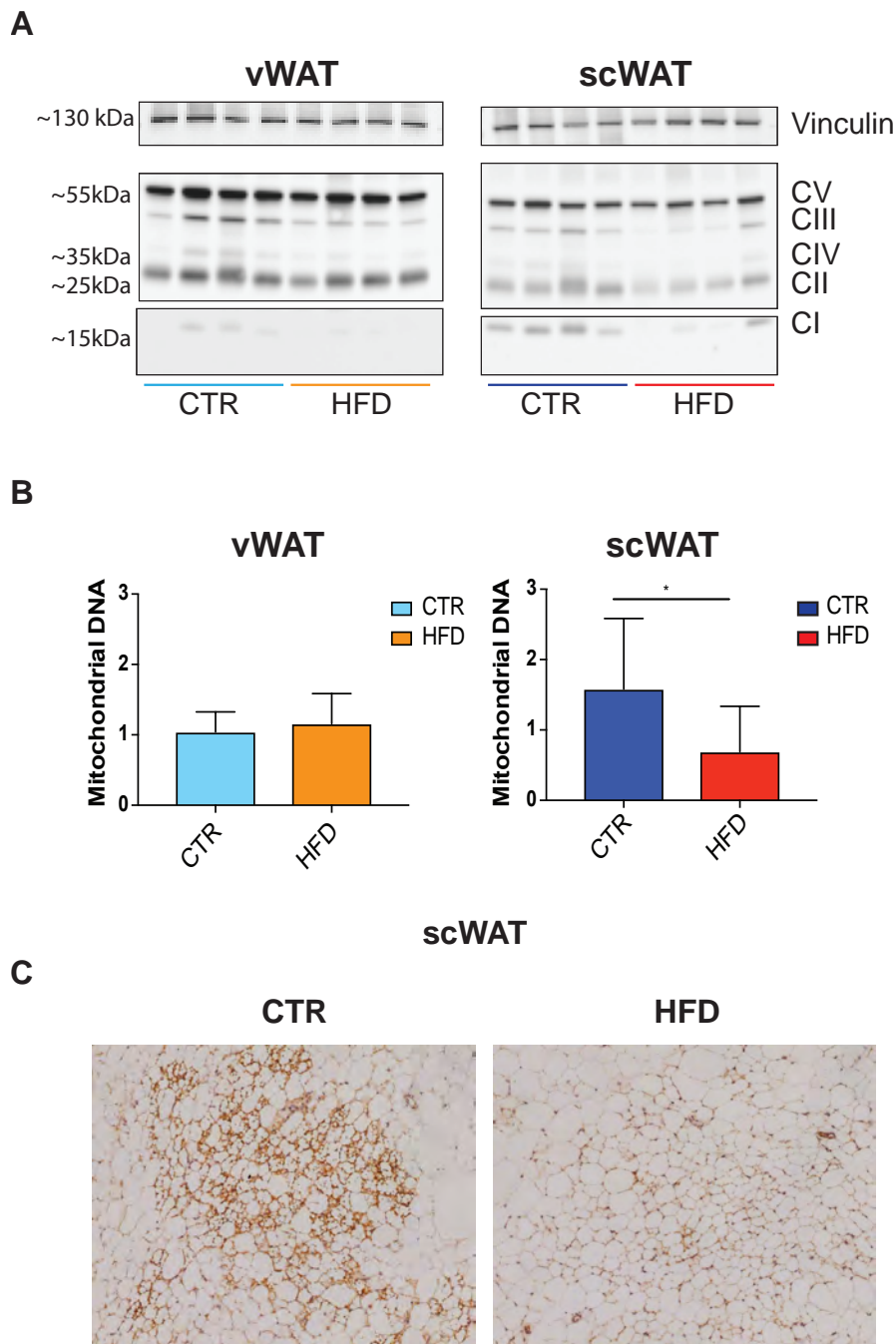


**Figure 24:** (A) Western blot performed using a cocktail of antibodies against different proteins of the electron transport chain complexes. In the picture four controls and four mice treated for 1 week with HFD are showed. Vinculin is used as loading control. (B) Mitochondrial DNA quantification. The y-axis represents the ratio between the expression of a mitochondrial 16S and a genomic gene ( $\ln 11$ ). (C) UCP1 immunohistochemistry. On the left control subcutaneous adipose tissue section where clusters of UCP1+ cells are visible. A reduction in UCP1+, small cells is detected in the subcutaneous adipose tissue of HFD treated mice, right panel. \* $p$ Val < 0.05.

### **IV.3.1 Adipocytes in culture maintain the characteristic of their origin, visceral or subcutaneous, but not the specific response to lipid overload**

Our results on WAT epigenomic and transcriptomic changes showed that one aspect that is really differentiating vWAT and scWAT acute response to HFD relates to the ability of the tissue to remodel its adipocyte cell population through adipocyte differentiation and proliferation. In order to dig into the mechanisms of how HFD treatment affects the adipogenic potential, we wondered whether the HFD would exert its effect directly on adipocytes and/or the action on cell differentiation is mediated by the tissue environment. To dissect these two components, we isolated the stromal vascular fraction (SVF), either from vWAT or scWAT, and differentiated adipocyte progenitors (APs) *in vitro*. APs are multipotent stem cells, which can fully differentiate into mature adipocytes. These are different from the pre-adipocytes that are one step further, as they already went through the first step of adipocyte differentiation.

We first assayed the efficiency of the differentiation protocol by checking the phenotypic change of these cells. As shown in Figure 25A and C, both vWAT and scWAT-derived primary APs efficiently differentiate to adipocytes and no noticeable differences were observed between the two types of cells. As expected, the differentiation was accompanied by an increased *Fabp4* expression compared to non-differentiated cells, further proving their transition to mature adipocytes. We then analyzed gene expression of specific markers of the two original adipose tissue depots, in order to check whether, upon a prolonged time in culture, the cells maintained their tissue identity. In particular, we checked some of the genes that we confirmed to be differentially expressed in the two tissues (see RNA-seq analysis, paragraph III page 109). Our results show that the expression of tissue specific markers, such as *Wt1*, *Tcf21*, *Tbx15* and *Lhx8*,

is kept along the 14 tested days and confirm that these cells in culture maintain tissue properties (Figure 25B).

We then inspected the mechanism by which HFD influences the adipogenic potential in the visceral adipose tissue by measuring the gene expression level of mature adipocyte markers, such as *Fabp4*, Peroxisome proliferator-activated receptor  $\gamma$  (*Pparg*) and CCAAT/ enhancer-binding protein  $\alpha$  (*Cebpa*). *In vivo Pparg* expression is reduced in both vWAT and scWAT at 1, 8 and 20 weeks, with a more marked drop in vWAT (Figure 26A). A similar behavior is observed for *Cebpa* whose expression, however, is not changing after 1 week of diet. Finally, an opposite regulation between vWAT and scWAT is occurring in the level of expression of *Fabp4*. In vWAT *Fabp4* levels increase after 1 week of diet, and then go down at 8 and 20 weeks. On the other hand, in the scWAT, the expression of this gene is increasing at both 1 and 8 week of HFD and remains stable at 20 weeks.

To mimic HFD effect *in vitro*, we treated differentiated adipocytes from vWAT and scWAT with palmitic acid (PA) during 24, 48 and 96 hours, because it is one of the widely used FA to induce inflammatory response in cultured adipocytes<sup>305</sup>. As shown in Figure 26B, the treatment with PA is not mimicking the effect of the HFD in the tissue with respect to the expression level of *Fabp4*, *Pparg* and *Cebpa*. The only significant change is a decreased expression of *Fabp4* after 96 hours of PA exposure on the primary adipocytes. In adipocyte cultures from scWAT treated with PA, all the tested genes were increased after 24h compared to the vehicle-treated, albeit these effects were fluctuating, with a reduction at 48h and an increase at 96h. These small changes in gene expression, even if statistically significant, were not considered as relevant due to their fluctuation. Thus, the treatment with PA of vWAT adipocyte culture is not inducing the same reduction of the adipogenic potential observed with the HFD in the vWAT.



Finally, following our observations of the changes affecting the action of the canonical Wnt/ $\beta$ catenin pathway in vWAT, we evaluated the expression level of *Wnt10b*. Unexpectedly, this gene was not expressed in either APs or mature adipocytes. The absence of WNT10b in the culture system may represent an explanation to the fact that, by mimicking the HFD treatment *in vitro*, we could not reproduce the effect on adipocyte differentiation observed in mice. Moreover, one possible explanation to the lack of Wnt10b in primary cultures might be that Wnt10b is not expressed by adipocytes, but by other cells that are present in the tissue. Interestingly, in our hands, primary culture cells obtained from vWAT were expressing Itgax (CD11c), a known marker of activated macrophage cells, suggesting that these last are probably not those cells expressing Wnt10b (Figure 26C).

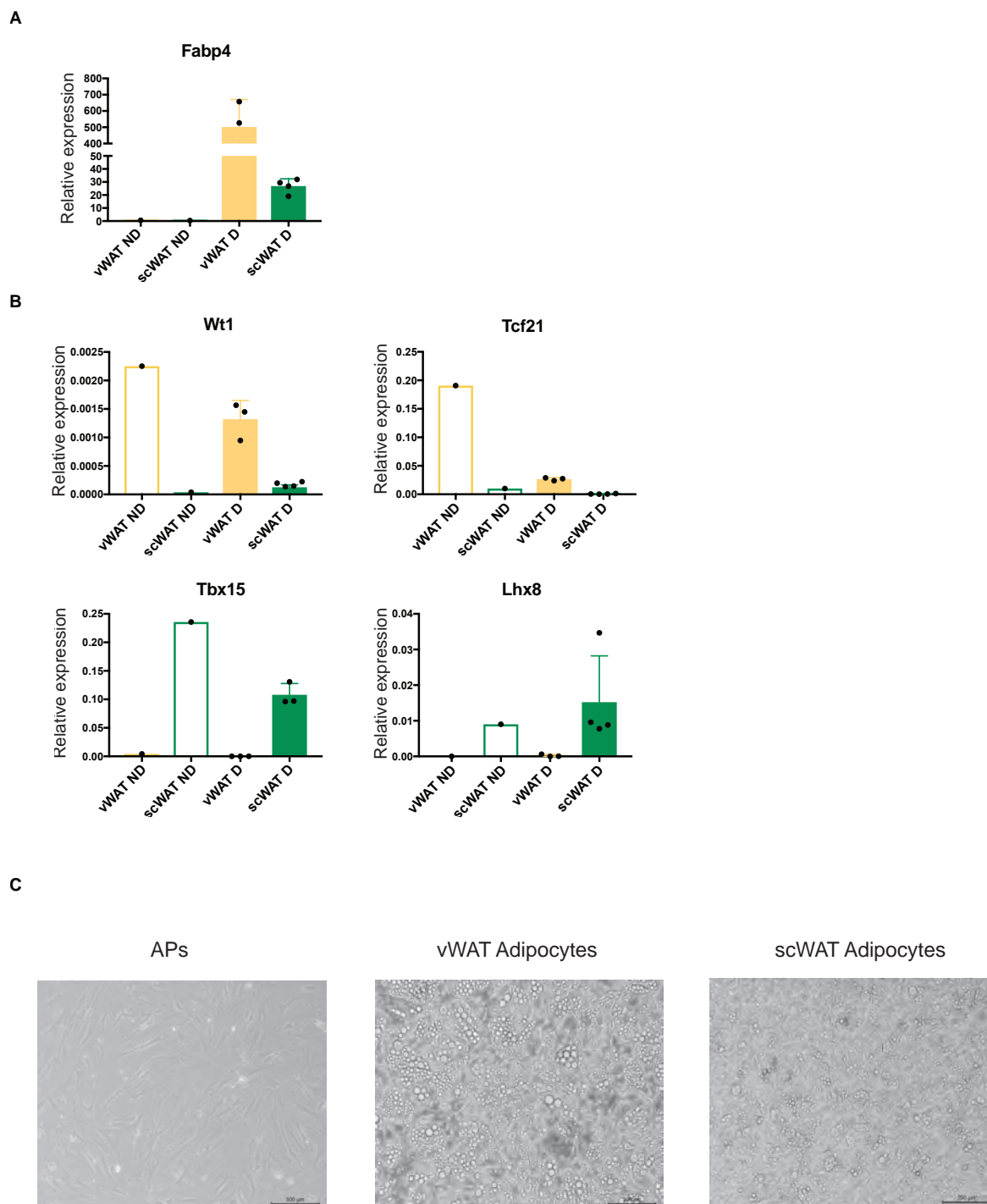


**Figure 25:** (A & B) Gene expression levels measured in non-differentiated or differentiated primary adipocytes isolated from visceral or subcutaneous adipose tissue. (A) *aP2* is used as marker of mature adipocytes. (B) Selection of genes that are visceral (*Wt1* and *Tcf21*) or subcutaneous (*Tbx15* and *Lhx8*) specific. (C) Adipocytes progenitors (APs) and mature adipocytes morphology. Before the starting of the differentiation protocol the APs show a fibroblast like shape that changes to a round lipid filled shape after some days of treatment with the differentiating cocktails.

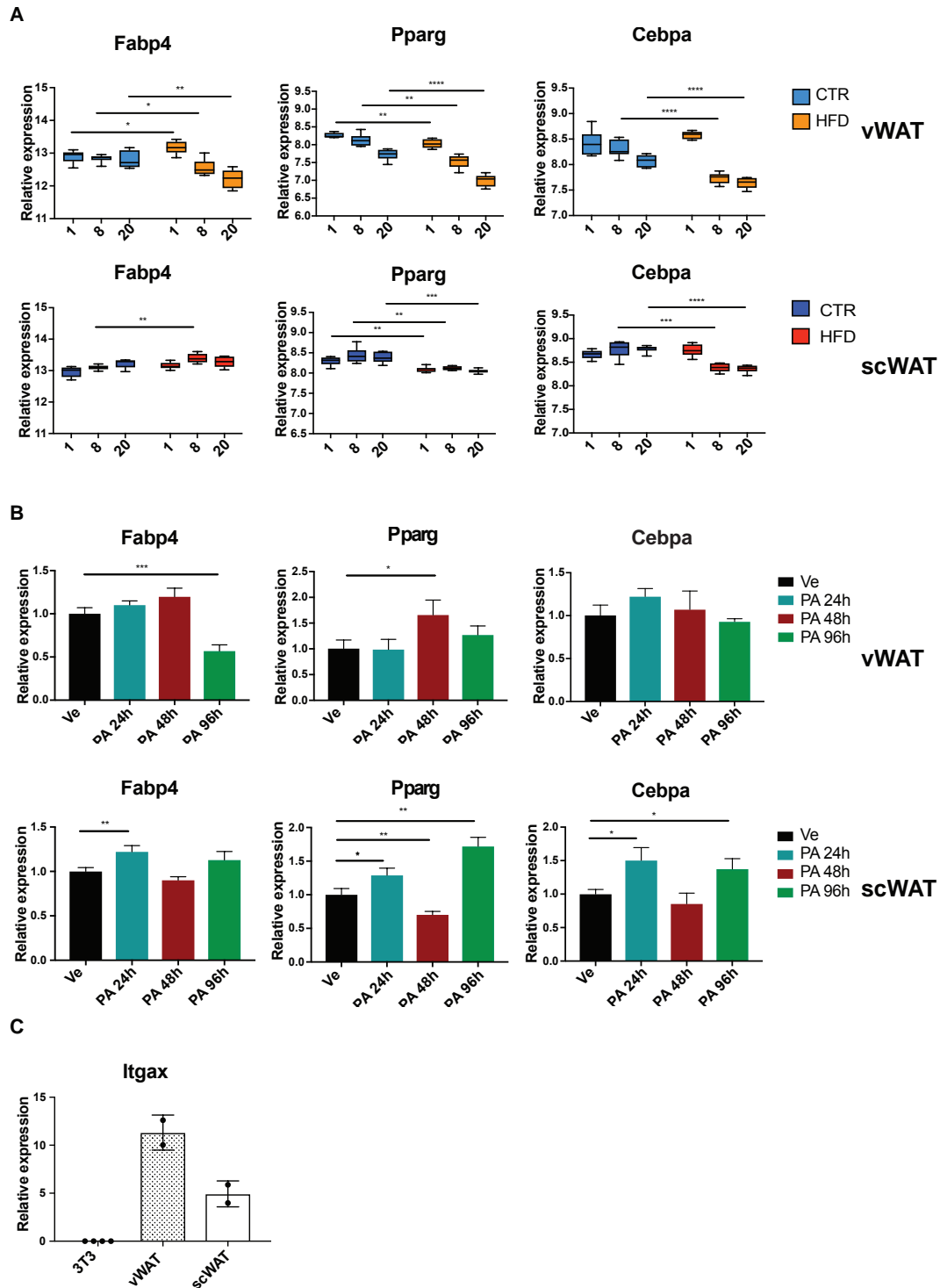


**Figure 26:** Gene expression levels of mature adipocyte specific genes measured in: (A) visceral and subcutaneous adipose tissue in controls and HFD treated mice for 1, 8 and 20 weeks; (B) differentiating cells treated with vehicle (ethanol 100%) or palmitic acid (200 $\mu$ M) for 24, 48 or 96 h. (C) *Itgax* expression level in 3T3 cells or primary cells isolated from visceral or subcutaneous adipose tissue \* $p$ Val < 0.05, \*\* $p$ Val < 0.01, \*\*\* $p$ Val < 0.001, \*\*\*\* $p$ Val < 0.0001.

Collectively, our data suggest that, upon 1 week of HFD feeding, vWAT undergoes a possible alteration in cell growth and differentiation sustained by epigenetic changes at the level of histone acetylation and RNAPol II occupancy. The increased expression of Wnt10b and the changes in  $\beta$ -catenin phosphorylation indicate that the canonical Wnt/ $\beta$ -catenin pathway may block cell differentiation. Moreover, the *in vitro* results and the finding that Wnt10b is not expressed in cell culture system suggest that not only adipocytes, but also other cells in the tissue matrix are involved in this mechanism. On the other hand, the main effect observed in scWAT is a reduction in mitochondrial activity and mass, as well as in beige adipocytes quantity.

In conclusion, the differences in the response to over-nutrition seem mediated by tissue intrinsic differences, which might ultimately lead to the different response to over nutrition in the two adipose tissue depots.

## V Analysis at the 8-week time-point confirmed the prevalence of inflammation in the vWAT

To explore the gene expression changes occurring in vWAT and scWAT when the inflammatory response is already established, we performed pathway analysis on the intermediate time point (8 weeks). Similarly to what we did at 1 week, we applied the SPIA tool to highlight the biological pathways differently deregulated in the two adipose tissues. The results obtained showed a clear inflammatory response in the vWAT where we observed a number of pathways linked to inflammation, including NF- $\kappa$ B and TNF $\alpha$  signaling (Figure 27). A substantial number of pro-apoptotic genes were also deregulated (*Endog*, *Aifm1*, *Birc2*, *Akt2*, *Capn2*, *Casp9*, *Nfkb1*, *Tnfrsf1a*, *Traf2*, *Dffa*, *Fas*, *Trp53*, *Casp3*, *Tradd*, *Map3k14*, *Casp8*, *Bax*, *Tnfrsf10b*, *Apaf1*, *Tnf*). This increased transcription of pro-apoptotic genes nicely fits with the hypothesis that the vWAT undergoes a hypertrophic expansion until the mature adipocytes reach their maximal size, after which the process of apoptosis is engaged due to the FA overload. This increased cell death could be at the basis of the inflammatory progression in this tissue, where the macrophages have the role of cleaning up the cell remnants and form the known crown-like structures around the dead adipocytes<sup>48</sup>. In the scWAT instead, there is a lower number of statistically significant deregulated pathways, reflecting a minor or absent inflammatory response. Interestingly, we observe among the pathway Cell Cycle and Systemic Lupus Erythematosus. As for the 1-week pathway analysis, the SLE pathway is appearing as significantly deregulated because of the increased expression of histone genes. This may suggest that the scWAT could go through a hyperplastic expansion only at this stage, with the activation of adipocyte progenitor expansion.

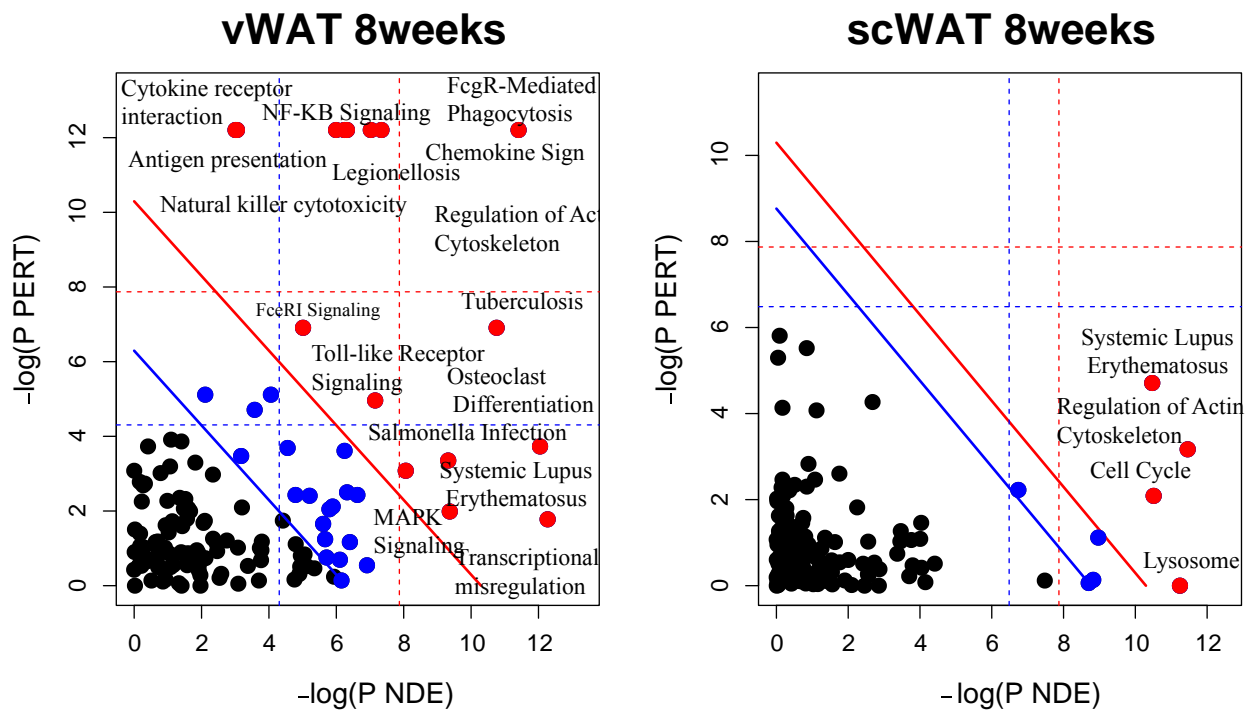


**Figure 27:** Signalling Pathway Impact Analysis (SPIA) performed at 8 weeks. Two-dimensional plots illustrating the relationship between the two types of evidence considered by SPIA. The x-axis shows the over-representation evidence ( $P_{NDE}$ ), while the y-axis shows the perturbation evidence ( $P_{PERT}$ ). Each pathway is represented by a point. Pathways above the oblique red line are significant at 5% after Bonferroni correction, while those above the oblique blue line are significant at 5% after FDR correction. The vertical and horizontal thresholds represent the same corrections for the two types of evidence considered individually.

## VI Omics integration

Since one of the ambitious goal of the project was to integrate different -omics datasets, namely the ChIP-seq, RNA-seq and Metabolomics, a conspicuous part the work was focused on the research and application of methods able to integrate datasets with very different kind of variables, i.e. metabolites levels and gene expression. For this purpose, we decided to apply a series of multivariate analysis, contained in the R package mixOmics with the final goal of identifying some candidate genes and metabolites, which could explain the different tissue behavior upon HFD treatment<sup>306</sup>. These bioinformatic approaches are well suited for large datasets where the number of variables (genes, metabolites and genomic regions) are much higher compared to the number of samples (biological replicates) and have the big advantage of reducing the dimensionality of the dataset by generating new variables, called components, which are created by the combinations of all the variables in the data. These components are then used to study the correlation between variables of the different dataset that should be integrated.

We performed the analysis at the early and intermediate time-point (1 & 8 weeks). To identify the key differences between vWAT and scWAT, we performed the analysis to contrast the response to HFD in the two tissues using a tool called DIABLO (Data Integration Analysis for Biomarker discovery using Latent variable approaches for Omics studies)<sup>307</sup>. DIABLO is applying a supervised Generalized Canonical Correlation Analysis (sGCCA) in order to identify correlated (co-expressed) variables, measured in heterogeneous dataset, which can explain the categorical outcome of interest (supervised analysis).

### VI.1.1 Data set preparation for integration

One important requirement for the application of this tool is that the variables in the different datasets are measured on the same samples. For this reason, the results from the untargeted metabolomics, that was performed in single mice, were averaged in pools containing the same mice as the RNA-seq, in order to have 6 replicates per condition.

The second important step is the refinement of the datasets, which is necessary to eliminate the possible noise coming from the entire dataset. Indeed, for this particular analysis, it is better to focus on a selected set of variables that are extremely significant for the biological output of interest. Thus, we selected a subpart of genes and metabolites, retrieving only those contributing the most to the differences in the response to the diet at 8 weeks between the two tissues.

For the RNA-seq, this step was performed using Limma, which fits samples into a linear model, and the following comparisons:

- Tissue difference in controls; subcutaneous CTR vs visceral CTR (SC CTR –V CTR)
- Tissue difference in HFD; subcutaneous HFD vs visceral HFD (SC HFD –V CTR)
- Interaction (V HFD –V CTR) - (SC HFD –SC CTR)

These comparisons returned a list of genes (5741 and 4717 for the 1 and 8 weeks, respectively), whose differences are statistically significant when comparing visceral and subcutaneous adipose tissue and upon HFD are uniquely regulated in the visceral fat. This analytical strategy was chosen because of the interest in identifying genes that could explain the progression of the inflammatory response in the vWAT.

The metabolomic dataset was refined by applying a Partial Least Squares Discriminant Analysis (PLS-DA), which is a supervised statistical method used for predictive model, where the difference between samples is maximized according to a known discriminative variable. In this case the discriminative variable was applied to the tissue difference (scWAT vs. vWAT)



independently of the diet. This method enabled us to identify 700 and 208 metabolites out of 1783 for the 1 and 8 weeks, respectively, which were extremely significant in the comparison between the tissues.

Once the datasets were refined, we put the different datasets together defining the blocks, in this case RNA-seq and Metabolomics, in which we want to evaluate the correlation. The second important step was to establish the optimal number of variables to select in each block. This was done by running a simulation model on a small random set of variables of the two blocks, which provide the number and the selected variables that can be used for the validation model.

MixOmic is providing many tools for graphical interpretation of the correlation between variables of the different blocks. The one that, for us, was the most interesting is the network which is plotting the variables with different colors, according to the dataset i.e. RNA-seq or metabolomics, as well as colored edges connecting these variables, representing the degree of correlation (from 0 to 1).

The networks obtained represent genes and metabolites, in red and light blue, respectively. Each node is linked by edges colored in green or red based on the correlation degree (Figure 28 & 29). The plot obtained at 8 weeks identified three different clusters. The first cluster analyzed can be associated to the basal difference of the tissue, since the genes appearing were already identified as being vWAT or scWAT specific (eg, *Wt1*, *Tcf21*, *Lhx8*, *Muc16*, *Tbx15*). Interestingly, all the metabolites present in this cluster are positively correlated to the scWAT specific genes. For instance, we observe the presence of many derivatives of glutamic acid, such as N-acetyl-aspartyl glutamic acid (NAAG), N-acetyl-aspartic acid (NAA) and N-acetyl glutamic acid (NAG). The amount of these metabolites is, indeed, much higher in control scWAT compared to vWAT. By inspecting the network obtained at 1 week we found, again, a cluster of genes and metabolites that are associated to the tissue differences. Indeed, it contains *Tbx15* and *Tcf21* together with

other genes that are transcribed more either in scWAT (*Shox2*, *Zfhx4*) or in vWAT (*Col6a5* and *Prepl*). As for the 8 weeks, we find NAAG and NAA as metabolites correlated to these genes, further suggesting that this is a signature of the tissue irrespectively of the diet and the mouse age.

The second cluster, observed in the network at 8 weeks, contains a mix of genes, some linked to cell differentiation (*Meis1*, *Gata6*, *Hoxa5*) and others to oxygen availability and hypoxia (*Agt* and *Hif3a*). These genes have a common behavior in their expression. On the one hand, we have genes whose expression is higher in basal condition in the scWAT (*Pcolce2*, *Kcnj14*) and then significantly upregulated with the diet in both tissues. On the other hand, we have genes that are more expressed in the vWAT in control condition and which are downregulated with the diet in both tissues. Interestingly, among the co-expressed metabolites we find glutamic acid and malic acid, whose levels are known to be increased in obesity in vWAT<sup>308</sup>. Glutamic acid, in our data set, is more abundant in scWAT in control condition but its levels increase with the diet only in the vWAT. A corresponding cluster was not clearly seen in the plot at 1 week. However, we find Glutamate Pyruvate Transaminase (*Gpt*) in one of the clusters in the network, suggesting that glutamate metabolism could be affected with the diet in the vWAT.

The last inspected cluster at 8 weeks contains a number of lipid species, Di-acyl glycerol (DGs), mono-acyl glycerol (MGs) and 2-arachidonoyl glycerol (2-AG) that are all upregulated in vWAT only after 8 weeks of diet. The 2-AG is an endogenous agonist of the cannabinoid receptors and a known regulator of food intake, which exerts an effect on fasting glycaemia and triglyceride levels in humans<sup>309,310</sup>. Interestingly, all the lipids becoming more abundant in vWAT are relatively long species with high number of carbon molecules (>C40). The only metabolite that

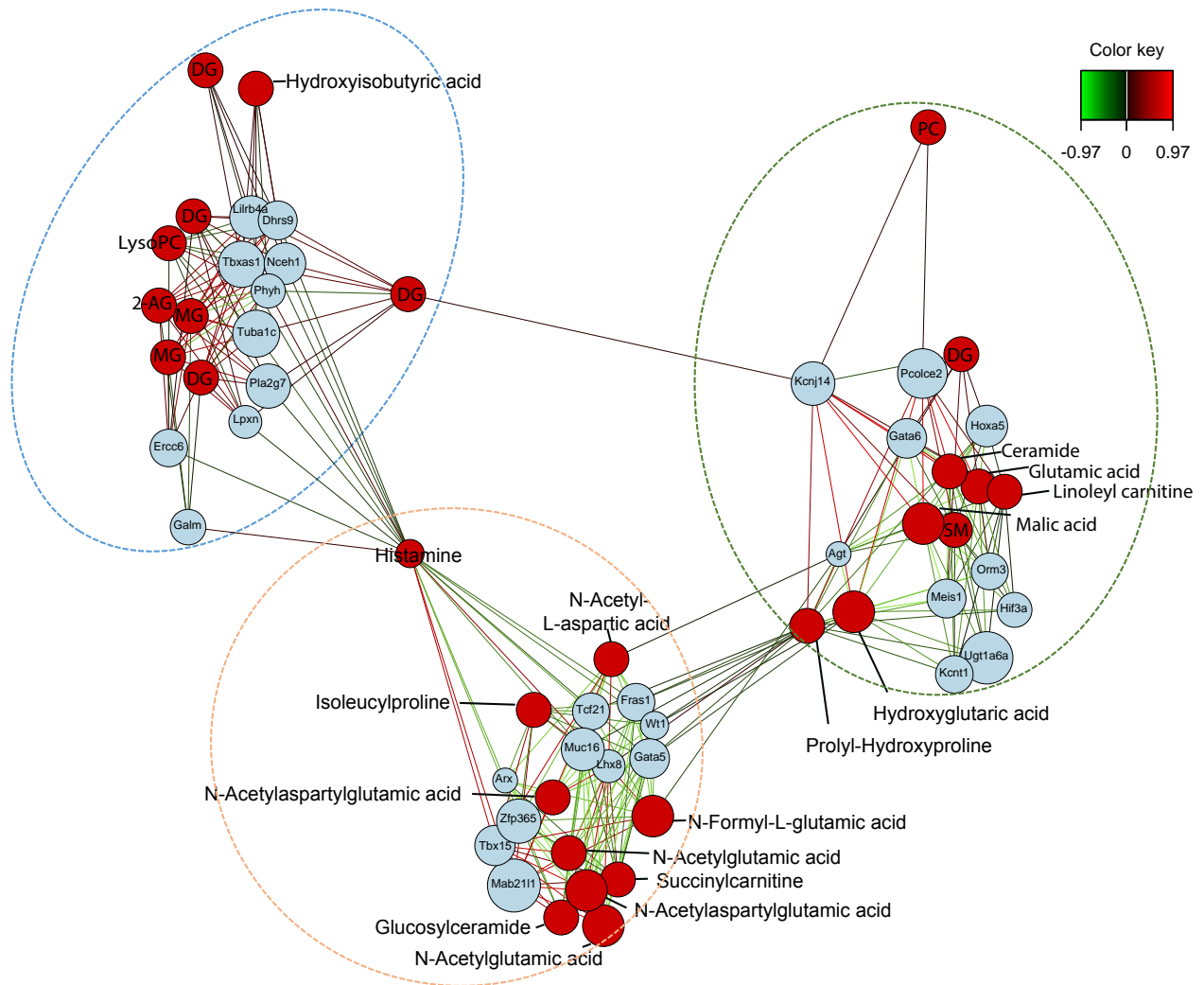


**Figure 28:** Network generated using DIABLO in R, showing the integration of RNA-seq and metabolomics at 8 weeks. In the pictures the red and the light blue nodes are metabolites and genes respectively. Each red node is linked to one or more blue one by an edge that can be red or green based on the positive or negative correlation between the corresponding gene and metabolite. The orange, the green and the blue dashed lines indicate cluster 1, 2 and 3, respectively.

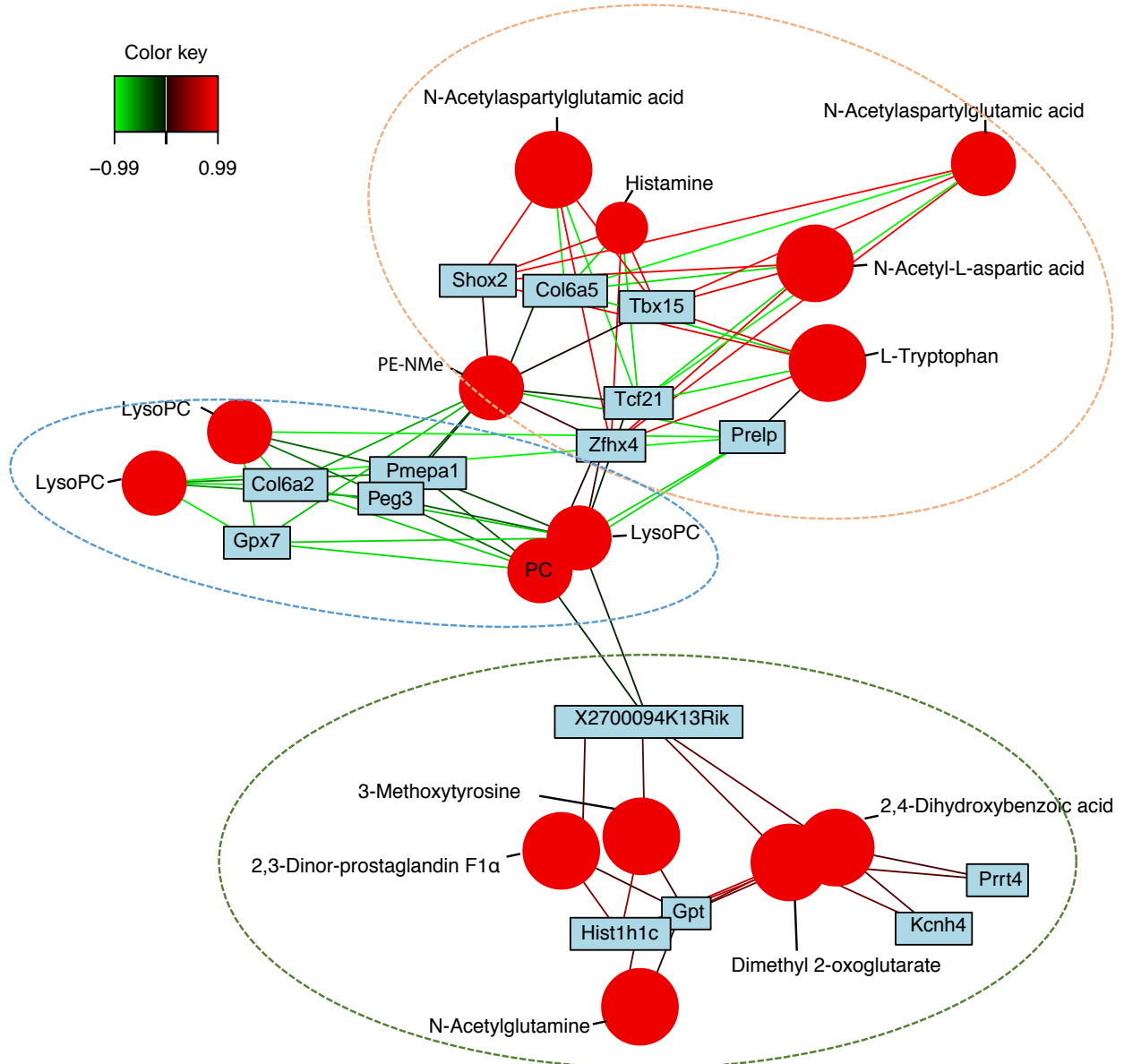


**Figure 29:** Network generated using DIABLO in R, showing the integration of RNA-seq and metabolomics at 1 week. In the pictures the red and the light blue nodes are metabolites and genes respectively. Each red node is linked to one or more blue one by an edge that can be red or green based on the positive or negative correlation between the corresponding gene and metabolite. . The orange, the green and the blue dashed lines indicate cluster 1, 2 and 3, respectively.

has a negative correlation with the genes in the cluster (Lyso- Phosphatidyl Choline, LysoPC) has instead a lower number of carbons (C24). Moreover, genes important for lipid metabolism appear in this cluster, such as the Phospholipase A2 group VII (*Pla2g7*) and the Dehydrogenase/reductase SDR family member 9 (*Dhrs9*). Interestingly, we observed a similar behavior in the network produced with the 1-week data set. Indeed, the lipid species highlighted at 1 week, LysoPc and PC, have all less than 28 carbons and are all downregulated with the diet in the two tissues.

The fact that the level of 2-AG, DGs, and MGs are significantly increased only in vWAT at 8 weeks, suggests that this cluster may be linked with the inflammatory response.

Collectively, pathway analysis and data integration approaches allowed to highlight the known differences in the inflammatory response between vWAT and scWAT. In addition, the data integration performed with DIABLO brought new interesting hypotheses on the intrinsic difference of the tissues and the characterization of the different response to over-feeding. One of these hypotheses, regarding the increased level of 2-AG in the vWAT upon HFD treatment is presently explored by Nasim Bararpour, from the group of Aurélien Thomas, in the frame of the collaborative project InflaWAT.



# **Discussion**

## **I Overview**

The overall aim of this thesis was to highlight the epigenetic and transcriptomic changes occurring along with the progression of obesity in the white adipose tissue (WAT). Our particular interest was in dissecting the modifications occurring in two different white depots, the visceral (vWAT) and the subcutaneous (scWAT) adipose tissues, because of their different susceptibility to develop inflammation upon prolonged over nutrition. Of note, inflammation is known to play a major role in the development of obesity-related metabolic diseases, such as insulin resistance and type 2 diabetes (T2D)<sup>2,171</sup>. The vWAT, more than the scWAT, is known to be one of the first site where the obesity-induced chronic, systemic and low grade inflammation, also known as metaflammation, originates<sup>24,215,311</sup>. Comparing the early responses of these two tissues would thus give some insights in the molecular mechanisms, either contributing to inflammation in the vWAT or protecting the scWAT from such a detrimental event.

To achieve this goal, we used a mouse model of diet-induced obesity and we performed ChIP-seq, RNA-seq and Metabolomics on vWAT and scWAT at different steps. The time points were chosen according to different stages of obesity development, namely the acute response (1 week), the appearance of macrophage infiltration in vWAT (8 weeks) and the chronic inflammation (20 weeks).



## **II Power and limits of the tools used**

### **Pathways analyses**

RNA-seq is a high-throughput gene expression approach that allows measuring the expression levels of thousands of genes contemporarily. However, this technique is just the first step of a biological investigation and serves to generate hypothesis based on the identified differentially expressed genes (DE). The approach used here (SPIA), for the identification of differentially regulated pathways in the different experimental conditions is a novel method which differs from the classic gene set enrichment analysis (GSEA), which is based only on the expression levels of the genes that belong to the pathway. The SPIA tool, indeed, integrates also the topology of the pathways improving the specificity and the sensitivity of the discoveries, being not biased by the arbitrary selection of fold change thresholds. The classical method is not suiting our project because it considers each functional category individually, thus, it is not appropriate for a system biology approach. The strength of the method that we used is that it takes into account the position of the gene in the pathway and its interaction with other genes both in the same and other pathways. In other words, if one gene is crucial in triggering the activity of the pathway, changes in the expression levels of this gene are considered much more influent than changes in several downstream genes in the pathway.

### **Integrating data sets of different nature, via DIABLO**

The integration of different Omics datasets is, to date, a big challenge for biologists, due to the lack of tools able to take into account very different variables coming from high throughput approaches such as data from epigenetics, transcriptomics and proteomics or metabolomics.

One of the first issues in the integration is linked to the experimental design, which has to be extremely rigorous in order to have measurements coming exactly from the same samples. This allows to overcome possible biases introduced by the sample variability and minimize only to the one coming from the different 'omics technological platforms used for the measurements.

The method used in this project to integrate RNA-seq and metabolomics is part of an R package, *mixOmics*<sup>306</sup>, and is called Data Integration analysis for Biomarker discovery using Latent variable approaches for Omics studies (DIABLO)<sup>307</sup>. The advantage of this tool is that it has an integrated algorithm to identify correlated variables i.e. genes and metabolites, which allows to identify interesting features that can help in generating hypothesis.

However, the major weakness of this approach is that it is based on a supervised correlation analysis, meaning that it is fundamental to declare in advance the different categories of interest i.e. tissue differences, diet-related changes etc. Moreover, in order to avoid difficulties in the interpretation of the results, a variable selection is needed first, in order to provide, from each dataset, only the variables that are contributing the most to the contrasts of interest.

Another strategy pursued to integrate RNA-seq and metabolomics is based on the identification of modules of correlated genes, meaning group of genes having the same expression changes in the different experimental conditions. For each module of genes, the correlation with specific trait of interest, such as the contrast between vWAT and scWAT, or between controls and HFD in one tissue at a specific time point, is then calculated. This first analysis is used to select a set of features to use for modeling the metabolic event in each tissue. The modeling part is mainly pursued by Thoung Van Du Tran and Marco Pagni, and does not belong to this thesis.

### III Intrinsic differences of the two white adipose tissue depots,

We first show that there are basal differences between the two analysed tissues. These differences can arise from many features, like the different origins of the adipocyte progenitors or the environmental dissimilarities, such as the peripheral innervation and the specific relationship with the circulation<sup>9-11</sup>.

With respect to the origin, the two WATs are developing separately. The scWAT appears in mice at embryonic day 16.5-17.5 in mice<sup>225,226</sup>, while the vWAT develops later, becoming visible at postnatal day 7<sup>227</sup>. At the cellular level, adipocytes are originating from adipocyte progenitors that are contained in the so-called stromal vascular fraction (SVF). These cells have a mesodermal origin, developing from the mesenchyme<sup>228</sup> and studies showing the apposition of vascular structures to the developing fat pad, advanced the hypothesis of a connection between adipogenesis and angiogenesis<sup>229,230</sup>. In the mature tissue, scWAT is not made uniquely of white adipocytes but it also hosts clusters of “beige” or “brite” (brown in white) adipocytes. This is consistent with what we observed in the histological section of scWAT, showing a strong difference in UCP1<sup>+</sup> cells, as well as in cell number, compared to vWAT. This difference in beige cell population also correlates with the dissimilarity in the expression of genes linked to lipid metabolism and oxidation, as shown by the pathway analysis in Figure 16. Finally, at epigenetic and transcriptomic levels, we could confirm the presence of genes that are specifically expressed in one or the other tissue, i.e. *Wt1* and *Tcf21*, *Tbx15* and *Lhx8* that are vWAT and scWAT specific, respectively.

Among other tissue intrinsic differences that could have an impact on diet-induced inflammation, we also highlighted metabolites whose abundance is unbalanced in the two tissues. The N-acetyl-aspartyl glutamic acid (NAAG) and histamine are indeed, highly present in the scWAT

independently of the diet and the age of the mice. This can be explained, at least in part by the higher expression in the vWAT of the *Folh1* gene, which is coding for the glutamate carboxypeptidase II. Knowing that this enzyme is metabolizing NAAG, generating N-acetyl-aspartate (NAA) and glutamate, we could infer that the levels of NAAG are lower in the vWAT because it is more metabolized.

However, tissue differences could also arise from other cell type apart from adipocytes. Indeed, the occurrence of histamine among the tissue specific metabolites can be related to the presence of mast cells in the tissue, as described by Altintas et al<sup>312</sup>.

#### **IV Inhibition of AP differentiation in the vWAT may cause hypertrophic adipocytes and cell death**

The analysis of the early changes occurring in white adipose tissue upon 1 week of high fat diet treatment highlighted an increase in histone gene transcription in the vWAT. A massive increase in histone gene transcription is normally linked with cell proliferation. Indeed, during the S-phase of the cell cycle, nucleosomes are disassembled and subsequently re-assembled with newly synthesized histones and DNA<sup>313</sup>. The observed augmentation of histone genes could be associated to adipocyte progenitor (APs) expansion as described by Jeffery et al<sup>14</sup>. In this paper the authors describe how 3 days of high fat feeding induce, in male mice, a rapid and transient proliferation of APs specifically in vWAT, suggesting that the hyperplastic expansion of the visceral fat is starting at the very beginning of the diet treatment.

On the other hand, our ChIP-seq analyses revealed that, upon HFD treatment, the vWAT undergoes a reduction in histone acetylation, already detected at 1 week and exacerbated at 8 weeks, on many genes of fatty acid metabolism, regulation of cell growth and differentiation.

Such decrease in H3K27Ac, which would imply a reduced activity of the corresponding genes, would suggest rather a decreased cell proliferation, in conflict with the literature.

These conflicting results, prompted us to develop the following hypothesis: the active expansion of APs occurring very early in the vWAT, as showed in the literature, is happening concomitantly to a block in the process of cell differentiation. This hypothesis is supported by the fact that many genes belonging to the non-canonical Wnt pathway, as well as other fundamental pathways for cell differentiation, i.e. *Ihh*, *Bmp8a*, appear in the group of genomic regions with reduced H3K27Ac at 1 and 8 weeks in the vWAT, but show no change in the scWAT. Along this hypothesis, the increased gene expression of *Wnt10b*, a known anti-adipogenic mediator, together with the reduced phosphorylation levels of  $\beta$ -catenin, which are observed in the vWAT uniquely, further support a negative effect of HFD on AP differentiation in vWAT. This inhibition in adipocyte differentiation could be the cause of the hypertrophic expansion of the tissue, due to mature adipocyte overload.

Of note, the storage capacity of a fat cell is not unlimited and once they reach their maximal size, adipocytes die<sup>48</sup>. This is consistent with the increased level of apoptotic genes, observed in vWAT after 8 weeks of HFD. The concomitant appearance of immune cell recruitment in the tissue underscores a possible correlation between the increased cell death rate and the inflammatory response. Finally, it might also explain, at least in part, the remarkable decrease of vWAT weight after 20 weeks of HFD (Figure 9). A similar behavior of vWAT in response to HFD was also reported by Strissel et al<sup>301</sup>, who observed an active process of remodeling after 16 weeks, in which the rate of adipocyte death (80%) exceeded the rate of tissue repair, resulting in net adipocyte and vWAT loss. The authors further showed that after 20 weeks of HFD, the frequency of adipocyte death was decreased while the number of newly formed adipocytes

increased by fourfold. As a consequence of the high prevalence of small adipocytes, the vWAT mass remained reduced despite the restoration of the cell number<sup>301</sup>.

Taken together, our results pinpoint the block in adipocyte differentiation as a key mechanism that characterizes the early response of vWAT to over nutrition. Moreover, this effect is proposed as a distinctive behavior that can explain the different response observed in the two white adipose tissue depots. Canonical Wnt pathway activation, and in particular WNT10b, are proposed to be the mediators of such differentiation shut off. Additional studies will be required to understand the molecular changes underlying the different activation of the Wnt signaling observed in vWAT and scWAT.

## **V Early changes occurring in over nutrition in scWAT**

In contrast to vWAT, scWAT is known to undergo a metabolically healthy expansion upon overnutrition in both humans and mice, but the reason explaining the different behavior of this tissue has not been elucidated yet. The scWAT, in the early phase of obesity development, is not undergoing a clonal expansion of adipocyte progenitors, as shown previously by Jeffery et al<sup>14</sup>. However, it still maintains its capacity to increase in size, a phenomenon that could be explained by two mechanisms.

According to our observations, in scWAT, short-term treatment with HFD induces a tissue-specific reduction of mitochondrial activity and mass, with disappearance of the UCP1<sup>+</sup> cells. These data suggest that, upon HFD, there is a loss of beige adipocytes in scWAT. The disappearance of beige adipocytes without cell death evidence could be explained by the trans-differentiation of these cells from beige to white adipocytes. The existence of such a mechanism

has been hypothesized by the Cinti group<sup>247</sup> with the demonstration that, upon cold stimulation, the number of beige adipocytes is increasing without any sign of cell death. Moreover, BrDU staining showed that these newly formed beige adipocytes are not derived from the clonal expansion of APs, because BrDU<sup>-</sup>, suggesting that they can only be generated by white cell trans-differentiated to beige adipocytes. Trans-differentiation could thus represent a way for the tissue to provide new mature adipocytes, which improve the storage of fatty acid excess, at the expense of the “burning” capacity of the tissue.

Another mechanism possibly contributing to scWAT ability of healthy expand in response to HFD is highlighted by our ChIP-seq analysis. Indeed, our data identified a group of genomic regions that lose acetylation after 1 and 8 weeks of diet only in vWAT and that are linked to genes, such as *Zfp423* (Figure 18C & D), involved in adipogenesis, at the level of both AP clonal expansion and differentiation. Interestingly, in normal condition, these regions have a lower acetylation, methylation, as well as a less important RNAPol II occupancy in the subcutaneous compared to the visceral adipose tissue. This peculiar epigenetic landscape suggests that, in scWAT the chromatin is more compacted and less prone to be transcribed at the level of these enhancers, making this tissue less prone to hyperplastic expansion. This is in line with tracing experiments performed using the Adipochaser mice, showing that the scWAT, when exposed to HFD, undergoes primarily hypertrophic expansion with low rate of adipogenesis<sup>314</sup>. Interestingly, *Wnt10b*, in normal condition, is expressed at higher level in scWAT compared to vWAT, in line with the idea that the scWAT is less prone to undergo adipogenesis. This observation strengthens the role of WNT10b, making it a possible key regulator of the hyperplastic expansion of the white adipose tissue.

After 8 weeks of HFD, scWAT changes are characterized by an increased expression of cell cycle-related and histone genes, as evidenced by pathway analysis performed at 8 weeks (Figure 27). This could indicate that, upon a prolonged exposure to overfeeding, the scWAT is undergoing a hyperplastic growth, which ensure a healthy expansion of the tissue. In line with this hypothesis, the expression levels of *Fabp4* in the scWAT are increasing at 8 weeks, suggesting that more adipocytes are present in the tissue at this stage of overnutrition (Figure 26A).

Taken together all these observations suggest that in the first phase of HFD treatment in scWAT the process of clonal expansion of the progenitors is not occurring, probably because of the beige adipocyte trans-differentiation to white. This process is providing the tissue with new mature white adipocytes, which can contribute to the storage of the excessive FAs. In contrast, at later time points of HFD feeding, the expansion of a new pool of pre-adipocytes is probably occurring, which could explain the progressive expansion of the tissue, as observed by the tissue weight after 20 weeks of diet (Figure 9).

In summary, adipose tissue dysfunctions, mainly at the level of the vWAT, are contributing to the onset of obesity-related secondary diseases such as insulin resistance. vWAT, despite a first attempt to increase the number of APs, undergoes a block in pre-adipocyte differentiation that prevents the formation of mature adipocytes. This is then causing the hypertrophic expansion of the mature adipocytes that once reached their maximal size undergo cell death and recruitment of immune cells. Thus, an early intervention, facilitating the differentiation of the primed pre-adipocytes, could be a strategy to help the vWAT to cope with the excess of fatty acids, reduce cell stress and death as well as improve the inflammatory response.



# **Appendix**

# **From chronic overnutrition to metaflammation and insulin resistance: adipose tissue and liver contribution**

*Tiziana Caputo, Federica Gilardi\*, and Béatrice Desvergne\**

*Center for Integrative Genomics, Genopode, Lausanne Faculty of Biology and Medicine CH-1015 Lausanne,  
Switzerland*

\*Corresponding authors

Review published in July 2017

<https://doi.org/10.1002/1873-3468.12742>

# From chronic overnutrition to metaflammation and insulin resistance: adipose tissue and liver contributions

Tiziana Caputo, Federica Gilardi and Béatrice Desvergne

Center for Integrative Genomics, Lausanne Faculty of Biology and Medicine, University of Lausanne, Switzerland

## Correspondence

F. Gilardi and B. Desvergne, Center for Integrative Genomics, Genopode Building, University of Lausanne, Genopode, CH 1015 Lausanne, Switzerland  
Fax: +41 21 692 4115  
Tel: +41 21 692 4110  
E-mail: Federica.gilardi@unil.ch (FG) and Beatrice.desvergne@unil.ch (BD)

(Received 16 May 2017, revised 28 June 2017, accepted 2 July 2017, available online 25 July 2017)

doi:10.1002/1873-3468.12742

Edited by László Nagy

**The close association of obesity with an increased risk of metabolic diseases, such as insulin resistance, type 2 diabetes, and nonalcoholic fatty liver disease, is now well established. In this review, we aim first to describe the inflammatory process activated in response to overnutrition, especially in the liver and the adipose tissue. We then discuss the systemic effects of low-grade inflammation on the onset of insulin resistance. Particular attention is given to a series of very recent reports that identify not only processes but also molecules (lipids and metabolites) that interfere with the normal insulin signaling. Finally, special notes concerning the roles of peroxisome proliferator-activated receptors in the various processes will be made.**

**Keywords:** insulin resistance; liver-adipose tissue cross-talk; metaflammation; PPARs; visceral white adipose tissue

Obesity is a complex chronic disorder with a multifactorial etiology, involving genetics, hormones, diet, and life style. It is characterized by a massive increase in adipose tissue due to the imbalance between daily energy intake and energy expenditure. In the last 30 years, obesity has become a worldwide epidemic affecting both adult and children and turning into an extremely important public health problem [1]. Indeed, it is associated with many different (co)morbidities, such as cardiovascular diseases, type 2 diabetes (T2D), hypertension, certain cancers, and sleep-disordered breathing such as sleep apnea contributing to an increase risk of mortality as well as reduced life expectancy. Although carrying a large amount of fat is not necessarily harmful, two interlinked systemic disorders contribute to the high morbidity, that is, insulin resistance and inflammation, the latter being thought to play an important role in the pathogenesis of the

former [2]. The link between these two processes is illustrated by the increased levels of several inflammatory cytokines in serum of T2D patients compared to healthy subjects. Up to 30% of obese patients are considered as 'metabolically healthy obese individuals' because of their normal fasting glucose, normotension, high insulin sensitivity, and inflammatory status [3,4]. This concept was substantiated in many clinical studies, although it has been recently challenged by a study showing that insulin-sensitive and insulin-resistant obese have similar insulin-dependent transcriptional response in subcutaneous adipose tissue [5].

Both the adipose tissue and the liver are primary targets of increased fluxes of fat upon obesity. In this review, we will first discuss the critical role of adipose tissue in metabolic homeostasis. We will mainly focus on how the altered circulating fatty acid levels affect adipose tissue homeostasis, modify the profile of

## Abbreviations

ATF6, Activating Transcription Factor 6; ATM, adipose-tissue macrophages; ER, endoplasmic reticulum; FFA, free fatty acids; GLUT4, glucose transporter 4; HGP, hepatic glucose production; IRE1, Inositol-Requiring Enzyme 1; NAFLD, nonalcoholic fatty liver disease; PERK, PKR-like ER Kinase; PPARs, peroxisome proliferator-activated receptors; ROS, radical oxygen species; TGs, triglycerides; UPR, unfolded protein response; WAT, white adipose tissue.

adipokines and cytokines secreted by the adipocyte, and favor the recruitment of immune cells. These events are indeed considered as important contributors to the pathogenesis of the metabolic syndrome. The inflammatory responses of the liver will then be discussed. Indeed, the rise in human obesity has been recently correlated with an increased prevalence of nonalcoholic fatty liver disease (NAFLD) [6]. NAFLD is considered as the hepatic manifestation of the metabolic syndrome and is characterized by an excessive accumulation of triglycerides (TGs) in the hepatocytes, known as ‘hepatosteatosis’, in the absence of alcohol abuse or viral infection. Based on epidemiological studies, the percentage of obese subjects showing signs of NAFLD (75%) is increasing exponentially compared to lean subjects (16%), whereas it is close to 100% among the obese patients with T2D [7]. Importantly, we will emphasize how the signaling cross-talks between liver and adipose tissue relies both on inflammatory and metabolic signals. In the section Linking metabolism and inflammation, we will more specifically discuss the nature and actions of different actors that contribute to the insulin resistance in the context of inflammation. A final section will summarize the role that the transcription factor peroxisome proliferator-activated receptors (PPARs) plays in the onset of inflammation and insulin resistance.

### **Profound remodeling of the visceral white adipose tissue in overnutrition and obesity**

In humans, adipose tissue is distributed over the entire body with many compartments that differ in terms of metabolic activity, sympathetic innervation, and contribution to local and systemic signaling. Although the brown adipose tissue (BAT) is orientated toward use of lipids, coupled to a thermogenic process, the white adipose tissue (WAT) is the main location for lipid storage, expanding in response to high fat or overnutrition (see Box 1). The WAT is prone to develop inflammation upon obesity and thus is the focus of the present review.

#### **Visceral WAT and subcutaneous WAT**

When considering the impact on the development of metabolic disorders, two main types of WAT have been identified: the subcutaneous WAT (scWAT) which is located under the dermal compartment of the skin, and the visceral WAT (vWAT) further divided into the mesenteric WAT wrapped around the intestine, the retroperitoneal WAT surrounding the kidney,

and the omental WAT positioned in the lower part of the abdominal cavity covering the stomach. This anatomic classification of the vWAT is not strictly reproduced in mice where omental fat is absent, and the tissue presenting the properties of visceral fat in mouse is the gonadal fat.

Visceral and subcutaneous adipose tissues have different behaviors, particularly highlighted in obesity and related metabolic disorders. These differences are of three types. Firstly, adipokine nature and secretion profile of vWAT and scWAT differ. For example, the expression and secretion of Interleukin 6 (IL6) and Plasminogen-Activator Inhibitor type 1 (PAI-1) are higher in the vWAT, whereas leptin and adiponectin are higher in subcutaneous WAT [8,9]. Secondly, the adipokines produced by the scWAT are secreted into the systemic circulation, whereas those produced by vWAT are secreted into the portal system, thus having a more direct impact on hepatic metabolism. Thirdly, the rate of lipolysis and fatty acid mobilization [10] is also different, the visceral adipose tissue appearing to be more sensitive to lipolytic effects of catecholamines and less sensitive to the antilipolytic effects of insulin, that mobilizes fatty acids into the portal vein. Although these differences are possibly due to the vWAT- vs scWAT-specific environment, which includes the innervation and vasculature proper to each depot, recent reports suggested that physiological heterogeneity within the adipose tissues could also stem from different developmental programs, leading to cell-autonomous differences [11–13].

These differences explain at least in part the major distinct response of each WAT depot upon obesity in human and in experimental models, including genetically induced obese mice, *ob/ob* and *db/db*, lacking the coding gene for leptin or for leptin receptor, respectively, as well as diet-induced obese mice.

In the rest of this chapter, we will thus discuss how the remodeling of the vWAT in overnutrition and obesity is a sequential process that starts with the development of mature hypertrophic adipocytes that have to face oxidative and endoplasmic reticulum (ER) stress. Their altered secretome initiates the inflammation process, with the recruitment of a large number of macrophages as well as the modification of the profile of pre-existing adipose tissue-resident macrophages (ATM). Finally, activated macrophages lead to the recruitment and activation of T lymphocytes, which altogether sustain the progression of obesity-induced inflammation. Recent knowledge concerning this process is discussed below. However, it must be reminded that the triggering stimuli as well as the exact temporal sequence of inflammatory cell infiltration and their

**Box 1.** The adipose tissue properties and its diverse depots**Heterogeneity of the adipose tissue (AT)**

Adipose tissue is a highly plastic tissue composed of preadipocytes, mature adipocytes, and stromal-vascular cells, coexisting with nerve terminals, blood vessels and lymph nodes, and immersed in a complex collagen matrix.

**The two main properties of AT**

- Capacity to store and to release lipids, depending on the energy demand of the organism.
- Secretion of bioactive peptides, called adipokines, that act both locally and systemically for the maintenance of energy homeostasis. Main adipokines are leptin, adiponectin, and resistin, which regulate feeding behavior and energy expenditure. Other cytokines can also be expressed by adipocytes.

Both the storage function and the secretome are altered upon overnutrition.

**The white, brown, and brite adipocytes**

The white adipocytes store lipids in one large lipid droplet surrounded by a thin layer of cytoplasm. The white adipose tissue (WAT) grows through increased cell size and increased cell number. The subcutaneous WAT (scWAT) and the visceral WAT (vWAT) have distinct properties (see the main text).

The brown adipocytes accumulate lipids in several small lipid droplets and are characterized by a high number of densely packed mitochondria and expression of the uncoupling protein UCP1. The stored lipids are mainly used in nonshivering thermogenesis. The brown adipose tissues (BAT) are, in humans, mainly localized in the para-clavicular and spinal region [227–229].

The brite or ‘brown-in-white [230]’ adipocytes correspond to inducible brown cells appearing in a predominantly white fat depot. The ‘browning’ process is induced by cold or beta-adrenergic stimuli and depends on the genetic background and on the location [231]. Raising the number and the activity of human brown cells can boost the whole-body energy expenditure, and is therefore the focus of enormous research efforts.

White adipocytes derive from mesenchymal stem cells, whereas brown adipocytes derive from precursor cells in the embryonic mesoderm [232].

cross-talk with stressed adipocytes is not completely clear, due to its intrinsic complexity and the difficulties in taking into account the various experimental contexts (e.g., animal model, type of diet, selected time points).

**Cellular and tissular responses of the vWAT in obesity**

White adipose tissue has the unique capacity to undergo dramatic remodeling in response to nutritional factors by increasing the size of individual cells (hypertrophy) and by recruiting new adipocytes from the resident pool of progenitors (hyperplasia). These processes, which aim to positively improve the lipid storage capacity of the body, are however accompanied, particularly in vWAT, by a reduction in tissue vascularization, leading to areas with lower oxygen availability and hypoxia [14,15]. This alters in the vWAT some cellular and tissular responses and results in an undesirable infiltration and activation of immune and inflammatory cells, observed both in experimental models and in humans.

The first response of the adipose tissue to the high levels of circulating lipids is an hypertrophic growth of the pre-existing mature adipocytes as a result of the triglyceride accumulation in the unilocular lipid droplet. The hyperplasia process also starts quite rapidly since in mice adipogenesis and adipocyte precursor proliferation are already activated 3 days after the beginning of a high-fat diet feeding in vWAT depots, with the subsequent creation of a pool of precursors that will turn into mature adipocytes over a prolonged exposition to the diet (7 weeks) [16]. Notably, the hypertrophic process—rather than the hyperplasia—seems to be the most damaging for the cells and thus for the tissue.

At the cellular level, one of the consequences of the hypertrophic response is the decrease in insulin-dependent glucose uptake because of a dysregulation of cortical actin remodeling and the consequent impairment of insulin-dependent glucose transporter 4 (GLUT4) translocation to the plasma membrane [17]. Another alteration in hypertrophic adipocytes is the accumulation of radical oxygen species (ROS) [18] and dysfunction of the ER, a membranous network controlling

synthesis, maturation, and trafficking of secreted and membrane proteins. The accumulation of unfolded proteins in the ER lumen induces an adaptive response known as unfolded protein response (UPR) that is mediated by three major transducers: the PKR-like ER Kinase (PERK), the Inositol-Requiring Enzyme 1 (IRE1), and the Activating Transcription Factor 6 (ATF6). Along this line, chronic obesity is associated with ER stress in adipose tissue [19] and free fatty acids (FFA; also called nonesterified fatty acids) induce ROS generation as well as ER stress by activation of UPR signaling pathways in adipocytes [20].

At the tissular levels, adipocyte hypertrophy is associated with a relative deficiency of vasculature that creates a local imbalance between oxygen supply and consumption, which, in turn, leads to an increase in the level of angiogenic factors and the expression of inflammation and ER stress-associated genes [21]. In mice exposed to high-fat diet, sign of hypoxia can be detected after 3 days of diet together with increased protein level of its main mediator, the hypoxia inducible factors (HIF1 $\alpha$ ), vascular endothelial growth factor expression levels, and accumulation of lactate. The link between hypoxia and the appearance of inflammation in vWAT was demonstrated in both mouse models of both HIF1 $\alpha$  genetic deletion and transgenic overexpression establishing its critical role in the inflammatory response and in the onset of insulin [15,22].

Altogether, these alterations are responsible at least in part for the subsequent inflammatory response and decreased insulin sensitivity, as discussed below.

### **Adipose tissue proinflammatory responses induced in obesity: secretion of proinflammatory cytokines and modulation of adipokine secretion**

The first evidence showing the implication of adipose tissue in the obesity-related inflammatory response came 20 years ago, when Hotamisligil *et al.* [23] demonstrated that the production of tumor necrosis factor alpha (TNF- $\alpha$ ) was induced in the visceral fat pad of obese rodents and that the neutralization of this cytokine improved their insulin sensitivity. Excessive nutrient consumption triggers an inflammatory process, also called ‘metaflammation’ [2,24], that is initiated and sustained by metabolic cells, which are at the interface between metabolic inputs and the inflammatory outputs. Metaflammation is characterized by being low-grade compared to the acute inflammatory response, and chronic, as cytokine expression and immune cell infiltration appear gradually and remain unresolved over time. WAT is likely the primary site where metaflammation originates, although, to a

certain degree, other metabolic tissues, such as liver (as discussed later), pancreas, and gut cells associated with the gut microbiota are also involved, with important consequences for metabolic homeostasis.

Upon nutrient overload, the inflammatory process is likely initiated by the cellular and tissular damages, described above. These alterations lead to two main processes. First, they increase the number of dead adipocytes showing necrotic-like abnormalities [25,26]. In turn, these necrotic events trigger the recruitment of inflammatory cells that secrete proinflammatory soluble mediators. In parallel, the adipocytes themselves undergo a global and profound change in their secretome profile, with not only an increased release of mediators of the clotting process, such as PAI-1, but also an increased expression and secretion of proinflammatory cytokines [27,28] and alterations in the level of several adipokines [29].

As mentioned above, TNF- $\alpha$  was the first identified major proinflammatory cytokine released from the obese adipose tissue, in mice and in humans [30,31]. It is mainly expressed by monocytes and macrophages that infiltrate the obese adipose tissue, as well as by obese adipocytes [23] and has a central role in many different inflammatory diseases.

The CC-motif Chemokine Ligand 2 (CCL2) also known as Macrophage Chemoattractant Protein 1 (MCP1), is one key chemokine expressed by the adipocytes whose levels positively correlate with the increased adiposity and whose presence is sufficient to induce the recruitment and infiltration of macrophages in the adipose tissue initiating the inflammatory response and obesity-related insulin resistance [32]. Although the work of Kirk *et al.* reported no differences in adipose tissue inflammation or macrophages accumulation in CCL2-deficient mice [33], other studies showed that lack of CCL2 or of its receptor CCR2 in the adipose tissue reduces macrophage accumulation and ameliorates the metabolic profile as well as the insulin sensitivity and hepatic steatosis of obese mice [32,34].

Interleukin 6 and IL18 are cytokines produced by the adipose tissue and positively correlated with the adiposity level [35,36], even in a regimen of weight loss [37,38]. However, the metabolic consequence of the increase in these two cytokines remains controversial, as discussed later.

The adipokines also play a role in modulating inflammatory responses. Adiponectin has anti-inflammatory properties, *via* inhibition of TNF- $\alpha$  synthesis in endothelial and hepatic cells and induction of the production of anti-inflammatory cytokines such as IL-10 and IL-1 receptor antagonist (IL-1RA) in macrophages and dendritic cells [39]. Adiponectin reduction observed in obesity limits these anti-inflammatory

effects. In contrast, leptin increases circulating levels of proinflammatory mediators released by various cell types, including macrophages. Leptin is an adipokine involved in the regulation of food intake through the central nervous system. Mice lacking leptin (*ob/ob* mice) are hyperphagic and develop obesity and insulin resistance, which can be reverted by the administration of leptin [40]. Leptin circulating levels are positively associated with the adipose tissue mass, suggesting a possible leptin resistance in obese patients as they do not show the expected anorexic response [40]. The proinflammatory activity of leptin is mainly mediated by its ability to increase the production of TNF- $\alpha$  and IL6 by monocytes, and of CC-chemokine ligands by macrophages [41–43]. In addition, it increases the production of IL2 and interferon  $\gamma$  (IFN $\gamma$ ) and suppresses the production of the anti-inflammatory cytokine IL4 in T cells [44]. In the obese adipose tissue, proinflammatory signals such as TNF- $\alpha$  [45], stimulate the production of leptin, which in turn maintains and exacerbates the inflammatory response.

Resistin is another major secreted adipokine whose levels increase with obesity and correlate with both inflammation and insulin resistance in animal models [46]. The proinflammatory action of resistin in human mononuclear cells is mediated by the increase in the expression levels of TNF- $\alpha$  and IL6 in monocytes [46] and of adhesion molecules (VCAM1, ICAM1, and pentraxin 3) in vascular cells that enhance leukocyte adhesion [47].

Altogether, the obesity- or overnutrition-driven changes in the secretion profiles of these cytokines and adipokines in the vWAT are part of the process that leads to the recruitment of inflammatory/immune cell in this tissue.

### Recruitment of inflammatory and immune cells in the WAT

Macrophages are at the front line of the inflammatory process, prevailing in terms of number and tissue remodeling activity [48]. In lean mice, around 10–15% of the vWAT cells are positive for F4/80<sup>+</sup>, which identifies macrophages. These so-called ATMs have an alternatively activated M2 phenotype (Arg1<sup>+</sup>, CD206<sup>+</sup>, CD301<sup>+</sup>) and localize in the interstitial spaces between adipocytes, uniformly distributed through the adipose tissue. M2 macrophages are crucial for the adipose tissue homeostasis, particularly for their production of IL10, a regulatory anti-inflammatory cytokine. However, upon obesity, the secretion by the hypertrophic adipocytes of proinflammatory cytokines such as CCL2, CCL5, and others [49] as well as that caused by the presence of increased number of necrotic adipocytes [50,51], leads to

the recruitment of circulating monocytes toward the stressed tissue, monocytes which then are activated in macrophages (Fig. 1). In total, in obese mice, macrophages can reach 45–60% of the vWAT cell population [52]. They localize primarily in ‘crown-like structure’ surrounding dying adipocytes [53,54] and have a classical proinflammatory M1 phenotype (CD11c<sup>+</sup>, nitric oxidase synthase 2<sup>+</sup>, TNF- $\alpha$ <sup>+</sup>). They produce proinflammatory cytokines, such as TNF- $\alpha$ , iNOS, and IL6, which further promote obesity-associated inflammation not only in mice [54] but also in obese patients where the accumulation of macrophages has been shown to correlate with higher circulating levels of TNF- $\alpha$  [55,56].

Another concurrent effect, which contributes to the worsening of obesity-related inflammation, is mediated by paracrine action of leptin on immune cells. Leptin has been reported as a strong mediator of monocytes proliferation, macrophages phagocytosis, cytokine expression, and chemotaxis [57] by stimulating the production of IL2, IL12, and IFN $\gamma$  [58]. Moreover, mast cells in the adipose tissue of obese mice contribute to leptin production, which in turn affects macrophage polarization toward the M1 proinflammatory status. Consistently, mast cells from leptin-deficient mice are able to polarize macrophages toward the less inflammatory M2 phenotype [59].

Finally, other stimuli in the context of obesity can influence macrophage recruitment and activation, such as fatty acids, fetuin-A, Krüppel-like factor 4 [60], or cold exposure [61]. Unsaturated fatty acids have been identified as promoters of macrophage activation in obesity through a mechanism mediated by the binding to the pattern recognition receptor Toll-like receptor 4 (TLR4) [62]. Recent observations suggested that FFAs are not direct ligands of TLR4 but bind *via* fetuin-A, a glycoprotein produced by the liver that may act as a transporter of FFAs in the circulation and as endogenous ligand for TLR4, presenting in this way FFAs to the receptor [63]. All these effects favor not only recruitment of macrophages to the inflated adipose tissue but also their polarization to M1 type. However, some studies have demonstrated a mixed M2/M1 phenotype in the adipose tissue of obese mice and humans [64–66], while others depicted a complex scenario where the most abundant ‘metabolically activated’ (MMe) macrophages have a different phenotype compared to classically activated M1 macrophages, suggesting that their activation is occurring *via* mechanisms that are different from those occurring during infection [67].

Currently, an active research field is studying ways to counteract the inflammatory response in WAT by pushing the rise in number and activity of brite (brown-in-white) cells, in order to not only boost the

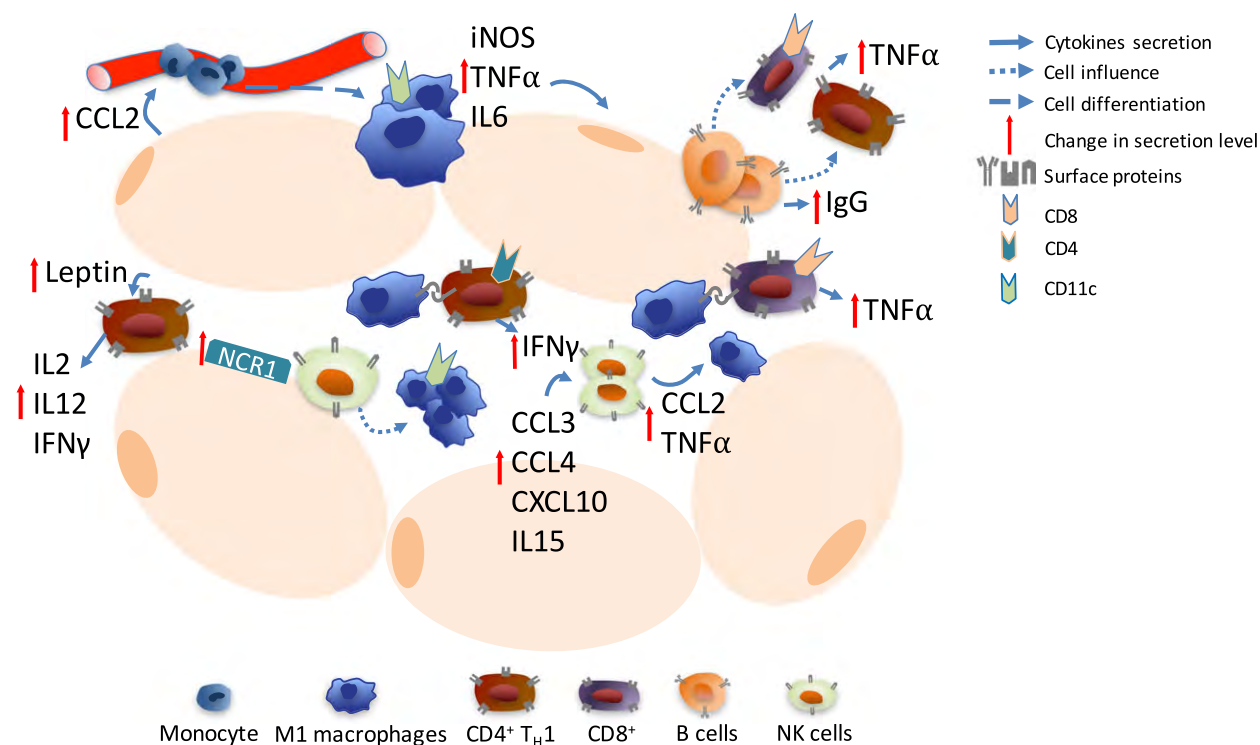


**Fig. 1.** Recruitment of inflammatory and immune cells in WAT. Upon overnutrition, adipocytes secrete proinflammatory cytokines: CC-motif chemokine ligand 2, 3, and 4 (CCL2, CCL3, CCL4), C-X-C motif chemokine 10 (CXCL10), interleukin 15 (IL15), which induce recruitment and activation of inflammatory and immune cells. Monocytes are recruited from the circulation and are activated to become M1 macrophages producing tumor necrosis factor alpha (TNF $\alpha$ ), Interleukin 6 (IL6), and inducible nitric oxide synthase (iNOS). M1 macrophages activate cells of the adaptive immune response: CD4<sup>+</sup> T helper 1 cells (T<sub>H</sub>1), CD8<sup>+</sup> T cells, producing interferon  $\gamma$  (IFN $\gamma$ ) and TNF $\alpha$ ; B cells, releasing immunoglobulins G (IgGs). Obese adipocytes favor the recruitment of natural killer cells (NK) through upregulation of NK cell-activating receptor (NCR1) ligand. The increased adipocyte secretion of leptin contributes to the activation of CD4<sup>+</sup> cells that worsen the inflammation via secretion of interleukin 2, 12 (IL2, IL12), and IFN $\gamma$ .

whole-body energy expenditure but also to improve adipose tissue inflammation and thus insulin resistance [68]. Indeed, prolonged cold exposure increases adiponectin secretion that in turn is responsible for the activation and recruitment of anti-inflammatory M2-type macrophages [69].

After the first wave of newly recruited M1 macrophages, that have the role to clear necrotic adipocytes and remodel the extracellular matrix [26], and with the persistence of excessive nutrient intake, the activation of the adaptive immune system response is occurring in the adipose tissue. Indeed, activated M1 cells act as antigen presenting cells, *via* MHC class I and II molecules, thereby initiating the response of the adaptive immune system and amplifying the adipose tissue obesity-driven inflammation (Fig. 1).

Among the immune cells of the adaptive response, CD4<sup>+</sup> T cells are thought to play an important role in the progression of the obesity-related inflammatory response. T helper lymphocytes expressing CD4 can be

subdivided into a T<sub>H</sub>1 and T<sub>H</sub>2 sublineage, based on their secretion profile. T<sub>H</sub>1-cells tend to secrete proinflammatory cytokines responsible for the elimination of pathogens and the perpetuation of the inflammatory response. On the other hand, T<sub>H</sub>2 cells produce anti-inflammatory cytokines including IL4, 5, 10, and 13, which promote antibody synthesis but inhibit several functions of phagocytic cells. Compared to the scWAT of obese mice as well as to vWAT of lean mice, the vWAT of diet-induced obese mice exhibits a higher number of proinflammatory CD4<sup>+</sup> T<sub>H</sub>1 cells secreting IFN $\gamma$  (Fig. 1). This contributes to the creation of a feed-forward loop in the obese vWAT, where the increased production of IFN $\gamma$  by T<sub>H</sub>1 cells favors the classical (proinflammatory) activation of macrophages [70]. The importance of another subset of CD4<sup>+</sup> T cells, the regulatory CD4<sup>+</sup>Foxp3<sup>+</sup> T<sub>reg</sub> cells, in the vWAT is highlighted by its relative defection upon inflammatory response of the adipose tissue in obesity. This particular population of WAT T<sub>reg</sub> seems to be



extremely important for metabolic processes and for the regulation of inflammatory response in vWAT. They are present in high number in lean mice (40–80% of CD4<sup>+</sup> T cells in vWAT), while they are dramatically reduced down to 30% of the initial population during obesity [71]. However, how this particular new cell compartment contributes to the worsening of the inflammatory response is not yet clarified.

Another immune cell type contributing to the creation of a modified milieu in the AT, are the CD8<sup>+</sup> T cells, whose depletion improves insulin sensitivity in diet-induced obese mice. These cells localize in close proximity to M1 cells in the crown-like structures, suggesting a possible cross-talk between CD8<sup>+</sup> and M1 cells. This hypothesis is also supported by the fact that M1 cells that are cocultured with CD8<sup>+</sup> cells increase their production of TNF- $\alpha$  [72] (Fig. 1).

B cells, another class of cells belonging to the adaptive immune system, are also playing a role in the pathogenesis of obesity-related insulin resistance. In mouse model of diet-induced obesity, B cells accumulate in vWAT at early stage (i.e., by 4 weeks), and contribute to the worsening of insulin sensitivity. This mechanism is in part mediated by their effect on CD8<sup>+</sup> and T<sub>H</sub>1 cells, which are induced to produce proinflammatory cytokines, and in part by their own release of Immunoglobulin G (IgGs). In line with this observation, B-cell depletion using CD20 monoclonal antibody reduced the levels of proinflammatory mediators such as IFN $\gamma$  and TNF- $\alpha$  and ameliorated glucose metabolism [73].

This already complex scenario has been recently enriched by two reports that highlighted the essential role of natural killer (NK) cells in this process. This specialized subset of lymphocytic cells has normally two functions. First, they can destroy tumor and infected cells using the cytolytic activities of enzymes such as perforin and granzyme. Second, they are able to modulate the activity of many immune cells by secreting many different pro- and anti-inflammatory cytokines, including TNF- $\alpha$ , IFN $\gamma$ , and IL10 [74] (Fig. 1). Two different groups demonstrated that NK cell number dramatically increase in the vWAT of mice exposed to high-fat diet (HFD) and that these cells have a major role in the recruitment and the M2-M1 macrophage polarization [75,76]. Wensveen *et al.* showed how NK cells start to accumulate in the vWAT within few days of high-fat diet, with the maximum number detected at 2 weeks, and this correlates with the upregulated expression of NK Cell-activating Receptor (NCR1) ligand in adipocytes. In turn, NCR1 is thought to activate vWAT-resident NK cells thereby inducing the production of IFN $\gamma$ , a strong modulator of M1 polarization (Fig. 1). Similar

results come from the work of Lee *et al.*, where the authors show how the modified milieu, created by a prolonged high-fat diet (12 weeks), induce in the vWAT the production of proinflammatory cytokines, such as CCL3, CCL4, CXCL10, and IL15, which serve as chemo-attractants for NK cells. NK cells are then responsible for the production of CCL2 and TNF- $\alpha$ , which will promote monocyte recruitment and activation, respectively. Together these works agree on the crucial role of NK cells in the early and late phases of obesity, showing how selective depletion of this particular immune cell population is able to improve metabolic phenotype and insulin resistance of HFD-treated mice.

### Local metabolic consequences of vWAT remodeling

Cellular and tissular damages together with the inflammation of the vWAT along obesity development have local metabolic consequences which are interconnected: a decreased insulin sensitivity and a limitation of the capacity of the vWAT to store lipids.

While section Linking metabolism and inflammation is dedicated to insulin signaling and its perturbation upon obesity, we can here mention two specific actions in adipocytes with that respect. First, the remodeling of the cortical actin in adipocytes impacts the insulin-dependent translocation of the glucose transporteur Glut4 to the membrane. Second, in mice, the enhanced secretion of the adipokine Resistin interferes with the normal insulin signaling by increasing the expression of the Suppressor Of Cytokine Signaling 3 (SOCS3), a known inhibitor of insulin action in adipocytes [77]. Other more systemic mechanisms are likely to operate and are reviewed in the section Metaflammation and specific aspects of PPARs.

One paradoxical consequence of the adipose tissue remodeling and its decreased insulin sensitivity during overnutrition is a limitation of the vWAT to further accumulate lipids. This occurs through several mechanisms. The first one is the fact that adipocytes are less sensitive to the antilipolytic effects of insulin. This results in a sustained lipolysis even in fed state, which augments the efflux of FFAs in the systemic circulation (Fig. 2). The second fact is that proinflammatory cytokines produced by inflamed WAT, such as IL6 and TNF- $\alpha$ , reduce the activity of lipoprotein lipase (LPL) [78] (Fig. 2), the enzyme that hydrolyzes TGs contained in very low-density lipoproteins (VLDLs) and chylomicrons at the surface of capillary endothelium [79]. This reduction thus impairs the uptake of FA into the adipose tissue for storage. Consistent with this important role in the regulation of lipid flux, LPL

upregulation in the adipose tissue protects against the ectopic accumulations of lipids by increasing the portion of FAs stored in the adipocytes with beneficial effects on obesity-induced insulin resistance [80]. Interestingly, scWAT maintains its ability to correctly store

lipids upon HFD feeding, as demonstrated in Interferon Regulatory Factors 5 (IRF5)-deficient mice [81]. Thus, a strategy directed at limiting vWAT expansion to the expenses of the scWAT might be beneficial for the whole-body homeostasis. However, some clinical

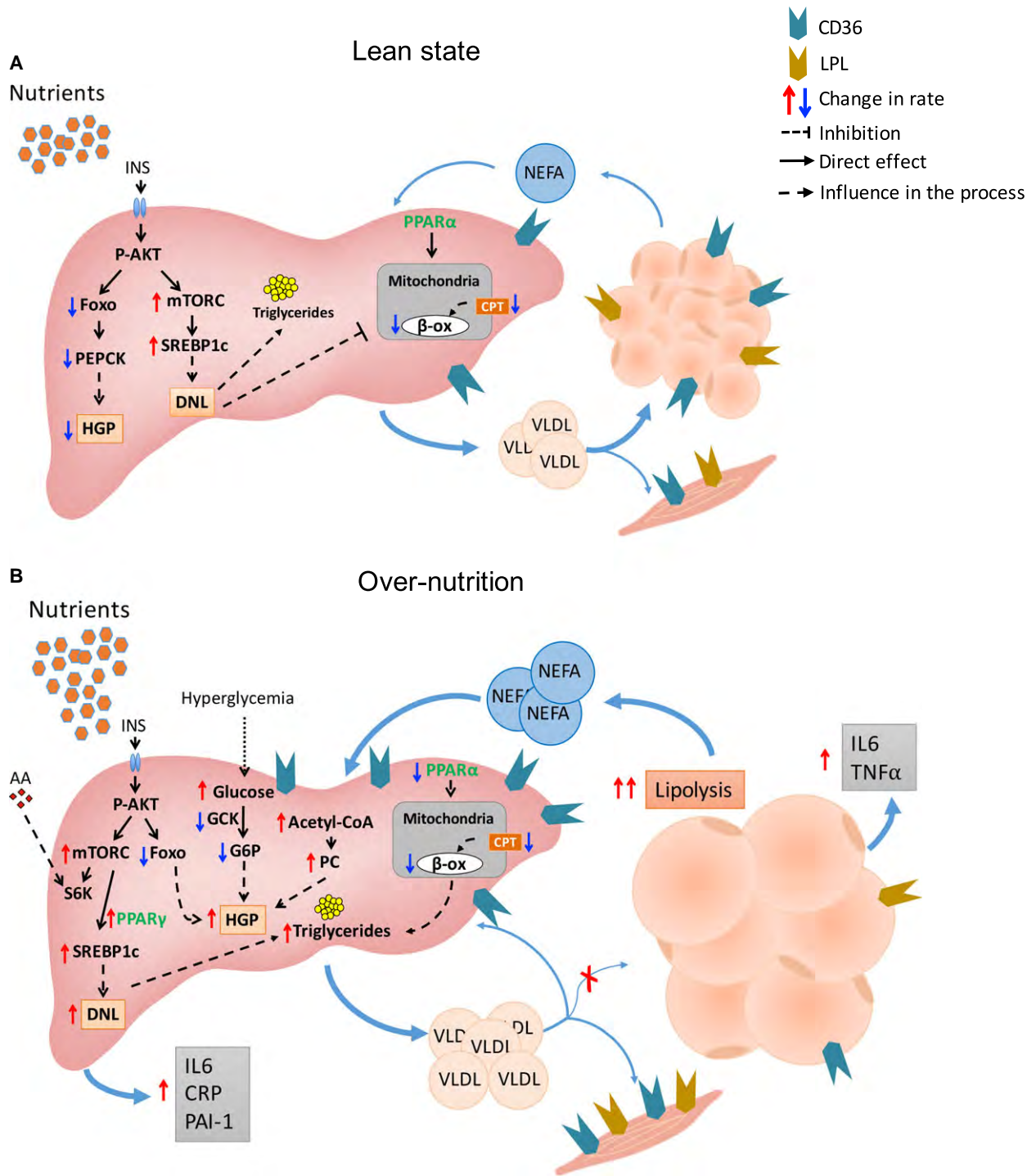


**Fig. 2.** Liver-adipose tissue cross-talk in lean and overnutrition state. A. Lean state. Insulin signaling in the liver induces phosphorylation of the protein kinase AKT. AKT-dependent downregulation of forkhead box (Foxo) transcription factor reduces the transcription of gluconeogenic genes, such as PhosphoEnolPyruvate CarboxyKinase (PEPCK), and hepatic glucose production (HGP). AKT-dependent upregulation of the mammalian target of rapamycin complex (mTORC) upregulates Sterol Regulatory Element-Binding Protein 1c (SREBP1c) thus inducing *de novo* lipogenesis (DNL) and triglyceride (TG) synthesis. DNL inhibits both the transport of fatty acids in the mitochondria via carnitine palmitoyl transferase carrier (CPT) and the  $\beta$ -oxidation ( $\beta$ -ox), which is controlled by peroxisome proliferator-activated receptors  $\alpha$  (PPAR $\alpha$ ). Hepatic TGs are secreted in the circulation in form of very low-density lipoproteins (VLDLs) to reach muscle and adipose tissue where they are taken up, through the action of CD36 and lipoprotein lipase (LPL). In adipose tissue, insulin inhibits the release of nonesterified fatty acids (NEFAs). (B) Overnutrition. In obesity, hepatic DNL and HGP are both active. PPAR $\gamma$  is upregulated in hepatosteatosis, further inducing DNL and hepatic TG content. Aminoacids (AA) derived from the diet influence mTORC/S6 kinase (S6K) pathway that, through an intertissue connection, affects LPL activity in the adipose tissue and thus increases circulating TGs. Hepatic VLDL secretion increases, but their uptake by adipose tissue is reduced because of the low expression of CD36 and LPL. Conversely, CD36 and LPL are more expressed in muscles and liver that therefore internalize more VLDLs. HGP upregulation is due to different processes: (a) lower utilization of glucose due to reduced glucokinase (GCK) activity, (b) increased adipose tissue lipolysis due to insulin resistance and consequent increase in the releasing of NEFAs in the circulation. Hepatic acetyl-CoA content and pyruvate carboxylase (PC) activity increase, with consequent higher transformation of pyruvate into glucose. In obesity, both liver and adipose tissue undergo an inflammatory response with production of proinflammatory cytokines: interleukin 6 (IL6), tumor necrosis factor alpha (TNF- $\alpha$ ), C-reactive protein (CRP), plasminogen activator inhibitor 1 (PAI-1).

studies are reporting the observation that vWAT and scWAT have no difference in terms of adipose tissue macrophage (ATM) accumulation in severe obese patients [82]. This controversy may be linked to the fact that in the extreme conditions of obesity even the scWAT loses the capacity to properly store lipids, leading to the accumulation of activated ATM.

Thus, inflammation and insulin resistance are major processes that, in the early phase, take place in the vWAT upon overnutrition and obesity development. The consequences are not only local but results in a systemic low-grade inflammation and increased levels of circulating FFA that will particularly affect the liver.

### Diet-induced modifications occurring in the liver

The liver has a central metabolic role. More specifically in the context of this review, the liver regulates metabolic homeostasis across the alternance of fed and fasting states on daily basis, as summarized in Box 2. In context of chronic overnutrition, the liver must cope on the one hand with the direct alteration of these homeostatic metabolic responses. On the other hand, the liver must also cope with metabolites and inflammatory signals coming from the adipose tissue as described above.

### NAFLD as a result of the imbalance between uptake and export of lipid in the liver

As clarified by the World Gastroenterology Association, NAFLD is a condition defined by excessive fat accumulation in the form of triglycerides (steatosis) in

the liver. A subgroup of NAFLD patients displays liver cell injury and inflammation in addition to excessive fat (steatohepatitis), a condition designated as nonalcoholic steatohepatitis (NASH).

In obesity, hepatosteatosis represents the first step of NAFLD. Hepatosteatosis correlates quite well with abdominal adiposity and its incidence is showing the same positive trend as obesity. In a simplified manner, hepatosteatosis results from increased fatty acid uptake, decreased fatty acid use, and decreased export in form of VLDL. Adipose tissue-derived FFAs are the major source of hepatic fatty acids and they represent 59% of liver fat in NAFLD patients [83]. The increased fatty acid uptake is sustained by the increased expression of CD36 in the liver and skeletal muscle of obese patients with NAFLD compared to obese subjects with normal intrahepatic TG content [84]. At the same time, the downregulation of CD36 and the enhanced lipolysis that take place in the adipose tissue, further exacerbate the flux of FFAs toward the liver and the skeletal muscle in NAFLD patients (Fig. 2). The role of FFA uptake in hepatosteatosis was further corroborated in animal model of NAFLD lacking transporters such as CD36 and FATPs, where reduction in liver fatty acid influx prevented steatosis [85,86].

The remaining part of hepatic TG stores derives from dietary fatty acids and *de novo* lipogenesis (DNL) (see Box 2 for DNL in physiological context). The increase in DNL precedes the development of steatosis and is due in part to the insulin resistance of the muscle, which provokes an increased flux of ingested carbohydrates toward the liver [87]. Compared to healthy subjects, in patients with NAFLD the newly synthesized lipids account for a much higher percentage of

**Box 2.** The healthy liver**Anatomy and cellular composition**

The liver is a central metabolic organ, which receives blood from:

- The gastrointestinal tract and the spleen via the hepatic portal circulation. This blood is rich in nutrients coming from the absorbed food. The first passage through the liver of potentially toxic substances allows their detoxification prior to reaching the systemic circulation,
- The hepatic artery, which delivers oxygen to the cells

The drained blood coming from both the portal vein and the hepatic artery join the general circulation via the inferior vena cava.

Eighty percent of the liver volume is occupied by hepatocytes, the parenchymal cells that perform the majority of hepatic metabolic activities.

Nonparenchymal cells consist of Kupffer cells (specialized macrophages), endothelial cells, and also NK, NKT, and CD4<sup>+</sup> T immune cells [233], which together play an important role in the hepatic immune response [234]. Stellate cells, which store vitamin A, are mainly quiescent in the healthy liver, and are rather characterized by their profibrotic activity in the damaged liver.

**The healthy liver in feeding condition**

The high levels of glucose reaching the liver in postprandial state first drive its condensation into glycogen to reconstitute the glycogen store.

The excess of glucose is used for *de novo* lipogenesis (DNL), in which pyruvate coming from glycolysis enters a process leading to palmitate via acetyl-CoA and malonyl CoA [235]. The fatty acids generated by DNL, together with dietary fatty acids are converted in triglycerides and released in the bloodstream in the form of very low-density lipoproteins (VLDLs).

Dietary amino acids can be used by the liver as a source of energy, or to generate proteins and glucose.

**The healthy liver in fasting condition**

Glycaemia levels are maintained through glycogenolysis and then through hepatic glucose production by gluconeogenesis.

The white adipose tissue releases FFAs in the bloodstream as lipolysis products, which are internalized in the liver via specific transporters.

Hepatic fatty acid oxidation produces ketone bodies, which will fuel extrahepatic tissues particularly upon prolonged fasting.

The nuclear receptor PPAR $\alpha$  is a lipid sensor and a key regulator of mitochondrial  $\beta$ -oxidation, peroxisomal  $\beta$ -oxidation, and other aspects of fatty acid metabolism [236,237], in the liver during fasting.

the total intrahepatic fatty acids (15–23% vs 5%) [88]. Highly lipogenic hepatocytes undergo a phenotypic change characterized by enhanced expression of adipogenic genes such as Sterol Regulatory Element-Binding Proteins (SREBPs), Adipose Differentiation-Related Protein (ADRP), and PPAR $\gamma$  [89,90].

At the same time, oxidation of fatty acids in the liver is reduced, contributing to their consequent accumulation in the liver. More particularly, the expression of the nuclear receptor PPAR $\alpha$  [91] is blunted, resulting in a reduction of fatty acid transport to the mitochondria, *via* reduction of Carnitine Palmitoyl Transferase 1 (CPT1) expression, and decreased fatty acid  $\beta$ -oxidation. Reciprocally, liver-specific deletion of PPAR $\alpha$  also caused the development of hepatic steatosis in aging in

mice fed a standard diet [92]. Finally, the TG outflow rate through VLDL contributes to the maintenance of hepatosteatosis. Although subjects with NAFLD have greater VLDL secretion than those with normal intrahepatic TG content, this secretion does not increase linearly with the increasing TG amount but rather reaches a plateau. Therefore, the increase in VLDL secretion rate, in NAFLD patients, is not able to compensate for the increased rate of TG accumulation [93].

Hepatosteatosis *per se* is not necessarily deleterious, and may remain clinically silent, that is, the metabolic functions of the liver are unaffected by the ‘simple’ accumulation of lipids. However, in a number of cases, which in humans reach one-third [94] of the NAFLD patients, complications can ultimately lead to NASH,

where inflammation and fibrosis are severely altering liver functions.

### **From NAFLD to NASH: the role of inflammation in the liver in obesity and overnutrition**

A prolonged overnutrition condition triggers in some case the progression of NAFLD from the simple hepatosteatosis to the development of inflammation, fibrosis, and NASH [95]. A ‘multihit’ hypothesis is presently widely accepted to explain this evolution. As described above, liver lipid accumulation and insulin resistance (see also Metaflammation and specific aspects of PPARs) appears early in NAFLD and worsens steatosis as a result of increased DNL. These alterations expose the liver to ‘multihits’, which include mitochondrial dysfunction, oxidative damage, altered hepatocyte apoptosis, increased levels of fibrogenic and proinflammatory mediators and activation of stellate and Kupffer cells [91]. We will focus below on the inflammatory process, which is a main contributor to the worsening of the liver status.

The inflammatory response of the liver parallels the increase in hepatic lipid accumulation and the development of obesity. Hepatic inflammatory mediators include C-reactive protein, PAI-1, fibrinogen, and IL-6, which mark the presence of a ‘subacute inflammation’ in the liver [96]. However, as for the adipose tissue, the immune cells are the major contributors of liver inflammation.

Two different populations of macrophages mainly drive the inflammatory response in liver: the resident macrophages, known as Kupffer cells, and the recruited macrophages, which migrate into the liver during obesity [97]. Kupffer cells derive from embryonic progenitors of the yolk sac and are found in the liver sinusoids in close proximity with sinusoidal endothelial cells [98], where they protect against pathogenic compounds. However, their activation, induced by toxic lipid droplets present in the liver, seems to represent the ‘first hit’ of NAFLD/NASH pathogenesis [99]. Activated Kupffer cells further enhance hepatic inflammation *via* the secretion of monocyte chemoattractant CCL2 [100], which triggers the recruitment and activation of monocytes from the bloodstream. These monocytes are able to infiltrate the liver as a result of liver injury and to differentiate into proinflammatory M1 macrophages [101]. The primary role of Kupffer cells is supported by the fact that their depletion, using clodronate injections, results in improved liver steatosis, and insulin resistance [102].

However, liver inflammation is also sustained by other immune cells that entertain complex cross-regulation and activation with Kupffer cells and

macrophages [103]. Dendritic cells are antigen-presenting cells that participate to the innate immune defense in the liver and provide support to macrophages. NK cells are the major lymphocyte population in the liver, representing 30–50% of total lymphocytes [104]. NKs as well as T cells are not contributing to the steady-state condition of the liver but are extremely important during the inflammatory response. Activated Kupffer cells are responsible for the stimulation of these cells through a signaling pathway initiated by TLRs. TLR2 or 3 induce Kupffer cell secretion of IL18 and IL1 $\beta$ , thus activating NK cells [105], while TLR4 is responsible for the upregulation of adhesion molecules such as ICAM1 and VCAM on Kupffer cells and hepatic stellate cells, which are then mediating T-cell trapping and activation [106]. In addition, neutrophils are polymorphonuclear leukocytes important in sustaining the liver inflammation process. Hepatic infiltration of neutrophils is an acute response to liver injury, hepatic stress, or systemic inflammatory signals [107] that aggravates the inflammatory reaction by the secretion of cytotoxic reactive oxygen and nitrogen species or of proinflammatory cytokines such as IL1 $\beta$  and TNF [108]. Neutrophil dysfunction is also associated with the development of liver fibrosis and cirrhosis in NASH. Indeed, the neutrophil-to-lymphocyte ratio is higher in patients with NASH and advanced fibrosis, and has been proposed as a noninvasive marker to predict advanced liver disease [109].

Chronic liver inflammation is also associated with tissue damage and remodeling as well as fibrosis [110]. Hepatic macrophages are able to induce differentiation of hepatic stellate cells, the primary cells involved in liver fibrosis, into myofibroblasts and to promote their survival with the secretion of TNF and IL1 [111]. The establishment of a modified microenvironment, where inflammation and fibrosis coexist enhancing liver injury, is thought to be at the base of the progression of liver steatosis to NASH.

### **The adipose tissue-liver cross-talk in metaflammation**

As described above, there are two main processes that start in the adipose tissue and have an impact on the liver environment: the development of systemic low-grade inflammation in obesity, and the increased afflux of FFAs to the liver due to increased lipolysis, together with the inhibition of LPL activity. The importance of WAT lipolysis was also recently highlighted by the efficiency of the pharmacological inhibition of the adipose triglyceride lipase in decreasing insulin resistance and hepatosteatosis in mice [112].

In addition to this metabolic regulation, adipose tissue-derived adipokines and pro-inflammatory cytokines can directly act on liver metabolism and the development of NAFLD [113]. Adiponectin, for example, has a protective role in the progression of hepatic steatosis to fibrosis and NASH. In the model of diet-induced obesity in rats, adiponectin overexpression stimulates hepatic  $\beta$ -oxidation and protects the liver from steatosis and inflammation, thus improving insulin sensitivity [114]. Indeed, adiponectin inhibits hepatic DNL and gluconeogenesis by reducing the expression of the lipogenic transcription factor SREBP1-c and the rate-limiting enzyme Phosphoenolpyruvate Carboxy Kinase (PEPCK), respectively [115]. In addition, adiponectin improves glucose utilization by activating an adenosine monophosphate-activated protein kinase (AMPK-dependent pathway) [116]. In agreement with mouse studies, adiponectin levels are reduced in patients with NAFLD [117] and negatively correlate with liver alanine aminotransferase (ALT) and  $\gamma$ -glutamyltranspeptidase [118], which are indicators of liver lesions.

Leptin, on the other hand, negatively influences the onset and the progression of NAFLD, being positively correlated with serum level of ALT in humans [119]. Moreover, it acts as profibrogenic mediator by stimulating the production of  $\alpha$ -smooth muscle actin ( $\alpha$ -SMA), collagen 1 and the tissue inhibitor of metalloproteinase 1 (TIMP1) in human stellate cells [120]. However, it has been shown that leptin produced by the adipose tissue has an insulin sensitizer effect in the liver and skeletal muscle with regularization of pancreatic  $\beta$ -cell activity [121]. TNF- $\alpha$  and IL-6 also correlated with the progression of NAFLD to NASH and with the onset of insulin resistance by increasing the production of SOCS3 in the liver [122].

Finally, the adipose tissue-derived FFAs may directly act as signaling molecules in the liver *via* interacting with the transcription factor PPAR $\alpha$ , triggering the expression of its target genes and more particularly fibroblast growth factor 21 (FGF21) [123,124]. In turn, FGF21 is part of the reciprocal cross-talk from the liver to the adipose tissue. It is produced mainly by the liver in the fasted state, and has a direct effect on adipose tissue, stimulating both lipolysis and the expression of adiponectin [125]. This signaling to adipose tissue is required for FGF21 activity on increasing insulin sensitivity. However, it also has adipose tissue-independent activity, more particularly on increasing energy expenditure [126]. It is considered as a good candidate for the treatment of T2D and metabolic syndrome primarily for its ability to reduce plasma TGs in rodents and humans [127,128]. FGF21 would act *via* reducing

VLDL secretion in the liver and redirecting TG-rich lipoproteins toward WAT, *via* increased activity of CD36 and LPL in this tissue [129]. Other hepatokines might be discovered, since systematic analyses of the secretome of steatotic hepatocytes identified 32 hepatokines differentially secreted by steatotic vs non-steatotic hepatocytes. Among them, Fetuin B is increased in patients with hepatosteatois, and its silencing in mice improved glucose tolerance [130].

### Linking metabolism and inflammation: insulin sensitivity as the central piece

With the onset of T2D, obese patients display an array of metabolic alterations including hyperinsulinemia, hyperglycemia, and hypertriglyceridemia. High levels of insulin are not able to lower the glycemia: thus the name of insulin resistance. This insulin signaling has been at best studied in the liver, but resistance appears in all metabolic tissues, particularly the adipose tissue, which will be discussed herein in light of their links to metaflammation.

### Insulin signaling in the liver and pathways to insulin resistance in the context of obesity

Insulin signaling has been extensively studied. An overview of insulin signaling in the liver, with a focus on the elements relevant for this review is shown in Figure 3.

Briefly, in terms of processes, the peak of insulin in the postprandial period drives both a reduction in hepatic glucose production (HGP), and an increase in the rate of lipid production *via* DNL. In insulin-resistant liver, the insulin-dependent activation in DNL is maintained, but there is a failure in decreasing glucose production, a process known as 'selective hepatic insulin resistance' [131] (Fig. 2).

In this context, the observation by Lu *et al.* that mice lacking Akt1, Akt2, and forkhead box transcription factor 1 (Foxo1) do not show any defect in insulin-mediated suppression of gluconeogenesis [132], raised the question whether other mediators could have a role in the postprandial reduction of HGP mediated by insulin [133]. The idea that an intertissue connection could participate in regulating this metabolic process comes from the observation that the insulin-dependent suppression of HGP is occurring even in mice with liver specific ablation of insulin receptor [134]. Subsequently, Perry *et al.* [135] demonstrated that HGP is highly sensitive to hepatic acetyl-CoA, whose concentration depends on the levels of circulating FFAs. When insulin fails to suppress

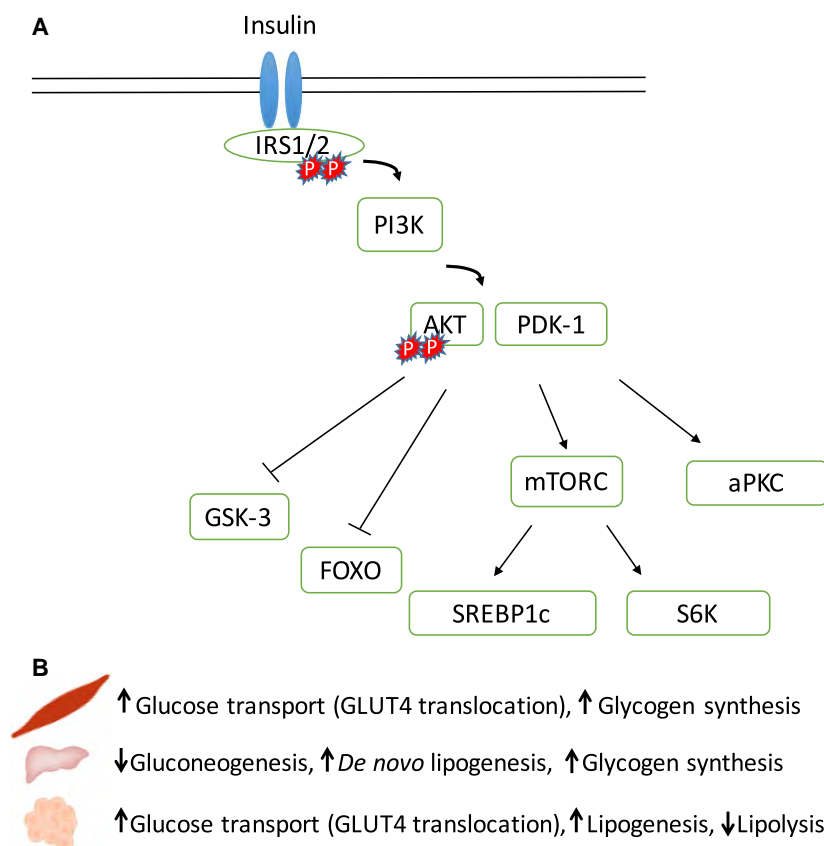


**Fig. 3.** Insulin signaling pathway. (A) The interaction of insulin with the membrane insulin receptor (IR) and insulin receptor substrate 1 and 2 (IRS1/IRS2) are represented. The activation of the phosphatidylinositol 3-kinase (PI3K) mediates the action of insulin on intermediary metabolism, *via* activation of AKT. PI3K-dependent activation of Sterol Regulatory Element-Binding Protein 1c (SREBP1c) and S6 Kinase (S6K) is mediated by the mammalian target of rapamycin complex 1 (mTORC1). In contrast, AKT activation inhibits the activity of Glycogen Synthase Kinase 3 (GSK-3) and the Forkhead box (FOXO) transcription factors, mainly resulting in the inhibition of the activity and transcription of downstream target. Other consequences of PI3K/AKT activation are the activation of the atypical Protein Kinase C (aPKC), which is responsible for the glucose transport in muscles and adipose tissue. (B) Metabolic pathways activated by insulin in muscle, liver, and adipose tissue.

lipolysis in adipose tissue, the high FFA flux to the liver determines a rise in the levels of hepatic acetyl-CoA, which, in turn, maintain high the pyruvate carboxylase activity and the conversion of pyruvate into glucose (Fig. 2). The critical role of FFAs in the regulation of HGP in obesity-related insulin resistance was also pointed by Titchenell *et al.* [136]. These authors suggested that, in fact, insulin action in the liver directly controls only hepatic lipogenesis, while HGP is regulated by insulin in an indirect way through the modulation of the levels of circulating FFAs. Both these reports thus highlighted the key role of FFAs as mediators of the tight connection between liver and adipose tissue in the regulation of HGP in insulin-resistant mice. It must be noted, however, that recent studies highlighted some contexts in which hepatic lipid production is necessary and even beneficial. More particularly, the accumulation of

monounsaturated fatty acids such as oleate rather than polyunsaturated fatty acids, seems rather protective against insulin resistance and glucose intolerance [123,137].

Finally, an additional level of complexity comes from the role of amino acids, which in obesity can activate the Mammalian Target Of Rapamycin Complex 1/S6 Kinase (mTORC1/S6K) signaling pathway [138]. This signal then activates an intertissue neuronal pathway acting on the adipose tissue that results in a reduction of LPL activity and consequent elevation in serum TGs [139].

### Molecular pathways that link inflammation and insulin resistance

The link between inflammation and the onset of insulin resistance in obese patients remained obscure until

the hypoglycemic effects of salicylates were reinvestigated, leading to the identification of the Inhibitor of Nuclear Factor  $\kappa$ B (I $\kappa$ B) kinase  $\beta$  (IKK $\beta$ )/NF $\kappa$ B axis as their molecular target [140]. Concomitantly, increased adiposity and dysregulation of lipid metabolism were shown to correlate with the activation of a diverse range of stress-responsive pathways including the Jun N-terminal Kinases (JNKs), IKK $\beta$ , and inflammasome, which are important mediators of the inflammatory response.

Jun N-terminal Kinases are members of the Mitogen-Activated Protein Kinases (MAPK) family, which are induced in response to cellular stress signals [141] and are able to phosphorylate and activate the protein cJun, a member of the Activator Protein-1 (AP-1) transcription factor family. Their role in the induction of insulin resistance has been largely studied in the past and several mechanisms are proposed to explain how JNKs can induce insulin resistance in response to excess of adiposity. First, JNKs are responsible for the phosphorylation of Irs1 in serine-307, inhibiting the interaction of Irs1 with the insulin receptor [142], whose signaling is normally occurring through the counter-regulatory serine/threonine phosphorylation. Second, JNK1 and 2 are proposed as key mediators in macrophages to allow their recruitment and activation in the obese vWAT. Mice lacking JNK1/2 specifically in myeloid cells are largely protected from the inflammation associated with diet-induced obesity, with less severe insulin resistance, decreased accumulation of macrophages and a relative lower expression of M1-specific cytokines [143]. Finally, JNKs have a role in the reduction of FA oxidation and in the onset of steatosis and insulin resistance in the liver, mainly acting as a negative regulator of PPAR $\alpha$  activity and FGF21 expression in hepatocytes, *via* the activation of the Nuclear Receptor Co-Repressor (NCoR1) complex [144].

The IKK $\beta$  is another inflammatory kinase playing a critical role in the onset of insulin resistance. Its activity is highly selective toward its physiological substrates, the I $\kappa$ B protein inhibitors of NF $\kappa$ B. Phosphorylation by IKK $\beta$  directs I $\kappa$ B $\alpha$  to proteasomal degradation, thus allowing the release of NF $\kappa$ B, a master transcriptional regulator of inflammation. Once delivered from its complex with I $\kappa$ B $\alpha$ , NF $\kappa$ B translocates into the nucleus, where it affects the expression of numerous target genes involved in insulin resistance [145,146]. It has been shown that NF $\kappa$ B is activated in the liver of mice fed a high-fat diet, whereas a reduction in its activity or an increased expression of IKK $\beta$  significantly improve glucose and lipid metabolism [145,147].

As described above, IRS1, the first transducer of insulin signaling, can be phosphorylated by JNKs (Fig. 3). Besides this regulation, IRS1 is also the target of other kinases such as RNA-activated Protein Kinase (PKR), Extracellular signal-Regulated Kinase (ERK), Protein Kinase C $\theta$  (PKC $\theta$ ), mTOR, and SOCS, whose activity is influenced by the inflammatory status. Thus, insulin signaling is sensitive to the antagonizing effects of multiple mediators belonging to different cellular pathways related to the inflammatory response. Further highlighting this interference, inflammatory kinases also counteract insulin sensitivity by directly activating transcription factors such as the AP-1, NF $\kappa$ B and interferon regulatory factors (IRFs) and thus modulating the expression of genes important not only in inflammation but also in glucose, cholesterol metabolism and fatty acid synthesis [148], as detailed below.

Many of the proinflammatory cytokines and adipokines that are produced in obese vWAT, including TNF- $\alpha$ , IL6, IL1 $\beta$ , and resistin, were shown to modulate the activation of the stress-response kinase JNK and IKK $\beta$ . Therefore, a feed-forward loop arises in obesity, where increased adiposity induces the production of proinflammatory cytokines, which, in turn, activate cellular signaling pathways leading to the onset of insulin resistance.

Tumor necrosis factor alpha was the first adipose tissue-secreted cytokine directly linking inflammation and insulin resistance [23]. It exerts its action on the adipose tissue by enhancing adipocyte lipolysis and increasing Irs1 serine phosphorylation through a mechanism dependent on the activation of JNK1/2 in visceral adipose tissue [149]. TNF- $\alpha$  levels are increased in the adipose tissue and in the plasma of obese individuals [30], where it correlates with markers of insulin resistance [31]. Moreover, mouse models of genetic loss-of-function for TNF- $\alpha$ , TNF Receptors 1/2, JNKs, are all protected when challenged with high-fat diet [150,151]. However, the use of TNF- $\alpha$  as target to treat insulin resistance in diabetic patients did not turn to be successful. Clinical trials using short- and long-term administration of TNF- $\alpha$  antagonists were able to reduce systemic inflammatory markers but showed poor effects on insulin resistance [152–154].

Interleukin 6 is a proinflammatory cytokine produced mainly by the adipose tissue that is thought to play a role in the onset of insulin resistance. This action would be mediated by IL6-induced reduction in GLUT4 and Irs1 expression levels through the activation of the JACK-STAT signaling pathway and the increased expression of SOCS3 [155]. However, the direct link between IL6 and obesity-induced insulin



resistance is controversial. On the one hand, it is thought to suppress insulin ability to modulate gluconeogenesis in liver and this was demonstrated both in mice [156] and *in vitro*, using HepG2 human cell line [157]. On the other hand, IL6 deficiency worsens hepatic insulin resistance and inflammation in a mouse model of diet-induced obesity [158]. These contradictory results on IL6 role in insulin resistance can be in part explained by its multiple action in different organs (i.e., skeletal muscle or liver) and in part by its different sources (i.e., muscle and adipose tissue).

The action of IL18 is also debated in the literature with negative effects on insulin sensitivity reported in a rat model of metabolic syndrome [159], whereas IL18-deficient mice show hyperphagia, obesity, and insulin resistance [160].

Finally, the adipokine resistin was initially reported as a major player in insulin resistance, thus its name. Mice lacking resistin are protected from diet-induced hyperglycemia, due to AMPK increased activity and reduced expression of gluconeogenic genes [161]. However, in humans, the role of resistin is less clear and quite debated, with reports showing a positive association between resistin levels and the development of obesity, insulin resistance and T2D [162] and others refuting any kind of association with the development of metabolic syndrome [163,164]. One of the possible explanations of the difference between mice and human is the different pattern of resistin expression, which, in mice, is totally restricted to adipocytes, whereas in humans is exclusively observed in macrophages and monocytes [165,166].

### Lipid mediators of insulin resistance

The altered lipid flux that prevails in obesity has been associated to insulin-resistant states, being both the cause and the result of insulin resistance. Circulating fatty acids can impair insulin signaling mainly in two ways.

On the one hand fatty acids can interfere with the downstream pathways of insulin binding [167], *via* the interaction of long saturated fatty acids, such as palmitate, with the receptors TLR2, TLR4 and Nucleotide-binding oligomerization domain, Leucine-rich Repeat (NLR) and Pysin domain containing 3 (NLRP3) [168,169]. Upon ligand binding, TLRs trigger a signaling cascade that leads to the activation of IKK $\beta$  and MAPKs such as p38, JNK, and ERK1/2. In parallel, NLRP3 can be activated by host-derived molecules, including excess ATP, glucose, ceramides, reactive oxygen species, that are abundant in obese individuals.

NLRP3 activation initiates the assembly of the inflammasome, a large multiprotein complex which governs the maturation of the proinflammatory cytokines IL-1 $\beta$  and IL-18 [170–172]. The key role of this complex in the obesity-induced adipose tissue inflammatory response has been demonstrated by the blunted response to ceramide of macrophages derived from the adipose tissue of Nlrp3 knockout mice, which display a reduction in macrophage M1 polarization in the fat tissue [172].

All these multiple pathways activated by overnutrition converge onto the stimulation of the major inflammatory kinases JNK and IKK $\beta$ , which, as described above, interfere with insulin signal transduction.

On the other hand, the accumulation of intracellular lipid products, such as diacylglycerols (DAG) and ceramides can directly be the cause of insulin resistance. This last mechanism raises the concept of lipotoxicity, as referred to the ability of excessive lipids to contribute to the pathophysiology of metabolic syndrome and T2D [173]. Once entered in the cell, fatty acids are rapidly esterified with coenzyme A to form acyl-CoAs. These intermediates are then transferred to a glycerol backbone to form mono-, di-, and triacylglycerols. In the liver, the link between DAG accumulation and insulin resistance is attributed to the activation of Protein Kinase C $\epsilon$  (PKC $\epsilon$ ) [174], which binds and inhibits insulin receptor kinase activity. By knocking down the hepatic PKC $\epsilon$  expression using specific antisense oligonucleotides, Samuel *et al.* were able to protect rats from lipid-induced hepatic insulin resistance, independently of the increased hepatic lipid levels [175].

Ceramides represent another class of fatty acid derivatives whose intracellular levels are strongly associated with insulin resistance [176,177]. Their biosynthesis occurs through the condensation of saturated fatty acids (preferentially palmitate) with amino acids (preferentially serine) to form 3-ketosphingamine, the scaffold for all sphingolipids. The sphingoid backbone subsequently acquires additional fatty acids leading to the production of a series of sphingolipids that include ceramides and other more complex products [178]. Inhibition of ceramide production through the administration of myriocin, a potent inhibitor of Serine Palmitoyl Transferase (SPTLC), prevents the development of insulin resistance and diabetes in obese mice [179,180]. This insulin sensitizing effect is mediated by a reduction in the circulating levels of leptin and a concomitant increase in adiponectin and FGF21. A decrease in ceramide production was also observed in mice carrying an intestinal-specific Farnesoid X Receptor (*Fxr*) gene deletion and resulted in a

downregulation of hepatic SREBP1c and decreased DNL [181]. Furthermore, supporting the beneficial effect of the hampering of ceramide production, myriocin administration, as well as Sptlc2 ablation specifically in adipose tissue, induces macrophage M2 polarization, most prominently in the scWAT, with concomitant increase in serum anti-inflammatory cytokine IL10 and reduction in proinflammatory cytokines IL6, MCP1, and TNF- $\alpha$  [182]. Conversely, elevated intracellular ceramide levels have been shown to stimulate the ability of phosphatase 2A to dephosphorylate AKT, thus interfering with insulin signaling [177]. Notably, both saturated fatty acids and TNF- $\alpha$  induce SPTLC expression, and the subsequent production of ceramide, *via* activation of TLR4 [176,183] and their action is mediated by IKK $\beta$ . In the case of the TNF $\alpha$ -mediated cascade, this is an emblematic example of how an inflammatory stimulus can promote the production of lipid intermediates, which, in turn, impairs insulin action.

Lastly, a compelling body of evidence has accumulated in recent years showing how intracellular fluctuations of several metabolites, as a function of the metabolic status, may influence the activity of chromatin regulators. The resulting epigenetic changes at the level of DNA and histone modifications have a major influence on the control of gene transcription during embryonic development as well as in the differentiated tissues of the adult organism.

Example of metabolites influencing chromatin-modifying enzymes include acetyl-CoA, which is the universal donor for acetylation reactions [184], and S-adenosylmethionine, which acts as a methyl donor

substrate stimulating DNA methyltransferase reactions [185]. The cross-talk between metabolites and epigenetic regulation is described elsewhere [186].

## Metaflammation and specific aspects of PPARs

Peroxisome proliferator-activated receptors (PPARs) are nuclear receptors that function as ligand-activated transcriptional regulators, with both activation and repression mechanisms, depending on the condition/target. Three PPAR isoforms exist, PPAR $\alpha$ , PPAR $\beta/\delta$ , and PPAR $\gamma$ , which are characterized by distinct functions and expression patterns (Table 1). Their peculiar role in the regulation of glucose and lipid metabolism and inflammation puts PPARs at the crossroad of many molecular pathways involved in metaflammation development. This paragraph will mainly consider PPAR activity in the adipose tissue and the liver, the tissue focus of this review, and their potential use as therapeutic target for the treatment of obesity [187,188].

The PPAR $\alpha$  has a crucial role in regulating hepatic fatty acid catabolism and clearance, as demonstrated by its target genes such as CPT1, Carnitine Acylcarnitine Translocase (SLC25A20), Medium-chain Acyl-CoA Dehydrogenase, Acyl-CoA Oxidase 1, that globally induce fatty acid oxidation [189]. In addition, PPAR $\alpha$  enhances the expression of the FGF21, a secreted factor that further stimulates hepatic fatty acid utilization, but that also improves systemic insulin sensitivity through its extrahepatic enhancement of glucose transporter 1 expression [127,190]. PPAR $\alpha$

**Table 1.** Peroxisome proliferator-activated receptors (PPARs). PPARs are ligand-activated transcription factors that bind, in form of heterodimers with the Retinoid-X-receptor (RXR), to specific DNA sequences called PPAR-Responsive Elements (PPRE), at the regulatory regions of target genes [238]. The three PPAR isoforms, PPAR $\alpha$ , PPAR $\beta/\delta$ , and PPAR $\gamma$ , are encoded in separate genes and share a high structural homology, except for their ligand-binding domain.

Receptor	Expression	Function	Natural ligands	Synthetic ligands
PPAR $\alpha$	Liver, skeletal muscle, heart, intestinal mucosa, and brown adipose tissue	Induces the expression of genes involved in lipid and lipoprotein metabolism, mitochondrial and peroxisomal fatty acid oxidation, ketone synthesis (reviewed in Ref. [240]) and has anti-inflammatory effects	Omega-3 dietary fatty acids and eicosanoids	Fibrates, Wy-14643
PPAR $\beta/\delta$	ubiquitously expressed, particularly in tissues with high metabolic rate, such as liver, skeletal muscle, heart, adipose tissue, and macrophages [239]	Regulates fatty acid oxidation, lipid and cholesterol metabolism, and has anti-inflammatory effects (reviewed in Ref. 241)	Unsaturated fatty acids and eicosanoids	GW501516, GW0742, L-165041
PPAR $\gamma$	It has two isoforms. PPAR $\gamma$ 1: ubiquitously expressed; PPAR $\gamma$ 2: white and brown adipose tissue [239]	Master regulator of adipocyte differentiation and lipid storage. It also regulates glucose and fatty acid transporters and has anti-inflammatory effects (reviewed in Ref. [242])	Prostaglandin and eicosanoids	TZDs, GW1929, GW2090, SR1664

displays also anti-inflammatory activity, by interfering with NF $\kappa$ B activation [191]. Altogether, these features make PPAR $\alpha$  an interesting therapeutic target for obesity, particularly in the presence of hepatosteatosis. Selective PPAR $\alpha$ -agonists, such as fibrates were efficiently used for decades in hyperlipidemic patients to lower plasma triglycerides [192]. However, and despite encouraging results obtained in mouse models of NAFLD, these molecules did not prove advantageous in the treatment of NAFLD/NASH in humans, likely due to their lower potency in humans, compared to mice [193] (reviewed in Ref. [193]). Furthermore, a number of side effects (i.e., increased risk of acute kidney injury, rhabdomyolysis, and gallstone formation) were associated with their long-lasting use [194].

Another key positive modulator of FA oxidation, particularly in skeletal muscle, is PPAR $\beta/\delta$ . However, in the liver, FA oxidation is mainly under the control of PPAR $\alpha$ , while PPAR $\beta/\delta$ -selective activation suppresses hepatic gluconeogenesis, enhances carbohydrate catabolism [195], and has anti-inflammatory effects in the liver by dampening Kupffer cell activation [196]. In the adipose tissue, PPAR $\beta/\delta$  inhibits FFA release. While the selective PPAR $\beta/\delta$  ligand GW501516 was discontinued from clinical trials for favoring tumor development in several organs, KD3010 [197] is currently in phase III clinical trial for the treatment of obesity, NASH, and T2D. A detailed description of other PPAR $\beta/\delta$  agonist can be found elsewhere [198].

In the adipose tissue, PPAR $\gamma$  is the master regulator of adipogenesis [199] and its activation with Thiazolidinediones (TZDs) leads to *de novo* differentiation of adipocytes. TZDs are potent insulin sensitizer agents, but their clinical use in the last years has been strongly limited due to the associated risk of increased body weight, bone fractures, congestive heart failure, and bladder cancer [200,201]. In humans, PPAR $\gamma$  activation triggers apoptosis of large fat cells in vWAT and scWAT and induces differentiation of preadipocytes only in scWAT [202], thus favoring scWAT adiposity [203]. The formation of new adipocytes with the activation of genes such as Fatty Acids-Binding Protein 4 (FABP4), CD36, LPL Fatty Acids Transporter (FATP1), and SREBP1 [204], improves the uptake and storage of plasmatic FFAs in AT, with the subsequent reduction in circulating TGs and of lipotoxic accumulation in nonstorage specialized tissues, such as liver and muscles [205]. TZDs also enhance FFA mobilization upon fasting and ameliorate the postprandial suppression of FFA release triggered by insulin [206]. Interestingly, chronic treatment of human adipocytes with TZDs initiates a 'browning program' characterized by induction of Uncoupling Protein 1 (Ucp1) [207,208] and

of several components of the mitochondrial transport chain [209], thus initiating a tissue remodeling program that is considered as a promising way to combat obesity through consumption of lipids to produce heat.

Besides their effects on adipogenesis, PPAR $\gamma$  agonists also promote the expression of components of the insulin signaling pathway, including the IRS2 and CAP [210,211], that contributes to enhance adipocyte insulin sensitivity. In addition, PPAR $\gamma$  activation restores the expression and secretion levels of different adipokines such as adiponectin, resistin [212], IL6, TNF- $\alpha$  [213], PAI-1, MCP1, and angiotensinogen [214] that are altered in obesity. Thus, TZDs display also beneficial effects on the development of adipose tissue inflammation upon chronic overnutrition. Importantly, such anti-inflammatory properties of PPAR $\gamma$  agonists are the result of their action not only in adipocytes but also in all the PPAR $\gamma$ -expressing immune cells residing in adipose tissue. In macrophages, PPAR $\gamma$  acts as negative regulator of classical proinflammatory M1 polarization [215] and promotes the shift toward the alternative M2 macrophage activation in response to IL4 [216], thus reducing the expression of inflammatory markers such as Metalloproteinase Domain-8 (ADAM8), Macrophage Inflammatory Protein 1 $\alpha$  (MIP-1 $\alpha$ ), Macrophage Antigen 1 (MAC-1), F4/80, and CD68 [217]. In M2 macrophages PPAR $\gamma$  is required to induce  $\beta$ -oxidation and mitochondrial biogenesis [218] as well as expression of Arginase 1 (Arg1), a specific M2 marker. In obesity, PPAR $\gamma$  has been proposed to play a crucial anti-inflammatory role in the so-called metabolically activated macrophages in the adipose tissue [67]. Consistently, mice lacking PPAR $\gamma$  in myeloid cells when challenged with a high-fat diet are more prone to develop obesity and insulin resistance, mainly due to mitochondrial dysfunction and altered glucose disposal in adipose tissue [218,219].

More recently, PPAR $\gamma$  has been shown to play a role also in regulating the accumulation of T<sub>reg</sub> cells in vWAT. T<sub>reg</sub>-specific PPAR $\gamma$  ablation reduces the population of vWAT T<sub>reg</sub> cells on normal chow diet, while injection of PPAR $\gamma$  agonist into HFD-treated mice specifically induces an expansion of T<sub>reg</sub> population in adipose tissue [220], with beneficial consequences on the tissue inflammatory pattern.

One special note must be made about hepatic PPAR $\gamma$  activity in obesity. PPAR $\gamma$ , whose hepatic expression is very low in lean subjects, is strongly upregulated in steatotic liver. As a consequence, TZD treatment in obese/NAFLD patients favors the transcription of the lipogenic transcription factors SREBP1c in the liver, thus increasing the hepatic production of TGs and the maintenance of steatosis [221].

This explains why, in spite of their ability to reduce lipotoxicity by favoring lipid storage in adipose tissue, TZDs are not able to counteract the development of NAFLD in mice exposed to high-fat diet.

In conclusion, although the long-lasting use of PPAR agonists highlighted the occurrence of considerable side effects that raise the necessity to improve their long-term safety profile, the modulation of PPAR activity is still an attractive possibility to ameliorate obesity-related inflammation, insulin resistance, and NAFLD. The development of safer PPAR agonists still requires a deeper understanding of PPAR signaling and their changes in obesity. As an example, in the obese state, PPAR $\gamma$  was recently shown to undergo phosphorylation at serine 273, a post-transcriptional modification that alters the transcriptional effects of PPAR $\gamma$  and its sensitivity to ligands [222,223]. The new synthetic compound SR1664, which was shown to block this phosphorylation of serine 273, has been recently proposed as an antidiabetic drug [224]. Another appealing approach that has been explored in the pharmacological use of PPAR agonists is the combination of the therapeutic benefits of the activation at least two PPAR isoforms with the development of dual PPAR agonists. Although so far most of these molecules displayed safety issues, saroglitazar, a dual PPAR $\alpha/\gamma$  activator, has currently been approved in India for the treatment of diabetic patients with NAFLD [225]. Finally, a more systematic consideration of species-related differences, when comparing the activity of PPAR agonists in mice and humans, would be also beneficial for the successful development of new therapeutic ligands [226]. The systematic and complementary use of system biology approaches, evaluating PPAR activity in a given tissue/cell, but integrating such information in the context of the whole organism, will perhaps allow accounting for PPAR agonist pleiotropic effects without considering only a single receptor-dependent pathway.

## Conclusions and perspectives

Obesity, especially visceral adipose tissue overload, is associated with many metabolic disturbances, and more particularly insulin resistance, dyslipidemia, and NAFLD. In the last years enormous efforts have been made to uncover new mechanisms contributing to the onset of insulin resistance. Particular progresses were made in understanding how nutritional overload, as well as particular classes of metabolites and lipids can induce a plethora of pathological modifications in different metabolic organs that can alter their physiological activity.

The low-grade inflammatory response or metaflammation is a well-established consequence of the diet-induced obesity and the characterization of the mechanism of recruitment and activation of different immune cell population is a very active research field. However, the attempt to study the modulation of the immune response playing with the balance between pro- and anti-inflammatory cells has been pursued mainly in mouse model whose immune system is, for some aspects, different from humans, leaving an open question on the feasibility of a treatment based on a delicate equilibrium that should favor metabolic outcome without causing other perturbations.

The hope to develop efficient cure to improve insulin resistance in obesity using unique target, such as PPARs (but also, for example, AKT or JNK pathways) faded away over the last years. The evidence that the model in which one factor is the primary responsible for the onset of insulin resistance is clearly too simplistic, as is the idea that targeting one single factor will correct the myriad of defects observed in the context of obesity and insulin resistance. Considering the fact that obesity is a disease where multiple organs, endocrine pathways, and inflammatory responses are involved, the future challenge will be to develop a holistic approach where knowledge of different systems are processed together in order to see how they are interconnected in humans. This is the ambitious goal of system medicine, and only its achievement will open the door for personalized medicine.

## References

- 1 Zimmet P, Magliano D, Matsuzawa Y, Alberti G and Shaw J (2005) The metabolic syndrome: a global public health problem and a new definition. *J Atheroscler Thromb* **12**, 295–300.
- 2 Gregor MF and Hotamisligil GS (2011) Inflammatory mechanisms in obesity. *Annu Rev Immunol* **29**, 415–445.
- 3 Bluher M (2010) The distinction of metabolically ‘healthy’ from ‘unhealthy’ obese individuals. *Curr Opin Lipidol* **21**, 38–43.
- 4 Samocha-Bonet D, Chisholm DJ, Tonks K, Campbell LV and Greenfield JR (2012) Insulin-sensitive obesity in humans – a ‘favorable fat’ phenotype? *Trends Endocrinol Metab* **23**, 116–124.
- 5 Ryden M, Hrydzinszko O, Mileti E, Raman A, Bornholdt J, Boyd M, Toft E, Qvist V, Naslund E, Thorell A *et al.* (2016) The adipose transcriptional response to insulin is determined by obesity, not insulin sensitivity. *Cell Rep* **16**, 2317–2326.

- 6 Lopez-Velazquez JA, Silva-Vidal KV, Ponciano-Rodriguez G, Chavez-Tapia NC, Arrese M, Uribe M and Mendez-Sanchez N (2014) The prevalence of nonalcoholic fatty liver disease in the Americas. *Ann Hepatol* **13**, 166–178.
- 7 Bellentani S and Marino M (2009) Epidemiology and natural history of non-alcoholic fatty liver disease (NAFLD). *Ann Hepatol* **8** (Suppl 1), S4–S8.
- 8 Montague CT, Prins JB, Sanders L, Digby JE and O'Rahilly S (1997) Depot- and sex-specific differences in human leptin mRNA expression: implications for the control of regional fat distribution. *Diabetes* **46**, 342–347.
- 9 Kershaw EE and Flier JS (2004) Adipose tissue as an endocrine organ. *J Clin Endocrinol Metab* **89**, 2548–2556.
- 10 Tchkonina T, Thomou T, Zhu Y, Karagiannides I, Pothoulakis C, Jensen MD and Kirkland JL (2013) Mechanisms and metabolic implications of regional differences among fat depots. *Cell Metab* **17**, 644–656.
- 11 Rosen ED and Spiegelman BM (2014) What we talk about when we talk about fat. *Cell* **156**, 20–44.
- 12 Gesta S, Bluher M, Yamamoto Y, Norris AW, Berndt J, Kralisch S, Boucher J, Lewis C and Kahn CR (2006) Evidence for a role of developmental genes in the origin of obesity and body fat distribution. *Proc Natl Acad Sci U S A* **103**, 6676–6681.
- 13 Tchkonina T, Lenburg M, Thomou T, Giorgadze N, Frampton G, Pirtskhalava T, Cartwright A, Cartwright M, Flanagan J, Karagiannides I *et al.* (2007) Identification of depot-specific human fat cell progenitors through distinct expression profiles and developmental gene patterns. *Am J Physiol Endocrinol Metab* **292**, E298–E307.
- 14 Hausman DB, DiGirolamo M, Bartness TJ, Hausman GJ and Martin RJ (2001) The biology of white adipocyte proliferation. *Obesity Rev* **2**, 239–254.
- 15 Lee YS, Kim JW, Osborne O, Oh DY, Sasik R, Schenk S, Chen A, Chung H, Murphy A, Watkins SM *et al.* (2014) Increased adipocyte O<sub>2</sub> consumption triggers HIF-1 $\alpha$ , causing inflammation and insulin resistance in obesity. *Cell* **157**, 1339–1352.
- 16 Jeffery E, Church CD, Holtrup B, Colman L and Rodeheffer MS (2015) Rapid depot-specific activation of adipocyte precursor cells at the onset of obesity. *Nat Cell Biol* **17**, 376–385.
- 17 Kim JI, Huh JY, Sohn JH, Choe SS, Lee YS, Lim CY, Jo A, Park SB, Han W and Kim JB (2015) Lipid-overloaded enlarged adipocytes provoke insulin resistance independent of inflammation. *Mol Cell Biol* **35**, 1686–1699.
- 18 Furukawa S, Fujita T, Shimabukuro M, Iwaki M, Yamada Y, Nakajima Y, Nakayama O, Makishima M, Matsuda M and Shimomura I (2004) Increased oxidative stress in obesity and its impact on metabolic syndrome. *J Clin Invest* **114**, 1752–1761.
- 19 Ozcan U, Cao Q, Yilmaz E, Lee AH, Iwakoshi NN, Ozdelen E, Tuncman G, Gorgun C, Glimcher LH and Hotamisligil GS (2004) Endoplasmic reticulum stress links obesity, insulin action, and type 2 diabetes. *Science* **306**, 457–461.
- 20 Kawasaki N, Asada R, Saito A, Kanemoto S and Imaizumi K (2012) Obesity-induced endoplasmic reticulum stress causes chronic inflammation in adipose tissue. *Sci Rep* **2**, 799.
- 21 Hosogai N, Fukuhara A, Oshima K, Miyata Y, Tanaka S, Segawa K, Furukawa S, Tochino Y, Komuro R, Matsuda M *et al.* (2007) Adipose tissue hypoxia in obesity and its impact on adipocytokine dysregulation. *Diabetes* **56**, 901–911.
- 22 Sun K, Halberg N, Khan M, Magalang UJ and Scherer PE (2013) Selective inhibition of hypoxia-inducible factor 1 $\alpha$  ameliorates adipose tissue dysfunction. *Mol Cell Biol* **33**, 904–917.
- 23 Hotamisligil GS, Shargill NS and Spiegelman BM (1993) Adipose expression of tumor necrosis factor- $\alpha$ : direct role in obesity-linked insulin resistance. *Science* **259**, 87–91.
- 24 Hotamisligil GS (2017) Inflammation, metaflammation and immunometabolic disorders. *Nature* **542**, 177–185.
- 25 Cinti S (2012) The adipose organ at a glance. *Dis Model Mech* **5**, 588–594.
- 26 Strissel KJ, Stancheva Z, Miyoshi H, Perfield JW 2nd, DeFuria J, Jick Z, Greenberg AS and Obin MS (2007) Adipocyte death, adipose tissue remodeling, and obesity complications. *Diabetes* **56**, 2910–2918.
- 27 Jernas M, Palming J, Sjöholm K, Jennische E, Svensson PA, Gabrielsson BG, Levin M, Sjögren A, Rudemo M, Lystig TC *et al.* (2006) Separation of human adipocytes by size: hypertrophic fat cells display distinct gene expression. *FASEB J* **20**, 1540–1542.
- 28 Winkler G, Kiss S, Keszthelyi L, Sapi Z, Ory I, Salamon F, Kovacs M, Vargha P, Szekeres O, Speer G *et al.* (2003) Expression of tumor necrosis factor (TNF)- $\alpha$  protein in the subcutaneous and visceral adipose tissue in correlation with adipocyte cell volume, serum TNF- $\alpha$ , soluble serum TNF-receptor-2 concentrations and C-peptide level. *Eur J Endocrinol* **149**, 129–135.
- 29 Ouchi N, Kihara S, Arita Y, Maeda K, Kuriyama H, Okamoto Y, Hotta K, Nishida M, Takahashi M, Nakamura T *et al.* (1999) Novel modulator for endothelial adhesion molecules: adipocyte-derived plasma protein adiponectin. *Circulation* **100**, 2473–2476.
- 30 Kern PA, Saghizadeh M, Ong JM, Bosch RJ, Deem R and Simsolo RB (1995) The expression of tumor necrosis factor in human adipose tissue. Regulation by

- obesity, weight loss, and relationship to lipoprotein lipase. *J Clin Invest* **95**, 2111–2119.
- 31 Hivert MF, Sullivan LM, Fox CS, Nathan DM, D'Agostino RB Sr, Wilson PW and Meigs JB (2008) Associations of adiponectin, resistin, and tumor necrosis factor- $\alpha$  with insulin resistance. *J Clin Endocrinol Metab* **93**, 3165–3172.
- 32 Kanda H, Tateya S, Tamori Y, Kotani K, Hiasa K, Kitazawa R, Kitazawa S, Miyachi H, Maeda S, Egashira K *et al.* (2006) MCP-1 contributes to macrophage infiltration into adipose tissue, insulin resistance, and hepatic steatosis in obesity. *J Clin Invest* **116**, 1494–1505.
- 33 Kirk EA, Sagawa ZK, McDonald TO, O'Brien KD and Heinecke JW (2008) Monocyte chemoattractant protein deficiency fails to restrain macrophage infiltration into adipose tissue [corrected]. *Diabetes* **57**, 1254–1261.
- 34 Tamura Y, Sugimoto M, Murayama T, Ueda Y, Kanamori H, Ono K, Ariyasu H, Akamizu T, Kita T, Yokode M *et al.* (2008) Inhibition of CCR2 ameliorates insulin resistance and hepatic steatosis in db/db mice. *Arterioscler Thromb Vasc Biol* **28**, 2195–2201.
- 35 Sopasakis VR, Sandqvist M, Gustafson B, Hammarstedt A, Schmelz M, Yang X, Jansson PA and Smith U (2004) High local concentrations and effects on differentiation implicate interleukin-6 as a paracrine regulator. *Obes Res* **12**, 454–460.
- 36 Wood IS, Wang B, Jenkins JR and Trayhurn P (2005) The pro-inflammatory cytokine IL-18 is expressed in human adipose tissue and strongly upregulated by TNF $\alpha$  in human adipocytes. *Biochem Biophys Res Comm* **337**, 422–429.
- 37 Ziccardi P, Nappo F, Giugliano G, Esposito K, Marfella R, Cioffi M, D'Andrea F, Molinari AM and Giugliano D (2002) Reduction of inflammatory cytokine concentrations and improvement of endothelial functions in obese women after weight loss over one year. *Circulation* **105**, 804–809.
- 38 Esposito K, Pontillo A, Ciotola M, Di Palo C, Grella E, Nicoletti G and Giugliano D (2002) Weight loss reduces interleukin-18 levels in obese women. *J Clin Endocrinol Metab* **87**, 3864–3866.
- 39 Wolf AM, Wolf D, Rumpold H, Enrich B and Tilg H (2004) Adiponectin induces the anti-inflammatory cytokines IL-10 and IL-1RA in human leukocytes. *Biochem Biophys Res Comm* **323**, 630–635.
- 40 Friedman JM and Halaas JL (1998) Leptin and the regulation of body weight in mammals. *Nature* **395**, 763–770.
- 41 Santos-Alvarez J, Goberna R and Sanchez-Margalet V (1999) Human leptin stimulates proliferation and activation of human circulating monocytes. *Cell Immunol* **194**, 6–11.
- 42 Kiguchi N, Maeda T, Kobayashi Y, Fukazawa Y and Kishioka S (2009) Leptin enhances CC-chemokine ligand expression in cultured murine macrophage. *Biochem Biophys Res Comm* **384**, 311–315.
- 43 Gainsford T, Willson TA, Metcalf D, Handman E, McFarlane C, Ng A, Nicola NA, Alexander WS and Hilton DJ (1996) Leptin can induce proliferation, differentiation, and functional activation of hemopoietic cells. *Proc Natl Acad Sci U S A* **93**, 14564–14568.
- 44 Lord GM, Matarese G, Howard JK, Baker RJ, Bloom SR and Lechler RI (1998) Leptin modulates the T-cell immune response and reverses starvation-induced immunosuppression. *Nature* **394**, 897–901.
- 45 Grunfeld C, Zhao C, Fuller J, Pollack A, Moser A, Friedman J and Feingold KR (1996) Endotoxin and cytokines induce expression of leptin, the ob gene product, in hamsters. *J Clin Invest* **97**, 2152–2157.
- 46 Bokarewa M, Nagaev I, Dahlberg L, Smith U and Tarkowski A (2005) Resistin, an adipokine with potent proinflammatory properties. *J Immunol* **174**, 5789–5795.
- 47 Verma S, Li SH, Wang CH, Fedak PW, Li RK, Weisel RD and Mickle DA (2003) Resistin promotes endothelial cell activation: further evidence of adipokine-endothelial interaction. *Circulation* **108**, 736–740.
- 48 Odegaard JI and Chawla A (2011) Alternative macrophage activation and metabolism. *Annu Rev Pathol* **6**, 275–297.
- 49 Ota T (2013) Chemokine systems link obesity to insulin resistance. *Diabetes Metab J* **37**, 165–172.
- 50 Cinti S, Mitchell G, Barbatelli G, Murano I, Ceresi E, Faloia E, Wang S, Fortier M, Greenberg AS and Obin MS (2005) Adipocyte death defines macrophage localization and function in adipose tissue of obese mice and humans. *J Lipid Res* **46**, 2347–2355.
- 51 Chawla A, Nguyen KD and Goh YP (2011) Macrophage-mediated inflammation in metabolic disease. *Nat Rev Immunol* **11**, 738–749.
- 52 Weisberg SP, McCann D, Desai M, Rosenbaum M, Leibel RL and Ferrante AW Jr (2003) Obesity is associated with macrophage accumulation in adipose tissue. *J Clin Invest* **112**, 1796–1808.
- 53 Lumeng CN, DelProposto JB, Westcott DJ and Saltiel AR (2008) Phenotypic switching of adipose tissue macrophages with obesity is generated by spatiotemporal differences in macrophage subtypes. *Diabetes* **57**, 3239–3246.
- 54 Lumeng CN, Bodzin JL and Saltiel AR (2007) Obesity induces a phenotypic switch in adipose tissue macrophage polarization. *J Clin Invest* **117**, 175–184.
- 55 Clement K, Viguier N, Poitou C, Carette C, Pelloux V, Curat CA, Sicard A, Rome S, Benis A, Zucker JD *et al.* (2004) Weight loss regulates inflammation-related genes in white adipose tissue of obese subjects. *FASEB J* **18**, 1657–1669.

- 56 Rouault C, Pellegrinelli V, Schilch R, Cotillard A, Poitou C, Tordjman J, Sell H, Clement K and Lacasa D (2013) Roles of chemokine ligand-2 (CXCL2) and neutrophils in influencing endothelial cell function and inflammation of human adipose tissue. *Endocrinology* **154**, 1069–1079.
- 57 Gruen ML, Hao M, Piston DW and Hasty AH (2007) Leptin requires canonical migratory signaling pathways for induction of monocyte and macrophage chemotaxis. *Am J Physiol Cell Physiol* **293**, C1481–C1488.
- 58 Mattioli B, Straface E, Quaranta MG, Giordani L and Viora M (2005) Leptin promotes differentiation and survival of human dendritic cells and licenses them for Th1 priming. *J Immunol* **174**, 6820–6828.
- 59 Zhou Y, Yu X, Chen H, Sjoberg S, Roux J, Zhang L, Ivoulsou AH, Bensaid F, Liu CL, Liu J *et al.* (2015) Leptin deficiency shifts mast cells toward anti-inflammatory actions and protects mice from obesity and diabetes by polarizing M2 macrophages. *Cell Metab* **22**, 1045–1058.
- 60 Liao X, Sharma N, Kapadia F, Zhou G, Lu Y, Hong H, Paruchuri K, Mahabeshwar GH, Dalmas E, Venteclef N *et al.* (2011) Kruppel-like factor 4 regulates macrophage polarization. *J Clin Invest* **121**, 2736–2749.
- 61 Nguyen KD, Qiu Y, Cui X, Goh YP, Mwangi J, David T, Mukundan L, Brombacher F, Locksley RM and Chawla A (2011) Alternatively activated macrophages produce catecholamines to sustain adaptive thermogenesis. *Nature* **480**, 104–108.
- 62 Konner AC and Bruning JC (2011) Toll-like receptors: linking inflammation to metabolism. *Trends Endocrinol Metab* **22**, 16–23.
- 63 Pal D, Dasgupta S, Kundu R, Maitra S, Das G, Mukhopadhyay S, Ray S, Majumdar SS and Bhattacharya S (2012) Fetuin-A acts as an endogenous ligand of TLR4 to promote lipid-induced insulin resistance. *Nat Med* **18**, 1279–1285.
- 64 Xu X, Grijalva A, Skowronski A, van Eijk M, Serlie MJ and Ferrante AW Jr (2013) Obesity activates a program of lysosomal-dependent lipid metabolism in adipose tissue macrophages independently of classic activation. *Cell Metab* **18**, 816–830.
- 65 Zeyda M and Stulnig TM (2007) Adipose tissue macrophages. *Immunol Lett* **112**, 61–67.
- 66 Bourlier V, Zakaroff-Girard A, Miranville A, De Barros S, Maumus M, Sengenès C, Galitzky J, Lafontan M, Karpe F, Frayn KN *et al.* (2008) Remodeling phenotype of human subcutaneous adipose tissue macrophages. *Circulation* **117**, 806–815.
- 67 Kratz M, Coats BR, Hisert KB, Hagman D, Mutskov V, Peris E, Schoenfelt KQ, Kuzma JN, Larson I, Billing PS *et al.* (2014) Metabolic dysfunction drives a mechanistically distinct proinflammatory phenotype in adipose tissue macrophages. *Cell Metab* **20**, 614–625.
- 68 Bartelt A and Heeren J (2014) Adipose tissue browning and metabolic health. *Nat Rev Endocrinol* **10**, 24–36.
- 69 Hui X, Gu P, Zhang J, Nie T, Pan Y, Wu D, Feng T, Zhong C, Wang Y, Lam KS *et al.* (2015) Adiponectin enhances cold-induced browning of subcutaneous adipose tissue via promoting M2 macrophage proliferation. *Cell Metab* **22**, 279–290.
- 70 Winer S, Chan Y, Paltser G, Truong D, Tsui H, Bahrami J, Dorfman R, Wang Y, Zielenski J, Mastronardi F *et al.* (2009) Normalization of obesity-associated insulin resistance through immunotherapy. *Nat Med* **15**, 921–929.
- 71 Feuerer M, Hill JA, Kretschmer K, von Boehmer H, Mathis D and Benoist C (2010) Genomic definition of multiple ex vivo regulatory T cell subphenotypes. *Proc Natl Acad Sci U S A* **107**, 5919–5924.
- 72 Nishimura S, Manabe I, Nagasaki M, Eto K, Yamashita H, Ohsugi M, Otsu M, Hara K, Ueki K, Sugiura S, *et al.* (2009) CD8+ effector T cells contribute to macrophage recruitment and adipose tissue inflammation in obesity. *Nat Med* **15**, 914–920.
- 73 Winer DA, Winer S, Shen L, Wadia PP, Yantha J, Paltser G, Tsui H, Wu P, Davidson MG, Alonso MN *et al.* (2011) B cells promote insulin resistance through modulation of T cells and production of pathogenic IgG antibodies. *Nat Med* **17**, 610–617.
- 74 Di Santo JP (2006) Natural killer cell developmental pathways: a question of balance. *Annu Rev Immunol* **24**, 257–286.
- 75 Lee BC, Kim MS, Pae M, Yamamoto Y, Eberle D, Shimada T, Kamei N, Park HS, Sasorith S, Woo JR *et al.* (2016) Adipose natural killer cells regulate adipose tissue macrophages to promote insulin resistance in obesity. *Cell Metab* **23**, 685–698.
- 76 Wensveen FM, Jelencic V, Valentic S, Sestan M, Wensveen TT, Theurich S, Glasner A, Mendrila D, Stimac D, Wunderlich FT *et al.* (2015) NK cells link obesity-induced adipose stress to inflammation and insulin resistance. *Nat Immunol* **16**, 376–385.
- 77 Steppan CM, Wang J, Whiteman EL, Birnbaum MJ and Lazar MA (2005) Activation of SOCS-3 by resistin. *Mol Cell Biol* **25**, 1569–1575.
- 78 Greenberg AS, Nordan RP, McIntosh J, Calvo JC, Scow RO and Jablons D (1992) Interleukin 6 reduces lipoprotein lipase activity in adipose tissue of mice in vivo and in 3T3-L1 adipocytes: a possible role for interleukin 6 in cancer cachexia. *Cancer Res* **52**, 4113–4116.
- 79 Wang H and Eckel RH (2009) Lipoprotein lipase: from gene to obesity. *Am J Physiol Endocrinol Metab* **297**, E271–E288.

- 80 Walton RG, Zhu B, Unal R, Spencer M, Sunkara M, Morris AJ, Charnigo R, Katz WS, Daugherty A, Howatt DA *et al.* (2015) Increasing adipocyte lipoprotein lipase improves glucose metabolism in high fat diet-induced obesity. *J Biol Chem* **290**, 11547–11556.
- 81 Dalmas E, Toubal A, Alzaid F, Blazek K, Eames HL, Lebozec K, Pini M, Hainault I, Montastier E, Denis RG *et al.* (2015) Irf5 deficiency in macrophages promotes beneficial adipose tissue expansion and insulin sensitivity during obesity. *Nat Med* **21**, 610–618.
- 82 Bigornia SJ, Farb MG, Mott MM, Hess DT, Carmine B, Fiscale A, Joseph L, Apovian CM and Gokce N (2012) Relation of depot-specific adipose inflammation to insulin resistance in human obesity. *Nutr Diabetes* **2**, e30.
- 83 Donnelly KL, Smith CI, Schwarzenberg SJ, Jessurun J, Boldt MD and Parks EJ (2005) Sources of fatty acids stored in liver and secreted via lipoproteins in patients with nonalcoholic fatty liver disease. *J Clin Invest* **115**, 1343–1351.
- 84 Fabbrini E, Magkos F, Mohammed BS, Pietka T, Abumrad NA, Patterson BW, Okunade A and Klein S (2009) Intrahepatic fat, not visceral fat, is linked with metabolic complications of obesity. *Proc Natl Acad Sci U S A* **106**, 15430–15435.
- 85 Doege H, Baillie RA, Ortegon AM, Tsang B, Wu Q, Punreddy S, Hirsch D, Watson N, Gimeno RE and Stahl A (2006) Targeted deletion of FATP5 reveals multiple functions in liver metabolism: alterations in hepatic lipid homeostasis. *Gastroenterology* **130**, 1245–1258.
- 86 Falcon A, Doege H, Fluit A, Tsang B, Watson N, Kay MA and Stahl A (2010) FATP2 is a hepatic fatty acid transporter and peroxisomal very long-chain acyl-CoA synthetase. *Am J Physiol Endocrinol Metab* **299**, E384–E393.
- 87 Petersen KF, Dufour S, Savage DB, Bilz S, Solomon G, Yonemitsu S, Cline GW, Befroy D, Zeman L, Kahn BB *et al.* (2007) The role of skeletal muscle insulin resistance in the pathogenesis of the metabolic syndrome. *Proc Natl Acad Sci U S A* **104**, 12587–12594.
- 88 Diraison F, Moulin P and Beylot M (2003) Contribution of hepatic de novo lipogenesis and reesterification of plasma non esterified fatty acids to plasma triglyceride synthesis during non-alcoholic fatty liver disease. *Diabetes Metab* **29**, 478–485.
- 89 Motomura W, Inoue M, Ohtake T, Takahashi N, Nagamine M, Tanno S, Kohgo Y and Okumura T (2006) Up-regulation of ADRP in fatty liver in human and liver steatosis in mice fed with high fat diet. *Biochem Biophys Res Comm* **340**, 1111–1118.
- 90 Schadinger SE, Bucher NL, Schreiber BM and Farmer SR (2005) PPARgamma2 regulates lipogenesis and lipid accumulation in steatotic hepatocytes. *Am J Physiol Endocrinol Metab* **288**, E1195–E1205.
- 91 Souza-Mello V, Gregorio BM, Cardoso-de-Lemos FS, de Carvalho L, Aguila MB and Mandarin-de-Lacerda CA (2010) Comparative effects of telmisartan, sitagliptin and metformin alone or in combination on obesity, insulin resistance, and liver and pancreas remodelling in C57BL/6 mice fed on a very high-fat diet. *Clin Sci (Lond)* **119**, 239–250.
- 92 Montagner A, Polizzi A, Fouche E, Ducheix S, Lippi Y, Lasserre F, Barquissau V, Regnier M, Lukowicz C, Benhamed F *et al.* (2016) Liver PPARalpha is crucial for whole-body fatty acid homeostasis and is protective against NAFLD. *Gut* **65**, 1202–1214.
- 93 Fabbrini E, Mohammed BS, Magkos F, Korenblat KM, Patterson BW and Klein S (2008) Alterations in adipose tissue and hepatic lipid kinetics in obese men and women with nonalcoholic fatty liver disease. *Gastroenterology* **134**, 424–431.
- 94 Sanyal AJ, Brunt EM, Kleiner DE, Kowdley KV, Chalasani N, Lavine JE, Ratziu V and McCullough A (2011) Endpoints and clinical trial design for nonalcoholic steatohepatitis. *Hepatology* **54**, 344–353.
- 95 Jou J, Choi SS and Diehl AM (2008) Mechanisms of disease progression in nonalcoholic fatty liver disease. *Semin Liver Dis* **28**, 370–379.
- 96 Stanton MC, Chen SC, Jackson JV, Rojas-Triana A, Kinsley D, Cui L, Fine JS, Greenfeder S, Bober LA and Jenh CH (2011) Inflammatory Signals shift from adipose to liver during high fat feeding and influence the development of steatohepatitis in mice. *J Inflamm* **8**, 8.
- 97 Obstfeld AE, Sugaru E, Thearle M, Francisco AM, Gayet C, Ginsberg HN, Ables EV and Ferrante AW Jr (2010) C-C chemokine receptor 2 (CCR2) regulates the hepatic recruitment of myeloid cells that promote obesity-induced hepatic steatosis. *Diabetes* **59**, 916–925.
- 98 Yona S, Kim KW, Wolf Y, Mildner A, Varol D, Breker M, Strauss-Ayali D, Viukov S, Guillemins M, Misharin A *et al.* (2013) Fate mapping reveals origins and dynamics of monocytes and tissue macrophages under homeostasis. *Immunity* **38**, 79–91.
- 99 Ganz M, Bukong TN, Csak T, Saha B, Park JK, Ambade A, Kodys K and Szabo G (2015) Progression of non-alcoholic steatosis to steatohepatitis and fibrosis parallels cumulative accumulation of danger signals that promote inflammation and liver tumors in a high fat-cholesterol-sugar diet model in mice. *J Transl Med* **13**, 193.
- 100 Seki E, de Minicis S, Inokuchi S, Taura K, Miyai K, van Rooijen N, Schwabe RF and Brenner DA (2009) CCR2 promotes hepatic fibrosis in mice. *Hepatology* **50**, 185–197.
- 101 Devisscher L, Verhelst X, Colle I, Van Vlierberghe H and Geerts A (2016) The role of macrophages in



- obesity-driven chronic liver disease. *J Leukoc Biol* **99**, 693–698.
- 102 Huang W, Metlakunta A, Dedousis N, Zhang P, Sipula I, Dube JJ, Scott DK and O'Doherty RM (2010) Depletion of liver Kupffer cells prevents the development of diet-induced hepatic steatosis and insulin resistance. *Diabetes* **59**, 347–357.
- 103 Heymann F and Tacke F (2016) Immunology in the liver—from homeostasis to disease. *Nat Rev Gastroenterol Hepatol* **13**, 88–110.
- 104 Klugewitz K, Adams DH, Emoto M, Eulenburg K and Hamann A (2004) The composition of intrahepatic lymphocytes: shaped by selective recruitment? *Trends Immunol* **25**, 590–594.
- 105 Tu Z, Bozorgzadeh A, Pierce RH, Kurtis J, Crispe IN and Orloff MS (2008) TLR-dependent cross talk between human Kupffer cells and NK cells. *J Exp Med* **205**, 233–244.
- 106 Schildberg FA, Wojtalla A, Siegmund SV, Endl E, Diehl L, Abdullah Z, Kurts C and Knolle PA (2011) Murine hepatic stellate cells veto CD8 T cell activation by a CD54-dependent mechanism. *Hepatology* **54**, 262–272.
- 107 Ramaiah SK and Jaeschke H (2007) Hepatic neutrophil infiltration in the pathogenesis of alcohol-induced liver injury. *Toxicol Mech Methods* **17**, 431–440.
- 108 Ramadori G, Moriconi F, Malik I and Dudas J (2008) Physiology and pathophysiology of liver inflammation, damage and repair. *J Physiol Pharmacol* **59** (Suppl 1), 107–117.
- 109 Alkhouri N, Morris-Stiff G, Campbell C, Lopez R, Tamimi TA, Yerian L, Zein NN and Feldstein AE (2012) Neutrophil to lymphocyte ratio: a new marker for predicting steatohepatitis and fibrosis in patients with nonalcoholic fatty liver disease. *Liver Int* **32**, 297–302.
- 110 Bataller R and Brenner DA (2005) Liver fibrosis. *J Clin Invest* **115**, 209–218.
- 111 Pradere JP, Kluwe J, De Minicis S, Jiao JJ, Gwak GY, Dapito DH, Jang MK, Guenther ND, Mederacke I, Friedman R *et al.* (2013) Hepatic macrophages but not dendritic cells contribute to liver fibrosis by promoting the survival of activated hepatic stellate cells in mice. *Hepatology* **58**, 1461–1473.
- 112 Schweiger M, Romauch M, Schreiber R, Grabner GF, Hutter S, Kotzbeck P, Benedikt P, Eichmann TO, Yamada S, Knittelfelder O *et al.* (2017) Pharmacological inhibition of adipose triglyceride lipase corrects high-fat diet-induced insulin resistance and hepatosteatosis in mice. *Nat Commun* **8**, 14859.
- 113 Roden M (2006) Mechanisms of Disease: hepatic steatosis in type 2 diabetes—pathogenesis and clinical relevance. *Nat Clin Pract Endocrinol Metab* **2**, 335–348.
- 114 Xu A, Wang Y, Keshaw H, Xu LY, Lam KS and Cooper GJ (2003) The fat-derived hormone adiponectin alleviates alcoholic and nonalcoholic fatty liver diseases in mice. *J Clin Invest* **112**, 91–100.
- 115 Shklyae S, Aslanidi G, Tennant M, Prima V, Kohlbrenner E, Kroutov V, Campbell-Thompson M, Crawford J, Shek EW, Scarpace PJ *et al.* (2003) Sustained peripheral expression of transgene adiponectin offsets the development of diet-induced obesity in rats. *Proc Natl Acad Sci U S A* **100**, 14217–14222.
- 116 Yamauchi T, Kamon J, Minokoshi Y, Ito Y, Waki H, Uchida S, Yamashita S, Noda M, Kita S, Ueki K *et al.* (2002) Adiponectin stimulates glucose utilization and fatty-acid oxidation by activating AMP-activated protein kinase. *Nat Med* **8**, 1288–1295.
- 117 Hui JM, Hodge A, Farrell GC, Kench JG, Kriketos A and George J (2004) Beyond insulin resistance in NASH: TNF-alpha or adiponectin? *Hepatology* **40**, 46–54.
- 118 Lopez-Bermejo A, Botas P, Funahashi T, Delgado E, Kihara S, Ricart W and Fernandez-Real JM (2004) Adiponectin, hepatocellular dysfunction and insulin sensitivity. *Clin Endocrinol (Oxf)* **60**, 256–263.
- 119 Poordad FF (2004) The role of leptin in NAFLD: contender or pretender? *J Clin Gastroenterol* **38**, 841–843.
- 120 Cao Q, Mak KM, Ren C and Lieber CS (2004) Leptin stimulates tissue inhibitor of metalloproteinase-1 in human hepatic stellate cells: respective roles of the JAK/STAT and JAK-mediated H<sub>2</sub>O<sub>2</sub>-dependant MAPK pathways. *J Biol Chem* **279**, 4292–4304.
- 121 Marroqui L, Gonzalez A, Neco P, Caballero-Garrido E, Vieira E, Ripoll C, Nadal A and Quesada I (2012) Role of leptin in the pancreatic beta-cell: effects and signaling pathways. *J Mol Endocrinol* **49**, R9–R17.
- 122 Sabio G, Das M, Mora A, Zhang Z, Jun JY, Ko HJ, Barrett T, Kim JK and Davis RJ (2008) A stress signaling pathway in adipose tissue regulates hepatic insulin resistance. *Science* **322**, 1539–1543.
- 123 Jaeger D, Schoiswohl G, Hofer P, Schreiber R, Schweiger M, Eichmann TO, Pollak NM, Poecher N, Grabner GF, Zierler KA *et al.* (2015) Fasting-induced G0/G1 switch gene 2 and FGF21 expression in the liver are under regulation of adipose tissue derived fatty acids. *J Hepatol* **63**, 437–445.
- 124 Inagaki T, Dutchak P, Zhao G, Ding X, Gautron L, Parameswara V, Li Y, Goetz R, Mohammadi M, Esser V *et al.* (2007) Endocrine regulation of the fasting response by PPARalpha-mediated induction of fibroblast growth factor 21. *Cell Metab* **5**, 415–425.
- 125 Lin Z, Tian H, Lam KS, Lin S, Hoo RC, Konishi M, Itoh N, Wang Y, Bornstein SR, Xu A *et al.* (2013) Adiponectin mediates the metabolic effects of FGF21

- on glucose homeostasis and insulin sensitivity in mice. *Cell Metab* **17**, 779–789.
- 126 BonDurant LD, Ameka M, Naber MC, Markan KR, Idiga SO, Acevedo MR, Walsh SA, Ornitz DM and Potthoff MJ (2017) FGF21 regulates metabolism through adipose-dependent and – independent mechanisms. *Cell Metab* **25**, 935–944. e934.
- 127 Kharitonov A, Shiyanova TL, Koester A, Ford AM, Micanovic R, Galbreath EJ, Sandusky GE, Hammond LJ, Moyers JS, Owens RA *et al.* (2005) FGF-21 as a novel metabolic regulator. *J Clin Invest* **115**, 1627–1635.
- 128 Gimeno RE and Moller DE (2014) FGF21-based pharmacotherapy–potential utility for metabolic disorders. *Trends Endocrinol Metab* **25**, 303–311.
- 129 Schlein C, Talukdar S, Heine M, Fischer AW, Krott LM, Nilsson SK, Brenner MB, Heeren J and Scheja L (2016) FGF21 lowers plasma triglycerides by accelerating lipoprotein catabolism in white and brown adipose tissues. *Cell Metab* **23**, 441–453.
- 130 Meex RC, Hoy AJ, Morris A, Brown RD, Lo JC, Burke M, Goode RJ, Kingwell BA, Kraakman MJ, Febbraio MA *et al.* (2015) Fetuin B is a secreted hepatocyte factor linking steatosis to impaired glucose metabolism. *Cell Metab* **22**, 1078–1089.
- 131 Brown MS and Goldstein JL (2008) Selective versus total insulin resistance: a pathogenic paradox. *Cell Metab* **7**, 95–96.
- 132 Lu M, Wan M, Leavens KF, Chu Q, Monks BR, Fernandez S, Ahima RS, Ueki K, Kahn CR and Birnbaum MJ (2012) Insulin regulates liver metabolism in vivo in the absence of hepatic Akt and Foxo1. *Nat Med* **18**, 388–395.
- 133 Li S, Brown MS and Goldstein JL (2010) Bifurcation of insulin signaling pathway in rat liver: mTORC1 required for stimulation of lipogenesis, but not inhibition of gluconeogenesis. *Proc Natl Acad Sci U S A* **107**, 3441–3446.
- 134 O-Sullivan I, Zhang W, Wasserman DH, Liew CW, Liu J, Paik J, DePinho RA, Stolz DB, Kahn CR, Schwartz MW *et al.* (2015) FoxO1 integrates direct and indirect effects of insulin on hepatic glucose production and glucose utilization. *Nat Commun* **6**, 7079.
- 135 Perry RJ, Camporez JP, Kursawe R, Titchenell PM, Zhang D, Perry CJ, Jurczak MJ, Abudukadier A, Han MS, Zhang XM *et al.* (2015) Hepatic acetyl CoA links adipose tissue inflammation to hepatic insulin resistance and type 2 diabetes. *Cell* **160**, 745–758.
- 136 Titchenell PM, Quinn WJ, Lu M, Chu Q, Lu W, Li C, Chen H, Monks BR, Chen J, Rabinowitz JD *et al.* (2016) Direct hepatocyte insulin signaling is required for lipogenesis but is dispensable for the suppression of glucose production. *Cell Metab* **23**, 1154–1166.
- 137 Benhamed F, Denechaud PD, Lemoine M, Robichon C, Moldes M, Bertrand-Michel J, Ratziu V, Serfaty L, Housset C, Capeau J *et al.* (2012) The lipogenic transcription factor ChREBP dissociates hepatic steatosis from insulin resistance in mice and humans. *J Clin Invest* **122**, 2176–2194.
- 138 Tremblay F, Lavigne C, Jacques H and Marette A (2007) Role of dietary proteins and amino acids in the pathogenesis of insulin resistance. *Annu Rev Nutr* **27**, 293–310.
- 139 Uno K, Yamada T, Ishigaki Y, Imai J, Hasegawa Y, Sawada S, Kaneko K, Ono H, Asano T, Oka Y *et al.* (2015) A hepatic amino acid/mTOR/S6K-dependent signalling pathway modulates systemic lipid metabolism via neuronal signals. *Nat Commun* **6**, 7940.
- 140 Kopp E and Ghosh S (1994) Inhibition of NF-kappa B by sodium salicylate and aspirin. *Science* **265**, 956–959.
- 141 Chang L and Karin M (2001) Mammalian MAP kinase signalling cascades. *Nature* **410**, 37–40.
- 142 Aguirre V, Uchida T, Yenush L, Davis R and White MF (2000) The c-Jun NH(2)-terminal kinase promotes insulin resistance during association with insulin receptor substrate-1 and phosphorylation of Ser(307). *J Biol Chem* **275**, 9047–9054.
- 143 Han MS, Jung DY, Morel C, Lakhani SA, Kim JK, Flavell RA and Davis RJ (2013) JNK expression by macrophages promotes obesity-induced insulin resistance and inflammation. *Science* **339**, 218–222.
- 144 Vernia S, Cavanagh-Kyros J, Garcia-Haro L, Sabio G, Barrett T, Jung DY, Kim JK, Xu J, Shulha HP, Garber M *et al.* (2014) The PPARalpha-FGF21 hormone axis contributes to metabolic regulation by the hepatic JNK signaling pathway. *Cell Metab* **20**, 512–525.
- 145 Yuan M, Konstantopoulos N, Lee J, Hansen L, Li ZW, Karin M and Shoelson SE (2001) Reversal of obesity- and diet-induced insulin resistance with salicylates or targeted disruption of Ikkbeta. *Science* **293**, 1673–1677.
- 146 Kim JK, Kim YJ, Fillmore JJ, Chen Y, Moore I, Lee J, Yuan M, Li ZW, Karin M, Perret P *et al.* (2001) Prevention of fat-induced insulin resistance by salicylate. *J Clin Invest* **108**, 437–446.
- 147 Cai D, Yuan M, Frantz DF, Melendez PA, Hansen L, Lee J and Shoelson SE (2005) Local and systemic insulin resistance resulting from hepatic activation of IKK-beta and NF-kappaB. *Nat Med* **11**, 183–190.
- 148 Hotamisligil GKS (2010) Endoplasmic reticulum stress and the inflammatory basis of metabolic disease. *Cell* **140**, 900–917.
- 149 Shoelson SE, Lee J and Goldfine AB (2006) Inflammation and insulin resistance. *J Clin Invest* **116**, 1793–1801.
- 150 Uysal KT, Wiesbrock SM, Marino MW and Hotamisligil GS (1997) Protection from obesity-

- induced insulin resistance in mice lacking TNF- $\alpha$  function. *Nature* **389**, 610–614.
- 151 Hirosumi J, Tuneman G, Chang L, Gorgun CZ, Uysal KT, Maeda K, Karin M and Hotamisligil GS (2002) A central role for JNK in obesity and insulin resistance. *Nature* **420**, 333–336.
- 152 Dominguez H, Storgaard H, Rask-Madsen C, Steffen Hermann T, Ihlemann N, Baunbjerg Nielsen D, Spohr C, Kober L, Vaag A and Torp-Pedersen C (2005) Metabolic and vascular effects of tumor necrosis factor- $\alpha$  blockade with etanercept in obese patients with type 2 diabetes. *J Vasc Res* **42**, 517–525.
- 153 Ofei F, Hurel S, Newkirk J, Sopwith M and Taylor R (1996) Effects of an engineered human anti-TNF- $\alpha$  antibody (CDP571) on insulin sensitivity and glycemic control in patients with NIDDM. *Diabetes* **45**, 881–885.
- 154 Wascher TC, Lindeman JH, Sourij H, Kooistra T, Pacini G and Roden M (2011) Chronic TNF- $\alpha$  neutralization does not improve insulin resistance or endothelial function in “healthy” men with metabolic syndrome. *Mol Med* **17**, 189–193.
- 155 Heinrich PC, Behrmann I, Muller-Newen G, Schaper F and Graeve L (1998) Interleukin-6-type cytokine signalling through the gp130/Jak/STAT pathway. *Biochem J* **334** (Pt 2), 297–314.
- 156 Kim HJ, Higashimori T, Park SY, Choi H, Dong J, Kim YJ, Noh HL, Cho YR, Cline G, Kim YB *et al.* (2004) Differential effects of interleukin-6 and -10 on skeletal muscle and liver insulin action in vivo. *Diabetes* **53**, 1060–1067.
- 157 Senn JJ, Klover PJ, Nowak IA, Zimmers TA, Koniaris LG, Furlanetto RW and Mooney RA (2003) Suppressor of cytokine signaling-3 (SOCS-3), a potential mediator of interleukin-6-dependent insulin resistance in hepatocytes. *J Biol Chem* **278**, 13740–13746.
- 158 Matthews VB, Allen TL, Risis S, Chan MH, Henstridge DC, Watson N, Zaffino LA, Babb JR, Boon J, Meikle PJ *et al.* (2010) Interleukin-6-deficient mice develop hepatic inflammation and systemic insulin resistance. *Diabetologia* **53**, 2431–2441.
- 159 Tan HW, Liu X, Bi XP, Xing SS, Li L, Gong HP, Zhong M, Wang ZH, Zhang Y and Zhang W (2010) IL-18 overexpression promotes vascular inflammation and remodeling in a rat model of metabolic syndrome. *Atherosclerosis* **208**, 350–357.
- 160 Netea MG, Joosten LA, Lewis E, Jensen DR, Voshol PJ, Kullberg BJ, Tack CJ, van Krieken H, Kim SH, Stalenhoef AF *et al.* (2006) Deficiency of interleukin-18 in mice leads to hyperphagia, obesity and insulin resistance. *Nat Med* **12**, 650–656.
- 161 Banerjee RR, Rangwala SM, Shapiro JS, Rich AS, Rhoades B, Qi Y, Wang J, Rajala MW, Poci A, Scherer PE *et al.* (2004) Regulation of fasted blood glucose by resistin. *Science* **303**, 1195–1198.
- 162 McTernan CL, McTernan PG, Harte AL, Levick PL, Barnett AH and Kumar S (2002) Resistin, central obesity, and type 2 diabetes. *Lancet* **359**, 46–47.
- 163 Lee JH, Chan JL, Yiannakouris N, Kontogianni M, Estrada E, Seip R, Orlova C and Mantzoros CS (2003) Circulating resistin levels are not associated with obesity or insulin resistance in humans and are not regulated by fasting or leptin administration: cross-sectional and interventional studies in normal, insulin-resistant, and diabetic subjects. *J Clin Endocrinol Metab* **88**, 4848–4856.
- 164 Kielstein JT, Becker B, Graf S, Brabant G, Haller H and Fliser D (2003) Increased resistin blood levels are not associated with insulin resistance in patients with renal disease. *Am J Kidney Dis* **42**, 62–66.
- 165 Patel L, Buckels AC, Kinghorn IJ, Murdock PR, Holbrook JD, Plumpton C, Macphee CH and Smith SA (2003) Resistin is expressed in human macrophages and directly regulated by PPAR gamma activators. *Biochem Biophys Res Comm* **300**, 472–476.
- 166 Savage DB, Sewter CP, Klenk ES, Segal DG, Vidal-Puig A, Considine RV and O’Rahilly S (2001) Resistin/Fizz3 expression in relation to obesity and peroxisome proliferator-activated receptor- $\gamma$  action in humans. *Diabetes* **50**, 2199–2202.
- 167 Glass CK and Olefsky JM (2012) Inflammation and lipid signaling in the etiology of insulin resistance. *Cell Metab* **15**, 635–645.
- 168 den Dekker WK, Cheng C, Pasterkamp G and Duckers HJ (2010) Toll like receptor 4 in atherosclerosis and plaque destabilization. *Atherosclerosis* **209**, 314–320.
- 169 Leemans JC, Cassel SL and Sutterwala FS (2011) Sensing damage by the NLRP3 inflammasome. *Immunol Rev* **243**, 152–162.
- 170 Tanti J-F and Jager J (2009) Cellular mechanisms of insulin resistance: role of stress-regulated serine kinases and insulin receptor substrates (IRS) serine phosphorylation. *Curr Opin Pharmacol* **9**, 753–762.
- 171 Stienstra R, Joosten LAB, Koenen T, van Tits B, van Diepen JA, van den Berg SAA, Rensen PCN, Voshol PJ, Fantuzzi G, Hijmans A *et al.* (2010) The inflammasome-mediated caspase-1 activation controls adipocyte differentiation and insulin sensitivity. *Cell Metab* **12**, 593–605.
- 172 Vandannagsar B, Youm Y-H, Ravussin A, Galgani JE, Stadler K, Mynatt RL, Ravussin E, Stephens JM and Dixit VD (2011) The NLRP3 inflammasome instigates obesity-induced inflammation and insulin resistance. *Nat Med* **17**, 179–188.

- 173 Samuel VT and Shulman GI (2012) Mechanisms for insulin resistance: common threads and missing links. *Cell* **148**, 852–871.
- 174 Samuel VT, Liu ZX, Qu X, Elder BD, Bilz S, Befroy D, Romanelli AJ and Shulman GI (2004) Mechanism of hepatic insulin resistance in non-alcoholic fatty liver disease. *J Biol Chem* **279**, 32345–32353.
- 175 Samuel VT, Liu ZX, Wang A, Beddow SA, Geisler JG, Kahn M, Zhang XM, Monia BP, Bhanot S and Shulman GI (2007) Inhibition of protein kinase Cepsilon prevents hepatic insulin resistance in nonalcoholic fatty liver disease. *J Clin Invest* **117**, 739–745.
- 176 Holland WL, Bikman BT, Wang LP, Yuguang G, Sargent KM, Bulchand S, Knotts TA, Shui G, Clegg DJ, Wenk MR *et al.* (2011) Lipid-induced insulin resistance mediated by the proinflammatory receptor TLR4 requires saturated fatty acid-induced ceramide biosynthesis in mice. *J Clin Invest* **121**, 1858–1870.
- 177 Stratford S, Hoehn KL, Liu F and Summers SA (2004) Regulation of insulin action by ceramide: dual mechanisms linking ceramide accumulation to the inhibition of Akt/protein kinase B. *J Biol Chem* **279**, 36608–36615.
- 178 Merrill AH Jr (2002) De novo sphingolipid biosynthesis: a necessary, but dangerous, pathway. *J Biol Chem* **277**, 25843–25846.
- 179 Holland WL, Brozinick JT, Wang LP, Hawkins ED, Sargent KM, Liu Y, Narra K, Hoehn KL, Knotts TA, Siesky A *et al.* (2007) Inhibition of ceramide synthesis ameliorates glucocorticoid-, saturated-fat-, and obesity-induced insulin resistance. *Cell Metab* **5**, 167–179.
- 180 Ussher JR, Koves TR, Cadete VJ, Zhang L, Jaswal JS, Swyrd SJ, Lopaschuk DG, Proctor SD, Keung W, Muoio DM *et al.* (2010) Inhibition of de novo ceramide synthesis reverses diet-induced insulin resistance and enhances whole-body oxygen consumption. *Diabetes* **59**, 2453–2464.
- 181 Jiang C, Xie C, Li F, Zhang L, Nichols RG, Krausz KW, Cai J, Qi Y, Fang ZZ, Takahashi S *et al.* (2015) Intestinal farnesoid X receptor signaling promotes nonalcoholic fatty liver disease. *J Clin Invest* **125**, 386–402.
- 182 Chaurasia B, Kaddai VA, Lancaster GI, Henstridge DC, Sriram S, Galam DL, Gopalan V, Prakash KN, Velan SS, Bulchand S *et al.* (2016) Adipocyte ceramides regulate subcutaneous adipose browning, inflammation, and metabolism. *Cell Metab* **24**, 820–834.
- 183 Dbaiibo GS, El-Assaad W, Krikorian A, Liu B, Diab K, Idriss NZ, El-Sabban M, Driscoll TA, Perry DK and Hannun YA (2001) Ceramide generation by two distinct pathways in tumor necrosis factor alpha-induced cell death. *FEBS Lett* **503**, 7–12.
- 184 Wellen KE, Hatzivassiliou G, Sachdeva UM, Bui TV, Cross JR and Thompson CB (2009) ATP-citrate lyase links cellular metabolism to histone acetylation. *Science* **324**, 1076–1080.
- 185 Detich N, Hamm S, Just G, Knox JD and Szyf M (2003) The methyl donor S-Adenosylmethionine inhibits active demethylation of DNA: a candidate novel mechanism for the pharmacological effects of S-Adenosylmethionine. *J Biol Chem* **278**, 20812–20820.
- 186 Xu W, Wang F, Yu Z and Xin F (2016) Epigenetics and cellular metabolism. *Genet Epigenet* **8**, 43–51.
- 187 Tan CK, Zhuang Y and Wahli W (2017) Synthetic and natural Peroxisome Proliferator-Activated Receptor (PPAR) agonists as candidates for the therapy of the metabolic syndrome. *Expert Opin Ther Targets* **21**, 333–348.
- 188 Gross B, Pawlak M, Lefebvre P and Staels B (2017) PPARs in obesity-induced T2DM, dyslipidaemia and NAFLD. *Nat Rev Endocrinol* **13**, 36–49.
- 189 Kersten S (2014) Integrated physiology and systems biology of PPARalpha. *Mol Metab* **3**, 354–371.
- 190 Kharitonov A, Wroblewski VJ, Koester A, Chen YF, Clutinger CK, Tigno XT, Hansen BC, Shanafelt AB and Etgen GJ (2007) The metabolic state of diabetic monkeys is regulated by fibroblast growth factor-21. *Endocrinology* **148**, 774–781.
- 191 Staels B, Koenig W, Habib A, Merval R, Lebre M, Torra IP, Delerive P, Fadel A, Chinetti G, Fruchart JC *et al.* (1998) Activation of human aortic smooth-muscle cells is inhibited by PPARalpha but not by PPARgamma activators. *Nature* **393**, 790–793.
- 192 Liu ZM, Hu M, Chan P and Tomlinson B (2015) Early investigational drugs targeting PPAR-alpha for the treatment of metabolic disease. *Expert Opin Investig Drugs* **24**, 611–621.
- 193 Tanaka N, Aoyama T, Kimura S and Gonzalez FJ (2017) Targeting nuclear receptors for the treatment of fatty liver disease. *Pharmacol Ther* **S0163-7258**, 30130–30134.
- 194 Jackevicius CA, Tu JV, Ross JS, Ko DT, Carreon D and Krumholz HM (2011) Use of fibrates in the United States and Canada. *JAMA* **305**, 1217–1224.
- 195 Sanderson LM, Boekschoten MV, Desvergne B, Muller M and Kersten S (2010) Transcriptional profiling reveals divergent roles of PPARalpha and PPARbeta/delta in regulation of gene expression in mouse liver. *Physiol Genomics* **41**, 42–52.
- 196 Odegaard JI, Ricardo-Gonzalez RR, Red Eagle A, Vats D, Morel CR, Goforth MH, Subramanian V, Mukundan L, Ferrante AW and Chawla A (2008) Alternative M2 activation of Kupffer cells by PPARdelta ameliorates obesity-induced insulin resistance. *Cell Metab* **7**, 496–507.
- 197 Iwaisako K, Haimerl M, Paik YH, Taura K, Kodama Y, Sirlin C, Yu E, Yu RT, Downes M, Evans RM

- et al.* (2012) Protection from liver fibrosis by a peroxisome proliferator-activated receptor delta agonist. *Proc Natl Acad Sci U S A* **109**, E1369–E1376.
- 198 Grewal AS, Beniwal M, Pandita D, Sekhon BS and Lather V (2016) Recent updates on peroxisome proliferator-activated receptor delta agonists for the treatment of metabolic syndrome. *Med Chem* **12**, 3–21.
- 199 Rosen ED, Sarraf P, Troy AE, Bradwin G, Moore K, Milstone DS, Spiegelman BM and Mortensen RM (1999) PPAR gamma is required for the differentiation of adipose tissue in vivo and in vitro. *Mol Cell* **4**, 611–617.
- 200 Soccio RE, Chen ER and Lazar MA (2014) Thiazolidinediones and the promise of insulin sensitization in type 2 diabetes. *Cell Metab* **20**, 573–591.
- 201 Cariou B, Charbonnel B and Staels B (2012) Thiazolidinediones and PPARgamma agonists: time for a reassessment. *Trends Endocrinol Metab* **23**, 205–215.
- 202 Adams M, Montague CT, Prins JB, Holder JC, Smith SA, Sanders L, Digby JE, Sewter CP, Lazar MA, Chatterjee VK *et al.* (1997) Activators of peroxisome proliferator-activated receptor gamma have depot-specific effects on human preadipocyte differentiation. *J Clin Invest* **100**, 3149–3153.
- 203 Miyazaki Y, Mahankali A, Matsuda M, Mahankali S, Hardies J, Cusi K, Mandarino LJ and DeFronzo RA (2002) Effect of pioglitazone on abdominal fat distribution and insulin sensitivity in type 2 diabetic patients. *J Clin Endocrinol Metab* **87**, 2784–2791.
- 204 Guan HP, Li Y, Jensen MV, Newgard CB, Steppan CM and Lazar MA (2002) A futile metabolic cycle activated in adipocytes by antidiabetic agents. *Nat Med* **8**, 1122–1128.
- 205 Yamauchi T, Kamon J, Waki H, Murakami K, Motojima K, Komeda K, Ide T, Kubota N, Terauchi Y, Tobe K *et al.* (2001) The mechanisms by which both heterozygous peroxisome proliferator-activated receptor gamma (PPARgamma) deficiency and PPARgamma agonist improve insulin resistance. *J Biol Chem* **276**, 41245–41254.
- 206 Oakes ND, Thalén PG, Jacinto SM and Ljung B (2001) Thiazolidinediones increase plasma-adipose tissue FFA exchange capacity and enhance insulin-mediated control of systemic FFA availability. *Diabetes* **50**, 1158–1165.
- 207 Petrovic N, Shabalina IG, Timmons JA, Cannon B and Nedergaard J (2008) Thermogenically competent nonadrenergic recruitment in brown preadipocytes by a PPARgamma agonist. *Am J Physiol Endocrinol Metab* **295**, E287–E296.
- 208 Ohno H, Shinoda K, Spiegelman BM and Kajimura S (2012) PPARgamma agonists induce a white-to-brown fat conversion through stabilization of PRDM16 protein. *Cell Metab* **15**, 395–404.
- 209 Sears DD, Hsiao G, Hsiao A, Yu JG, Courtney CH, Ofrecio JM, Chapman J and Subramaniam S (2009) Mechanisms of human insulin resistance and thiazolidinedione-mediated insulin sensitization. *Proc Natl Acad Sci U S A* **106**, 18745–18750.
- 210 Smith U, Gogg S, Johansson A, Olausson T, Rotter V and Svalstedt B (2001) Thiazolidinediones (PPARgamma agonists) but not PPARalpha agonists increase IRS-2 gene expression in 3T3-L1 and human adipocytes. *FASEB J* **15**, 215–220.
- 211 Ribon V, Johnson JH, Camp HS and Saltiel AR (1998) Thiazolidinediones and insulin resistance: peroxisome proliferator-activated receptor gamma activation stimulates expression of the CAP gene. *Proc Natl Acad Sci U S A* **95**, 14751–14756.
- 212 Steppan CM, Bailey ST, Bhat S, Brown EJ, Banerjee RR, Wright CM, Patel HR, Ahima RS and Lazar MA (2001) The hormone resistin links obesity to diabetes. *Nature* **409**, 307–312.
- 213 Peraldi P, Xu M and Spiegelman BM (1997) Thiazolidinediones block tumor necrosis factor-alpha-induced inhibition of insulin signaling. *J Clin Invest* **100**, 1863–1869.
- 214 Hammarstedt A, Andersson CX, Rotter Sopasakis V and Smith U (2005) The effect of PPARgamma ligands on the adipose tissue in insulin resistance. *Prostaglandins Leukot Essent Fatty Acids* **73**, 65–75.
- 215 Chawla A (2010) Control of macrophage activation and function by PPARs. *Circ Res* **106**, 1559–1569.
- 216 Huang JT, Welch JS, Ricote M, Binder CJ, Willson TM, Kelly C, Witztum JL, Funk CD, Conrad D and Glass CK (1999) Interleukin-4-dependent production of PPAR-gamma ligands in macrophages by 12/15-lipoxygenase. *Nature* **400**, 378–382.
- 217 Xu H, Barnes GT, Yang Q, Tan G, Yang D, Chou CJ, Sole J, Nichols A, Ross JS, Tartaglia LA *et al.* (2003) Chronic inflammation in fat plays a crucial role in the development of obesity-related insulin resistance. *J Clin Invest* **112**, 1821–1830.
- 218 Odegaard JI, Ricardo-Gonzalez RR, Goforth MH, Morel CR, Subramanian V, Mukundan L, Red Eagle A, Vats D, Brombacher F, Ferrante AW *et al.* (2007) Macrophage-specific PPARgamma controls alternative activation and improves insulin resistance. *Nature* **447**, 1116–1120.
- 219 Hevener AL, Olefsky JM, Reichart D, Nguyen MT, Bandyopadhyay G, Leung HY, Watt MJ, Benner C, Febbraio MA, Nguyen AK *et al.* (2007) Macrophage PPAR gamma is required for normal skeletal muscle and hepatic insulin sensitivity and full antidiabetic effects of thiazolidinediones. *J Clin Invest* **117**, 1658–1669.

- 220 Cipolletta D, Feuerer M, Li A, Kamei N, Lee J, Shoelson SE, Benoist C and Mathis D (2012) PPAR-gamma is a major driver of the accumulation and phenotype of adipose tissue Treg cells. *Nature* **486**, 549–553.
- 221 Fraulob JC, Souza-Mello V, Aguila MB and Mandarim-de-Lacerda CA (2012) Beneficial effects of rosuvastatin on insulin resistance, adiposity, inflammatory markers and non-alcoholic fatty liver disease in mice fed on a high-fat diet. *Clin Sci (Lond)* **123**, 259–270.
- 222 Banks AS, McAllister FE, Camporez JP, Zushin PJ, Jurczak MJ, Laznik-Bogoslavski D, Shulman GI, Gygi SP and Spiegelman BM (2015) An ERK/Cdk5 axis controls the diabetogenic actions of PPARgamma. *Nature* **517**, 391–395.
- 223 Choi JH, Banks AS, Estall JL, Kajimura S, Bostrom P, Laznik D, Ruas JL, Chalmers MJ, Kamenecka TM, Bluher M *et al.* (2010) Anti-diabetic drugs inhibit obesity-linked phosphorylation of PPARgamma by Cdk5. *Nature* **466**, 451–456.
- 224 Vitale SG, Lagana AS, Nigro A, La Rosa VL, Rossetti P, Rapisarda AM, La Vignera S, Condorelli RA, Corrado F, Buscema M *et al.* (2016) Peroxisome proliferator-activated receptor modulation during metabolic diseases and cancers: master and minions. *PPAR Res* **2016**, 6517313.
- 225 Rotman Y and Sanyal AJ (2017) Current and upcoming pharmacotherapy for non-alcoholic fatty liver disease. *Gut* **66**, 180–190.
- 226 Pap A, Cuaranta-Monroy I, Peloquin M and Nagy L (2016) Is the mouse a good model of human PPARgamma-related metabolic diseases? *Int J Mol Sci* **17**, 1236.
- 227 Cypess AM, Lehman S, Williams G, Tal I, Rodman D, Goldfine AB, Kuo FC, Palmer EL, Tseng YH, Doria A *et al.* (2009) Identification and importance of brown adipose tissue in adult humans. *N Engl J Med* **360**, 1509–1517.
- 228 van Marken Lichtenbelt WD, Vanhommerig JW, Smulders NM, Drossaerts JM, Kemerink GJ, Bouvy ND, Schrauwen P and Teule GJ (2009) Cold-activated brown adipose tissue in healthy men. *N Engl J Med* **360**, 1500–1508.
- 229 Virtanen KA, Lidell ME, Orava J, Heglind M, Westergren R, Niemi T, Taittonen M, Laine J, Savisto NJ, Enerback S *et al.* (2009) Functional brown adipose tissue in healthy adults. *N Engl J Med* **360**, 1518–1525.
- 230 Petrovic N, Walden TB, Shabalina IG, Timmons JA, Cannon B and Nedergaard J (2010) Chronic peroxisome proliferator-activated receptor gamma (PPARgamma) activation of epididymally derived white adipocyte cultures reveals a population of thermogenically competent, UCP1-containing adipocytes molecularly distinct from classic brown adipocytes. *J Biol Chem* **285**, 7153–7164.
- 231 Guerra C, Koza RA, Yamashita H, Walsh K and Kozak LP (1998) Emergence of brown adipocytes in white fat in mice is under genetic control. Effects on body weight and adiposity. *J Clin Invest* **102**, 412–420.
- 232 Moseti D, Regassa A and Kim WK (2016) Molecular regulation of adipogenesis and potential anti-adipogenic bioactive molecules. *Int J Mol Sci* **17**, 124.
- 233 Baratta JL, Ngo A, Lopez B, Kasabwalla N, Longmuir KJ and Robertson RT (2009) Cellular organization of normal mouse liver: a histological, quantitative immunocytochemical, and fine structural analysis. *Histochem Cell Biol* **131**, 713–726.
- 234 Fox ES, Thomas P and Broitman SA (1987) Comparative studies of endotoxin uptake by isolated rat Kupffer and peritoneal cells. *Infect Immun* **55**, 2962–2966.
- 235 Rui L (2014) Energy metabolism in the liver. *Compr Physiol* **4**, 177–197.
- 236 Mandard S, Muller M and Kersten S (2004) Peroxisome proliferator-activated receptor alpha target genes. *Cell Mol Life Sci* **61**, 393–416.
- 237 Braissant O, Foufelle F, Scotto C, Dauca M and Wahli W (1996) Differential expression of peroxisome proliferator-activated receptors (PPARs): tissue distribution of PPAR-alpha, -beta, and -gamma in the adult rat. *Endocrinology* **137**, 354–366.
- 238 Desvergne B, Michalik L and Wahli W (2006) Transcriptional regulation of metabolism. *Physiol Rev* **86**, 465–514.
- 239 Bookout AL, Jeong Y, Downes M, Yu RT, Evans RM and Mangelsdorf DJ (2006) Anatomical profiling of nuclear receptor expression reveals a hierarchical transcriptional network. *Cell* **126**, 789–799.
- 240 Pawlak M, Lefebvre P and Staels B (2015) Molecular mechanism of PPARalpha action and its impact on lipid metabolism, inflammation and fibrosis in non-alcoholic fatty liver disease. *J Hepatol* **62**, 720–733.
- 241 Tan NS, Vazquez-Carrera M, Montagner A, Sng MK, Guillou H and Wahli W (2016) Transcriptional control of physiological and pathological processes by the nuclear receptor PPARbeta/delta. *Prog Lipid Res* **64**, 98–122.
- 242 Ahmadian M, Suh JM, Hah N, Liddle C, Atkins AR, Downes M and Evans RM (2013) PPARgamma signaling and metabolism: the good, the bad and the future. *Nat Med* **19**, 557–566.

## **References**

- 1 Zimmet, P., Magliano, D., Matsuzawa, Y., Alberti, G. & Shaw, J. The metabolic syndrome: a global public health problem and a new definition. *J Atheroscler Thromb* **12**, 295-300 (2005).
- 2 Gregor, M. F. & Hotamisligil, G. S. Inflammatory mechanisms in obesity. *Annu Rev Immunol* **29**, 415-445, doi:10.1146/annurev-immunol-031210-101322 (2011).
- 3 Bluher, M. The distinction of metabolically 'healthy' from 'unhealthy' obese individuals. *Curr Opin Lipidol* **21**, 38-43, doi:10.1097/MOL.0b013e3283346ccc (2010).
- 4 Samocha-Bonet, D., Chisholm, D. J., Tonks, K., Campbell, L. V. & Greenfield, J. R. Insulin-sensitive obesity in humans - a 'favorable fat' phenotype? *Trends Endocrinol Metab* **23**, 116-124, doi:10.1016/j.tem.2011.12.005 (2012).
- 5 Ryden, M. *et al.* The Adipose Transcriptional Response to Insulin Is Determined by Obesity, Not Insulin Sensitivity. *Cell Rep* **16**, 2317-2326, doi:10.1016/j.celrep.2016.07.070 (2016).
- 6 Montague, C. T., Prins, J. B., Sanders, L., Digby, J. E. & O'Rahilly, S. Depot- and sex-specific differences in human leptin mRNA expression: implications for the control of regional fat distribution. *Diabetes* **46**, 342-347 (1997).
- 7 Kershaw, E. E. & Flier, J. S. Adipose tissue as an endocrine organ. *J Clin Endocrinol Metab* **89**, 2548-2556, doi:10.1210/jc.2004-0395 (2004).
- 8 Tchkonja, T. *et al.* Mechanisms and metabolic implications of regional differences among fat depots. *Cell metabolism* **17**, 644-656, doi:10.1016/j.cmet.2013.03.008 (2013).
- 9 Rosen, E. D. & Spiegelman, B. M. What we talk about when we talk about fat. *Cell* **156**, 20-44, doi:10.1016/j.cell.2013.12.012 (2014).
- 10 Gesta, S. *et al.* Evidence for a role of developmental genes in the origin of obesity and body fat distribution. *Proceedings of the National Academy of Sciences of the United States of America* **103**, 6676-6681, doi:10.1073/pnas.0601752103 (2006).
- 11 Tchkonja, T. *et al.* Identification of depot-specific human fat cell progenitors through distinct expression profiles and developmental gene patterns. *Am J Physiol Endocrinol Metab* **292**, E298-307, doi:10.1152/ajpendo.00202.2006 (2007).
- 12 Hausman, D. B., DiGirolamo, M., Bartness, T. J., Hausman, G. J. & Martin, R. J. The biology of white adipocyte proliferation. *Obesity reviews : an official journal of the International Association for the Study of Obesity* **2**, 239-254 (2001).
- 13 Lee, Y. S. *et al.* Increased adipocyte O<sub>2</sub> consumption triggers HIF-1 $\alpha$ , causing inflammation and insulin resistance in obesity. *Cell* **157**, 1339-1352, doi:10.1016/j.cell.2014.05.012 (2014).
- 14 Jeffery, E., Church, C. D., Holtrup, B., Colman, L. & Rodeheffer, M. S. Rapid depot-specific activation of adipocyte precursor cells at the onset of obesity. *Nature cell biology* **17**, 376-385, doi:10.1038/ncb3122 (2015).



- 15 Kim, J. I. *et al.* Lipid-overloaded enlarged adipocytes provoke insulin resistance independent of inflammation. *Molecular and cellular biology* **35**, 1686-1699, doi:10.1128/MCB.01321-14 (2015).
- 16 Furukawa, S. *et al.* Increased oxidative stress in obesity and its impact on metabolic syndrome. *The Journal of clinical investigation* **114**, 1752-1761, doi:10.1172/JCI21625 (2004).
- 17 Ozcan, U. *et al.* Endoplasmic reticulum stress links obesity, insulin action, and type 2 diabetes. *Science* **306**, 457-461, doi:10.1126/science.1103160 (2004).
- 18 Kawasaki, N., Asada, R., Saito, A., Kanemoto, S. & Imaizumi, K. Obesity-induced endoplasmic reticulum stress causes chronic inflammation in adipose tissue. *Scientific reports* **2**, 799, doi:10.1038/srep00799 (2012).
- 19 Hosogai, N. *et al.* Adipose tissue hypoxia in obesity and its impact on adipocytokine dysregulation. *Diabetes* **56**, 901-911, doi:10.2337/db06-0911 (2007).
- 20 Sun, K., Halberg, N., Khan, M., Magalang, U. J. & Scherer, P. E. Selective inhibition of hypoxia-inducible factor 1alpha ameliorates adipose tissue dysfunction. *Mol Cell Biol* **33**, 904-917, doi:10.1128/MCB.00951-12 (2013).
- 21 Hotamisligil, G. S., Shargill, N. S. & Spiegelman, B. M. Adipose expression of tumor necrosis factor-alpha: direct role in obesity-linked insulin resistance. *Science* **259**, 87-91 (1993).
- 22 Hotamisligil, G. S. Inflammation, metaflammation and immunometabolic disorders. *Nature* **542**, 177-185, doi:10.1038/nature21363 (2017).
- 23 Cinti, S. The adipose organ at a glance. *Disease models & mechanisms* **5**, 588-594, doi:10.1242/dmm.009662 (2012).
- 24 Strissel, K. J. *et al.* Adipocyte death, adipose tissue remodeling, and obesity complications. *Diabetes* **56**, 2910-2918, doi:10.2337/db07-0767 (2007).
- 25 Jernas, M. *et al.* Separation of human adipocytes by size: hypertrophic fat cells display distinct gene expression. *FASEB journal : official publication of the Federation of American Societies for Experimental Biology* **20**, 1540-1542, doi:10.1096/fj.05-5678fje (2006).
- 26 Winkler, G. *et al.* Expression of tumor necrosis factor (TNF)-alpha protein in the subcutaneous and visceral adipose tissue in correlation with adipocyte cell volume, serum TNF-alpha, soluble serum TNF-receptor-2 concentrations and C-peptide level. *European journal of endocrinology* **149**, 129-135 (2003).
- 27 Ouchi, N. *et al.* Novel modulator for endothelial adhesion molecules: adipocyte-derived plasma protein adiponectin. *Circulation* **100**, 2473-2476 (1999).
- 28 Kern, P. A. *et al.* The expression of tumor necrosis factor in human adipose tissue. Regulation by obesity, weight loss, and relationship to lipoprotein lipase. *The Journal of clinical investigation* **95**, 2111-2119, doi:10.1172/JCI117899 (1995).
- 29 Hivert, M. F. *et al.* Associations of adiponectin, resistin, and tumor necrosis factor-alpha with insulin resistance. *J Clin Endocrinol Metab* **93**, 3165-3172, doi:10.1210/jc.2008-0425 (2008).

- 30 Kanda, H. *et al.* MCP-1 contributes to macrophage infiltration into adipose tissue, insulin resistance, and hepatic steatosis in obesity. *The Journal of clinical investigation* **116**, 1494-1505, doi:10.1172/JCI26498 (2006).
- 31 Kirk, E. A., Sagawa, Z. K., McDonald, T. O., O'Brien, K. D. & Heinecke, J. W. Monocyte chemoattractant protein deficiency fails to restrain macrophage infiltration into adipose tissue [corrected]. *Diabetes* **57**, 1254-1261, doi:10.2337/db07-1061 (2008).
- 32 Tamura, Y. *et al.* Inhibition of CCR2 ameliorates insulin resistance and hepatic steatosis in db/db mice. *Arteriosclerosis, thrombosis, and vascular biology* **28**, 2195-2201, doi:10.1161/ATVBAHA.108.168633 (2008).
- 33 Sopasakis, V. R. *et al.* High local concentrations and effects on differentiation implicate interleukin-6 as a paracrine regulator. *Obesity research* **12**, 454-460, doi:10.1038/oby.2004.51 (2004).
- 34 Wood, I. S., Wang, B., Jenkins, J. R. & Trayhurn, P. The pro-inflammatory cytokine IL-18 is expressed in human adipose tissue and strongly upregulated by TNF $\alpha$  in human adipocytes. *Biochemical and biophysical research communications* **337**, 422-429, doi:10.1016/j.bbrc.2005.09.068 (2005).
- 35 Ziccardi, P. *et al.* Reduction of inflammatory cytokine concentrations and improvement of endothelial functions in obese women after weight loss over one year. *Circulation* **105**, 804-809 (2002).
- 36 Esposito, K. *et al.* Weight loss reduces interleukin-18 levels in obese women. *The Journal of clinical endocrinology and metabolism* **87**, 3864-3866, doi:10.1210/jcem.87.8.8781 (2002).
- 37 Wolf, A. M., Wolf, D., Rumpold, H., Enrich, B. & Tilg, H. Adiponectin induces the anti-inflammatory cytokines IL-10 and IL-1RA in human leukocytes. *Biochemical and biophysical research communications* **323**, 630-635, doi:<http://dx.doi.org/10.1016/j.bbrc.2004.08.145> (2004).
- 38 Friedman, J. M. & Halaas, J. L. Leptin and the regulation of body weight in mammals. *Nature* **395**, 763-770, doi:10.1038/27376 (1998).
- 39 Santos-Alvarez, J., Goberna, R. & Sanchez-Margalet, V. Human leptin stimulates proliferation and activation of human circulating monocytes. *Cellular immunology* **194**, 6-11, doi:10.1006/cimm.1999.1490 (1999).
- 40 Kiguchi, N., Maeda, T., Kobayashi, Y., Fukazawa, Y. & Kishioka, S. Leptin enhances CC-chemokine ligand expression in cultured murine macrophage. *Biochemical and biophysical research communications* **384**, 311-315, doi:10.1016/j.bbrc.2009.04.121 (2009).
- 41 Gainsford, T. *et al.* Leptin can induce proliferation, differentiation, and functional activation of hemopoietic cells. *Proceedings of the National Academy of Sciences of the United States of America* **93**, 14564-14568 (1996).
- 42 Lord, G. M. *et al.* Leptin modulates the T-cell immune response and reverses starvation-induced immunosuppression. *Nature* **394**, 897-901, doi:10.1038/29795 (1998).

- 43 Grunfeld, C. *et al.* Endotoxin and cytokines induce expression of leptin, the ob gene product, in hamsters. *The Journal of clinical investigation* **97**, 2152-2157, doi:10.1172/JCI118653 (1996).
- 44 Bokarewa, M., Nagaev, I., Dahlberg, L., Smith, U. & Tarkowski, A. Resistin, an adipokine with potent proinflammatory properties. *J Immunol* **174**, 5789-5795 (2005).
- 45 Verma, S. *et al.* Resistin promotes endothelial cell activation: further evidence of adipokine-endothelial interaction. *Circulation* **108**, 736-740, doi:10.1161/01.CIR.0000084503.91330.49 (2003).
- 46 Odegaard, J. I. & Chawla, A. Alternative macrophage activation and metabolism. *Annu Rev Pathol* **6**, 275-297, doi:10.1146/annurev-pathol-011110-130138 (2011).
- 47 Ota, T. Chemokine systems link obesity to insulin resistance. *Diabetes Metab J* **37**, 165-172, doi:10.4093/dmj.2013.37.3.165 (2013).
- 48 Cinti, S. *et al.* Adipocyte death defines macrophage localization and function in adipose tissue of obese mice and humans. *Journal of lipid research* **46**, 2347-2355, doi:10.1194/jlr.M500294-JLR200 (2005).
- 49 Chawla, A., Nguyen, K. D. & Goh, Y. P. Macrophage-mediated inflammation in metabolic disease. *Nat Rev Immunol* **11**, 738-749, doi:10.1038/nri3071 (2011).
- 50 Weisberg, S. P. *et al.* Obesity is associated with macrophage accumulation in adipose tissue. *J Clin Invest* **112**, 1796-1808, doi:10.1172/JCI19246 (2003).
- 51 Lumeng, C. N., DelProposto, J. B., Westcott, D. J. & Saltiel, A. R. Phenotypic switching of adipose tissue macrophages with obesity is generated by spatiotemporal differences in macrophage subtypes. *Diabetes* **57**, 3239-3246, doi:10.2337/db08-0872 (2008).
- 52 Lumeng, C. N., Bodzin, J. L. & Saltiel, A. R. Obesity induces a phenotypic switch in adipose tissue macrophage polarization. *The Journal of clinical investigation* **117**, 175-184, doi:10.1172/JCI29881 (2007).
- 53 Clement, K. *et al.* Weight loss regulates inflammation-related genes in white adipose tissue of obese subjects. *FASEB J* **18**, 1657-1669, doi:10.1096/fj.04-2204com (2004).
- 54 Rouault, C. *et al.* Roles of chemokine ligand-2 (CXCL2) and neutrophils in influencing endothelial cell function and inflammation of human adipose tissue. *Endocrinology* **154**, 1069-1079, doi:10.1210/en.2012-1415 (2013).
- 55 Gruen, M. L., Hao, M., Piston, D. W. & Hasty, A. H. Leptin requires canonical migratory signaling pathways for induction of monocyte and macrophage chemotaxis. *American journal of physiology. Cell physiology* **293**, C1481-1488, doi:10.1152/ajpcell.00062.2007 (2007).
- 56 Mattioli, B., Straface, E., Quaranta, M. G., Giordani, L. & Viora, M. Leptin promotes differentiation and survival of human dendritic cells and licenses them for Th1 priming. *Journal of immunology* **174**, 6820-6828 (2005).
- 57 Zhou, Y. *et al.* Leptin Deficiency Shifts Mast Cells toward Anti-Inflammatory Actions and Protects Mice from Obesity and Diabetes by Polarizing M2 Macrophages. *Cell metabolism* **22**, 1045-1058, doi:10.1016/j.cmet.2015.09.013 (2015).

- 58 Liao, X. *et al.* Kruppel-like factor 4 regulates macrophage polarization. *The Journal of clinical investigation* **121**, 2736-2749, doi:10.1172/JCI45444 (2011).
- 59 Nguyen, K. D. *et al.* Alternatively activated macrophages produce catecholamines to sustain adaptive thermogenesis. *Nature* **480**, 104-108, doi:10.1038/nature10653 (2011).
- 60 Konner, A. C. & Bruning, J. C. Toll-like receptors: linking inflammation to metabolism. *Trends in endocrinology and metabolism: TEM* **22**, 16-23, doi:10.1016/j.tem.2010.08.007 (2011).
- 61 Pal, D. *et al.* Fetuin-A acts as an endogenous ligand of TLR4 to promote lipid-induced insulin resistance. *Nature medicine* **18**, 1279-1285, doi:10.1038/nm.2851 (2012).
- 62 Xu, X. *et al.* Obesity activates a program of lysosomal-dependent lipid metabolism in adipose tissue macrophages independently of classic activation. *Cell metabolism* **18**, 816-830, doi:10.1016/j.cmet.2013.11.001 (2013).
- 63 Zeyda, M. & Stulnig, T. M. Adipose tissue macrophages. *Immunol Lett* **112**, 61-67, doi:10.1016/j.imlet.2007.07.003 (2007).
- 64 Bourlier, V. *et al.* Remodeling phenotype of human subcutaneous adipose tissue macrophages. *Circulation* **117**, 806-815, doi:10.1161/CIRCULATIONAHA.107.724096 (2008).
- 65 Kratz, M. *et al.* Metabolic dysfunction drives a mechanistically distinct proinflammatory phenotype in adipose tissue macrophages. *Cell metabolism* **20**, 614-625, doi:10.1016/j.cmet.2014.08.010 (2014).
- 66 Bartelt, A. & Heeren, J. Adipose tissue browning and metabolic health. *Nat Rev Endocrinol* **10**, 24-36, doi:10.1038/nrendo.2013.204 (2014).
- 67 Hui, X. *et al.* Adiponectin Enhances Cold-Induced Browning of Subcutaneous Adipose Tissue via Promoting M2 Macrophage Proliferation. *Cell metabolism* **22**, 279-290, doi:10.1016/j.cmet.2015.06.004 (2015).
- 68 Winer, S. *et al.* Normalization of obesity-associated insulin resistance through immunotherapy. *Nature medicine* **15**, 921-929, doi:10.1038/nm.2001 (2009).
- 69 Feuerer, M. *et al.* Genomic definition of multiple ex vivo regulatory T cell subphenotypes. *Proceedings of the National Academy of Sciences of the United States of America* **107**, 5919-5924, doi:10.1073/pnas.1002006107 (2010).
- 70 Nishimura, S. *et al.* CD8<sup>+</sup> effector T cells contribute to macrophage recruitment and adipose tissue inflammation in obesity. *Nature medicine* **15**, 914-920, doi:10.1038/nm.1964 (2009).
- 71 Winer, D. A. *et al.* B cells promote insulin resistance through modulation of T cells and production of pathogenic IgG antibodies. *Nat Med* **17**, 610-617, doi:10.1038/nm.2353 (2011).
- 72 Di Santo, J. P. Natural killer cell developmental pathways: a question of balance. *Annual review of immunology* **24**, 257-286, doi:10.1146/annurev.immunol.24.021605.090700 (2006).

- 73 Lee, B. C. *et al.* Adipose Natural Killer Cells Regulate Adipose Tissue Macrophages to Promote Insulin Resistance in Obesity. *Cell metabolism* **23**, 685-698, doi:10.1016/j.cmet.2016.03.002 (2016).
- 74 Wensveen, F. M. *et al.* NK cells link obesity-induced adipose stress to inflammation and insulin resistance. *Nature immunology* **16**, 376-385, doi:10.1038/ni.3120 (2015).
- 75 Stepan, C. M., Wang, J., Whiteman, E. L., Birnbaum, M. J. & Lazar, M. A. Activation of SOCS-3 by resistin. *Molecular and cellular biology* **25**, 1569-1575, doi:10.1128/MCB.25.4.1569-1575.2005 (2005).
- 76 Greenberg, A. S. *et al.* Interleukin 6 reduces lipoprotein lipase activity in adipose tissue of mice in vivo and in 3T3-L1 adipocytes: a possible role for interleukin 6 in cancer cachexia. *Cancer research* **52**, 4113-4116 (1992).
- 77 Wang, H. & Eckel, R. H. Lipoprotein lipase: from gene to obesity. *Am J Physiol Endocrinol Metab* **297**, E271-288, doi:10.1152/ajpendo.90920.2008 (2009).
- 78 Walton, R. G. *et al.* Increasing adipocyte lipoprotein lipase improves glucose metabolism in high fat diet-induced obesity. *The Journal of biological chemistry* **290**, 11547-11556, doi:10.1074/jbc.M114.628487 (2015).
- 79 Dalmas, E. *et al.* Irf5 deficiency in macrophages promotes beneficial adipose tissue expansion and insulin sensitivity during obesity. *Nat Med* **21**, 610-618, doi:10.1038/nm.3829 (2015).
- 80 Bigornia, S. J. *et al.* Relation of depot-specific adipose inflammation to insulin resistance in human obesity. *Nutr Diabetes* **2**, e30, doi:10.1038/nutd.2012.3 (2012).
- 81 Donnelly, K. L. *et al.* Sources of fatty acids stored in liver and secreted via lipoproteins in patients with nonalcoholic fatty liver disease. *The Journal of clinical investigation* **115**, 1343-1351, doi:10.1172/JCI23621 (2005).
- 82 Fabbrini, E. *et al.* Intrahepatic fat, not visceral fat, is linked with metabolic complications of obesity. *Proceedings of the National Academy of Sciences of the United States of America* **106**, 15430-15435, doi:10.1073/pnas.0904944106 (2009).
- 83 Doege, H. *et al.* Targeted deletion of FATP5 reveals multiple functions in liver metabolism: alterations in hepatic lipid homeostasis. *Gastroenterology* **130**, 1245-1258, doi:10.1053/j.gastro.2006.02.006 (2006).
- 84 Falcon, A. *et al.* FATP2 is a hepatic fatty acid transporter and peroxisomal very long-chain acyl-CoA synthetase. *American journal of physiology. Endocrinology and metabolism* **299**, E384-393, doi:10.1152/ajpendo.00226.2010 (2010).
- 85 Petersen, K. F. *et al.* The role of skeletal muscle insulin resistance in the pathogenesis of the metabolic syndrome. *Proc Natl Acad Sci U S A* **104**, 12587-12594, doi:10.1073/pnas.0705408104 (2007).
- 86 Diraison, F., Moulin, P. & Beylot, M. Contribution of hepatic de novo lipogenesis and reesterification of plasma non esterified fatty acids to plasma triglyceride synthesis during non-alcoholic fatty liver disease. *Diabetes Metab* **29**, 478-485 (2003).

- 87 Motomura, W. *et al.* Up-regulation of ADRP in fatty liver in human and liver steatosis in mice fed with high fat diet. *Biochemical and biophysical research communications* **340**, 1111-1118, doi:10.1016/j.bbrc.2005.12.121 (2006).
- 88 Schadinger, S. E., Bucher, N. L., Schreiber, B. M. & Farmer, S. R. PPARgamma2 regulates lipogenesis and lipid accumulation in steatotic hepatocytes. *Am J Physiol Endocrinol Metab* **288**, E1195-1205, doi:10.1152/ajpendo.00513.2004 (2005).
- 89 Souza-Mello, V. *et al.* Comparative effects of telmisartan, sitagliptin and metformin alone or in combination on obesity, insulin resistance, and liver and pancreas remodelling in C57BL/6 mice fed on a very high-fat diet. *Clin Sci (Lond)* **119**, 239-250, doi:10.1042/CS20100061 (2010).
- 90 Montagner, A. *et al.* Liver PPARalpha is crucial for whole-body fatty acid homeostasis and is protective against NAFLD. *Gut* **65**, 1202-1214, doi:10.1136/gutjnl-2015-310798 (2016).
- 91 Fabbrini, E. *et al.* Alterations in adipose tissue and hepatic lipid kinetics in obese men and women with nonalcoholic fatty liver disease. *Gastroenterology* **134**, 424-431, doi:10.1053/j.gastro.2007.11.038 (2008).
- 92 Sanyal, A. J. *et al.* Endpoints and clinical trial design for nonalcoholic steatohepatitis. *Hepatology* **54**, 344-353, doi:10.1002/hep.24376 (2011).
- 93 Jou, J., Choi, S. S. & Diehl, A. M. Mechanisms of disease progression in nonalcoholic fatty liver disease. *Semin Liver Dis* **28**, 370-379, doi:10.1055/s-0028-1091981 (2008).
- 94 Stanton, M. C. *et al.* Inflammatory Signals shift from adipose to liver during high fat feeding and influence the development of steatohepatitis in mice. *Journal of inflammation* **8**, 8, doi:10.1186/1476-9255-8-8 (2011).
- 95 Obstfeld, A. E. *et al.* C-C chemokine receptor 2 (CCR2) regulates the hepatic recruitment of myeloid cells that promote obesity-induced hepatic steatosis. *Diabetes* **59**, 916-925, doi:10.2337/db09-1403 (2010).
- 96 Yona, S. *et al.* Fate mapping reveals origins and dynamics of monocytes and tissue macrophages under homeostasis. *Immunity* **38**, 79-91, doi:10.1016/j.immuni.2012.12.001 (2013).
- 97 Ganz, M. *et al.* Progression of non-alcoholic steatosis to steatohepatitis and fibrosis parallels cumulative accumulation of danger signals that promote inflammation and liver tumors in a high fat-cholesterol-sugar diet model in mice. *Journal of translational medicine* **13**, 193, doi:10.1186/s12967-015-0552-7 (2015).
- 98 Seki, E. *et al.* CCR2 promotes hepatic fibrosis in mice. *Hepatology* **50**, 185-197, doi:10.1002/hep.22952 (2009).
- 99 Devisscher, L., Verhelst, X., Colle, I., Van Vlierberghe, H. & Geerts, A. The role of macrophages in obesity-driven chronic liver disease. *Journal of leukocyte biology* **99**, 693-698, doi:10.1189/jlb.5RU0116-016R (2016).
- 100 Huang, W. *et al.* Depletion of liver Kupffer cells prevents the development of diet-induced hepatic steatosis and insulin resistance. *Diabetes* **59**, 347-357, doi:10.2337/db09-0016 (2010).

- 101 Heymann, F. & Tacke, F. Immunology in the liver--from homeostasis to disease. *Nat Rev Gastroenterol Hepatol* **13**, 88-110, doi:10.1038/nrgastro.2015.200 (2016).
- 102 Klugewitz, K., Adams, D. H., Emoto, M., Eulenburg, K. & Hamann, A. The composition of intrahepatic lymphocytes: shaped by selective recruitment? *Trends Immunol* **25**, 590-594, doi:10.1016/j.it.2004.09.006 (2004).
- 103 Tu, Z. *et al.* TLR-dependent cross talk between human Kupffer cells and NK cells. *J Exp Med* **205**, 233-244, doi:10.1084/jem.20072195 (2008).
- 104 Schildberg, F. A. *et al.* Murine hepatic stellate cells veto CD8 T cell activation by a CD54-dependent mechanism. *Hepatology* **54**, 262-272, doi:10.1002/hep.24352 (2011).
- 105 Ramaiah, S. K. & Jaeschke, H. Hepatic neutrophil infiltration in the pathogenesis of alcohol-induced liver injury. *Toxicol Mech Methods* **17**, 431-440, doi:10.1080/00952990701407702 (2007).
- 106 Ramadori, G., Moriconi, F., Malik, I. & Dudas, J. Physiology and pathophysiology of liver inflammation, damage and repair. *J Physiol Pharmacol* **59 Suppl 1**, 107-117 (2008).
- 107 Alkhouri, N. *et al.* Neutrophil to lymphocyte ratio: a new marker for predicting steatohepatitis and fibrosis in patients with nonalcoholic fatty liver disease. *Liver Int* **32**, 297-302, doi:10.1111/j.1478-3231.2011.02639.x (2012).
- 108 Batailler, R. & Brenner, D. A. Liver fibrosis. *The Journal of clinical investigation* **115**, 209-218, doi:10.1172/JCI24282 (2005).
- 109 Pradere, J. P. *et al.* Hepatic macrophages but not dendritic cells contribute to liver fibrosis by promoting the survival of activated hepatic stellate cells in mice. *Hepatology* **58**, 1461-1473, doi:10.1002/hep.26429 (2013).
- 110 Schweiger, M. *et al.* Pharmacological inhibition of adipose triglyceride lipase corrects high-fat diet-induced insulin resistance and hepatosteatosis in mice. *Nat Commun* **8**, 14859, doi:10.1038/ncomms14859 (2017).
- 111 Roden, M. Mechanisms of Disease: hepatic steatosis in type 2 diabetes--pathogenesis and clinical relevance. *Nat Clin Pract Endocrinol Metab* **2**, 335-348, doi:10.1038/ncpendmet0190 (2006).
- 112 Xu, A. *et al.* The fat-derived hormone adiponectin alleviates alcoholic and nonalcoholic fatty liver diseases in mice. *J Clin Invest* **112**, 91-100, doi:10.1172/JCI17797 (2003).
- 113 Shklyaev, S. *et al.* Sustained peripheral expression of transgene adiponectin offsets the development of diet-induced obesity in rats. *Proceedings of the National Academy of Sciences of the United States of America* **100**, 14217-14222, doi:10.1073/pnas.2333912100 (2003).
- 114 Yamauchi, T. *et al.* Adiponectin stimulates glucose utilization and fatty-acid oxidation by activating AMP-activated protein kinase. *Nat Med* **8**, 1288-1295, doi:10.1038/nm788 (2002).
- 115 Hui, J. M. *et al.* Beyond insulin resistance in NASH: TNF-alpha or adiponectin? *Hepatology* **40**, 46-54, doi:10.1002/hep.20280 (2004).

- 116 Lopez-Bermejo, A. *et al.* Adiponectin, hepatocellular dysfunction and insulin sensitivity. *Clin Endocrinol (Oxf)* **60**, 256-263 (2004).
- 117 Poordad, F. F. The role of leptin in NAFLD: contender or pretender? *J Clin Gastroenterol* **38**, 841-843 (2004).
- 118 Cao, Q., Mak, K. M., Ren, C. & Lieber, C. S. Leptin stimulates tissue inhibitor of metalloproteinase-1 in human hepatic stellate cells: respective roles of the JAK/STAT and JAK-mediated H<sub>2</sub>O<sub>2</sub>-dependant MAPK pathways. *The Journal of biological chemistry* **279**, 4292-4304, doi:10.1074/jbc.M308351200 (2004).
- 119 Marroqui, L. *et al.* Role of leptin in the pancreatic beta-cell: effects and signaling pathways. *Journal of molecular endocrinology* **49**, R9-17, doi:10.1530/JME-12-0025 (2012).
- 120 Sabio, G. *et al.* A stress signaling pathway in adipose tissue regulates hepatic insulin resistance. *Science* **322**, 1539-1543, doi:10.1126/science.1160794 (2008).
- 121 Jaeger, D. *et al.* Fasting-induced G0/G1 switch gene 2 and FGF21 expression in the liver are under regulation of adipose tissue derived fatty acids. *J Hepatol* **63**, 437-445, doi:10.1016/j.jhep.2015.02.035 (2015).
- 122 Inagaki, T. *et al.* Endocrine regulation of the fasting response by PPARalpha-mediated induction of fibroblast growth factor 21. *Cell metabolism* **5**, 415-425, doi:10.1016/j.cmet.2007.05.003 (2007).
- 123 Lin, Z. *et al.* Adiponectin mediates the metabolic effects of FGF21 on glucose homeostasis and insulin sensitivity in mice. *Cell metabolism* **17**, 779-789, doi:10.1016/j.cmet.2013.04.005 (2013).
- 124 BonDurant, L. D. *et al.* FGF21 Regulates Metabolism Through Adipose-Dependent and -Independent Mechanisms. *Cell metabolism* **25**, 935-944 e934, doi:10.1016/j.cmet.2017.03.005 (2017).
- 125 Kharitononkov, A. *et al.* FGF-21 as a novel metabolic regulator. *The Journal of clinical investigation* **115**, 1627-1635, doi:10.1172/JCI23606 (2005).
- 126 Gimeno, R. E. & Moller, D. E. FGF21-based pharmacotherapy--potential utility for metabolic disorders. *Trends Endocrinol Metab* **25**, 303-311, doi:10.1016/j.tem.2014.03.001 (2014).
- 127 Schlein, C. *et al.* FGF21 Lowers Plasma Triglycerides by Accelerating Lipoprotein Catabolism in White and Brown Adipose Tissues. *Cell metabolism* **23**, 441-453, doi:10.1016/j.cmet.2016.01.006 (2016).
- 128 Meex, R. C. *et al.* Fetuin B Is a Secreted Hepatocyte Factor Linking Steatosis to Impaired Glucose Metabolism. *Cell metabolism* **22**, 1078-1089, doi:10.1016/j.cmet.2015.09.023 (2015).
- 129 Brown, M. S. & Goldstein, J. L. Selective versus total insulin resistance: a pathogenic paradox. *Cell metabolism* **7**, 95-96, doi:10.1016/j.cmet.2007.12.009 (2008).
- 130 Lu, M. *et al.* Insulin regulates liver metabolism in vivo in the absence of hepatic Akt and Foxo1. *Nature medicine* **18**, 388-395, doi:10.1038/nm.2686 (2012).



- 131 Li, S., Brown, M. S. & Goldstein, J. L. Bifurcation of insulin signaling pathway in rat liver: mTORC1 required for stimulation of lipogenesis, but not inhibition of gluconeogenesis. *Proceedings of the National Academy of Sciences of the United States of America* **107**, 3441-3446, doi:10.1073/pnas.0914798107 (2010).
- 132 I, O. S. *et al.* FoxO1 integrates direct and indirect effects of insulin on hepatic glucose production and glucose utilization. *Nature communications* **6**, 7079, doi:10.1038/ncomms8079 (2015).
- 133 Perry, R. J. *et al.* Hepatic acetyl CoA links adipose tissue inflammation to hepatic insulin resistance and type 2 diabetes. *Cell* **160**, 745-758, doi:10.1016/j.cell.2015.01.012 (2015).
- 134 Titchenell, P. M. *et al.* Direct Hepatocyte Insulin Signaling Is Required for Lipogenesis but Is Dispensable for the Suppression of Glucose Production. *Cell metabolism* **23**, 1154-1166, doi:10.1016/j.cmet.2016.04.022 (2016).
- 135 Benhamed, F. *et al.* The lipogenic transcription factor ChREBP dissociates hepatic steatosis from insulin resistance in mice and humans. *J Clin Invest* **122**, 2176-2194, doi:10.1172/JCI41636 (2012).
- 136 Tremblay, F., Lavigne, C., Jacques, H. & Marette, A. Role of dietary proteins and amino acids in the pathogenesis of insulin resistance. *Annu Rev Nutr* **27**, 293-310, doi:10.1146/annurev.nutr.25.050304.092545 (2007).
- 137 Uno, K. *et al.* A hepatic amino acid/mTOR/S6K-dependent signalling pathway modulates systemic lipid metabolism via neuronal signals. *Nat Commun* **6**, 7940, doi:10.1038/ncomms8940 (2015).
- 138 Kopp, E. & Ghosh, S. Inhibition of NF-kappa B by sodium salicylate and aspirin. *Science* **265**, 956-959 (1994).
- 139 Chang, L. & Karin, M. Mammalian MAP kinase signalling cascades. *Nature* **410**, 37-40, doi:10.1038/35065000 (2001).
- 140 Aguirre, V., Uchida, T., Yenush, L., Davis, R. & White, M. F. The c-Jun NH(2)-terminal kinase promotes insulin resistance during association with insulin receptor substrate-1 and phosphorylation of Ser(307). *The Journal of biological chemistry* **275**, 9047-9054 (2000).
- 141 Han, M. S. *et al.* JNK expression by macrophages promotes obesity-induced insulin resistance and inflammation. *Science* **339**, 218-222, doi:10.1126/science.1227568 (2013).
- 142 Vernia, S. *et al.* The PPARalpha-FGF21 hormone axis contributes to metabolic regulation by the hepatic JNK signaling pathway. *Cell metabolism* **20**, 512-525, doi:10.1016/j.cmet.2014.06.010 (2014).
- 143 Yuan, M. *et al.* Reversal of obesity- and diet-induced insulin resistance with salicylates or targeted disruption of Ikkbeta. *Science* **293**, 1673-1677, doi:10.1126/science.1061620 (2001).
- 144 Kim, J. K. *et al.* Prevention of fat-induced insulin resistance by salicylate. *J Clin Invest* **108**, 437-446, doi:10.1172/JCI11559 (2001).
- 145 Cai, D. *et al.* Local and systemic insulin resistance resulting from hepatic activation of IKK-beta and NF-kappaB. *Nat Med* **11**, 183-190, doi:10.1038/nm1166 (2005).

- 146 Hotamisligil, G. k. S. Endoplasmic Reticulum Stress and the Inflammatory Basis of Metabolic Disease. *Cell* **140**, 900-917, doi:<http://dx.doi.org/10.1016/j.cell.2010.02.034> (2010).
- 147 Shoelson, S. E., Lee, J. & Goldfine, A. B. Inflammation and insulin resistance. *J Clin Invest* **116**, 1793-1801, doi:10.1172/JCI29069 (2006).
- 148 Uysal, K. T., Wiesbrock, S. M., Marino, M. W. & Hotamisligil, G. S. Protection from obesity-induced insulin resistance in mice lacking TNF-alpha function. *Nature* **389**, 610-614, doi:10.1038/39335 (1997).
- 149 Hirosumi, J. *et al.* A central role for JNK in obesity and insulin resistance. *Nature* **420**, 333-336, doi:10.1038/nature01137 (2002).
- 150 Dominguez, H. *et al.* Metabolic and vascular effects of tumor necrosis factor-alpha blockade with etanercept in obese patients with type 2 diabetes. *J Vasc Res* **42**, 517-525, doi:10.1159/000088261 (2005).
- 151 Ofei, F., Hurel, S., Newkirk, J., Sopwith, M. & Taylor, R. Effects of an engineered human anti-TNF-alpha antibody (CDP571) on insulin sensitivity and glycemic control in patients with NIDDM. *Diabetes* **45**, 881-885 (1996).
- 152 Wascher, T. C. *et al.* Chronic TNF-alpha neutralization does not improve insulin resistance or endothelial function in "healthy" men with metabolic syndrome. *Mol Med* **17**, 189-193, doi:10.2119/molmed.2010.00221 (2011).
- 153 Heinrich, P. C., Behrmann, I., Muller-Newen, G., Schaper, F. & Graeve, L. Interleukin-6-type cytokine signalling through the gp130/Jak/STAT pathway. *Biochem J* **334** ( Pt 2), 297-314 (1998).
- 154 Kim, S., Sked, M. & Ji, Q. Non-intrusive eye gaze tracking under natural head movements. *Conf Proc IEEE Eng Med Biol Soc* **3**, 2271-2274, doi:10.1109/IEMBS.2004.1403660 (2004).
- 155 Senn, J. J. *et al.* Suppressor of cytokine signaling-3 (SOCS-3), a potential mediator of interleukin-6-dependent insulin resistance in hepatocytes. *The Journal of biological chemistry* **278**, 13740-13746, doi:10.1074/jbc.M210689200 (2003).
- 156 Matthews, V. B. *et al.* Interleukin-6-deficient mice develop hepatic inflammation and systemic insulin resistance. *Diabetologia* **53**, 2431-2441, doi:10.1007/s00125-010-1865-y (2010).
- 157 Tan, H. W. *et al.* IL-18 overexpression promotes vascular inflammation and remodeling in a rat model of metabolic syndrome. *Atherosclerosis* **208**, 350-357, doi:10.1016/j.atherosclerosis.2009.07.053 (2010).
- 158 Netea, M. G. *et al.* Deficiency of interleukin-18 in mice leads to hyperphagia, obesity and insulin resistance. *Nature medicine* **12**, 650-656, doi:10.1038/nm1415 (2006).
- 159 Banerjee, R. R. *et al.* Regulation of fasted blood glucose by resistin. *Science* **303**, 1195-1198, doi:10.1126/science.1092341 (2004).
- 160 McTernan, C. L. *et al.* Resistin, central obesity, and type 2 diabetes. *Lancet* **359**, 46-47 (2002).

- 161 Lee, J. H. *et al.* Circulating resistin levels are not associated with obesity or insulin resistance in humans and are not regulated by fasting or leptin administration: cross-sectional and interventional studies in normal, insulin-resistant, and diabetic subjects. *The Journal of clinical endocrinology and metabolism* **88**, 4848-4856, doi:10.1210/jc.2003-030519 (2003).
- 162 Kielstein, J. T. *et al.* Increased resistin blood levels are not associated with insulin resistance in patients with renal disease. *Am J Kidney Dis* **42**, 62-66 (2003).
- 163 Patel, L. *et al.* Resistin is expressed in human macrophages and directly regulated by PPAR gamma activators. *Biochemical and biophysical research communications* **300**, 472-476 (2003).
- 164 Savage, D. B. *et al.* Resistin / Fizz3 expression in relation to obesity and peroxisome proliferator-activated receptor-gamma action in humans. *Diabetes* **50**, 2199-2202 (2001).
- 165 Glass, C. K. & Olefsky, J. M. Inflammation and lipid signaling in the etiology of insulin resistance. *Cell metabolism* **15**, 635-645, doi:10.1016/j.cmet.2012.04.001 (2012).
- 166 den Dekker, W. K., Cheng, C., Pasterkamp, G. & Duckers, H. J. Toll like receptor 4 in atherosclerosis and plaque destabilization. *Atherosclerosis* **209**, 314-320, doi:<http://dx.doi.org/10.1016/j.atherosclerosis.2009.09.075> (2010).
- 167 Leemans, J. C., Cassel, S. L. & Sutterwala, F. S. Sensing damage by the NLRP3 inflammasome. *Immunological Reviews* **243**, 152-162, doi:10.1111/j.1600-065X.2011.01043.x (2011).
- 168 Tanti, J.-F. & Jager, J. Cellular mechanisms of insulin resistance: role of stress-regulated serine kinases and insulin receptor substrates (IRS) serine phosphorylation. *Current Opinion in Pharmacology* **9**, 753-762, doi:<http://dx.doi.org/10.1016/j.coph.2009.07.004> (2009).
- 169 Stienstra, R. *et al.* The Inflammasome-Mediated Caspase-1 Activation Controls Adipocyte Differentiation and Insulin Sensitivity. *Cell metabolism* **12**, 593-605, doi:<http://dx.doi.org/10.1016/j.cmet.2010.11.011> (2010).
- 170 Vandanmagsar, B. *et al.* The NLRP3 inflammasome instigates obesity-induced inflammation and insulin resistance. *Nature medicine* **17**, 179-188 (2011).
- 171 Samuel, V. T. & Shulman, G. I. Mechanisms for insulin resistance: common threads and missing links. *Cell* **148**, 852-871, doi:10.1016/j.cell.2012.02.017 (2012).
- 172 Samuel, V. T. *et al.* Mechanism of hepatic insulin resistance in non-alcoholic fatty liver disease. *The Journal of biological chemistry* **279**, 32345-32353, doi:10.1074/jbc.M313478200 (2004).
- 173 Samuel, V. T. *et al.* Inhibition of protein kinase Cepsilon prevents hepatic insulin resistance in nonalcoholic fatty liver disease. *J Clin Invest* **117**, 739-745, doi:10.1172/JCI30400 (2007).
- 174 Holland, W. L. *et al.* Lipid-induced insulin resistance mediated by the proinflammatory receptor TLR4 requires saturated fatty acid-induced ceramide biosynthesis in mice. *J Clin Invest* **121**, 1858-1870, doi:10.1172/JCI43378 (2011).

- 175 Stratford, S., Hoehn, K. L., Liu, F. & Summers, S. A. Regulation of insulin action by ceramide: dual mechanisms linking ceramide accumulation to the inhibition of Akt/protein kinase B. *The Journal of biological chemistry* **279**, 36608-36615, doi:10.1074/jbc.M406499200 (2004).
- 176 Merrill, A. H., Jr. De novo sphingolipid biosynthesis: a necessary, but dangerous, pathway. *The Journal of biological chemistry* **277**, 25843-25846, doi:10.1074/jbc.R200009200 (2002).
- 177 Holland, W. L. *et al.* Inhibition of ceramide synthesis ameliorates glucocorticoid-, saturated-fat-, and obesity-induced insulin resistance. *Cell metabolism* **5**, 167-179, doi:10.1016/j.cmet.2007.01.002 (2007).
- 178 Ussher, J. R. *et al.* Inhibition of de novo ceramide synthesis reverses diet-induced insulin resistance and enhances whole-body oxygen consumption. *Diabetes* **59**, 2453-2464, doi:10.2337/db09-1293 (2010).
- 179 Jiang, C. *et al.* Intestinal farnesoid X receptor signaling promotes nonalcoholic fatty liver disease. *J Clin Invest* **125**, 386-402, doi:10.1172/JCI76738 (2015).
- 180 Chaurasia, B. *et al.* Adipocyte Ceramides Regulate Subcutaneous Adipose Browning, Inflammation, and Metabolism. *Cell metabolism* **24**, 820-834, doi:10.1016/j.cmet.2016.10.002 (2016).
- 181 Dbaibo, G. S. *et al.* Ceramide generation by two distinct pathways in tumor necrosis factor alpha-induced cell death. *FEBS Lett* **503**, 7-12 (2001).
- 182 Wellen, K. E. *et al.* ATP-citrate lyase links cellular metabolism to histone acetylation. *Science* **324**, 1076-1080, doi:10.1126/science.1164097 (2009).
- 183 Detich, N., Hamm, S., Just, G., Knox, J. D. & Szyf, M. The methyl donor S-Adenosylmethionine inhibits active demethylation of DNA: a candidate novel mechanism for the pharmacological effects of S-Adenosylmethionine. *The Journal of biological chemistry* **278**, 20812-20820, doi:10.1074/jbc.M211813200 (2003).
- 184 Xu, W., Wang, F., Yu, Z. & Xin, F. Epigenetics and Cellular Metabolism. *Genet Epigenet* **8**, 43-51, doi:10.4137/GEG.S32160 (2016).
- 185 Tan, C. K., Zhuang, Y. & Wahli, W. Synthetic and natural Peroxisome Proliferator-Activated Receptor (PPAR) agonists as candidates for the therapy of the metabolic syndrome. *Expert Opin Ther Targets* **21**, 333-348, doi:10.1080/14728222.2017.1280467 (2017).
- 186 Gross, B., Pawlak, M., Lefebvre, P. & Staels, B. PPARs in obesity-induced T2DM, dyslipidaemia and NAFLD. *Nat Rev Endocrinol* **13**, 36-49, doi:10.1038/nrendo.2016.135 (2017).
- 187 Kersten, S. Integrated physiology and systems biology of PPARalpha. *Mol Metab* **3**, 354-371, doi:10.1016/j.molmet.2014.02.002 (2014).
- 188 Kharitononkov, A. *et al.* The metabolic state of diabetic monkeys is regulated by fibroblast growth factor-21. *Endocrinology* **148**, 774-781, doi:10.1210/en.2006-1168 (2007).

- 189 Staels, B. *et al.* Activation of human aortic smooth-muscle cells is inhibited by PPARalpha but not by PPARgamma activators. *Nature* **393**, 790-793, doi:10.1038/31701 (1998).
- 190 Liu, Z. M., Hu, M., Chan, P. & Tomlinson, B. Early investigational drugs targeting PPAR-alpha for the treatment of metabolic disease. *Expert Opin Investig Drugs* **24**, 611-621, doi:10.1517/13543784.2015.1006359 (2015).
- 191 Tanaka, N., Aoyama, T., Kimura, S. & Gonzalez, F. J. Targeting nuclear receptors for the treatment of fatty liver disease. *Pharmacol Ther*, doi:10.1016/j.pharmthera.2017.05.011 (2017).
- 192 Jackevicius, C. A. *et al.* Use of fibrates in the United States and Canada. *JAMA* **305**, 1217-1224, doi:10.1001/jama.2011.353 (2011).
- 193 Sanderson, L. M., Boekschoten, M. V., Desvergne, B., Muller, M. & Kersten, S. Transcriptional profiling reveals divergent roles of PPARalpha and PPARbeta/delta in regulation of gene expression in mouse liver. *Physiol Genomics* **41**, 42-52, doi:10.1152/physiolgenomics.00127.2009 (2010).
- 194 Odegaard, J. I. *et al.* Alternative M2 activation of Kupffer cells by PPARdelta ameliorates obesity-induced insulin resistance. *Cell metabolism* **7**, 496-507, doi:10.1016/j.cmet.2008.04.003 (2008).
- 195 Iwaisako, K. *et al.* Protection from liver fibrosis by a peroxisome proliferator-activated receptor delta agonist. *Proceedings of the National Academy of Sciences of the United States of America* **109**, E1369-1376, doi:10.1073/pnas.1202464109 (2012).
- 196 Grewal, A. S., Beniwal, M., Pandita, D., Sekhon, B. S. & Lather, V. Recent Updates on Peroxisome Proliferator-Activated Receptor delta Agonists for the Treatment of Metabolic Syndrome. *Med Chem* **12**, 3-21 (2016).
- 197 Rosen, E. D. *et al.* PPAR gamma is required for the differentiation of adipose tissue in vivo and in vitro. *Mol Cell* **4**, 611-617 (1999).
- 198 Soccio, R. E., Chen, E. R. & Lazar, M. A. Thiazolidinediones and the promise of insulin sensitization in type 2 diabetes. *Cell metabolism* **20**, 573-591, doi:10.1016/j.cmet.2014.08.005 (2014).
- 199 Cariou, B., Charbonnel, B. & Staels, B. Thiazolidinediones and PPARgamma agonists: time for a reassessment. *Trends Endocrinol Metab* **23**, 205-215, doi:10.1016/j.tem.2012.03.001 (2012).
- 200 Adams, M. *et al.* Activators of peroxisome proliferator-activated receptor gamma have depot-specific effects on human preadipocyte differentiation. *The Journal of clinical investigation* **100**, 3149-3153, doi:10.1172/JCI119870 (1997).
- 201 Miyazaki, Y. *et al.* Effect of pioglitazone on abdominal fat distribution and insulin sensitivity in type 2 diabetic patients. *The Journal of clinical endocrinology and metabolism* **87**, 2784-2791, doi:10.1210/jcem.87.6.8567 (2002).
- 202 Guan, H. P. *et al.* A futile metabolic cycle activated in adipocytes by antidiabetic agents. *Nature medicine* **8**, 1122-1128, doi:10.1038/nm780 (2002).

- 203 Yamauchi, T. *et al.* The mechanisms by which both heterozygous peroxisome proliferator-activated receptor gamma (PPARgamma) deficiency and PPARgamma agonist improve insulin resistance. *The Journal of biological chemistry* **276**, 41245-41254, doi:10.1074/jbc.M103241200 (2001).
- 204 Oakes, N. D., Thalen, P. G., Jacinto, S. M. & Ljung, B. Thiazolidinediones increase plasma-adipose tissue FFA exchange capacity and enhance insulin-mediated control of systemic FFA availability. *Diabetes* **50**, 1158-1165 (2001).
- 205 Petrovic, N., Shabalina, I. G., Timmons, J. A., Cannon, B. & Nedergaard, J. Thermogenically competent nonadrenergic recruitment in brown preadipocytes by a PPARgamma agonist. *Am J Physiol Endocrinol Metab* **295**, E287-296, doi:10.1152/ajpendo.00035.2008 (2008).
- 206 Ohno, H., Shinoda, K., Spiegelman, B. M. & Kajimura, S. PPARgamma agonists induce a white-to-brown fat conversion through stabilization of PRDM16 protein. *Cell metabolism* **15**, 395-404, doi:10.1016/j.cmet.2012.01.019 (2012).
- 207 Sears, D. D. *et al.* Mechanisms of human insulin resistance and thiazolidinedione-mediated insulin sensitization. *Proceedings of the National Academy of Sciences of the United States of America* **106**, 18745-18750, doi:10.1073/pnas.0903032106 (2009).
- 208 Smith, U. *et al.* Thiazolidinediones (PPARgamma agonists) but not PPARalpha agonists increase IRS-2 gene expression in 3T3-L1 and human adipocytes. *FASEB J* **15**, 215-220, doi:10.1096/fj.00-0020com (2001).
- 209 Ribon, V., Johnson, J. H., Camp, H. S. & Saltiel, A. R. Thiazolidinediones and insulin resistance: peroxisome proliferator-activated receptor gamma activation stimulates expression of the CAP gene. *Proceedings of the National Academy of Sciences of the United States of America* **95**, 14751-14756 (1998).
- 210 Steppan, C. M. *et al.* The hormone resistin links obesity to diabetes. *Nature* **409**, 307-312, doi:10.1038/35053000 (2001).
- 211 Peraldi, P., Xu, M. & Spiegelman, B. M. Thiazolidinediones block tumor necrosis factor-alpha-induced inhibition of insulin signaling. *The Journal of clinical investigation* **100**, 1863-1869, doi:10.1172/JCI119715 (1997).
- 212 Hammarstedt, A., Andersson, C. X., Rotter Sopasakis, V. & Smith, U. The effect of PPARgamma ligands on the adipose tissue in insulin resistance. *Prostaglandins, leukotrienes, and essential fatty acids* **73**, 65-75, doi:10.1016/j.plefa.2005.04.008 (2005).
- 213 Chawla, A. Control of macrophage activation and function by PPARs. *Circulation research* **106**, 1559-1569, doi:10.1161/CIRCRESAHA.110.216523 (2010).
- 214 Huang, J. T. *et al.* Interleukin-4-dependent production of PPAR-gamma ligands in macrophages by 12/15-lipoxygenase. *Nature* **400**, 378-382, doi:10.1038/22572 (1999).
- 215 Xu, H. *et al.* Chronic inflammation in fat plays a crucial role in the development of obesity-related insulin resistance. *J Clin Invest* **112**, 1821-1830, doi:10.1172/JCI19451 (2003).
- 216 Odegaard, J. I. *et al.* Macrophage-specific PPARgamma controls alternative activation and improves insulin resistance. *Nature* **447**, 1116-1120, doi:10.1038/nature05894 (2007).

- 217 Hevener, A. L. *et al.* Macrophage PPAR gamma is required for normal skeletal muscle and hepatic insulin sensitivity and full antidiabetic effects of thiazolidinediones. *The Journal of clinical investigation* **117**, 1658-1669, doi:10.1172/JCI31561 (2007).
- 218 Cipolletta, D. *et al.* PPAR-gamma is a major driver of the accumulation and phenotype of adipose tissue Treg cells. *Nature* **486**, 549-553, doi:10.1038/nature11132 (2012).
- 219 Fraulob, J. C., Souza-Mello, V., Aguila, M. B. & Mandarim-de-Lacerda, C. A. Beneficial effects of rosuvastatin on insulin resistance, adiposity, inflammatory markers and non-alcoholic fatty liver disease in mice fed on a high-fat diet. *Clinical science* **123**, 259-270, doi:10.1042/CS20110373 (2012).
- 220 Banks, A. S. *et al.* An ERK/Cdk5 axis controls the diabetogenic actions of PPARgamma. *Nature* **517**, 391-395, doi:10.1038/nature13887 (2015).
- 221 Choi, J. H. *et al.* Anti-diabetic drugs inhibit obesity-linked phosphorylation of PPARgamma by Cdk5. *Nature* **466**, 451-456, doi:10.1038/nature09291 (2010).
- 222 Vitale, S. G. *et al.* Peroxisome Proliferator-Activated Receptor Modulation during Metabolic Diseases and Cancers: Master and Minions. *PPAR Res* **2016**, 6517313, doi:10.1155/2016/6517313 (2016).
- 223 Rotman, Y. & Sanyal, A. J. Current and upcoming pharmacotherapy for non-alcoholic fatty liver disease. *Gut* **66**, 180-190, doi:10.1136/gutjnl-2016-312431 (2017).
- 224 Pap, A., Cuaranta-Monroy, I., Peloquin, M. & Nagy, L. Is the Mouse a Good Model of Human PPARgamma-Related Metabolic Diseases? *Int J Mol Sci* **17**, doi:10.3390/ijms17081236 (2016).
- 225 Birsoy, K. *et al.* Analysis of gene networks in white adipose tissue development reveals a role for ETS2 in adipogenesis. *Development* **138**, 4709-4719, doi:10.1242/dev.067710 (2011).
- 226 Greenwood, M. R. & Hirsch, J. Postnatal development of adipocyte cellularity in the normal rat. *Journal of lipid research* **15**, 474-483 (1974).
- 227 Han, J. *et al.* The spatiotemporal development of adipose tissue. *Development* **138**, 5027-5037, doi:10.1242/dev.067686 (2011).
- 228 Billon, N. *et al.* The generation of adipocytes by the neural crest. *Development* **134**, 2283-2292, doi:10.1242/dev.002642 (2007).
- 229 Cinti, S., Cigolini, M., Bosello, O. & Bjorntorp, P. A morphological study of the adipocyte precursor. *J Submicrosc Cytol* **16**, 243-251 (1984).
- 230 Fukumura, D. *et al.* Paracrine regulation of angiogenesis and adipocyte differentiation during in vivo adipogenesis. *Circ Res* **93**, e88-97, doi:10.1161/01.RES.0000099243.20096.FA (2003).
- 231 Seale, P. *et al.* PRDM16 controls a brown fat/skeletal muscle switch. *Nature* **454**, 961-967, doi:10.1038/nature07182 (2008).
- 232 Feldmann, H. M., Golozoubova, V., Cannon, B. & Nedergaard, J. UCP1 Ablation Induces Obesity and Abolishes Diet-induced Thermogenesis in Mice Exempt from Thermal Stress

- by Living at Thermoneutrality. *Cell metabolism* **9**, 203-209, doi:10.1016/j.cmet.2008.12.014 (2009).
- 233 Lowell, B. B. *et al.* Development of Obesity in Transgenic Mice after Genetic Ablation of Brown Adipose-Tissue. *Nature* **366**, 740-742, doi:DOI 10.1038/366740a0 (1993).
- 234 Cannon, B. & Nedergaard, J. Thermogenesis challenges the adipostat hypothesis for body-weight control. *P Nutr Soc* **68**, 401-407, doi:10.1017/S0029665109990255 (2009).
- 235 Vallerand, A. L., Lupien, J. & Bukowiecki, L. J. Cold-Exposure Reverses the Diabetogenic Effects of High-Fat Feeding. *Diabetes* **35**, 329-334, doi:DOI 10.2337/diabetes.35.3.329 (1986).
- 236 Cypess, A. M. *et al.* Identification and importance of brown adipose tissue in adult humans. *N Engl J Med* **360**, 1509-1517, doi:10.1056/NEJMoa0810780 (2009).
- 237 van Marken Lichtenbelt, W. D. *et al.* Cold-activated brown adipose tissue in healthy men. *N Engl J Med* **360**, 1500-1508, doi:10.1056/NEJMoa0808718 (2009).
- 238 Virtanen, K. A. *et al.* Functional brown adipose tissue in healthy adults. *N Engl J Med* **360**, 1518-1525, doi:10.1056/NEJMoa0808949 (2009).
- 239 Young, P., Arch, J. R. S. & Ashwell, M. Brown Adipose-Tissue in the Parametrial Fat Pad of the Mouse. *Febs Letters* **167**, 10-14, doi:Doi 10.1016/0014-5793(84)80822-4 (1984).
- 240 Wu, J., Cohen, P. & Spiegelman, B. M. Adaptive thermogenesis in adipocytes: Is beige the new brown? *Genes & development* **27**, 234-250, doi:10.1101/gad.211649.112 (2013).
- 241 Himms-Hagen, J. *et al.* Multilocular fat cells in WAT of CL-316243-treated rats derive directly from white adipocytes. *Am J Physiol-Cell Ph* **279**, C670-C681 (2000).
- 242 Petrovic, N. *et al.* Chronic peroxisome proliferator-activated receptor gamma (PPARgamma) activation of epididymally derived white adipocyte cultures reveals a population of thermogenically competent, UCP1-containing adipocytes molecularly distinct from classic brown adipocytes. *The Journal of biological chemistry* **285**, 7153-7164, doi:10.1074/jbc.M109.053942 (2010).
- 243 Schulz, T. J. *et al.* Identification of inducible brown adipocyte progenitors residing in skeletal muscle and white fat. *Proceedings of the National Academy of Sciences of the United States of America* **108**, 143-148, doi:10.1073/pnas.1010929108 (2011).
- 244 Fu, J. *et al.* Molecular pathways regulating the formation of brown-like adipocytes in white adipose tissue. *Diabetes Metab Res Rev* **31**, 433-452, doi:10.1002/dmrr.2600 (2015).
- 245 Vargas-Castillo, A., Fuentes-Romero, R., Rodriguez-Lopez, L. A., Torres, N. & Tovar, A. R. Understanding the Biology of Thermogenic Fat: Is Browning A New Approach to the Treatment of Obesity? *Arch Med Res* **48**, 401-413, doi:10.1016/j.arcmed.2017.10.002 (2017).
- 246 Rosenwald, M., Perdikari, A., Rulicke, T. & Wolfrum, C. Bi-directional interconversion of brite and white adipocytes. *Nat Cell Biol* **15**, 659-667, doi:10.1038/ncb2740 (2013).



- 247 Cinti, S. Transdifferentiation properties of adipocytes in the adipose organ. *Am J Physiol-Endoc M* **297**, E977-E986, doi:10.1152/ajpendo.00183.2009 (2009).
- 248 Rothwell, N. J. & Stock, M. J. Luxuskonsumption, Diet-Induced Thermogenesis and Brown Fat - the Case in Favor. *Clin Sci* **64**, 19-23, doi:DOI 10.1042/cs0640019 (1983).
- 249 Rosen, E. D. & MacDougald, O. A. Adipocyte differentiation from the inside out. *Nat Rev Mol Cell Bio* **7**, 885-896, doi:10.1038/nrm2066 (2006).
- 250 Lefterova, M. I. & Lazar, M. A. New developments in adipogenesis. *Trends Endocrinol Metab* **20**, 107-114, doi:10.1016/j.tem.2008.11.005 (2009).
- 251 Tontonoz, P. & Spiegelman, B. M. Fat and beyond: The diverse biology of PPAR gamma. *Annu Rev Biochem* **77**, 289-312, doi:10.1146/annurev.biochem.77.061307.091829 (2008).
- 252 Rosen, E. D., Walkey, C. J., Puigserver, P. & Spiegelman, B. M. Transcriptional regulation of adipogenesis. *Genes & development* **14**, 1293-1307 (2000).
- 253 Tamori, Y., Masugi, J., Nishino, N. & Kasuga, M. Role of peroxisome proliferator-activated receptor-gamma in maintenance of the characteristics of mature 3T3-L1 adipocytes. *Diabetes* **51**, 2045-2055, doi:DOI 10.2337/diabetes.51.7.2045 (2002).
- 254 Wang, N. D. *et al.* Impaired Energy Homeostasis in C/Ebp-Alpha Knockout Mice. *Science* **269**, 1108-1112, doi:DOI 10.1126/science.7652557 (1995).
- 255 Fajas, L. *et al.* Regulation of peroxisome proliferator-activated receptor gamma expression by adipocyte differentiation and determination factor 1/sterol regulatory element binding protein 1: implications for adipocyte differentiation and metabolism. *Mol Cell Biol* **19**, 5495-5503 (1999).
- 256 Shimba, S., Wada, T., Hara, S. & Tezuka, M. EPAS1 promotes adipose differentiation in 3T3-L1 cells. *Journal of Biological Chemistry* **279**, 40946-40953, doi:10.1074/jbc.M400840200 (2004).
- 257 Nanbu-Wakao, R. *et al.* Stimulation of 3T3-L1 adipogenesis by signal transducer and activator of transcription 5. *Mol Endocrinol* **16**, 1565-1576, doi:DOI 10.1210/me.16.7.1565 (2002).
- 258 Floyd, Z. E. & Stephens, J. M. STAT5A promotes adipogenesis in nonprecursor cells and associates with the glucocorticoid receptor during adipocyte differentiation. *Diabetes* **52**, 308-314, doi:DOI 10.2337/diabetes.52.2.308 (2003).
- 259 Chen, Z., Torrens, J. I., Anand, A., Spiegelman, B. M. & Friedman, J. M. Krox20 stimulates adipogenesis via C/EBP beta-dependent and -independent mechanisms. *Cell metabolism* **1**, 93-106, doi:10.1016/j.cmet.2004.12.009 (2005).
- 260 Mori, T. *et al.* Role of Kruppel-like factor 15 (KLF15) in transcriptional regulation of adipogenesis. *Journal of Biological Chemistry* **280**, 12867-12875, doi:10.1074/jbc.M410515200 (2005).
- 261 Sue, N. *et al.* Targeted disruption of the basic Kruppel-like factor gene (Klf3) reveals a role in adipogenesis. *Molecular and Cellular Biology* **28**, 3967-3978, doi:10.1128/Mcb.01942-07 (2008).

- 262 Birsoy, K., Chen, Z. & Friedman, J. Transcriptional regulation of adipogenesis by KLF4. *Cell metabolism* **7**, 339-347, doi:10.1016/j.cmet.2008.02.001 (2008).
- 263 Oishi, Y. *et al.* Kruppel-like transcription factor KLF5 is a key regulator of adipocyte differentiation. *Cell metabolism* **1**, 27-39, doi:10.1016/j.cmet.2004.11.005 (2005).
- 264 Li, D. *et al.* Kruppel-like factor-6 promotes preadipocyte differentiation through histone deacetylase 3-dependent repression of DLK1. *Journal of Biological Chemistry* **280**, 26941-26952, doi:10.1074/jbc.M500463200 (2005).
- 265 Banerjee, S. S. *et al.* The Kruppel-like factor KLF2 inhibits peroxisome proliferator-activated receptor-gamma expression and adipogenesis. *Journal of Biological Chemistry* **278**, 2581-2584, doi:10.1074/jbc.M210859200 (2003).
- 266 Clevers, H. Wnt/beta-catenin signaling in development and disease. *Cell* **127**, 469-480, doi:10.1016/j.cell.2006.10.018 (2006).
- 267 Gordon, M. D. & Nusse, R. Wnt signaling: Multiple pathways, multiple receptors, and multiple transcription factors. *Journal of Biological Chemistry* **281**, 22429-22433, doi:10.1074/jbc.R600015200 (2006).
- 268 He, X., Semenov, M., Tamai, K. & Zeng, X. LDL receptor-related proteins 5 and 6 in Wnt/beta-catenin signaling: Arrows point the way. *Development* **131**, 1663-1677, doi:10.1242/dev.01117 (2004).
- 269 Mao, J. H. *et al.* Low-density lipoprotein receptor-related protein-5 binds to Axin and regulates the canonical Wnt signaling pathway. *Molecular Cell* **7**, 801-809, doi:Doi 10.1016/S1097-2765(01)00224-6 (2001).
- 270 Zeng, X. *et al.* Initiation of Wnt signaling: control of Wnt coreceptor Lrp6 phosphorylation/activation via frizzled, dishevelled and axin functions. *Development* **135**, 367-375, doi:10.1242/dev.013540 (2008).
- 271 Hatsell, S., Rowlands, T., Hiremath, M. & Cowin, P. beta-catenin and Tcfs in mammary development and cancer. *J Mammary Gland Biol* **8**, 145-158, doi:Doi 10.1023/A:1025944723047 (2003).
- 272 Komiya, Y. & Habas, R. Wnt signal transduction pathways. *Organogenesis* **4**, 68-75 (2008).
- 273 Ross, S. E. *et al.* Inhibition of adipogenesis by Wnt signaling. *Science* **289**, 950-953 (2000).
- 274 Moldes, M. *et al.* Peroxisome-proliferator-activated receptor gamma suppresses Wnt/beta-catenin signalling during adipogenesis. *Biochem J* **376**, 607-613, doi:10.1042/BJ20030426 (2003).
- 275 Liu, J. J., Wang, H., Zuo, Y. & Farmer, S. R. Functional interaction between peroxisome proliferator-activated receptor gamma and beta-catenin. *Molecular and Cellular Biology* **26**, 5827-5837, doi:10.1128/Mcb.00441-06 (2006).
- 276 Bennett, C. N. *et al.* Regulation of osteoblastogenesis and bone mass by Wnt10b. *Proceedings of the National Academy of Sciences of the United States of America* **102**, 3324-3329, doi:10.1073/pnas.0408742102 (2005).

- 277 Longo, K. A. *et al.* Wnt10b inhibits development of white and brown adipose tissues. *Journal of Biological Chemistry* **279**, 35503-35509, doi:10.1074/jbc.M402937200 (2004).
- 278 Topol, L. *et al.* Wnt-5a inhibits the canonical Wnt pathway by promoting GSK-3-independent beta-catenin degradation. *J Cell Biol* **162**, 899-908, doi:10.1083/jcb.200303158 (2003).
- 279 Westfall, T. A. *et al.* Wnt-5/pipetail functions in vertebrate axis formation as a negative regulator of Wnt/beta-catenin activity. *J Cell Biol* **162**, 889-898, doi:10.1083/jcb.200303107 (2003).
- 280 Nishizuka, M., Koyanagi, A., Osada, S. & Imagawa, M. Wnt4 and Wnt5a promote adipocyte differentiation. *FEBS Lett* **582**, 3201-3205, doi:10.1016/j.febslet.2008.08.011 (2008).
- 281 Gregor, M. F. & Hotamisligil, G. k. S. Inflammatory Mechanisms in Obesity. *Annual Review of Immunology* **29**, 415-445, doi:10.1146/annurev-immunol-031210-101322 (2011).
- 282 Jin, C., Henao-Mejia, J. & Flavell, R. A. Innate Immune Receptors: Key Regulators of Metabolic Disease Progression. *Cell Metabolism* **17**, 873-882, doi:<http://dx.doi.org/10.1016/j.cmet.2013.05.011> (2013).
- 283 Desvergne, B., Michalik, L. & Wahli, W. Transcriptional Regulation of Metabolism. *Physiol. Rev.* **86**, 465-514, doi:10.1152/physrev.00025.2005 (2006).
- 284 Gut, P. & Verdin, E. The nexus of chromatin regulation and intermediary metabolism. *Nature* **502**, 489-498 (2013).
- 285 Natoli, G., Ghisletti, S. & Barozzi, I. The genomic landscapes of inflammation. *Genes & Development* **25**, 101-106 (2011).
- 286 Dobin, A. *et al.* STAR: ultrafast universal RNA-seq aligner. *Bioinformatics* **29**, 15-21, doi:10.1093/bioinformatics/bts635 (2013).
- 287 Anders, S., Pyl, P. T. & Huber, W. HTSeq-a Python framework to work with high-throughput sequencing data. *Bioinformatics* **31**, 166-169, doi:10.1093/bioinformatics/btu638 (2015).
- 288 Wang, L. G., Wang, S. Q. & Li, W. RSeQC: quality control of RNA-seq experiments. *Bioinformatics* **28**, 2184-2185, doi:10.1093/bioinformatics/bts356 (2012).
- 289 Li, B. & Dewey, C. N. RSEM: accurate transcript quantification from RNA-Seq data with or without a reference genome. *Bmc Bioinformatics* **12**, doi:Artn 323 10.1186/1471-2105-12-323 (2011).
- 290 Robinson, M. D., McCarthy, D. J. & Smyth, G. K. edgeR: a Bioconductor package for differential expression analysis of digital gene expression data. *Bioinformatics* **26**, 139-140, doi:10.1093/bioinformatics/btp616 (2010).
- 291 Law, C. W., Chen, Y. S., Shi, W. & Smyth, G. K. voom: precision weights unlock linear model analysis tools for RNA-seq read counts. *Genome Biol* **15**, doi:ARTN R29 10.1186/gb-2014-15-2-r29 (2014).

- 292 Dettmer, K., Aronov, P. A. & Hammock, B. D. Mass spectrometry-based metabolomics. *Mass Spectrometry Reviews* **26**, 51-78, doi:10.1002/mas.20108 (2007).
- 293 Ritchie, M. E. *et al.* limma powers differential expression analyses for RNA-sequencing and microarray studies. *Nucleic Acids Res* **43**, doi:ARTN e47  
10.1093/nar/gkv007 (2015).
- 294 Risso, D., Ngai, J., Speed, T. P. & Dudoit, S. Normalization of RNA-seq data using factor analysis of control genes or samples. *Nat Biotechnol* **32**, 896-902, doi:10.1038/nbt.2931 (2014).
- 295 Tarca, A. L. *et al.* A novel signaling pathway impact analysis. *Bioinformatics* **25**, 75-82, doi:10.1093/bioinformatics/btn577 (2009).
- 296 Yu, G. C., Wang, L. G., Han, Y. Y. & He, Q. Y. clusterProfiler: an R Package for Comparing Biological Themes Among Gene Clusters. *OmicS* **16**, 284-287, doi:10.1089/omi.2011.0118 (2012).
- 297 Mikkelsen, T. S. *et al.* Comparative Epigenomic Analysis of Murine and Human Adipogenesis. *Cell* **143**, 156-169, doi:10.1016/j.cell.2010.09.006 (2010).
- 298 Ghisletti, S. *et al.* Identification and Characterization of Enhancers Controlling the Inflammatory Gene Expression Program in Macrophages. *Immunity* **32**, 317-328 (2010).
- 299 Raghav, S. K. *et al.* Integrative Genomics Identifies the Corepressor SMRT as a Gatekeeper of Adipogenesis through the Transcription Factors C/EBP beta and KAISO. *Mol Cell* **46**, 335-350, doi:10.1016/j.molcel.2012.03.017 (2012).
- 300 van der Heijden, R. A. *et al.* High-fat diet induced obesity primes inflammation in adipose tissue prior to liver in C57BL/6j mice. *Aging* **7**, 256-268 (2015).
- 301 Strissel, K. J. *et al.* Adipocyte death, adipose tissue remodeling, and obesity complications. *Diabetes* **56**, 2910-2918, doi:10.2337/db07-0767 (2007).
- 302 Xu, H. Y. *et al.* Chronic inflammation in fat plays a crucial role in the development of obesity-related insulin resistance. *Journal of Clinical Investigation* **112**, 1821-1830, doi:10.1172/JCI200319451 (2003).
- 303 Chen, N. & Wang, J. Wnt/beta-Catenin Signaling and Obesity. *Front Physiol* **9**, 792, doi:10.3389/fphys.2018.00792 (2018).
- 304 Bennett, C. N. *et al.* Regulation of Wnt signaling during adipogenesis. *The Journal of biological chemistry* **277**, 30998-31004, doi:10.1074/jbc.M204527200 (2002).
- 305 Bradley, R. L., Fisher, F. F. & Maratos-Flier, E. Dietary fatty acids differentially regulate production of TNF-alpha and IL-10 by murine 3T3-L1 adipocytes. *Obesity* **16**, 938-944, doi:10.1038/oby.2008.39 (2008).
- 306 Rohart, F., Gautier, B., Singh, A. & Le Cao, K. A. mixOmics: An R package for 'omics feature selection and multiple data integration. *Plos Comput Biol* **13**, doi:ARTN e1005752  
10.1371/journal.pcbi.1005752 (2017).
- 307 Singh, A. *et al.* DIABLO: from multi-omics assays to biomarker discovery, an integrative approach. *bioRxiv*, 067611, doi:10.1101/067611 (2018).

- 
- 308 Nagao, H. *et al.* Increased Dynamics of Tricarboxylic Acid Cycle and Glutamate Synthesis in Obese Adipose Tissue IN VIVO METABOLIC TURNOVER ANALYSIS. *Journal of Biological Chemistry* **292**, 4469-4483, doi:10.1074/jbc.M116.770172 (2017).
- 309 Kunos, G., Osei-Hyiaman, D., Liu, J., Godlewski, G. & Batkai, S. Endocannabinoids and the Control of Energy Homeostasis. *Journal of Biological Chemistry* **283**, 33021-33025, doi:10.1074/jbc.R800012200 (2008).
- 310 Di Marzo, V. *et al.* Leptin-regulated endocannabinoids are involved in maintaining food intake. *Nature* **410**, 822-825, doi:Doi 10.1038/35071088 (2001).
- 311 Polyak, A. *et al.* The fractalkine/Cx3CR1 system is implicated in the development of metabolic visceral adipose tissue inflammation in obesity. *Brain Behav Immun* **38**, 25-35, doi:10.1016/j.bbi.2014.01.010 (2014).
- 312 Altintas, M. M. *et al.* Mast cells, macrophages, and crown-like structures distinguish subcutaneous from visceral fat in mice. *Journal of lipid research* **52**, 480-488, doi:10.1194/jlr.M011338 (2011).
- 313 Gunesdogan, U., Jackle, H. & Herzig, A. Histone supply regulates S phase timing and cell cycle progression. *Elife* **3**, e02443, doi:10.7554/eLife.02443 (2014).
- 314 Wang, Q. A., Tao, C., Gupta, R. K. & Scherer, P. E. Tracking adipogenesis during white adipose tissue development, expansion and regeneration. *Nature Medicine* **19**, 1338+, doi:10.1038/nm.3324 (2013).